Part I : Dynamics of Fluid-Filled Porous Media under Wave Action

Part II: Excitation of Surf-Beats in the Ocean

by

Mostafa Ameen Foda

B.Sc. Cairo University (1973)
M.Eng. McGill University (1977)

Submitted in partial fulfillment
of the requirements for the degree of
Doctor of Science

at the

Massachusetts Institute of Technology

(1980)

Signature Redacted

Signature of Author.....
Department of Civil Engineering, May 1980

Signature Redacted

Certified by.....
Thesis Supervisor

Signature Redacted

Accepted by.....
Chairman, Departmental Committee on Graduate Students
of the Department of Civil Engineering

Part I: Dynamics of Fluid-Filled Porous Media under Wave Action

Part II: Excitation of Surf-Beats in the Ocean

by

Mostafa Ameen Foda

Submitted to the Department of Civil Engineering in May 1980 in partial fulfillment of the requirements for the Degree of Doctor of Science

ABSTRACT

Part I:

Wave-induced stresses in a porous elastic medium are studied on the basis of Biot's linearized theory. For sufficiently high frequencies which are pertinent to ocean waves and seismic waves, a boundary layer of Stokes type is shown to exist near the free surface of the solid. Outside the boundary layer, fluid and solid skeleton move together essentially according to the laws of classical elasticity. This division simplifies considerably the analysis of Biot's equations; and several examples of potential interest to foundation engineering and geophysics are treated.

Part II:

The interaction between low frequency trapped waves and incident waves groups in the ocean is studied and two possible generation mechanisms for such trapped modes are investigated. One is a resonance mechanism when the directional spread of the incident waves results in incident wave grouping in both the longshore and the offshore directions that resonantly excites trapped modes having scales commensurate with those of the incident group. The second is a side-band instability when the low frequency trapped modes are unstable in the presence of incident waves. By accounting further for nonlinear radiation damping, the evolution of trapped modes is traced from initial growth until steady state is reached.

Thesis Supervisor: Chiang C. Mei
Title: Professor of Civil Engineering

Acknowledgement

Part I of this study was funded by a grant from U.S. National Science Foundation Earthquake Engineering Program (ENV 7710236). Part II was funded by (1) U.S. Office of Naval Research Fluid Dynamics Program (NR-062-228), Contract N00014,76-C-0124, (2) U.S. National Science Foundation Fluid Mechanics Program (CME-7717817). The supports of NSF and ONR are very much appreciated.

The author is indebted to his supervisor Professor Chiang C. Mei for his constant encouragement, timely criticism and invaluable advice during the course of this study. His friendship will be cherished forever.

The author finds no words that fully express his appreciation and gratitude to his dear wife Manal. She is always cheerful, giving confidence when there is doubt and comfort when there is distress. She has done a lot of enduring as well and has been and always will be my very best friend.

Tnaks are also due to Mrs. Stephanie George for her excellent typing of the thesis.

TO MY FATHER

TABLE OF CONTENTS

LIST OF FIGURES

Part I

LIST OF SYMBOLS

Part I

k = permeability

v_i = velocity of solid matrix

u_i = velocity of fluid

p = pore pressure in the fluid

σ_{ij} = effective stress in the solid

τ_{ij} = total stress in the composite medium

ϵ_{ij} = effective strain in the solid

$G=E/2(1+\nu)$ = shear modulus of solid matrix

$\lambda=2\nu G/(1-2\nu)$ = Lame constant of solid matrix

β = bulk modulus of fluid

n^1 = static void ratio, n' = perturbed void ratio, n = total void ratio

$\left.\begin{matrix}\rho_s \\ \rho_w\end{matrix}\right\}$ = density of $\begin{pmatrix}\text{solid} \\ \text{fluid}\end{pmatrix}$

ξ_i, ξ, η, τ = dimensionless independent variables in the outer region

X_i, X, Y, T = dimensionless independent variables in the boundary layer

$\tilde{u}_i, \tilde{v}_i, \tilde{\sigma}_{ij}, \tilde{\tau}_{ij}, \tilde{p}$ = dimensionless unknowns in the outer region

$\hat{u}_i, \hat{v}_i, \hat{\sigma}_{ij}, \hat{\tau}_{ij}, \hat{p}$ = dimensionless corrections in the boundary layer

Part II

A = incident wave amplitude

$\mathcal{A}$ = non-dimensional incident wave amplitude

Cg = incident wave group velocity

D = trapped wave amplitude

F_{nm}, G_{nm}, H_{nm} = the inhomogeneous forcings for the perturbation scheme problem sets

g = gravitational acceleration

h = water depth

$J_o, Y_o, H_o^{(1)}$ = Bessel's Functions

k = incident wave number

K = trapped wave number

$\mathcal{L}_n$ = Laguerre polynomial of order n

L_n = trapped wave n^{th} modal shape

P = the inhomogeneous forcing for ϕ_{21} potential

q = nondimensional water depth = kh

S = secular forcings for the trapped wave

x, y, z = cartizian coordinates

t = time

Greek letters

β = scaled beach slope

γ_b = ratio of wave height to local water depth at breaking point

γ_j = coefficients in the trapped wave evolution equation

ε = the small perturbation parameter that characterizes the sea bottom slope

η = water elevation from still water level

θ, Θ = slow-phase functions

ϕ, Φ = velocity potentials

ψ = fast-phase function

ω = incident wave frequency

Ω = trapped wave frequency

ξ = Irribarrin parameter

Part I

DYNAMICS OF FLUID-FILLED POROUS MEDIA UNDER WAVE ACTION

INTRODUCTION

In past decades, increasing engineering activities in the off-shore area and the progress achieved in modern earthquake engineering have created an impetus for seeking a better understanding of the dynamics of fluid-saturated porous media. The subject is also of interest in acoustics, geophysics and engineering soil mechanics. It also lies within the realm of the broader and more comprehensive theory of mixture (e.g., Bowen, 1976; Prevost, 1980) which is of practical importance in many branches of applied physics.

The class or problems considered herein will be those where the dynamical response of the fluid saturated porous media is required under wave-like forcing. For example, in the field of off-shore engineering, the determination of the pressures and stresses in sea-beds, induced by waves is important for the design of various ocean and near-shore structures. Such structures include gravity-type breakwaters, off-shore oil storage tanks, and drilling rigs. Such knowledge is also important when one considers the problem of floatation of buried pipelines and the burial of rubble-mounds, teterapods and other blocks and submarine land slide. It is also important to investigate the stability of such off-shore structures under the effect of cyclic loading due to earthquakes or sea waves. However, this subject is not yet well understood, partially because the dynamical behavior of soils under wave action is not well understood physically and difficult to model mathematically. The

objective here is to adopt the simple but consistent model of Biot, widely used in geophysics, and establish an effective analytical means that not only reduces the mathematical difficulties inherited in the problem, but also provides better understanding of the physics under such circumstances.

CONTINUUM APPROACH TO POROUS MEDIA DYNAMICS

A microscopic cross-sectional view of a typical saturated soil media is shown in Figure 1, where the randomly shaped and oriented

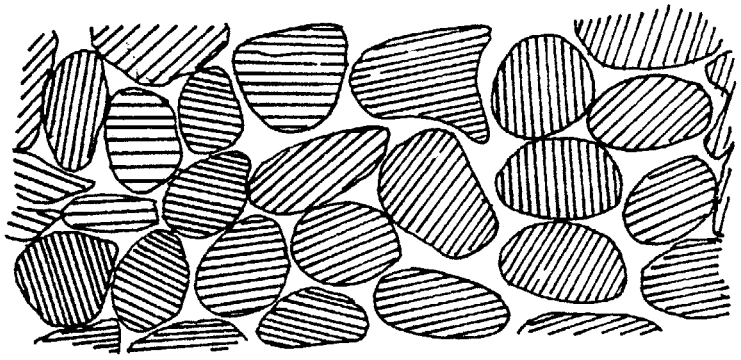

Figure 1

solid particles are immersed in water, which may contain tiny pockets of air. The space occupied by the fluid is called the pore space, while the solid particles are interconnected at isolated points, forming a continuous solid network.

As a first fundamental step towards formulating the mathematical model of such complicated physical system, we usually employ the concept of a continuum. This means that we overlook the microscopic details of the system and average over a fictitious elementary

volume, which is taken to be large enough compared to the size of the pores so that it may be treated as homogeneous, and at the same time small enough compared to the scale of the macroscopic phenomena in which we are interested, so that it may be considered as infinitesimal in the mathematical treatment.

The obvious reason for employing the continuum approach is that it is practically impossible to describe in any exact mathematical manner the complicated geometry at the microscopic level. The process of passing from the microscopic level to the macroscopic level of continuum at which only averaged phenomena are considered is certainly not a unique one. In the literature, one can find numerous continuum models for studying saturated porous-media. For example, geologists who are interested in fluid flow through porous media put the main emphasis on the fluid phase, while solid dynamicists who are interested in stress fields in porous materials, put their emphasis on the solid phase. Of course, each one of these models varies in its complexity and the assumptions involved as these relate to the main function and domain of application of the model. However, the success of any formulation should be measured against its ability to account for the important physical processes taking place at the macroscopic scale and then correctly translate them in some mathematical form. The formulation should consist of the laws of conservation of momentum (Newton's Second Law), conservation of mass and the various constitutive equations for the fluid and the solid phases.

It is mainly these constitutive equations used in a certain model that characterize the nature and the limitation of such a model. For example, it is known that if loading is applied to the solid skeleton of the soil, it will undergo certain displacements. To describe this in the continuum formulation, one needs a stress-strain constitutive relation that correctly represents such process. However, depending on the kind of soil, the nature of loadings and other characteristics of the problem at hand, one would arrive at a certain stress-strain relation that would be vastly different from that obtained under different circumstances. Even then, depending on the degree of complexity of the model, one would simplify the obtained relation to a certain idealized situation, thus sacrificing certain quantitative aspects of the problem, but keeping the essential qualitative features in, for the sake of reducing the mathematical difficulties of treatment.

SOLID-FLUID INTERACTION IN A POROUS MEDIA

When deriving the equations of conservation of momentum for the solid phase as well as for the fluid phase, as a part of the continuum governing equation, an especially important component would be the terms representing the different effects each phase impose on the other. Of course, the fluid will have the obvious static effect of "buoyancy" on the solid particles. However, as the fluid moves relative to the solid, two more subtle effects on both

the fluid and the solid will occur. First, due to the fluid viscosity, the fluid phase will dissipate energy by friction on the solid surfaces, and as a result exerts a viscous drag force on the solid skeleton. Secondly, due to the fluid inertia, the relative acceleration between the fluid and the solid will give rise to D'Alembert force component. This effect is usually called "the virtual mass" effect in classical hydrodynamics.

On the other hand, under stress, the solid skeleton will suffer displacements, causing changes in the pore space and consequently causing the fluid to move.

Terzaghi (1925) in his theory of soil consolidation was the first to recognize that accounting for such mutual interaction between water and soil will explain how soil settles, or consolidates, under loading. Terzaghi's theory was developed for one-dimensional, quasi-static settlements. Biot (1940, 1956a-b) extended Terzaghi's work to three dimensions, and included the effects of inertia in the formulation. Biot's theory has the following basic assumptions: (1) isotropy of the material, (2) reversibility of stress-strain relations under final equilibrium conditions, (3) linearity of stress-strain relation, (4) small strains, (5) the pore fluid is compressible, (6) the fluid flows through the porous skeleton according to Darcy's law. Of these basic assumptions, (2) and (3) are the most restrictive. However, for small enough strains, when the grain pattern is not too much disturbed, the assumption of reversibility seems to be applicable. The assumption of isotropy is not essential and anisotropy can easily be introduced as a

refinement (e.g. Madsen, 1978). Darcy's law will represent the fluid viscous drag effect. For the virtual mass effect, Biot introduced the "added mass coefficients" in the inertia terms of the equations to account for it. However, it is very difficult to, analytically or experimentally, assess for these coefficients (Deresiewicz, 1962). A further discussion of this point will be given later.

Biot's theory can be considered as a mere special case (Atkin and Craine, 1976a,b) of the more general and elaborate theory of mixtures, which has been developed to describe the behavior of multiphase materials. The general theoretical framework which forms the basis of mixtures' theories was first developed by Truesdell and Topin (1960). Since then, the theoretical description of multiphase media has received repeated attention in the literature, and fundamental equations for a dynamical theory of interacting continua have been derived [see Atkin and Craine (1976) and Bowen (1976]. The mixtures theories deal in general with an arbitrary number of constituents. However, the application to porous materials remains one of the important areas of application of such theories, viewing porous media as a mixture of deformable fluid and solid, each of which is regarded as a continuum and each following its own motion. It is assumed that at any time t each place $\vec{x}$ of the mixture is occupied simultaneously by m different particles (m=2 for saturated porous media), one for each constituent. Then, the governing equations will consist of statements of conservation of mass and

momentum for each constituent, as well as for the mixture as a whole, plus the appropriate constitutive equations. It will be shown later in the formulation that by linearizing these mixture theory equations, Biot's linear theory will be reproduced (Bowen, 1976; Atkin and Craine, 1976a,b; and Prevost, 1980).

LINEAR THEORY IN POROUS MEDIA DYNAMICS

There are various evidences in the literature that in certain contexts, linearized theory may be adequate in describing the dynamics of saturated porous media. For example, it is the partial success of Terzaghi's linear theory (1925) in predicting the settlement for many types of soils that provided one of the strongest incentives in the creation of a science of soil mechanics. Biot's linearized theory (1940, 1956a,b) has been the basis of most of the subsequent work in the acoustics and geophysics literature (see Rice and Cleary, 1976; Deresiewicz, 1962). Yamamoto et al. (1978) and Yamamato (1977) used Biot's linear theory for propagating sea waves over a sand layer of finite or infinite depth. By adjusting fluid compressibility due to possible entrainment of tiny air pockets, they succeed in verifying the theoretically predicted pore pressure by laboratory experiments. Biot's theory was used also to study elastic wave propagation in saturated porous media by de Josselin de Jong (1956), Geertsma and Smit (1961), Jones (1960) and Deresiewicz (1961-62). However, the majority of these studies involved very simple one-dimensional geometries that bear little engineering importance.

The reason for this is the great difficulty in the mathematical treatment of Biot's equations. The equations couple the pore pressure and the solid displacements. In plane-strain problems, the coupled equations amount to a sixth-order partial differential equation. Indeed, the Biot formulation is precisely analogous (Biot, 1956b) to the well established theory of linear coupled thermoelasticity (e.g. Nowaki, 1964) where temperature plays a similar role as pore pressure, so an abundance of available solutions might be expected. Unfortunately the neglect of coupling terms that is so commonly and justifiably used to simplify the equations in thermoelasticity (e.g. Boley and Weiner, 1960) is certainly not appropriate for fluid saturated porous media. Thus one usually has to resort to one of a small number of formal procedures (e.g., Biot, 1956a,b; McNamee and Gibson, 1960) in order to solve the equations. In all these approaches, the algebraic details become rather complicated. An effective analytical means of treating Biot's equation is therefore desirable in order to have a better understanding of the physics and to solve problems involving more realistic geometry.

BOUNDARY LAYER APPROXIMATION

By incorporating inertia effects in the formulation, Biot was the first to study the propagation of stress waves in poroelastic media. He found that there is one rotational wave and two dilatational waves, so that in addition to the usual elastic waves, one rotational and one dilatational, there exists a new wave which Biot called

"wave of the second kind." All three waves attenuate as they propagate in the media due to the viscous dissipation effect of the fluid. However, as noted by Biot (1956a), the attenuation length scale of the wave of the second kind is very short compared with that of the two other waves. In fact, it can be shown that the wave of the second kind behaves like a diffusion or heat conduction phenomenon where attenuation is very high, while in a first order calculation, the two other waves can be considered unattenuated. An important implication of Biot's finding is that two vastly different length scales are inherent and therefore there exists a boundary layer. In his study of the steady advance of semi-infinite cracks in poroelastic media, Simons (1977) neglected intertial effects in Biot's Equations, then at the limit of very rapid propagation he identified boundary layers at the crack's face.

In this thesis, we will first verify the existance of such boundary layers for the case of time harmonic forcing (for both quasi-static and dynamic problems) by comparing some obtained one-dimensional exact solutions of Biot's Equations with those obtained using the boundary layer approximation. It will be shown that for sufficiently high frequencies which are pertinent to ocean waves (quasi-static problems) and seismic waves (dynamic problems), the boundary layer analysis gives a good approximate solution to Biot's coupled equations. At the same time, it will be shown that this approximation simplifies considerably the analysis of Biot's Equations. The boundary layer analysis is then generalized to two-

and three-dimensional poroelastic problems with a free surface. It will be demonstrated that such problems may be reduced to first solving a conventional elasto-static (ocean waves), or elastodynamic (seismic waves) problems, and then making a boundary layer correction near the free surface. A variety of plane strains problems are then treated, in order to show the efficiency of the boundary layer approximations in solving a broad class of practical engineering problems.

1. Governing Equations

We will derive the conservation of mass and momentum equations for saturated porous media, following the mixtures' theory (Prevost, 1980).

We consider a binary mixture of solid and water. The porosity n is defined as the volume of water dV_w in a unit volume of the mixture dV:

$$n = \frac{dV_w}{dV} \tag{1.1}$$

Clearly, the volume fraction of solid n_s is then given by

$$n_s = \frac{dV_s}{dV} = 1-n \tag{1.2}$$

It will be assumed further (Biot, 1956) that the areal fraction of water and solid are given by

$$\frac{dA_w}{dA} = n \quad \text{for water}$$

$$\frac{dA_s}{dA} = 1-n \quad \text{for solid} \tag{1.3}$$

where A_w, A_s are the areas occupied by water and solid, respectively, in the elementary area dA.

We define $\{\rho^w_s\}$ as the mass of $\{^{\text{water}}_{\text{solid}}\}$ within a unit volume of mixture. Thus, $\{\rho_w, \rho_s\}$, based on the net volume of $\{^{\text{water}}_{\text{solid}}\}$ are given by:

$$\rho^w = n\rho_w \tag{1.4a}$$

$$\rho^s = n_s\rho_s = (1-n)\rho_s \tag{1.4b}$$

Assuming the mixture to be chemically inert, the axiom of balance of mass gives

$$\frac{\partial \rho^w}{\partial t} + \nabla\cdot\rho^w\underline{u} = \dot{\rho}^w + \rho^w \nabla\cdot\underline{u} = 0 \tag{1.5a}$$

$$\frac{\partial \rho^s}{\partial t} + \nabla\cdot\rho^s\underline{v} = \dot{\rho}^s + \rho^s \nabla\cdot\underline{v} = 0 \tag{1.5b}$$

where overhead dot denotes material derivatives, and $\underline{u}$, $\underline{v}$ the intrinsic or seepage velocities of fluid and solid.

Substituting (1.4) into (1.5), we have alternatively,

$$\dot{n} + n\ \nabla\cdot\underline{u} = -n\frac{\dot{\rho}_w}{w} \tag{1.6a}$$

$$\dot{n}_s + n_s\ \nabla\cdot\underline{v} = -n_s\frac{\dot{\rho}_s}{s} \tag{1.6b}$$

In our applications, the solid media are rocks or soils, rather

than rubber-like foams and hence, we will assume that the solid grains compressibility, which is different from the solid skeleton compressibility, is negligible. This means that:

$$\dot{\rho}_s = 0 \tag{1.7}$$

But, by definition, and using (1.2):

$$\dot{n}_s = \frac{\partial n_s}{\partial t} + \underline{v}.\nabla n_s = -\frac{\partial n}{\partial t} - \underline{v}.\nabla n$$

$$= -\dot{n} + (\underline{u} - \underline{v}).\nabla n$$

it then follows from (1.6b) that

$$-n + (1-n)\ \nabla.\underline{v} + (\underline{u} - \underline{v}).\nabla n = 0 \tag{1.8}$$

Adding (1.6a) and (1.8) we get the so-called storage equation

$$n\ \nabla.\underline{u} + (1-n)\ \nabla.\underline{v} + \underline{u} - \underline{v}).\nabla n = -n\ \frac{\dot{\rho}_w}{\rho_w} \tag{1.9}$$

Next we consider the surface forces acting on an area element dA with unit normal N. We define the partial stress vectors $\underline{t}^w$ and $\underline{t}^s$ as the force acting on water and solid, respectively, divided by dA. Then, the partial stress tensors, $\underline{\underline{\sigma}}^w$ and $\underline{\underline{\sigma}}^s$ are defined as:

$$\underline{t}^w = \underline{N}.\underline{\underline{\sigma}}^w$$

$$\underline{t}^s = \underline{N}.\underline{\underline{\sigma}}^s \tag{1.10}$$

From (1.3), it follows that the "net partial stress tensors" $\underline{\underline{\sigma}}_w$ and $\underline{\underline{\sigma}}_s$, where stresses are measured against the respective areas dA_w and dA_s, are given by:

$$\underline{\underline{\sigma}}^w = n\ \underline{\underline{\sigma}}_w$$

$$\underline{\underline{\sigma}}^s = (1-n)\underline{\underline{\sigma}}_s \tag{1.11}$$

We assume that the pore fluid net partial stress tensor is given

by (Biot, 1956):

$$\underline{\underline{\sigma}}_w = -p\underline{\underline{I}} \tag{1.12}$$

where $\underline{\underline{I}}$ is the identity tensor and p is the pore pressure. The partial stress tensor corresponding to the solid phase is given by (Prevost, 1980)

$$\underline{\underline{\sigma}}^s = \underline{\underline{\sigma}} + n_s \underline{\underline{\sigma}}_w \tag{1.13}$$

where, $n_s \underline{\underline{\sigma}}_w$ accounts for the effect of the pore fluid stress on the individual solid grain, which is assumed completely surrounded by the pore fluid with negligible contact areas with neighbouring grains. The tensor $\underline{\underline{\sigma}}$ is the effective stress tensor, first introduced by Terzaghi (1925), which characterizes the integranular forces on solid grains, in excess of the pore fluid stress.

In terms of the partial stress tensors (1.11), we may write the balance of linear momentum equations for water and solid as follows:

$$\rho^w \dot{\underline{u}} = \nabla \cdot \underline{\underline{\sigma}}^w + \rho^w \underline{g} + \underline{f} \tag{1.14}$$

$$\rho^s \dot{\underline{v}} = \nabla \cdot \underline{\underline{\sigma}}^s + \rho^s \underline{g} - \underline{f} \tag{1.15}$$

where $\underline{g}$ is the body force per unit volume of mixture (e.g. gravity) and $\underline{f}$ is the force exerted on the water by the solid, which, by Newton's third law, is equal to the negative of the force exerted by the water on the solid.

Equations of State

We have already assumed that the solid grains are incompressible (1.7), and the fluid stress tensor is given by (1.12). We will further assume that the pore pressure is related to the fluid density by the linear equation of state:

$$dp = \beta \frac{d\rho_w}{\bar{\rho}_w} \tag{1.16}$$

where $\bar{\rho}_w$ is a constant reference density and β the bulk modulus. The pure water bulk modulus is very large ($\beta_o = 1.9 \times 10^9 N/m^2$).

It may be shown, however, that if the entrainment of air in the pores keeps the degree of saturation S below one, then the effective bulk modulus of the fluid is given by:

$$\frac{1}{\beta} = \frac{1}{\beta_o} + \frac{1-S}{p_o} \quad \text{(Verruijt, 1969)} \tag{1.17}$$

where p_o denotes the absolute pore pressure. As was estimated by Yamamoto et al. (1978) and Madsen (1978), for S=0.95 and P_o=1 atm, $\beta = 9.5 \times 10^5 N/m^2$. We assume that β in (1.16) represents the effective bulk modulus accounting for possible content of air.

For the solid skeleton, Hook's law is assumed between the effective stress and solid strains,

$$\frac{\partial}{\partial t} \sigma_{ij} = G\left(\frac{\partial v_i}{\partial x_j} + \frac{\partial v_j}{\partial x_i} + \frac{2\nu}{1-2\nu} \delta_{ij} \frac{\partial v_k}{\partial x_k}\right) \tag{1.18}$$

r equivalently,

$$\frac{\partial v_i}{\partial x_j} + \frac{\partial v_j}{\partial x_i} = \frac{1}{G}\left(\frac{\partial \sigma_{ij}}{\partial t} - \frac{\nu}{1+\nu} \delta_{ij} \frac{\partial \sigma_{kk}}{\partial t}\right) \tag{1.19}$$

where G is the shear modulus and ν the Poisson ratio. Notice however that in Biot's formulation, the constitutive stress-strain relation was assumed between the solid strains and the partial stresses $\underline{\underline{\sigma}}^s$, instead of the effective stresses $\underline{\underline{\sigma}}$,

Finally, the inter-phase force $\underline{f}$ is assumed to be given by Darcy's law

$$\underline{f} = \frac{n^2}{k} (\underline{v} - \underline{u}) \tag{1.20}$$

where k is the coefficient of permeability.

Linearized Governing Equations

Let the superscript $( )^1$ denote static values, while the dynamic perturbations are denoted by $( )'$, i.e.,

$$p = p^1 + p' \qquad n = n^1 + n' \; ; \quad n^1 = \text{constant}$$

$$\underline{\underline{\sigma}} = \underline{\underline{\sigma}}^1 + \underline{\underline{\sigma}}' \qquad \rho_w = \rho_w^1 + \rho_w' \qquad \rho^w = \rho^{w^1} + \rho^{w'}$$

$$\underline{v} = \underline{v}' \qquad \underline{u} = \underline{u}' \qquad \text{etc.}$$

The linearized version of (1.6a) is

$$\frac{\partial n'}{\partial t} + n^1 \nabla \cdot \underline{u}' + \frac{n^1}{\beta} \frac{\partial p'}{\partial t} = 0 \tag{1.21}$$

after using (1.16). Similarly from (1.8)

$$- \frac{\partial n'}{\partial t} + (1-n^1) \nabla \cdot \underline{v}' = 0 \tag{1.22}$$

Adding (1.21) and (1.22), or from (1.9), we get the linearized storage equation

$$n^1 \nabla \cdot \underline{u}' + (1-n^1) \nabla \cdot \underline{v}' = - \frac{n^1}{\beta} \frac{\partial p'}{\partial t} \tag{1.23}$$

Now, the linear version of the momentum equations (1.14) and (1.15) is:

$$n^1 \rho_w^1 \frac{\partial \underline{u}'}{\partial t} = -n^1 \nabla (p^1+p') - p^1 \nabla n' + (\rho^{w^1} + \rho^{w'}) \underline{g} + \underline{f}' \qquad (1.24)$$

$$(1-n^1) \rho_s^1 \frac{\partial \underline{v}'}{\partial t} = \nabla \cdot (\underline{\underline{\sigma}}^1 + \underline{\underline{\sigma}}') - (1-n^1)\nabla(p^1+p') + p^1 \nabla n' + (\rho^{s^1} + \rho^{s'})\underline{g} - \underline{f}' \qquad (1.25)$$

But at the static equilibrium ($\frac{\partial}{\partial t} = 0$), the static values satisfy

$$0 = -n^1 \nabla p^1 + \rho^{w^1} \underline{g} \qquad (1.26)$$

$$0 = \nabla \cdot \underline{\underline{\sigma}}^1 - (1-n^1) \nabla p^1 + \rho^{s^1} \underline{g} \qquad (1.27)$$

Further, if we let P_o, ω and L to be the characteristic stress frequency and length, respectively, of the dynamic problem, then, by Hook's law (1.19), the characteristic dynamic velocity is $O(P_o \omega L/G)$. Thus, from (1.5),

$$\left(\frac{\rho^{\alpha'} \underline{g}}{\nabla p'}\right) \sim \rho_\alpha^1 \, gL/G \qquad \alpha = w,s \qquad (1.28)$$

and from (1.22) and (1.26):

$$\left(\frac{p^1 \nabla n'}{\nabla p'}\right) \sim \rho_w \, gL/G \qquad (1.29)$$

G is typically $10^8 \sim 10^{10}$ N/m^2, L $\sim$ 10-100m so that the above ratio is in the range of $10^{-2} \sim 10^{-5}$ and is negligible.

Therefore, subtracting (1.24), (1.25) from their static version (1.26), (1.27) and neglecting gravity terms [(1.28), (1.29)] and invoking Darcy's law we have finally:

$$\text{Solid:} \quad (1-n)\rho_s \frac{\partial v_i}{\partial t} = \frac{\partial \sigma_{ij}}{\partial x_j} - (1-n) \frac{\partial p}{\partial x_i} + \frac{n^2}{k} (u_i - v_i) \quad (1.30)$$

$$\text{Fluid:} \quad n\rho_w \frac{\partial u_i}{\partial t} = -n \frac{\partial p}{\partial x_i} - \frac{n^2}{k} (u_i - v_i) \quad (1.31)$$

where we have omitted the superscripts, for convenience, with the understanding that n, ρ_w, ρ_s and k are the static values, assumed constant, while v_i, u_i, p and σ_{ij} are the dynamical perturbations. Using this convention, the storage equation (1.23) is re-written as:

$$n \frac{\partial}{\partial x_j} (u_j - v_j) + \frac{\partial v_j}{\partial x_j} = - \frac{n}{\beta} \frac{\partial P}{\partial t} \quad (1.32)$$

Thus, if the boundary conditions permit, we may solve (1.30), (1.31), (1.32) with (1.18) for u_i, v_i and p. Afterwards n' is found from (1.21) or (1.22).

These are Biot's Equations (1956), but in the original formulation Biot also included apparent inertia force in the inter-phase force vector $\underline{f}$. This is caused by hydrodynamic reaction to the relative acceleration between solid and the surrounding fluid. The apparent mass is, of course, difficult to assess theoretically or experimentally, hence they are often omitted by some authors (Deresiewicz, 1962; Prevost, 1980). This omission is quite justifiable in our cases as will be discussed later.

2. ONE-DIMENSIONAL COMPRESSIONAL WAVES IN A LAYER

We assume that

$$u_i = [u(x,t),\ 0,\ 0] \qquad v_i = [v(x,t),\ 0,\ 0] \tag{2.1}$$

Denote the stress component σ_{11} by σ, then

$$\frac{\partial \sigma}{\partial t} = E\ \frac{\partial v}{\partial x} \tag{2.2}$$

The governing equations may be simplified to

$$n\ \rho_w \frac{\partial u}{\partial t} = -n\ \frac{\partial p}{\partial x} - \frac{n^2}{k}\ (u - v) \qquad \text{from (1.31)} \tag{2.3}$$

$$(1 - n)\rho_s \frac{\partial v}{\partial t} = \frac{\partial \sigma}{\partial x} - (1 - n)\ \frac{\partial p}{\partial x} + \frac{n^2}{k}\ (u - v) \qquad \text{from (1.30)} \tag{2.4}$$

$$n\ \frac{\partial}{\partial x}\ (u - v) + \frac{\partial v}{\partial x} = -\ \frac{n}{\beta}\ \frac{\partial p}{\partial t} \qquad \text{from (1.32)} \tag{2.5}$$

Alternatively we may use the sum of (2.3) and (2.4)

$$n\ \rho_w \frac{\partial u}{\partial t} + (1 - n)\rho_s \frac{\partial v}{\partial t} = \frac{\partial \sigma}{\partial x} - \frac{\partial p}{\partial x} \tag{2.6}$$

instead of (2.4).

2.1 Exact Solution for Harmonic Motion

Assume that forcing is applied to the fluid and to the solid at the top of a layer. The boundary conditions are:

$$p = P_o e^{-i\omega t}\ , \qquad \sigma = \sigma_o e^{-i\omega t}\ , \qquad x = L \tag{2.7.a-b}$$

$$u = 0, \qquad v = 0, \qquad x = 0 \tag{2.8.a-b}$$

We shall construct the solution by superposing propagating waves of the type:

$$\begin{bmatrix} u \\ v \\ p \\ \sigma \end{bmatrix} = \begin{bmatrix} U \\ V \\ P \\ \Sigma \end{bmatrix} e^{-i(\frac{\omega}{c} x + \omega t)} \tag{2.9}$$

Substituting into (2.2) to (2.6), a set of homogeneous algebraic equations is obtained for U, V, P and Σ

$$(-n \rho_w i\omega + \frac{n^2}{k})U + (-\frac{n^2}{k})V + (-n \frac{i\omega}{c})P + (0)\Sigma = 0$$

$$(-\frac{n^2}{k})U + [\frac{n^2}{k} - (1 - n)\rho_s i\omega]V + [-(1 - n)\frac{i\omega}{c}]P + (\frac{i\omega}{c})\Sigma = 0$$

$$(0)U + (-\frac{i\omega}{c})V + (0)P + (\frac{i\omega}{E})\Sigma = 0$$

$$(n \frac{i\omega}{c})U + [(1 - n)\frac{i\omega}{c}]V + (\frac{n}{\beta} i\omega)P + (0)\Sigma = 0 \tag{2.10.a-d}$$

For nontrivial solution the coefficient determinant must vanish, leading to a quadratic equation for c^2

$$Qc^4 - Sc^2 + 1 = 0 \tag{2.11}$$

where

$$Q = \frac{-n}{i\omega k}(Q_o - i\mu Q_1); \quad S = \frac{-n}{i\omega k}(S_o - i\mu S_1)$$

$$Q_o = \frac{n\rho_w + (1 - n)\rho_s}{\beta E}; \quad S_o = \frac{\beta + nE}{n\beta E}$$

$$Q_1 = \frac{(1 - n)\rho_s}{n\beta E}; \quad S_1 = \frac{(1 - n)\rho_s \beta/\rho_w + nE}{n^2 \beta E} \tag{2.12}$$

$$\mu = \rho_w \omega k$$

the exact solutions are

$$c = \pm c_1, \text{ and } \pm c_2 \tag{2.13.a}$$

where

$$\begin{Bmatrix} c_1 \\ c_2 \end{Bmatrix} = [[S \pm (S^2 - 4Q)^{1/2}]/2Q]^{1/2} \tag{2.13.b}$$

In practice, the non-dimensional parameter $\mu \equiv \rho_w \omega k = 10^{-6} \sim 10^{-4}$ is nearly always small, we may approxmate c^2 by

$$c^2 = \frac{S_o}{2Q_o}(1 \pm 1) - \frac{S_o}{2Q_o} i\mu\{(1 \pm 1)(\frac{S_1}{S_o} - \frac{Q_1}{Q_o}) \mp \frac{2Q_o}{S_o^2 n\rho_w}\} + O(\mu^2) \tag{2.14}$$

To the leading order

$$c_1 = \left(\frac{\beta/n + E}{n\rho_w + (1-n)\rho_s} \right)^{1/2} [1 + O(\mu)] \tag{2.15.a}$$

and

$$c_2 = \frac{1-i}{\sqrt{2}} \left(\frac{\omega k \beta E}{\beta + nE}\right)^{1/2} [1 + O(\mu)] \tag{2.15.b}$$

It will be assumed for generality that $\beta/E = O(1)$. Although in fully saturated water without air content, $\beta \simeq 10^9$ (N/m^2) >> $E = 10^7$ (N/m^2) and further simplification is possible.

Thus two modes of waves are possible. Mode 1 has a real propagations speed c_1 which is of the order $\sqrt{\beta/\rho}$ or $\sqrt{E/\rho}$. Mode 2 has a complex propagation speed; the real part is $O(\mu)^{1/2}$ and has an attenuation distance $O(\frac{kE}{\omega})^{1/2}$ of the order

$$\delta = O(|c_2|/\omega) \quad = O[k\beta E/\omega(\beta+nE)]^{1/2} \tag{2.16}$$

For a variety of soils and frequencies the magnitude of δ is a very small quantity compared to L or to the wavelength of Mode 1 (see Table 1 later on p. 28). The results corresponding to (2.15) have been found by Biot.

Returning now to the finite layer, to each of the four possible values of c: $\pm c_1$ and $\pm c_2$, there is a propagating wave mode. We now

construct a general solution by superposition of these modes:

$$\begin{bmatrix} u \\ v \\ p \\ \sigma \end{bmatrix} = e^{-i\omega t} \begin{bmatrix} U_1 & U_2 & U_3 & U_4 \\ V_1 & V_2 & V_3 & V_4 \\ P_1 & P_2 & P_3 & P_4 \\ \Sigma_1 & \Sigma_2 & \Sigma_3 & \Sigma_4 \end{bmatrix} \begin{bmatrix} e^{-i\omega x/c_1} \\ e^{+i\omega x/c_1} \\ e^{-i\omega x/c_2} \\ e^{i\omega x/c_2} \end{bmatrix} \tag{2.17}$$

Corresponding to the same index j, U_j, V_j, P_j, Σ_j are however related by Eqs. (2.10.a-d) and any three may be solved in terms of the fourth. Therefore, the sixteen coefficients can be reduced to four which are then determined from the four boundary conditions. We forego the algebra and only give the results:

$$u = i\{(\frac{\sigma_o}{E}\Gamma_2 + \frac{P_o}{\beta}\gamma_2)\frac{c_1 \sin\frac{\omega x}{c_1}}{(\gamma_1-\gamma_2)\cos\frac{\omega L}{c_1}} - (\frac{\sigma_o}{E}\Gamma_1 + \frac{P_o}{\beta}\gamma_1)\frac{c_2 \sin\frac{\omega x}{c_2}}{(\gamma_1-\gamma_2)\cos\frac{\omega L}{c_2}}\}e^{-i\omega t}$$

$$v = i\{\gamma_1(\frac{\sigma_o}{E}\Gamma_2 + \frac{P_o}{\beta}\gamma_2)\frac{c_1 \sin\frac{\omega x}{c_1}}{(\gamma_1-\gamma_2)\cos\frac{\omega L}{c_1}} - \gamma_2(\frac{\sigma_o}{E}\Gamma_1 + \frac{P_o}{\beta}\gamma_1)\frac{c_2 \sin\frac{\omega x}{c_2}}{(\gamma_1-\gamma_2)\cos\frac{\omega L}{c_2}}\}e^{-i\omega t}$$

$$p = \{-(\frac{\sigma_o\beta}{E}\Gamma_2 + P_o\gamma_2)\frac{\Gamma_1 \cos\frac{\omega x}{c_1}}{(\gamma_1-\gamma_2)\cos\frac{\omega L}{c_1}} + (\frac{\sigma_o\beta}{E}\Gamma_1 + P_o\gamma_1)\frac{\Gamma_2 \cos\frac{\omega x}{c_2}}{(\gamma_1-\gamma_2)\cos\frac{\omega L}{c_2}}\}e^{-i\omega t}$$

$$\sigma = \{(\sigma_o\Gamma_2 + \frac{P_oE}{\beta}\gamma_2)\frac{\gamma_1 \cos\frac{\omega x}{c_1}}{(\gamma_1-\gamma_2)\cos\frac{\omega L}{c_1}} - (\sigma_o\Gamma_1 + \frac{P_oE}{\beta}\gamma_1)\frac{\gamma_2 \cos\frac{\omega x}{c_2}}{(\gamma_1-\gamma_2)\cos\frac{\omega L}{c_2}}\}e^{-i\omega t}$$

(2.18.a-d)

where

$$\Gamma_i = 1 + \frac{1-n}{n}\gamma_i \quad ; \quad i = 1,2 \tag{2.19.a}$$

and

$$\gamma = \frac{\frac{in}{k} - \beta \frac{\omega}{c^2} + \rho_w \omega}{\frac{in}{k} + \frac{1-n}{n} \beta \frac{\omega}{c^2}} \qquad \begin{matrix} \gamma_1 = \gamma(c_1) \\ \gamma_2 = \gamma(c_2) \end{matrix} \tag{2.19.b}$$

with c_1 and c_2 given by (2.13b)

Many physical features can of course be deduced from (2.18), particularly for the practical case of small $\rho_w \omega k$. By using the approximate expressions for c_1 and c_2 in Eq. (2.15), we see that all results contain two parts. The first part varies over a very long scale c_1/ω. Because $\gamma_1 \cong 1$, the corresponding u and v are approximately the same. The second part vanishes exponentially when $|x - L| >> |c_2|/\omega$ which is a very short distance from the free surface. The corresponding u is different from v, implying friction between fluid and solid. This picture is certainly reasonable from an intuitive point of view, since for small k only near the free surface can the fluid be squeezed in and out. Deep within the porous layer, the resistance is so large that fluid and solid must move together as a composite material. It may be shown that

$$\gamma_2 \cong \frac{-\beta}{nE} \left[1 - (1 - \frac{1}{n}) \frac{\beta + nE}{nE}\right]^{-1} \tag{2.20}$$

so that (2.18.a-d) are now much simplified by neglecting $0(\rho_w \omega k)$. In particular, the total stress τ is given, from (2.18.c,d) by:

$$\tau = \tau_o \frac{\cos \frac{\omega x}{c_1}}{\cos \frac{\omega L}{c_1}} \quad ; \qquad \tau_o = \sigma_o - P_o \tag{2.21}$$

It is interesting to note that τ does not contain two parts as in (2.18), but only one, having a length scale $0(c_1/\omega)$, with no dependence on c_2.

Also, from (2.18.c)

$$p = \frac{-\tau_o \beta}{\beta+nE} \frac{\cos \frac{\omega x}{c_1}}{\cos \frac{\omega L}{c_1}} + \frac{\sigma_o \beta + P_o nE}{\beta+nE} e^{-i(x-L)\omega/c_2} \qquad (2.21.a)$$

The exponential may also be written as

$$\exp\left[\frac{1-i}{\sqrt{2}} \frac{\omega(x-L)}{|c_2|} \right]$$

Both (2.21) and (2.21.a) will be used for comparison later.

2.2 Boundary Layer Analysis

Guided by the observations from the exact solutions, we now seek an alternate approximate method to tackle the case of small permeability *directly*. The approach is to introduce first the dimensionless outer variables by the following transformation,

$$\begin{bmatrix} u^o \\ v^o \end{bmatrix} = \frac{\sigma_o \omega L}{\beta} \begin{bmatrix} \tilde{u} \\ \tilde{v} \end{bmatrix} \quad , \quad \begin{bmatrix} p^o \\ \sigma^o \end{bmatrix} = \sigma_o \begin{bmatrix} \tilde{p} \\ \tilde{\sigma} \end{bmatrix}$$

$$x = L\tilde{x} \qquad t = \tilde{t}/\omega \qquad (2.22)$$

where the variables on the right are dimensionless, and those on the left are physical. The outer solution will be sought to the leading order, which will not be capable of satisfying certain boundary conditions. A boundary layer correction is then added as a remedy.

Substituting (2.22) into (2.2), (2.3), (2.5) and (2.6) in succession, we have in dimensionless form:

$$\tilde{v}_{\tilde{x}} = (\beta/E)\tilde{\sigma}_{\tilde{t}} \qquad (2.23)$$

$$\frac{\rho_w \omega k}{n} \tilde{u}_{\tilde{t}} = - \frac{k\beta}{n\omega L^2} \tilde{p}_{\tilde{x}} - (\tilde{u} - \tilde{v}) \tag{2.24}$$

$$n(\tilde{u} - \tilde{v})_{\tilde{x}} + \tilde{v}_{\tilde{x}} = -n\tilde{p}_{\tilde{t}} \tag{2.25}$$

$$\frac{\omega^2 L^2}{\beta} [n\rho_w \tilde{u}_{\tilde{t}} + (1 - n)\rho_s \tilde{v}_{\tilde{t}}] = \tilde{\sigma}_{\tilde{x}} - \tilde{p}_{\tilde{x}} \tag{2.26}$$

For small $\rho_w \omega k$ the leading approximation of (2.24) is clearly

$$\tilde{u} = \tilde{v} \tag{2.27}$$

Thus the fluid and solid move together in most of the physical region, as was found earlier. As an immediate consequence, the apparent inertia is justifiably omitted in the outer region since it is non-zero only when there is a relative motion between solid and fluid. Furthermore, it follows from (2.25) and (2.23) that

$$\tilde{p} = - \frac{\beta}{nE} \tilde{\sigma} \tag{2.28}$$

Eliminating $\tilde{p}$, $\tilde{\sigma}$, and $\tilde{v}$ between (2.25) and (2.26) we get

$$\tilde{u}_{\tilde{x}\tilde{x}} = \frac{\omega^2 L[n\rho_w + (1-n)\rho_s]}{E + \beta/n} \tilde{u}_{\tilde{t}\tilde{t}} \tag{2.29}$$

which can be expressed in physical variables

$$u^o_{xx} = \frac{1}{c_1^2} u^o_{tt} \tag{2.30}$$

where c_1 is given by the approximate formula 2.15.a.

For harmonic motion the solution which satisfies the bottom conditions must be, in physical variables

$$u^o = v^o = \frac{inc_1}{\beta} B \sin \frac{\omega x}{c_1} e^{-i\omega t} \tag{2.31.a}$$

$$\begin{pmatrix} p^o \\ \sigma^o \end{pmatrix} = \begin{pmatrix} 1 \\ -\frac{nE}{\beta} \end{pmatrix} B \cos \frac{\omega x}{c_1} \qquad e^{-i\omega t} \tag{2.31.b}$$

Clearly the boundary conditions (2.7) on the free surface cannot yet be satisfied.

Let us denote by u^b, v^b, p^b and σ^b the corrections in the boundary layer, to be added to the outer solutions u^o, v^o, p^o and σ^o for the total solution which would be valid everywhere. Let the boundary layer length scale be δ whose magnitude is to be decided. The normalized variables are as follows

$$\begin{pmatrix} u^b \\ v^b \end{pmatrix} = \frac{\sigma_o \omega \delta}{\beta} \begin{pmatrix} \hat{u} \\ \hat{v} \end{pmatrix} \quad , \quad \begin{pmatrix} p^b \\ \sigma^b \end{pmatrix} = \sigma_o \begin{pmatrix} \hat{p} \\ \hat{\sigma} \end{pmatrix} \tag{2.32}$$

$$(x - L) = \delta X \qquad t = T/\omega$$

Note that the boundary layer velocities are of $0(\delta)$ compared to the outer solution in order that the strains are comparable.

The dimensionless versions of (2.2), (2.3), (2.5) and (2.6) are

$$\hat{v}_X = \frac{\beta}{E} \hat{\sigma}_T \tag{2.33}$$

$$\frac{\rho_w \omega k}{n} \hat{u}_T = -\frac{1}{n} \frac{\beta k}{\omega \delta^2} \hat{p}_X - (\hat{u} - \hat{v}) \tag{2.34}$$

$$\frac{\omega^2 \delta^2}{\beta} [n\rho_w \hat{u}_T + (1-n)\rho_s \hat{v}_T] = \hat{\sigma}_X - \hat{p}_X \tag{2.35}$$

$$(\hat{u} - \hat{v})_X + \frac{1}{n} \hat{v}_X = -\hat{p}_T \tag{2.36}$$

For small k it is clear from (2.34) that we must choose $\delta = 0(\beta k/\omega)^{1/2}$ to have a distinguishing limit. Consequently, to the leading order

$$-\frac{1}{n}\frac{\beta k}{\omega\delta^2}\hat{p}_X = \hat{u} - \hat{v} \tag{2.37}$$

Thus the static form of Darcy's law is in effect. Eq. (2.35) becomes

$$\hat{p} = \hat{\sigma} \tag{2.38}$$

implying that the boundary layer correction of the total stress $\hat{\sigma} - \hat{p}$ is zero. An important consequence of this is that the constant B in (2.31) can be found immediately by applying the condition:

$$\sigma - p = \tau = \tau_o \qquad \text{at} \qquad x = L$$

on (2.31) to obtain

$$B = \frac{-\beta\ \tau_o}{(nE + \beta)\ \cos\ (\frac{\omega L}{c_1})} \tag{2.31.c}$$

which confirms (2.21). Hence, the outer solution can be completely found in advance of the boundary layer analysis, which is needed now to obtain the solution within the boundary layer region.

The remaining equations (2.33) and (2.36) retain their forms, but can be used with (2.37) and (2.38) to get a single equation

$$\hat{p}_{XX} - \delta^2\omega\frac{\beta+nE}{kE\beta}\hat{p}_T = 0 \tag{2.39}$$

which is a heat equation; its physical form is

$$p^b_{xx} = \frac{\beta+nE}{kE\beta}p^b_t \tag{2.40}$$

Since all inertia terms are negligible in this approximation, it means in particular that apparent inertia is negligible in the boundary layer as well as outside. Eq. (2.40) is also the Terzaghi equation for one-

dimensional consolidation. Indeed, since the only time scale is the consolidation (diffusion) time in such problems, the entire soil depth is the boundary layer.

For harmonic motion the boundary layer structure is the same as Stokes layer in the viscous fluid. The thickness of the layer is clearly

$$\delta = \left[\frac{kE\beta}{\omega(\beta+nE)}\right]^{1/2} = \frac{|c_2|}{\omega} \tag{2.41}$$

where c_2 is the approximation given by (2.15.b). The solution is easily found to be, in physical variables

$$\left.\begin{aligned} p^b = \sigma^b &= A\, e^{-i\omega(x-L)/c_2} \\ \begin{pmatrix} u^b \\ v^b \end{pmatrix} &= \begin{pmatrix} \frac{1-n}{n} c_2 \\ 1 \end{pmatrix} \frac{A}{E} e^{-i\omega(x-L)/c_2} \end{aligned}\right\} e^{-i\omega t} \tag{2.42}$$

We now use the sum of Eq. (2.31) and (2.42) to satisfy the remaining boundary condition at x = L.

$$p^o + p^b = B \cos\frac{\omega L}{c_1} + A = P_o \tag{2.43}$$

or

$$\sigma^o + \sigma^b = -\frac{nE}{\beta} B \cos\frac{\omega L}{c_1} + A = \sigma_o \tag{2.44}$$

with B given by (2.31.c). The coefficient A is thus given by

$$A = \frac{(P_o nE + \sigma_o \beta)}{nE+\beta} \tag{2.45}$$

Inserting these results in (2.31) and (2.42), the total pore pressure inside the boundary layer is the same as (2.21.a). Similar agreement may be shown for u, v and σ.

Note that if $\sigma_o = 0$ but $P_o \neq 0$ and if the fluid is highly incompressible so that $E/\beta \ll 1$, then $A \simeq 0$ and there is essentially no boundary layer near the surface.

As an application we remark that the special case of $\sigma_o = 0$ in (2.7.b) is relevant to the one-dimensional microseism in a poro-elastic layer if

$$P_o = -\frac{\rho_w}{8} A_o^2 \omega^2 \tag{2.46}$$

It is known (Longuet-Higgins, 1950) that a standing sea wave of amplitude A_o and frequency $\omega/2$ can induce a second order pressure given by (2.46) which is spatially uniform and remains appreciable far beneath the sea surface. The theory of this section will give the forced response in a finite solid layer. Resonance is expected near $\omega L/c_1 = (n + \frac{1}{2})\pi$. Very near resonance, the boundary layer approximation is inadequate and the full solution (2.18) in which c_1 is complex is needed. In reality the elasticity of the layer beneath further introduces radiation damping and limits the resonance peak.

As an additional example, we add the solution for the one-dimensional problem due to seismic excitation at x = 0, while the top boundary is stress-free, i.e.,

$$\begin{aligned} u = v &= U_o\, e^{-i\omega t} && x = 0 \\ p = \sigma &= 0 && x = L \end{aligned} \tag{2.47}$$

The exact solution is

$$p = -\frac{\beta}{nc_1}\sigma \tag{2.48}$$

$$\sigma = U_o \frac{E}{c} \frac{e^{-i\omega L/c_1}}{\cos \frac{\omega L}{c_1}} \left(\cos \frac{\omega x}{c_1} - \cos \frac{\omega L}{c_1}\right) e^{-i\omega t} \tag{2.49}$$

with c_1 given by (2.13). Interestingly there is no boundary layer. If one applies the approximate method then the outer solution dominates the entire layer, and is also given by (2.48) and (2.49) except that c_1 is given by (2.15.a).

2.3 Numerical Results for Microseism due to Standing Sea Waves

In all numerical examples of this study the following soil properties are chosen:

$$\rho_w = 10^3 \text{ Kg/m}^3 \quad , \quad \rho_s = 2.7 \times 10^3 \text{ Kg/m}^3 \quad , \quad n = 0.3 \quad , \quad \text{and}$$

$$\nu = 0.333.$$

Figure 2.1 gives the response for $\frac{G}{\beta} = 0.0044$ when there is no air in pore water and $G = 10^7$ N/m^2. (The corresponding E is 2.7×10^7 N/m^2.) The depth of the layer is 25 m while $T = 2\pi/\omega = 5$ sec. The value of $\omega L/c_1$ is 0.75 which is not resonant. For such a large fluid bulk modulus, the load is entirely taken up by water. Also shown are the responses for $G/\beta = 1$ and $G = 10^6$ N/m^2. For fine sand (solid curve) the boundary layer is very thin, otherwise p and σ vary weakly in depth. For coarse sand the depth dependence is very large. For both sands, fluid and solid share the load quite evenly.

Figure 2.2 gives the response near the first resonances for $G = \beta = 10^6$ N/sec in depth L = 65 m for $T = 2\pi/\omega = 5$ sec. The corresponding $\omega L/c_1$ is 1.8. Maximum amplification is attained at the bottom. In this near-resonant case, the outer solution dominates so that the effect of permeability k is weak and the curves apply for both coarse and fine

sands.

For the same $G = \beta = 10^6$ N/sec^2 and L = 65 m, the pressure at the bottom is plotted in Figure 2.3 showing the first resonant peak. Being far from the free surface the outer solution dominates and the dependence on permeability is weak, and cannot be shown. The peak amplification is very high $\sim O(10^3)$ and may be estimated from (2.18) by standard arguments.

We have also calculated the cases ($\sigma_o \neq 0$, $P_o \neq 0$, $U_o = 0$) and ($\sigma_o = P_o = 0$, $U_o \neq 0$). The results are quite similar except for the details near the boundaries, hence are not presented here.

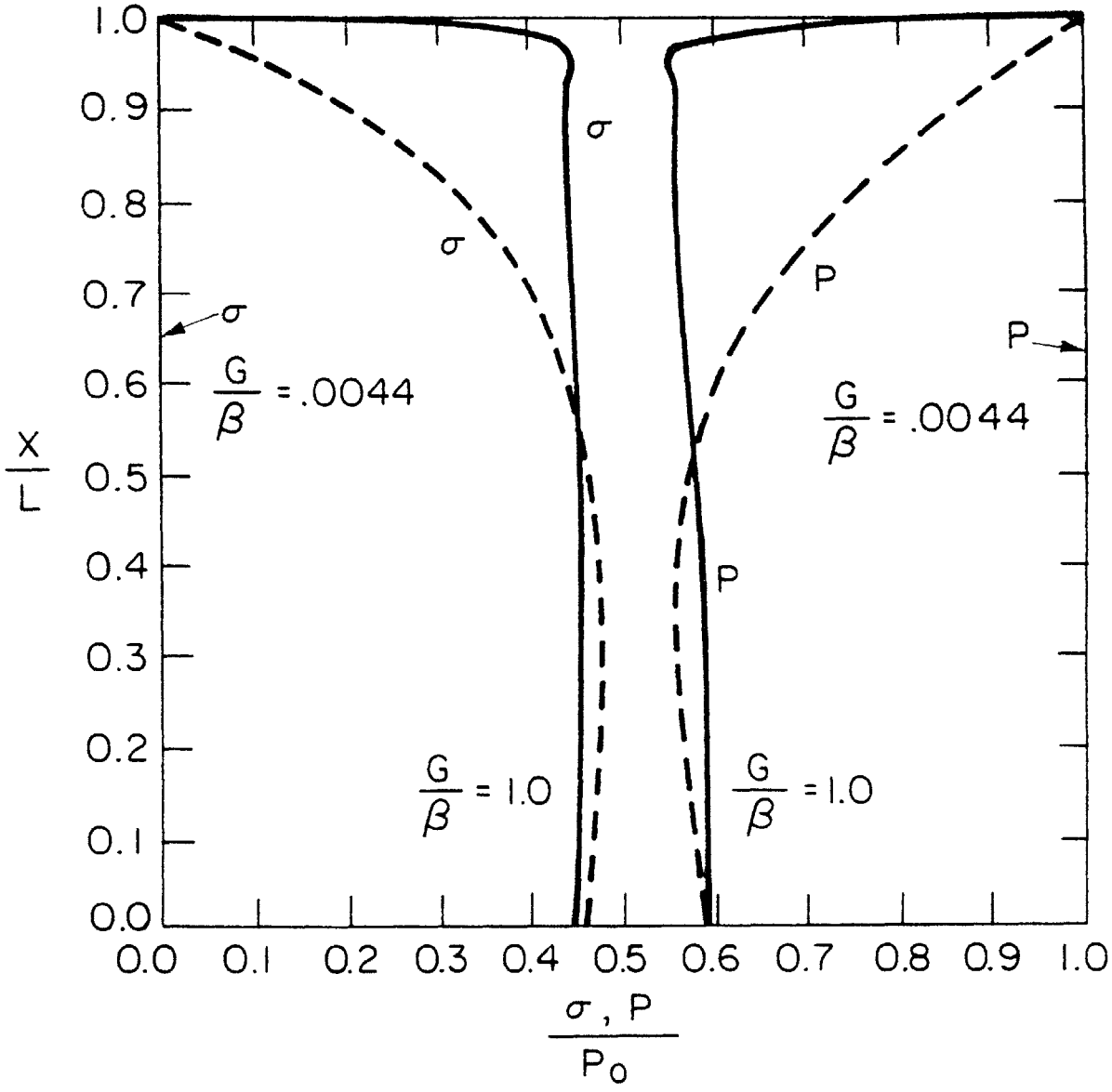

Figure (2.1)

Non-resonant response at $\omega L/c_1 = 0.75$ of one-dimensional microseism in 25 ms deep poro-elastic layer. The dimensionless pressure p/P_o and effective stress $/P_o$ are shown for fine sand _____, $k=10^{-8}$ m^3sec/kg; and coarse sand ------, $k=10^{-6}$ m^3sec/kg. For each sand, $G/\beta = .0044$ and 1 ($G=10^7 N/m^2$).

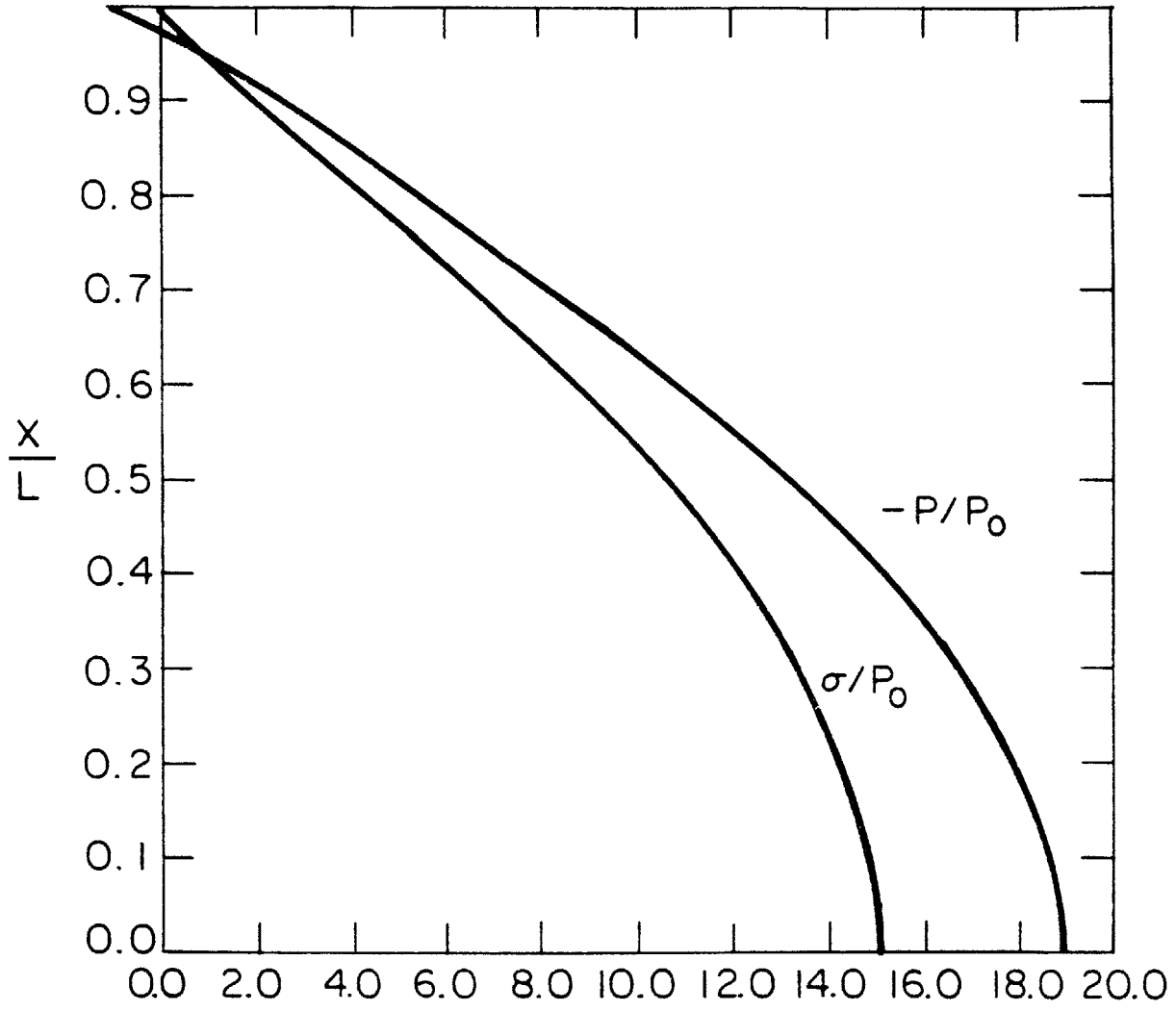

Figure (2.2)

Near resonant response ($\omega L/c_1 = 1.8$) for one-dimensional microseism in a 65 ms deep pror-elastic layer. $G=\beta=10^6$ N/m^2. Effect of permeability is negligible here so that the shown curves apply for both fine and coarse sand except for slight differences near the free surface.

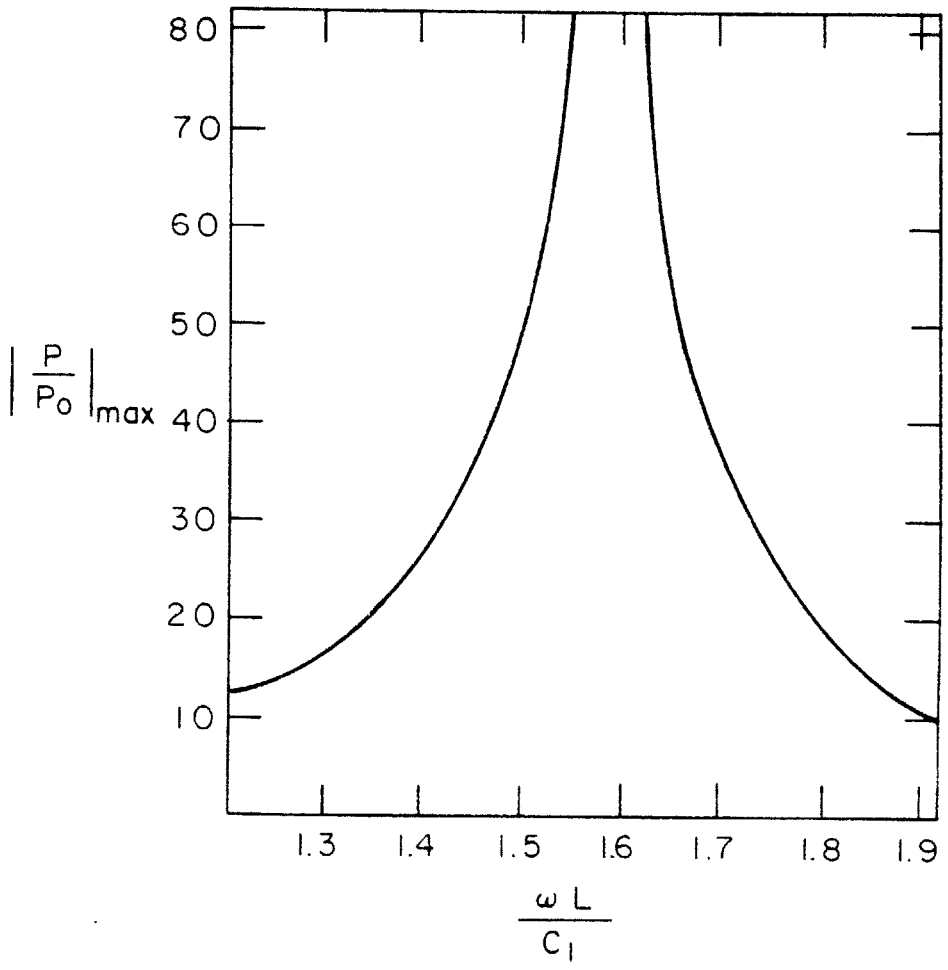

Figure (2.3)

Dynamic pressure amplitude at the layer bottom vs. frequency showing the first resonant peak, for the same soil properties as in Figure 2.2.

3. APPROXIMATIONS FOR TWO- OR THREE-DIMENSIONAL PROBLEMS IN A HORIZONTAL LAYER

Adding (1.30) and (1.31) and using Hookes Law (1.18) we get

$$G(\nabla^2\vec{v} + \frac{1}{1-2\nu}\nabla\nabla\cdot\vec{v}) - \nabla p_t = n\rho_w \vec{u}_{tt} + (1-n)\rho_s \vec{v}_{tt} \tag{3.1}$$

Also u - v may be eliminated from (1.31) and (1.32) to give

$$k\nabla^2 p = \nabla\cdot\vec{v} + \frac{n}{\beta} p_t - k\rho_w(\nabla\cdot\vec{u})_t \tag{3.2}$$

We now split the stress field into the outer solution and the boundary layer correction, i.e.,

$$( ) = ( )^o + ( )^b \tag{3.3}$$

3.1 The Outer Problem

The following variables will be introduced:

$$x_i = L\xi_i \qquad t = \tau/\omega \tag{3.4}$$

$$\begin{pmatrix} u_i^o \\ v_i^o \end{pmatrix} = \frac{P_o \omega L}{G} \begin{pmatrix} \tilde{u}_i \\ \tilde{v}_i \end{pmatrix}, \quad \begin{pmatrix} p^o \\ \sigma_{ij}^o \end{pmatrix} = P_o \begin{pmatrix} \tilde{p} \\ \tilde{\sigma}_{ij} \end{pmatrix} \tag{3.5}$$

Substituting into Eqs. (1.19), (1.32), (1.31) and (1.30), we have

$$\frac{\partial \tilde{v}_i}{\partial \xi_j} + \frac{\partial \tilde{v}_j}{\partial \xi_i} = \frac{\partial \tilde{\sigma}_{ij}}{\partial \tau} - \frac{\nu}{1+\nu}\delta_{ij}\frac{\partial \tilde{\sigma}_{kk}}{\partial \tau} \tag{3.6}$$

$$n\frac{\partial}{\partial \xi_j}(\tilde{u}_j - \tilde{v}_j) + \frac{\partial \tilde{v}_j}{\partial \xi_j} = -\frac{nG}{\beta}\frac{\partial \tilde{p}}{\partial \tau} \tag{3.7}$$

$$\rho_w \frac{\omega^2 L^2}{G} n \frac{\partial \tilde{u}_i}{\partial \tau} = -n\frac{\partial \tilde{p}}{\partial \xi_i} - \frac{n^2 \omega L^2}{Gk}(\tilde{u}_i - \tilde{v}_i) \tag{3.8}$$

$$\frac{\rho_s \omega^2 L^2}{G}(1-n)\frac{\partial \tilde{v}_i}{\partial \tau} = \frac{\partial \tilde{\sigma}_{ij}}{\partial \xi_j} - (1-n)\frac{\partial \tilde{p}}{\partial \xi_i} + \frac{n^2 \omega L^2}{Gk}(\tilde{u}_i - \tilde{v}_i) \tag{3.9}$$

The dimensionless forms of (3.1) and (3.2) are

$$\nabla^2\vec{v} + \frac{1}{1-2\nu}\nabla(\nabla\cdot\vec{v}) - \nabla\frac{\partial\tilde{p}}{\partial\tau} = \frac{\rho_w\omega^2L^2}{G}\,n\,\frac{\partial^2\vec{u}}{\partial\tau^2} + \frac{\rho_s\omega^2L^2}{G}\,(1-n)\,\frac{\partial^2\vec{v}}{\partial\tau^2} \qquad (3.10)$$

$$\nabla^2\tilde{p} = \frac{\omega L^2}{Gk}\nabla\cdot\vec{v} + \frac{\omega L^2}{\beta k}\,n\,\frac{\partial\tilde{p}}{\partial\tau} - \frac{\rho_w\omega^2L^2}{G}\,\frac{\partial}{\partial\tau}(\nabla\cdot\vec{u}) \qquad (3.11)$$

where $(\nabla)_i = \partial/\partial\xi_i$ in the outer problem.

Again we leave G/β to be arbitrary, i.e., $O(1)$. There are still two dimensionless parameters

$$\frac{\rho_w\omega^2L^2}{G} = \frac{L^2}{\ell^2} \qquad n\frac{\omega L^2}{Gk} = \frac{L^2}{\delta^2}$$

where $O(\ell)$ is the wavelength of the shear wave and $(Gk/\omega)^{1/2}$ will be shown to be the order of the boundary layer thickness. There are at least two cases which are of practical interest.

(a) *Excitation by seismic waves:* Here the frequency is $O(\omega) = 10$ rad/sec and if there is no other physical length so that $L = \ell$, $= O(100\sim500$ m), only one parameter remains. From Table 1 on p. 28 which summarizes the properties of a variety of soils, we find $n\omega L^2/Gk \gg 1$ for most ground materials. The response of the ground, especially near the free surface, to seismic excitation is of obvious interest. While Eqs. (3.6) and (3.7) remain the same, Eq. (3.8) may be simplified to

$$\vec{u} = \vec{v} \qquad (3.12)$$

Thus the fluid and solid again move as a whole and apparent inertia is unimportant. Using this fact we get further

$$\nabla^2\vec{v} + \frac{1}{1-2\nu}\nabla(\nabla\cdot\vec{v}) - \nabla\frac{\partial\tilde{p}}{\partial\tau} = \frac{\omega^2L^2}{G}\,[n\rho_w + (1-n)\rho_s]\frac{\partial^2\vec{v}}{\partial\tau^2} \qquad (3.13)$$

and

$$\nabla\cdot\vec{v} + \frac{nG}{\beta}\frac{\partial\tilde{p}}{\partial\tau} = 0 \qquad (3.14)$$

which means physically that dilation of the solid matrix is responsible for the pore pressure and vice versa. Let us decompose $\vec{v}$ into an irrotational part and a solenoidal part

$$\vec{v} = \nabla\tilde{\phi} + \vec{v}_s \qquad \text{with} \qquad \nabla\cdot\vec{v}_s = 0 \tag{3.15}$$

Eq. (3.14) then gives

$$\nabla^2\tilde{\phi} + \frac{nG}{\beta}\frac{\partial\tilde{p}}{\partial\tau} = 0 \tag{3.16}$$

Taking the divergence of (3.13) and using (3.16) we get

$$\nabla^2\left(\frac{\partial\tilde{p}}{\partial\tau}\right) = \frac{\omega^2L^2[n\rho_w + (1-n)\rho_s]}{\frac{2(1-\nu)}{1-2\nu}G + \frac{\beta}{n}}\frac{\partial^2}{\partial\tau^2}\frac{\partial\tilde{p}}{\partial\tau} \tag{3.17}$$

By virtue of (3.16) one may replace $\partial\tilde{p}/\partial\tau$ by $\nabla^2\tilde{\phi} = \nabla\cdot\vec{v}$ in the equation above. Taking the curl of (3.13) and defining

$$\vec{\Omega} = \nabla \times \vec{v} = \nabla \times \vec{v}_s \tag{3.18}$$

we get

$$\nabla^2\vec{\Omega} = \frac{\omega^2L^2}{G}[n\rho_w + (1-n)\rho_s]\frac{\partial^2\vec{\Omega}}{\partial\tau^2} \tag{3.19}$$

Eqs. (3.17) and (3.19) suggest the introduction of an effective density

$$\rho_e = n\rho_w + (1-n)\rho_s \tag{3.20.a}$$

and an effective Lamé constant

$$\lambda_e = \lambda + \frac{\beta}{n} = \frac{2\nu G}{1-2\nu} + \frac{\beta}{n} \tag{3.20.b}$$

The corresponding effective Poisson's ratio is

$$\nu_e = \frac{\lambda_e}{G} \Big/ 2\left(1 + \frac{\lambda_e}{G}\right)$$

$$= \left(\frac{2\nu}{1-2\nu} + \frac{\beta}{nG}\right) \Big/ 2\left(\frac{1}{1-2\nu} + \frac{\beta}{nG}\right) \qquad (3.20.c)$$

which is plotted against ν and β/nG in Figure 3.1. Eq. (3.17) implies the speed of the compression waves to be

$$c_p^2 = (\lambda_e + 2G)/\rho_e \qquad (3.21.a)$$

while Eq. (3.19) implies the speed of the shear waves to be

$$c_s^2 = G/\rho_e \qquad (3.21.b)$$

Thus the outer problem is essentially reduced to the usual elastodynamics with the wave speeds depending on the fluid and solid properties and the void ratio.

(b) *Excitation by gravity waves in the sea:* Consider the porous medium to be the bottom of the sea. As offshore structures or pipelines are sometimes installed in depths of 30 m or more, gravity waves within the frequency range $\omega \cong 0.5 \sim 1$ rad/sec can either generate sufficient pressure directly at the sea bottom, or excite the sea bed indirectly through the bottom-seated structure, thereby inducing pore pressure and stresses in the sea bed. The imposed length scale L can either be the gravity wavelength, i.e., $50 \sim 200$ m or the lateral dimension of the structure which is assumed to be O(50) m. The ratio $n\omega L^2/Gk$ can still be much greater than one even for coarse sand. Thus there are ample opportunities for (3.12) to hold; and this is assumed. The shear wave speed in the sea bed lies within the range $150 \sim 500$ m/sec, thus the wave length ℓ is $1000 \sim 5000$ m, hence $L^2/\ell^2 \ll 1$. As an immediate consequence, the inertia term on the right of (3.13)

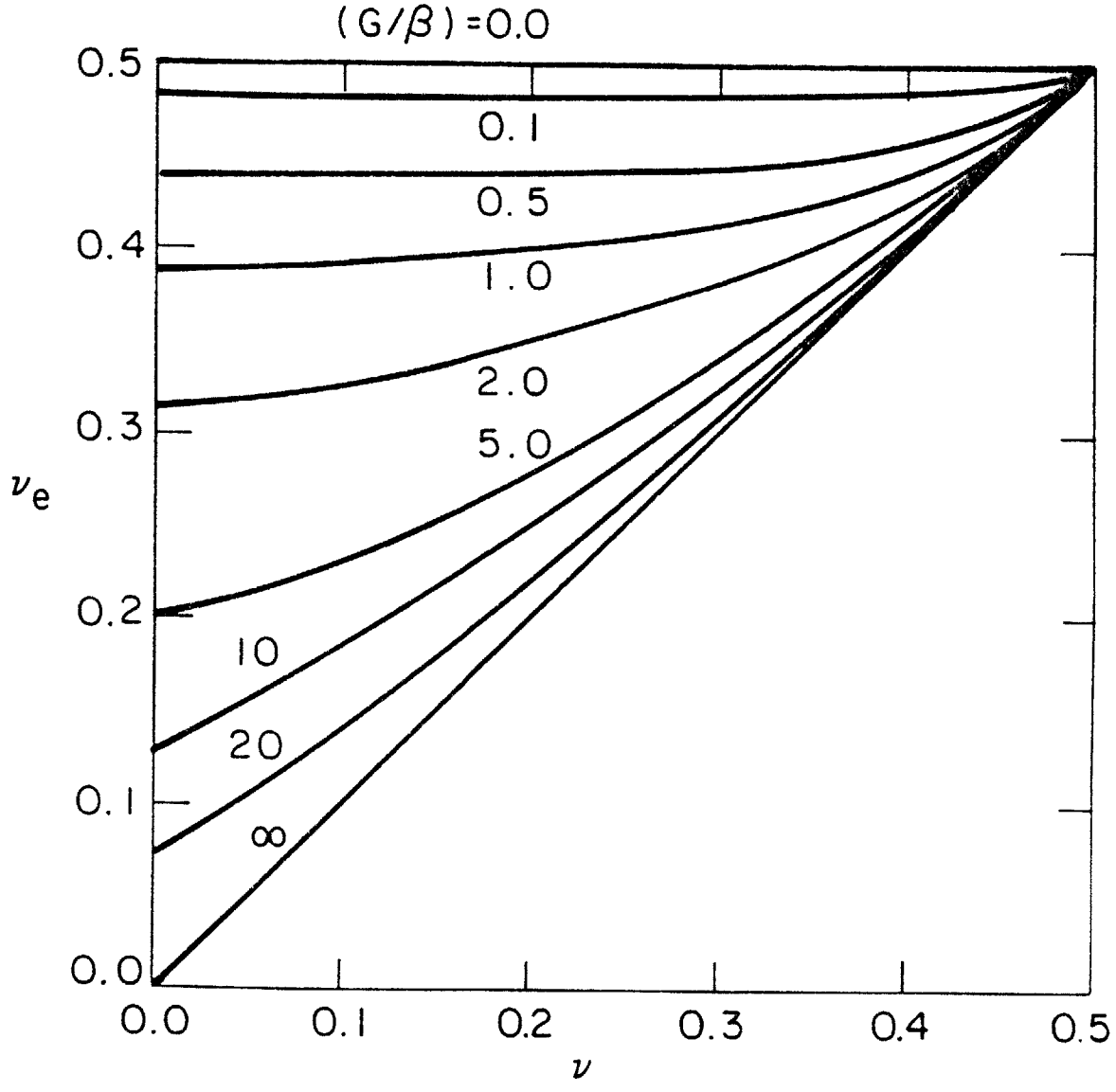

Figure (3.1)

Effective Poisson's ratio ν_e against the soil's actual Poisson's ratio ν and G/β.

can be neglected

$$\nabla^2 \vec{\tilde{v}} + \frac{1}{1-2\nu} \nabla(\nabla \cdot \vec{\tilde{v}}) - \nabla \frac{\partial \tilde{p}}{\partial \tau} \cong 0 \tag{3.22}$$

But this is just the elastostatic equation with a "body force" whose potential is $\frac{\partial \tilde{p}}{\partial \tau}$. Upon taking the divergence and using (3.14) we further obtain

$$\frac{\partial}{\partial \tau} \nabla^2 \tilde{p} \cong 0 \tag{3.23}$$

thus the "body force" potential is harmonic. Alternatively we may add (3.8) and (3.9) and ignore the inertia terms to get

$$\frac{\partial \tilde{\sigma}_{ij}}{\partial \xi_j} = \frac{\partial \tilde{p}}{\partial \xi_i} \tag{3.24}$$

This result can also be deduced by combining (1.30) and (1.31) after ignoring the inertia term in each.

In general, i.e., for both seismic and gravity waves, the outer pore pressure is not independent of the effective stress field because of (3.14). From (3.6) we get by tensor contraction

$$2\nabla \cdot \vec{\tilde{v}} = \frac{(1-2\nu)}{1+\nu} \frac{\partial \tilde{\sigma}_{kk}}{\partial \tau} \tag{3.25}$$

It follows from (3.14) that

$$\tilde{\sigma}_{kk} = - \frac{2(1+\nu)}{1-2\nu} \frac{nG}{\beta} \tilde{p} \tag{3.26}$$

For later use it is convient to introduce the total outer stress by

$$\tilde{\tau}_{ij} = \tilde{\sigma}_{ij} - \tilde{p}\, \delta_{ij} \tag{3.27}$$

which is related to the solid displacements $\tilde{v}_j$ by

$$\frac{\partial}{\partial\tau}\tilde{\tau}_{ij} = \left(\frac{\partial\tilde{v}_i}{\partial\xi_j} + \frac{\partial\tilde{v}_j}{\partial\xi_i}\right) + \frac{\lambda_e}{G}\delta_{ij}\frac{\partial\tilde{v}_k}{\partial\xi_k} \tag{3.28}$$

after using (1.18) and (3.26).

3.2 Boundary Layer Correction Near the Ground Surface - General Aspects

Since near the ground surface the pore fluid has greater freedom to flow in and out, there must be a relative motion between fluid and the solid skeleton. Thus there is a boundary layer within which $\frac{\partial}{\partial y} >> \frac{\partial}{\partial x}$ and $\frac{\partial}{\partial z}$. We expect p^b and the dominant part of σ^b_{ij} to be comparable in order of magnitude to similar quantities in the outer region.

Referring to Eq. (3.1) the dominant term is clearly $G\frac{\partial^{2\to b}v}{\partial y^2}$, relative to which the inertia terms are negligible, e.g.

$$(1-n)\rho_s\frac{\partial^{2\to b}v}{\partial t^2} \Big/ G\frac{\partial^{2\to b}v}{\partial y^2} \sim \rho_s\omega^2\delta^2/G \sim \delta^2/\ell^2 << 1 \tag{3.29}$$

Taking the curl of the remaining static equation we easily get

$$\nabla^2(\nabla\times\vec{v}^b) \cong \frac{\partial^2}{\partial y^2}(\nabla\times\vec{v}^b) \cong 0 \tag{3.30.a}$$

Because $\nabla \times \vec{v}^b$ vanishes identically outside the boundary layer, $|y| >> \delta$, it must be zero throughout, i.e.,

$$\nabla \times \vec{v}^b \cong 0 \tag{3.30.b}$$

Thus the boundary layer correction of the solid velocity is irrotational, which in turn implies that the horizontal velocities are much less than the vertical

$$v_i^b/v_2^b = O(\delta/L) \qquad i = 1,3 \tag{3.31}$$

Using this fact the dominant part of Eq. (3.1) becomes

$$G\left(\frac{\partial^2 v_i^b}{\partial y^2} + \frac{1}{1-2\nu} \frac{\partial^2 v_2^b}{\partial x_i \partial y} \right) - \frac{\partial^2 p^b}{\partial x_i \partial t} \cong 0 \qquad i = 1,3 \tag{3.32.a}$$

$$G\left(\frac{\partial^2 v_2^b}{\partial y^2} + \frac{1}{1-2\nu} \frac{\partial^2 v_2^b}{\partial y^2} \right) - \frac{\partial^2 p^b}{\partial y \partial t} \cong 0 \tag{3.32.b}$$

while the dominant part of Eq. (3.2) is

$$k \frac{\partial^2 p^b}{\partial y^2} = \frac{\partial v_2^b}{\partial y} + \frac{n}{\beta} \frac{\partial p^b}{\partial t} \tag{3.33}$$

where we have ignored the term $k\rho_w \frac{\partial^2 u_2^b}{\partial y \partial t}$ with an error

$$k\rho_w \frac{\partial^2 u_2^b}{\partial y \partial t} \Big/ k \frac{\partial^2 p}{\partial y^2} = O\left(\frac{u_2^b}{p_o} \delta\omega\rho_w\right) \tag{3.34}$$

For the moment the validity of such an omission is not obvious and to be further discussed.

Integrating (3.32.b) in y and noting that v_2^b, $p^b \to 0$ outside the boundary layer, we have

$$G \frac{2(1-\nu)}{1-2\nu} \frac{\partial v_2^b}{\partial y} = \frac{\partial p^b}{\partial t} \tag{3.35}$$

which may be substituted in (3.33) to get

$$k \frac{\partial^2 p^b}{\partial y^2} = \left(\frac{n}{\beta} + \frac{1}{G} \frac{1-2\nu}{2(1-\nu)}\right) \frac{\partial p^b}{\partial t} \tag{3.36}$$

which is a heat equation! Clearly the scale of the boundary layer thickness is

$$\delta = \sqrt{\frac{\overline{k}}{\omega}} \left[\frac{n}{\beta} + \frac{1}{G} \frac{1-2\nu}{2(1-\nu)}\right]^{-1/2} \tag{3.37}$$

Thus the boundary layer thickness is very small if any of the following

situations prevail, small permeability, high frequency, small bulk modulus of the pore fluid and small shear modulus in the solid. Sample values and other properties of earth materials are listed in Table 1.

Since $O(p^b) = P_o$, Eq. (3.35) implies that $v_2^b = O(P_o\omega\delta/G)$, which is small. Anticipating that $u_2^b = O(v_2^b)$ the error represented by Eq. (3.34) is $O(\rho_w\omega^2\delta^2/G) = O(\delta^2/\ell^2)$ and is legitimately ignored. The same argument also justifies the omission of apparent inertia. Finally, the horizontal displacement components v_i^b, i = 1,3 is $O(\frac{\delta}{L} v_2^b) = O(P_o\omega\delta^2/GL)$ which is even smaller than the vertical component.

We now introduce the dimensionless variables

$$x,z = L(X,Z) \ , \quad y = \delta Y \ , \quad t = T/\omega$$

$$(p^b,\sigma_{ij}^b) = P_o(\hat{p},\hat{\sigma}_{ij})$$

$$(u_i^b,v_i^b) = \frac{P_o\omega L}{G}\frac{\delta^2}{L^2}(\hat{u}_i,\hat{v}_i) \qquad i = 1,3$$

$$(u_2^b,v_2^b) = \frac{P_o\omega L}{G}\frac{\delta}{L}(\hat{u}_2,\hat{v}_2) \tag{3.38}$$

In terms of these (3.36) becomes

$$\frac{\partial^2\hat{p}}{\partial Y^2} = \frac{\partial\hat{p}}{\partial T} \tag{3.39}$$

and (3.35) becomes

$$\frac{2(1-\nu)}{1-2\nu}\frac{\partial\hat{v}_2}{\partial Y} = \frac{\partial\hat{p}}{\partial T} \tag{3.40}$$

Finally from (3.32.a)

$$\frac{\partial^2\hat{v}_i}{\partial Y^2} = \frac{\partial^2\hat{p}}{\partial X_i\partial T} - \frac{1}{1-2\nu}\frac{\partial^2\hat{v}_2}{\partial X_i\partial Y} = \frac{1-2\nu}{2(1-\nu)}\frac{\partial^2\hat{p}}{\partial X_i\partial T} \ , \quad i = 1,3 \tag{3.41}$$

Material	Dolomite	Granite	Limestone	Sandstone	Sand	Dense or Firm Soil	Soil of Medium Firmness	Soft Silt or Clay
Poisson's ratio ν	0.3	0.23-0.27	0.27-0.3	0.12-0.20	typical value $\tilde{}$ 0.33			
Porosity n	0.035		0.13	0.18	.25-.3	.25-.3	.3-.5	.15-.3
Shear Modulus $G(10^6\ N/m^2)$	45×10^3	30×10^3	40×10^3	10×10^3	200	120	40	15
Permeability $k(\frac{m^3\ sec}{kg})$	7×10^{-13}	10^{-16}	5×10^{-14}	2×10^{-10}	10^{-6}-10^{-9}	10^{-8}-10^{-10}		$\leq10^{-10}$
Shear Wave Velocity C_s(m/sec)	3950	3230	2900		330	250	150	90
Compressional Wave Velocity C_p(m/sec)		5790	5980	2900	$\tilde{}$ 1460 if fully saturated			
Boundary Layer Thickness for ω = 1 rad/s Eq. (3.37)	0.18	0.002	0.05	1.50	10.0~1.0	7.0 ~ 0.1		0,05

Table 1: Physical properties of certain ground materials.

[Compiled from: Lambe & Whitman (1967), Jaeger & Cook (1976) and Terzaghi and Peck (1948)]

after using (3.40). Thus inside the boundary layer one only need to solve $\hat{p}$ from (3.39), $\hat{v}_i$ and $\hat{v}_2$ can be formally expressed in terms of $\hat{p}$ via (3.40) and (3.41). It is interesting that Eq. (1.31) reduces to

$$0 = -\frac{\partial \hat{p}}{\partial X_i} - \left(\frac{n\omega\delta^2}{kG}\right)(\hat{u}_i - \hat{v}_1) \quad , \quad i=1,2,3 \tag{3.42}$$

which is the static Darcy's law. The fluid velocity $\hat{u}_i$ may be found in principle, but is of relatively minor interest.

The boundary layer corrections can be formally solved at once for simple harmonic waves

$$\begin{Bmatrix} \hat{p} \\ \hat{v}_2 \\ \hat{v}_i \end{Bmatrix} = \begin{Bmatrix} A(X_i) \\ \frac{1-i}{\sqrt{2}} \frac{1-2\nu}{2(1-\nu)} A \\ \frac{1-2\nu}{2(1-\nu)} \frac{\partial A}{\partial X_i} \end{Bmatrix} e^{Y(1-i)/\sqrt{2}} \; e^{-iT} \tag{3.43}$$

Written in dimensionless outer variables we have

$$\begin{bmatrix} \hat{p} \\ \hat{v}_2 \\ \hat{v}_i \end{bmatrix} = \begin{bmatrix} A(\xi_i) \\ \varepsilon \frac{1-i}{\sqrt{2}} \frac{1-2\nu}{2(1-\nu)} A \\ \varepsilon^2 \frac{1-2\nu}{2(1-\nu)} \frac{\partial A}{\partial \xi_i} \end{bmatrix} e^{(1-i)\eta/(\sqrt{2}\varepsilon)} \; e^{-i\tau} \tag{3.44}$$

where

$$\varepsilon = \delta/L \tag{3.45}$$

The corresponding stress components are obviously dominated by $\partial v_2/\partial \eta$:

$$\begin{bmatrix} \hat{\sigma}_{11} \\ \hat{\sigma}_{22} \\ \hat{\sigma}_{12} \end{bmatrix} = \begin{bmatrix} \frac{\nu}{1-\nu} A + O(\varepsilon^2) \\ A + O(\varepsilon^2) \\ O(\varepsilon) \end{bmatrix} e^{(1-i)\eta/(\sqrt{2}\varepsilon)} \, e^{-i\tau} \qquad (3.46)$$

The total stress components are

$$\hat{\tau}_{11} = \hat{\sigma}_{11} - \hat{p} = -\frac{1-2\nu}{1-\nu} A \, e^{(1-i)\eta/(\sqrt{2}\varepsilon)} \, e^{-i\tau}$$

$$\hat{\tau}_{22} = \hat{\sigma}_{22} - \hat{p} \cong 0$$

$$\hat{\tau}_{12} \cong 0 \qquad (3.47)$$

The second and third of (3.47) are the consequence of neglecting inertia and $\partial/\partial y >> \partial/\partial x$. Now, in many practical problems the total traction on the free surface i.e., $\tilde{\tau}_{22} + \hat{\tau}_{22}$ and $\tilde{\tau}_{12} + \hat{\tau}_{12}$, is prescribed. Because the boundary layer corrections $\hat{\tau}_{22}$ and $\hat{\tau}_{12}$ are zero to the leading order, the boundary conditions are simply that $\tilde{\tau}_{22}$ and $\tilde{\tau}_{12}$ are specified, thus the total stress field of the outer problem can be completely determined *a priori*. The outer pore pressure is then calculated from (3.26) and (3.27), after which the outer effective stresses can be found. The pore pressure and hence the effective stresses inside the boundary layer, i.e., A, can only be determined from the boundary condition on p, or σ_{22}, at the ground surface.

Thus from many known solutions of elastostatics or elastodynamics with a free surface, one can easily construct solutions of poroelasticity.

In the following sections a variety of plane-strain problems will be investigated.

4. Gravity Waves Propagating Over an Infinitely Thick Porous Sea Bed

This is the problem treated by Yamamoto et al., with further extension by Madsen. A progressive wave passes a water layer of depth h. The wave pressure at the top of the sea bed is, in physical variables:

$$p = P_o\, e^{i(Kx-\omega t)} \quad \text{with} \quad P_o = \rho g A_o \,\text{sech}\, Kh$$

$$\omega^2 = gK \tanh Kh \qquad (4.1.a\text{-}c)$$

where A_o is the wave amplitude and (4.1.c) the dispersion relation of the gravity wave. Equation (4.1) is obtained by ignoring the porosity and the deformation of the sea bed. This is a legitimate first approximation because the velocities of the solid and of the pore fluid are of the order $u = O(P_o\omega/KG)$ (cf. (3.5)) while the fluid velocity above the sea bed is $u_w = O(gKA/\omega)$, so that the ratio is $u/u_w = O((\frac{\omega}{K})^2/c_s^2)$ where ω/K is the water wave velocity. For a water depth of H = 10 m, $\omega/K = (gh)^{1/2} = O(10\ \text{m/sec})$ while the shear wave speed c_s in the solid is $100 \sim 500$ m/sec. Hence the bed can be regarded as impervious and rigid when computing the hydrodynamic pressure above and at the mud line.

Clearly the motion is two-dimensional and strain in the solid is plane, i.e., $\varepsilon_{33} = \varepsilon_{13} = \varepsilon_{23} = 0$. In the remainder of the section, dimensionless variables are used. In view of (3.24) we apply Airy's stress function to the total stresses, as follows

$$\tilde{\tau}_{11} = \tilde{\sigma}_{11} - \tilde{p} = \frac{\partial^2 F}{\partial \eta^2}, \quad \tilde{\tau}_{22} = \tilde{\sigma}_{22} - \tilde{p} = \frac{\partial^2 F}{\partial \xi^2}$$

$$\tilde{\tau}_{12} = \tilde{\sigma}_{12} = -\frac{\partial^2 F}{\partial \xi \partial \eta} \qquad (4.2)$$

The Airy function satisfies

$$\left(\frac{\partial^2}{\partial\xi^2} + \frac{\partial^2}{\partial\eta^2}\right)^2 F = 0 \tag{4.3}$$

where p is harmonic. In dimensionless outer variables†, the solution inside the sea bed is

$$\tilde{p} = D\, e^{\eta}\, e^{i(\xi-\tau)}$$

$$F = (B + C\eta)e^{\eta}\, e^{i(\xi-\tau)} \tag{4.4}$$

both of which vanish at $y \sim -\infty$. The corresponding solid stresses are

$$\left.\begin{aligned} \tilde{\tau}_{11} &= [B + C(2 + \eta)] \\ \tilde{\tau}_{22} &= (-B - C\eta) \\ \tilde{\tau}_{12} &= -i[B + C(1+\eta)] \end{aligned}\right\} e^{\eta} e^{i(\xi-\tau)} \tag{4.5}$$

Imposing the boundary conditions on the ground surface that

$$\tilde{\tau}_{22} = e^{-i(\xi-\tau)} \text{ and } \tilde{\tau}_{12} = 0 \quad \text{on} \quad \eta = 0 \tag{4.7}$$

we get

$$B = 1 \quad \text{and} \quad C = -1 \tag{4.8}$$

For plane strain, $\tilde{\sigma}_{33} = \nu(\tilde{\sigma}_{11} + \tilde{\sigma}_{22})$; Equation (3.26) reduces to

$$\tilde{\sigma}_{11} + \tilde{\sigma}_{22} = -\frac{2}{1-2\nu}\frac{nG}{\beta}\tilde{p} \qquad \text{all} \quad \eta < 0 \tag{4.9.a}$$

or

$$\tilde{\tau}_{11} + \tilde{\tau}_{22} = -2\tilde{p}(1+m) \ , \qquad m = \frac{nG/\beta}{1-2\nu} \ , \qquad \eta < 0 \tag{4.9.b}$$

†In §4 and 5 the normalizing length is actually K^{-1} = wavelength/2π.

which leads to

$$D = -\frac{C}{1+m} = \frac{1}{1+m} \tag{4.10}$$

The outer solution is thus determined completely. Note for highly incompressible fluid $m << 1$, solid dilatation is very small, by virtue of (4.9).

In terms of the dimensionless outer variables, the boundary layer correction is

$$\begin{pmatrix} \hat{p} \\ \hat{\sigma}_{11} \\ \hat{\sigma}_{22} \\ \hat{\sigma}_{12} \end{pmatrix} = \begin{pmatrix} 1 \\ \nu/(1-\nu) \\ 1 \\ 0 \end{pmatrix} A\, e^{(1-i)\eta/(\sqrt{2}\varepsilon)}\, e^{i(\xi-\tau)} \tag{4.11}$$

from (3.46). To determine A we apply the condition that

$$\tilde{p} + \hat{p} = e^{i(\xi-\tau)} \quad \text{on} \quad \eta = 0 \tag{4.12}$$

which gives

$$A = \frac{m}{1+m} \tag{4.13}$$

In summary the total solution is

$$\left.\begin{aligned} \tilde{p} + \hat{p} &= \{\frac{1}{1+m} e^{\eta} + \frac{m}{1+m} e^{(1-i)\eta/(\sqrt{2}\varepsilon)}\} \\ \tilde{\sigma}_{11} + \hat{\sigma}_{11} &= \{[-\frac{m}{1+m} - \eta]e^{\eta} + \frac{\nu}{1-\nu}\frac{m}{1+m} e^{(1-i)\eta/(\sqrt{2}\varepsilon)}\} \\ \tilde{\sigma}_{22} + \hat{\sigma}_{22} &= \{(-\frac{m}{1+m} + \eta)e^{\eta} + \frac{m}{1+m} e^{(1-i)\eta/(\sqrt{2}\varepsilon)}\} \\ \tilde{\sigma}_{12} + \hat{\sigma}_{12} &= i\eta e^{\eta} \end{aligned}\right\} e^{i(\xi-\tau)} \tag{4.14}$$

In Appendix (II), it is shown that the above solution is in complete agreement with the leading order approximation of Yamamoto et al. for small k. In particular, if the fluid bulk modulus is large so that $m \ll 1$, then $A \ll 1$ and the boundary layer disappears. Further information may be found in the cited references.

5. Gravity Waves Propagating Over a Porous Layer of Finite Thickness

5.1 The Approximate Solution

The problem is almost the same as in §4, except that the depth of the porous layer is now finite. Assuming that the layer is in welded contact with an impervious and perfectly rigid bed rock on which the boundary conditions are

$$v_1 = v_2 = 0 \qquad u_2 = 0 \ (\text{i.e., } \frac{\partial p}{\partial y} = 0) \tag{5.1}$$

As mentioned in the introduction, existing solution to this problem is quite numerical.

Again we introduce Airy's function F for the total outer stresses $\tilde{\tau}_{ij}$. The displacement components may be related to F by the relations of Love (1930, p. 205)

$$2\tilde{V}_1 = -\frac{\partial F}{\partial \xi} + \Gamma \int \nabla^2 F \, d\xi \tag{5.2.a}$$

$$2\tilde{V}_2 = -\frac{\partial F}{\partial \eta} + \Gamma \int \nabla^2 F \, d\eta \tag{5.2.b}$$

where, [see Appendix I]:

$$\Gamma = \frac{\lambda_e + 2G}{2(\lambda_e + G)} = \frac{\lambda + 2G - G/(1+m)}{2(\lambda + G)} \tag{5.2.c}$$

Let H be the layer depth normalized by $\frac{L}{2\pi} = K^{-1}$ where L is the gravity wave length. The solution which satisfies the traction conditions at $\eta = 0$ and $V_1 = V_2 = 0$ at $\eta = -H$ is worked out straightforwardly in Appendix III:

$$F = [\cosh \eta + \Omega_1 \sinh \eta + \eta(\Omega_2 \sinh \eta - \Omega_1 \cosh \eta)]e^{i(\xi - \tau)} \tag{5.3.a}$$

where

$$\Omega_1 = \Lambda^{-1}[(4H + 2(1-4\Gamma) \sinh 2H] \tag{5.3.b}$$

$$\Omega_2 = \Lambda^{-1}[2 - 2(1-4\Gamma)\cosh 2H] \tag{5.3.c}$$

$$\Lambda = 2(1-4\Gamma)\cosh 2H - [1+4H^2 + (1-4\Gamma)^2] \tag{5.3.d}$$

Note that for all ν, λ and m, $(1-4\Gamma) < 0$ so that Ω_2 and Λ are both negative. From F the following stresses may be deduced

$$\tilde{p} = -\frac{1}{1+m}(\Omega_2 \cosh \eta - \Omega_1 \sinh \eta)e^{i(\xi-\tau)} \tag{5.4.a}$$

$$\tilde{\sigma}_{11} = \tilde{\tau}_{11} + \tilde{p} = \{[1 + \Omega_2 \frac{(1+2m)}{1+m}] \cosh \eta - \Omega_1 \frac{m}{1+m} \sinh \eta + \eta(\Omega_2 \sinh \eta - \Omega_1 \cosh \eta)\}e^{i(\xi-\tau)} \tag{5.4.b}$$

$$\tilde{\sigma}_{22} = \tilde{\tau}_{22} + \tilde{p} = -\{(1 + \frac{\Omega_2}{1+m}) \cosh \eta + \Omega_1 \frac{m}{1+m} \sinh \eta + \eta(\Omega_2 \sinh \eta - \Omega_1 \cosh \eta)\}e^{i(\xi-\tau)} \tag{5.4.c}$$

$$\tilde{\sigma}_{12} = \tilde{\tau}_{12} = -i\{(1 + \Omega_2) \sinh \eta + \eta(\Omega_2 \cosh \eta - \Omega_1 \sinh \eta)\}e^{i(\xi-\tau)} \tag{5.4.d}$$

Inside the free surface boundary layer, the pressure correction is given by Eq. (4.11.a) with

$$A = 1 + \frac{\Omega_2}{1+m} \tag{5.5}$$

The corresponding corrections of $\hat{\sigma}_{ij}$ follow from (4.11.b,c,d). Adding the outer and the boundary layer solutions we see that the normal stresses σ_{11} and σ_{22} are out of phase with σ_{12} by $\pm\pi/2$.

At the bottom y = -H the normal derivative of the outer pressure $\partial\tilde{p}/\partial y$ is not zero. To satisfy the no-flux condition a boundary layer correction $\hat{p}$ is in principle needed. But for $\partial\hat{p}/\partial\eta = -\frac{\partial\tilde{p}}{\partial\eta} = O(1)$, $\hat{p}$ is of the order $O(\delta/L)$. The result is

$$\hat{p} = \frac{\partial \tilde{p}}{\partial \eta}\bigg|_{-H} \frac{1+i}{\sqrt{2}} \varepsilon \exp\left(-\frac{1-i}{\sqrt{2}} \frac{\eta+H}{\varepsilon}\right) \tag{5.6}$$

The smallness of $\hat{p}$ and $\hat{\sigma}_{ij}$ is equally true near any rigid and impervious boundary; this will lead to considerable simplification in analyzing foundation stresses under a rigid structure such as a caisson. On the other hand, if the sea bed rests on an elastic layer with a different porosity, there will be boundary layers at the interface which can be analyzed in a similar manner.

Let us mention a few limiting cases of the present solution. For an infinite layer, $H \to \infty$, we have from (5.3) that $\Omega_2 \to -1$ and $A \to m/(1+m)$ which agrees with (4.13). Also $\Omega_1 \to 1.0$ so that

$$F \to (e^{\eta} - \eta e^{\eta}) e^{i(\xi-\tau)} \tag{5.7}$$

which agrees with §4.

For highly incompressible fluid $m \ll 1$ we have $\Gamma \to 1/2$, and from (5.3.c) that

$$\Omega_2 \cong -\frac{1 + \cosh^2 H}{\cosh 2H + 1 + 2H^2} \tag{5.8}$$

The amplitude of $\hat{p}$ is

$$A \cong H^2/(\cosh^2 H + H^2) \tag{5.9}$$

In the two extremes $H \to 0$ (shallow layer) and ∞ (deep layer), $A \to 0$ so that there is no free surface boundary layer. The maximum of A occurs when

$$H \tanh H \cong 1 \qquad \text{or} \qquad H = 1.2 \tag{5.10}$$

5.2 Numerical Results

In Figure 5.1, Yamamoto's numerical results are compared with our analytical theory. The sea wave parameters are for North Sea conditions: water wave length L = 324 M (period = 15 sec in water depth 70 m), layer depth = 25 m (H = 0.48). For this wave and $G/\beta = 0.0044$, $\delta = 0.98$ m for fine sand and $\delta = 9.8$ m for coarse sand. Discrepancies of 5% and 0.5% were at first found near the bottom between Yamamoto's and our leading order approximation which ignores the boundary layer. After adding the small correction according to (5.6) the discrepancy disappears, as shown in Figure 5.1. Note that for the coarse sand δ is not small compared to the layer depth, yet there is excellent agreement. In Figure 5.2 we show some additional results for a rather compressible fluid with $G/\beta = 1.0$ for the same two values of k. Here $\delta = 0.66$ m for fine sand and 6.6 m for coarse sand. Again for fine sand the pore pressure diminishes rapidly with depth to a constant value. The effective vertical normal stress σ_{22} also rises to a constant value rapidly. For a coarse sand the variation with depth of both p and σ_{22} is rather gradual. For both sands the effective shear stress σ_{12} is independent of permeability but depends on λ, G, β, n and ν which affect m and the coefficient Γ, Eq. (5.2.c). Comparing Figures (5.1) and (5.2) it is clear that compressiblity helps to enhance the sharing of load between fluid and solid.

5.3 Stress Angle and Momentary Tension in the Solid

The assumption of an elastic skeleton is a valid one only if the solid is not granular and the stress and strain are infinitesimal, while the important engineering problem of *failure* is concerned with large strain

and is outside the realm of the present theory. Nevertheless it is interesting to discuss the stress states with a view to a qualitative understanding of the parameters which may induce failure and more severely tension in the solid. This is perhaps useful since there does not seem to be any other theory which treats the soil and the pore fluid behavior on equal footing and lends itself to analytical considerations.

An important variable in studying failure in soils and rocks is the stress angle ϕ which is defined for plane strain problems in cohesionless material by

$$\frac{1}{2}(\bar{\sigma}_{11} + \bar{\sigma}_{22}) \sin\phi = [\frac{1}{4}(\bar{\sigma}_{22} - \bar{\sigma}_{11})^2 + \bar{\sigma}_{12}^2]^{1/2} \tag{5.11}$$

(Eq. (23), p. 98, Jaeger and Cook (1976) with $S_o = 0$.) If the simple criterion of Coulomb is adopted, then under static conditions, a sliding failure exists if $\phi > \phi_f$ where ϕ_f is a constant material property called the *angle of internal friction*.

We may calculate the stress angle at each point for each instant by taking $\bar{\sigma}_{ij}$ to be the total effective stress which is the sum of static and dynamic stresses. Due to gravity the static stresses are given by

$$\begin{aligned}
\sigma^1_{22} &= (1-n)(\rho_s - \rho_w)gy \\
\sigma^1_{11} &= \frac{\nu}{1-\nu}(1-n)(\rho_s - \rho_w)gy \\
\sigma^1_{12} &= 0
\end{aligned} \tag{5.12}$$

The static weight of the water layer above is born by the static pressure in the pore fluid.

The dynamic stresses are given by adding the outer solution $\tilde{\sigma}_{ij}$ (5.4) to the boundary layer correction [(4.11) and (5.5)]. Therefore, we have,

$$\bar{\sigma}_{ij} = \sigma^{1}_{ij} + (\tilde{\sigma}_{ij} + \hat{\sigma}_{ij}) \tag{5.13}$$

Alternatively, we may calculate the maximum depth d at which ϕ rises to a specific value ϕ_f if only for one instant of a wave period. This can be calculated by putting $\phi = \phi_f$ in (5.11) and substituting $\bar{\sigma}_{ij}$ from (5.13), then maximizing for the depth d.

Mohr circles as shown in Figure (5.3) are commonly used as a graphical representation of Equation (5.11). The procedure starts by representing the stress field (5.13) by the two points $R\ (-\bar{\sigma}_{11}, -\bar{\sigma}_{12})$ and $S(-\bar{\sigma}_{22}, \bar{\sigma}_{12})$ with the normal stresses $\bar{\sigma}_{11}$, $\bar{\sigma}_{22}$ measured along the obscissa, the shear stress $\bar{\sigma}_{12}$ along the ordinate. This is done here following the traditional sign convention for stresses in soil mechanics literature, i.e., a stress is positive when it acts as a compression, (thus $-\bar{\sigma}_{11}$ is used instead of $\bar{\sigma}_{11}$, etc.). Mohr circle is defined as the circle that passes through R and S with its center on the abscissa. Then, it can be shown that the angle ϕ in (5.11) is the angle between the tangent to the circle that passes through the origin, and the abscissa as in Figure (5.3). Under static loadings, R and S receed to R_o and S_o on the abscissa, representing (5.12). As the gravity wave with frequency ω progresses over the sea bed, the points R and S, representing (5.13), will

rotate around R_o and S_o with the same frequency ω, with their path of rotation determined by (5.4) and (4.11). From these equations it is seen first that both σ_{11} and σ_{22} are out-of-phase with σ_{12} by $\pm \frac{\pi}{2}$. Thus, R and S each lies on an ellipse, having perpendicular major and minor radii, with centers at R_o and S_o respectively as shown in Figure (5.3). Second, if the boundary layer corrections are small at the depth d, it is seen from (5.4b and c) that σ_{11} and σ_{22} can either be out-of-phase by π or in phase. The former case occurs if $m \ll 1$ (incompressible fluid), while the latter may occur for $m \sim O(1)$. In Figure (5.3), the former case is illustrated by the points R and S, while the latter by R and S_1. It is however evident from the figure that the latter case (normal stresses are mainly in-phase) is the less critical of the two possibilities, as it produces lesser values of ϕ, implying a smaller depth d for the failure zone.

Another parameter that affects the depth d is of course the sea bottom pressure amplitude P_o which is related to the sea wave amplitude by (4.1). For the sea depth and wave length considered, a wave amplitude A=1 m would correspond roughly to P_o=5 KN/m^2.

We take $\phi_f = 30°$ which is a typical failure angle for sand. The corresponding variation of the depth d with P_o is shown in Figure (5.4) for two different situations. The first is that of a completely saturated sand (coarse or fine) where $G/\beta = 0.0044$, while the second is of a more compressible fluid $G/\beta = 1.0$. It is seen

from the figure that the depth d is much reduced by letting the fluid more compressible. This can be explained from (5.4) which yields $\tilde{\sigma}_{11}$ and $\tilde{\sigma}_{22}$ out of phase by π for the first situation ($G/\beta = 0.0044$, i.e., $m<<1$), but in phase, and thus less critical, for the second ($G/\beta = 1.0$).

Let us examine the possibility of having tension in the solid. This is of course a more severe situation than what was just discussed, as the start of tension corresponds to $\phi_f = \pi/2$. Since the free surface of water is given by $\zeta = A_o \exp[i(\xi-\tau)]$ from (5.4d) we see that $\sigma_{12} = \bar{\sigma}_{12} = 0$ when a crest or a trough where $\exp[i(\xi-\tau)] = +1$ and -1 respectively. Now if at a point $\bar{\sigma}_{12}$ vanishes and one or both of $\bar{\sigma}_{11}$ and $\bar{\sigma}_{12}$ is positive (tension), a granular solid would *liquefy* for this instant.

Consider the vertical line under a crest. Note that the static stress σ^1_{11} and σ^1_{22} are always compressible and increase linearly with depth. At y=0, the dynamic stress σ_{22} is zero also but σ_{11} can be positive for sufficiently large wave pressure $P_o >> 0$. Hence at the critical depth $\sigma^1_{11} + \sigma_{11} = 0$ or $(\rho_s - \rho_w)gD = O(P_o) = O(\rho_w gA/\cosh Kh)$. If $A/\cosh Kh = O(\delta)$ which is often the case in nature the critical depth D is then comparable to the boundary layer thickness, i.e., tension occurs throughout $-D < y < 0$ with $D = O(\delta)$. Large P_o of course increases D.

In Figure 5.5 we show D versus P_o. For three of the curves give the maximum D above which $\bar{\sigma}_{11}$ is tensile when a crest passes (labelled 1C). For $G/\beta = 1$ the fine sand tension occurs under a trough, the curve 2T shows the maximum D above which $\bar{\sigma}_{22}$ is tensile. Note the curve 1T that for sufficiently large P_o, $\bar{\sigma}_{11}$ can also be tensile under a trough in a region totally beneath y=0.

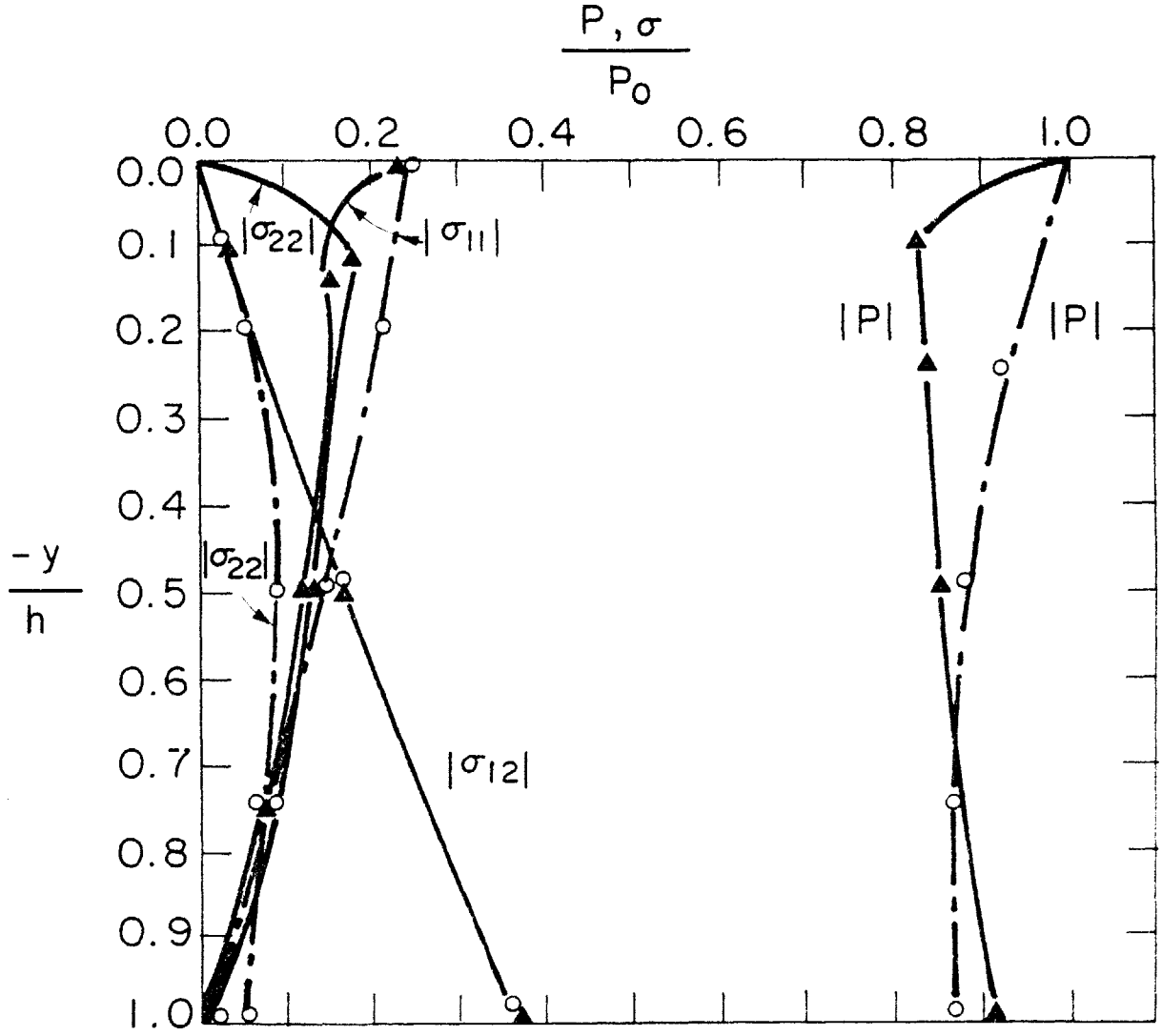

Figure (5.1)

Comparison between the present analytical theory and Yamamoto (1977) numerical results for the response of 125 ms deep poroelastic layer under gravity waves of length 324 ms, period 15 sec in 70 m water depth. Results are shown for: fine sand, $k=10^{-8}$ m^3 sec/kg (_____ present theory, Δ Yamamoto); and coarse sand, $k=10^{-6}$ m^3 sec/kg (———•———•——— present theory, O Yamamoto). For both sands, $G/\beta = .0044$ (completely saturated).

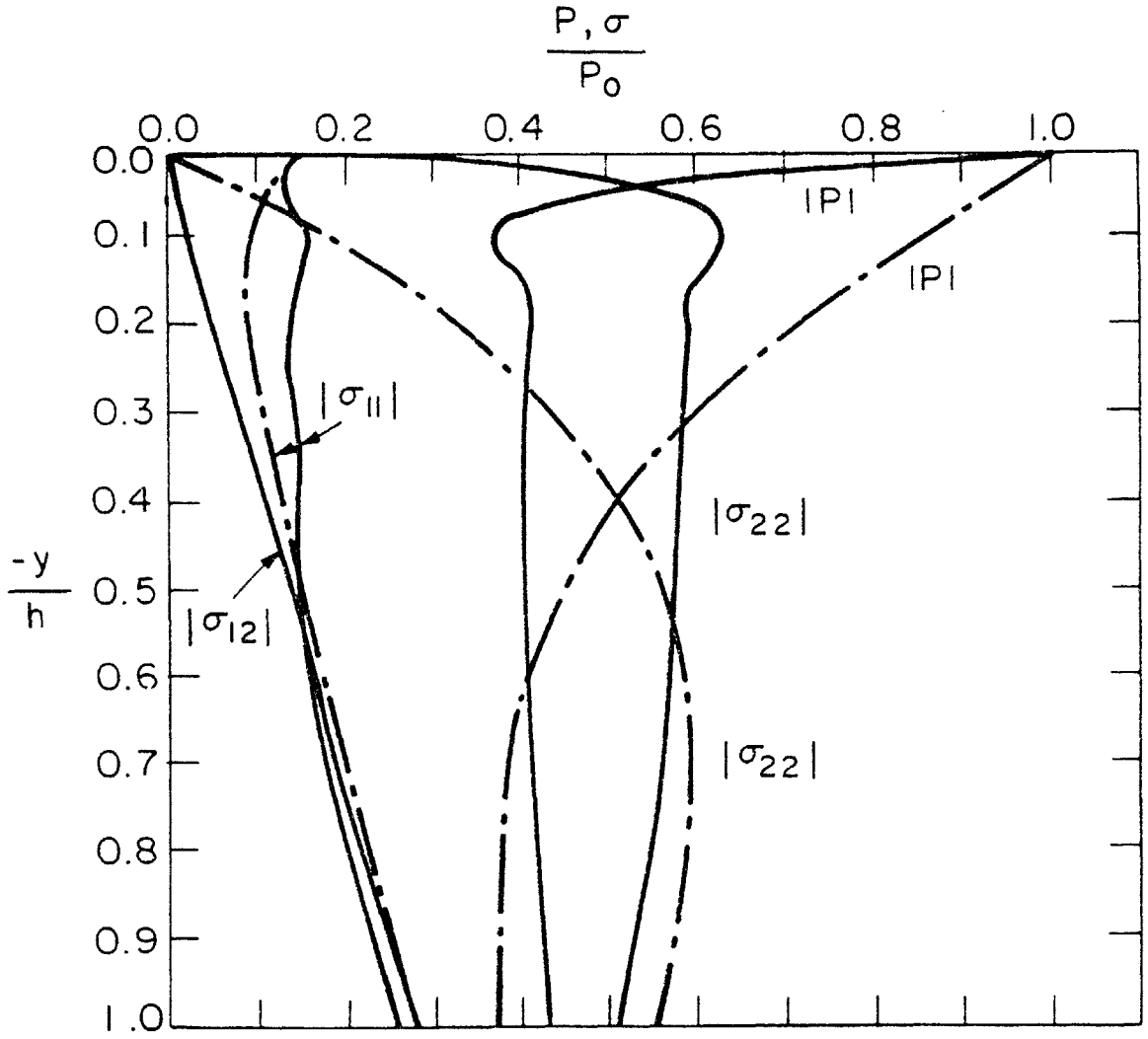

Figure (5.2)

Response of a poro-elastic layer of finite depth to sea waves. Some data as for Figure 5.1 except that $G/\beta = 1.0$ instead, i.e., fluid is more compressible due to air entrainment.

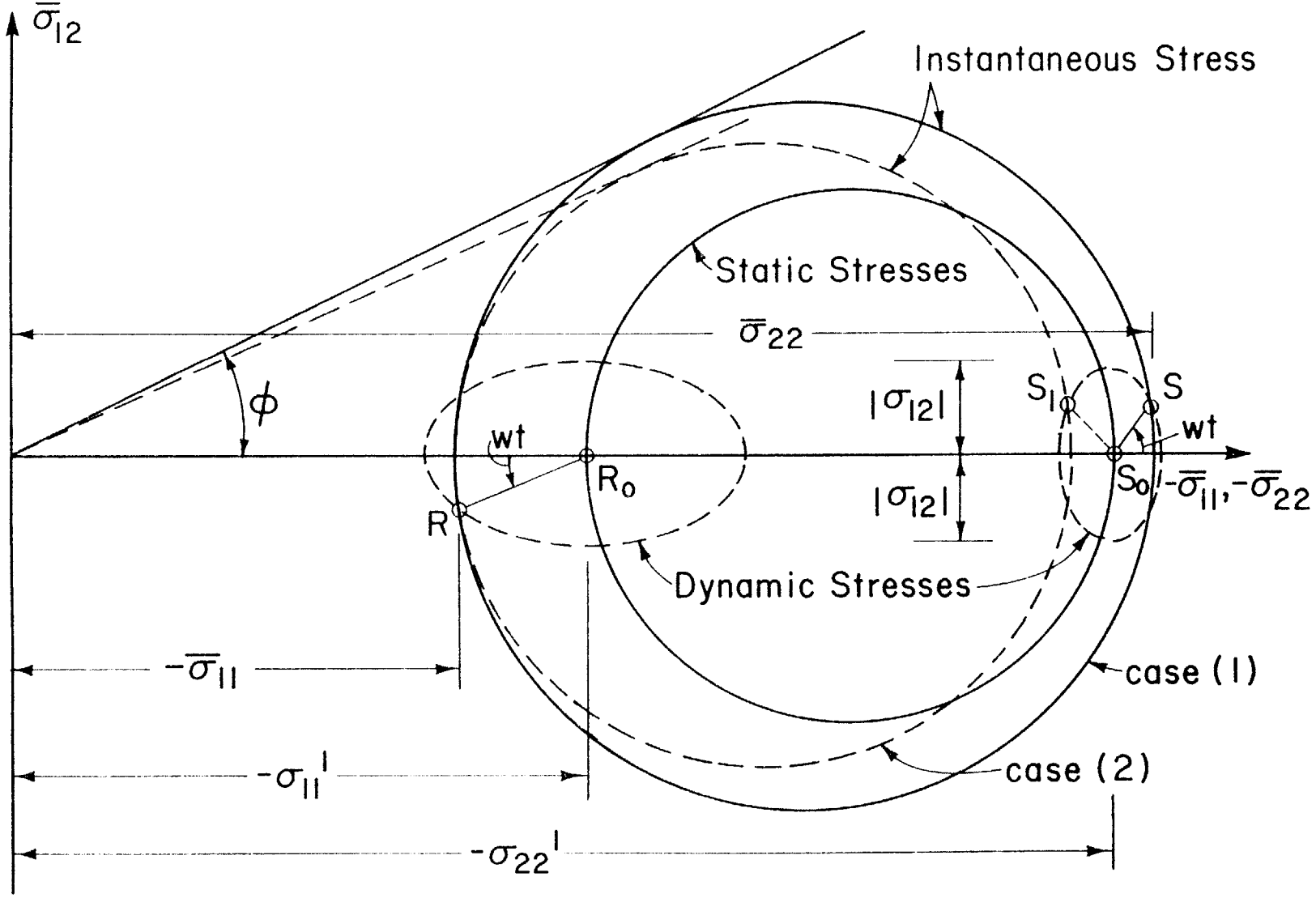

Figure (5.3)

Mohr circles for case (1), dynamic stresses out-of-phase by π ($m \ll 1$); case (2), dynamic stresses in-phase ($m \sim 0(1)$).

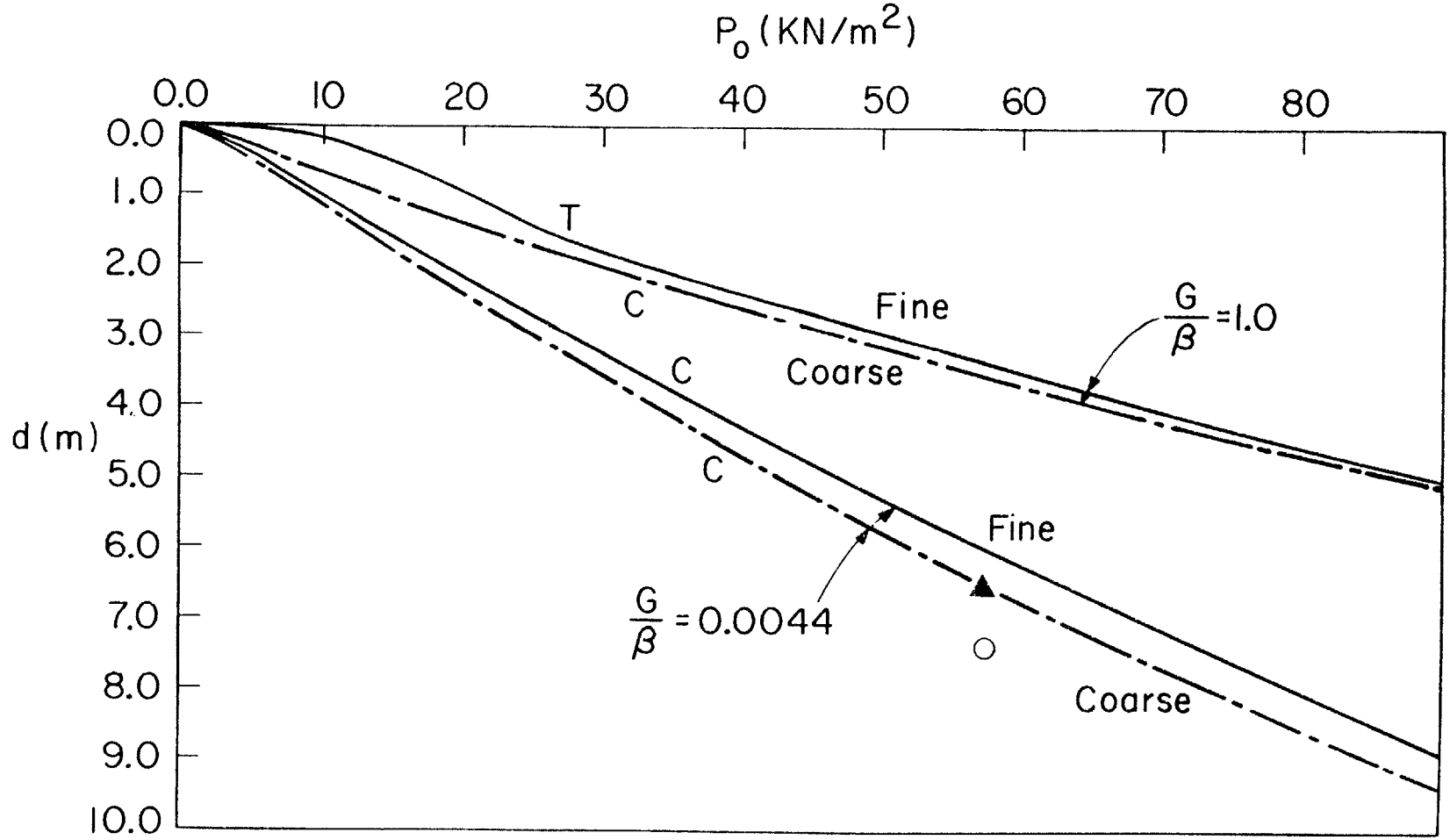

Figure (5.4)

Depth d at which = 30° momentarily as a function of wave pressure P_o at sea bottom. Same data as in Figures 5.1 and 5.2. For reference P_o = 10 KN/m^2 corresponds to A_o=2.0m. c - under a crest, T - under a trough.

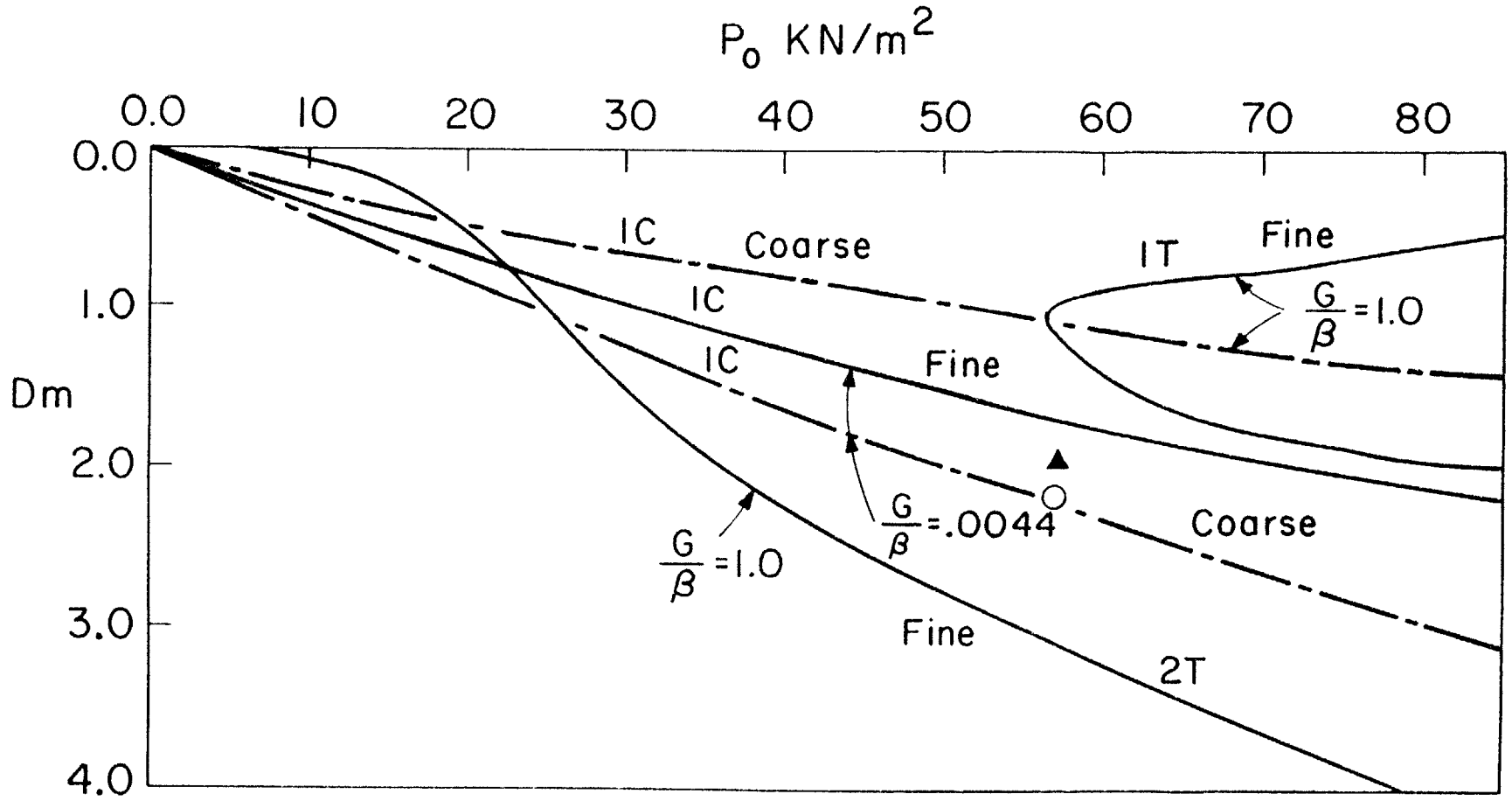

Figure (5.5)

Region of momentary tension as a function of wave pressure P_o at sea bottom. Same data as in Figures 5.1 and 5.2 1C: $\sigma_{11} < 0$ for $0 > y > -d$ under a crest; 2T: $\sigma_{22} \neq 0$ for $0 > y > -d$ under a trough; 1T: $\sigma_{11} < 0$ for $-d_1 > y > -d_2$ under a trough.

6. RESPONSE TO LOCALIZED PRESSURE OSCILLATING AT GRAVITY WAVE FREQUENCIES, WITH APPLICATION TO THE NEAR FIELD OF A PIPE LINE

6.1 General Solution

Let the hydrodynamic pressure on the sea bed be, in physical variables

$$p = \mathbb{P}(x)e^{-i\omega t}, \quad -\infty < x < \infty \tag{6.1}$$

where $\mathbb{P}$ has a Fourier transform. If we assume that the characteristic length L of $\mathbb{P}$ satisfies the condition that $L/\delta >> 1$ but $L/\ell << 1$, then the outer problem is again an elastostatic problem. The boundary conditions at the ground surface are

$$\begin{aligned} \tau_{22} &= -\mathbb{P}(x)e^{-i\omega t} \\ \tau_{12} &= 0 \end{aligned} \qquad y = 0 \tag{6.2}$$

The sea bed is assumed to be infinitely deep. The solution for such a half space problem is well known and can easily be obtained by Fourier transform.

Let us again employ the Airy stress function F for the outer solutions as in Eq. (4.2). Expressing F as a Fourier integral

$$F = \frac{1}{2\pi}\int_{-\infty}^{\infty} d\lambda\, e^{i\lambda\xi}\bar{F}(\lambda,\eta) \tag{6.3}$$

it is easy to find that

$$\bar{F} = \frac{\overline{\mathbb{P}}}{\lambda^2}(1 - |\lambda|\eta)e^{|\lambda|\eta}\, e^{-i\tau} \tag{6.4}$$

Substituting (6.4) in (6.3), the stress components may be obtained from (4.2).

$$\tilde{\tau}_{11} = \frac{1}{2\pi}\int_{-\infty}^{\infty} d\lambda\ e^{i\lambda\xi}(-\overline{\mathbb{P}})(1 + |\lambda|\eta)e^{|\lambda|\eta}\ e^{-i\tau}$$

$$\tilde{\tau}_{22} = \frac{1}{2\pi}\int_{-\infty}^{\infty} d\lambda\ e^{i\lambda\xi}(-\overline{\mathbb{P}})(1 - |\lambda|\eta)e^{|\lambda|\eta}\ e^{-i\tau} \qquad (6.5)$$

$$\tilde{\tau}_{12} = \frac{1}{2\pi}\int_{-\infty}^{\infty} d\lambda\ e^{i\lambda x}(-i\overline{\mathbb{P}})\lambda\eta\ e^{|\lambda|\eta}\ e^{-i\tau}$$

Note that

$$\tilde{\tau}_{11} + \tilde{\tau}_{22} = -\frac{2}{2\pi}\int_{-\infty}^{\infty} d\lambda\ e^{i\lambda\xi}\,\overline{\mathbb{P}}\,(\lambda)e^{|\lambda|\eta}\ e^{-i\tau} \qquad (6.6)$$

This may be used in (4.9.b) to calculate the pore pressure in the outer region.

$$\tilde{p} = \frac{1}{1+m}\,\frac{1}{2\pi}\int_{-\infty}^{\infty} d\lambda\ e^{i\lambda\xi}\,\overline{\mathbb{P}(\lambda)}e^{|\lambda|\eta}\ e^{-i\tau} \qquad (6.7)$$

We now turn to the boundary layer correction. Making use of (3.44.a) and applying the pressure boundary condition at $\eta = Y = 0$

$$A + \tilde{p}(\xi,0) = \mathbb{P}(\xi) \qquad (6.8)$$

The result is simply

$$A = \frac{m}{1+m}\,\mathbb{P}(\xi) \qquad (6.9)$$

For further discussion we need to specify $\mathbb{P}(\xi)$.

6.2 Disturbances Due to a Small Pipe Line Fixed Near the Sea Bed

Pipe lines laid directly on or very near the top of the sea bed are used to transport oil from offshore terminals to the mainland. The safety of the pipe lines against the sea waves depends in part on the

strength of the supporting sea bed. The stress and pore pressure inside the bed beneath the pipe are therefore of important concern. Now the typical pipe diameters for transporting oil are L = O(1 m) which is much larger that δ only if the permeability is very small. Referring to Table 1 we must confine this section to very fine sand mixed with silt or clay. For coarse sand one must have much larger pipe diameter for our results to be relevant. Since the pipe diameter is much less than the gravity wavelength, wave scattering is insignificant and the flow near the pipe is, to the leading order, that of a uniform horizontal current past a log on a rigid sea bed. The instantaneous current flow velocity is

$$U\, e^{-i\omega t} \tag{6.10.a}$$

where

$$U = \frac{gKA}{\omega} \operatorname{sech} Kh \tag{6.10.b}$$

Let there be no flow separation near the pipe, which is a reasonable assumption for small enough A or large enough Kh. The solution by Jeffrey (see Milne-Thomson, 1967) is then appropriate if the pipe line rests on the bed. In particular, the velocity potential in the sea water along the bed is

$$\phi(x,0) = \frac{a\pi U}{2} \frac{\sinh 2a\pi/x}{\sinh^2 a\pi/x} \tag{6.11}$$

Note that $\phi(x,0)$ is odd in x, has the asymptotic behavior

$$\phi(x,0) \tilde{=} Ux[1 + \frac{1}{3}(\frac{a\pi}{x})^2] \,, \quad \text{for} \quad |x/a| << 1 \tag{6.12}$$

and is discontinuous on two sides of the contact point, x = 0, i.e.,

$$\phi(x,0^{\pm}) = \pm\, a\, U[1 + e^{-2a\pi/|x|}] \qquad x \gtrless 0 \tag{6.13}$$

Note further that $\partial\phi/\partial x \to 0$ as $x \to \pm\infty$. Excluding the effect of the

undisturbed progressive waves, the local disturbance caused by the pipes is therefore

$$\Delta\phi = \frac{Ua\pi}{2} \frac{\sinh 2a\pi/x}{\sinh^2 a\pi/x} - Ux \tag{6.14}$$

which is plotted as a solid line in Figure 6.1. The corresponding pressure perturbation

$$\Delta p(x,0) = +i\rho\omega\Delta\phi \tag{6.15}$$

must look much the same. The function (6.14) is, however, too complicated for analytical considerations. In reality there is likely a small gap between the pipe and the sea bed; the actual pressure disturbance is likely continuous at the point x = 0. We therefore adopt a simple two-paramter model that

$$\mathbb{P}(x) = \frac{\Delta p(x,0)}{i\pi KaP_o} = \frac{2b\xi}{\xi^2+b^2} \qquad \text{with} \qquad \xi = 3x/\pi a \tag{6.16}$$

where P_o is given by (4.1.b). The choice of b = 1/2 makes (6.16) a very good approximation to (6.14) and (6.15) as shown by the dashed line in Figure 6.1.

The Fourier transform of (6.16) is of course simple

$$\overline{\mathbb{P}}(\lambda) = -2b\pi i(\operatorname{sgn}\lambda)e^{-b|\lambda|} \tag{6.17}$$

Furthermore, all the Fourier integrals in (6.5) and (6.7) can be explicitly evaluated to give

$$\begin{pmatrix}\tilde{\tau}_{11}\\ \tilde{\tau}_{22}\end{pmatrix} = 2b\left\{\frac{-\xi}{\xi^2 + (\eta-b)^2} \mp \frac{2\xi\eta(b-\eta)}{[\xi^2 + (\eta-b)^2]^2}\right\} e^{-i\tau}$$

$$\tilde{\tau}_{12} = 2b\eta \frac{\xi^2 - (\eta-b)^2}{[\xi^2 + (\eta-b)^2]^2} e^{-i\tau}, \quad \tilde{p} = \frac{2b}{1+m} \frac{\xi}{\xi^2 + (\eta-b)^2} e^{-i\tau} \tag{6.18}$$

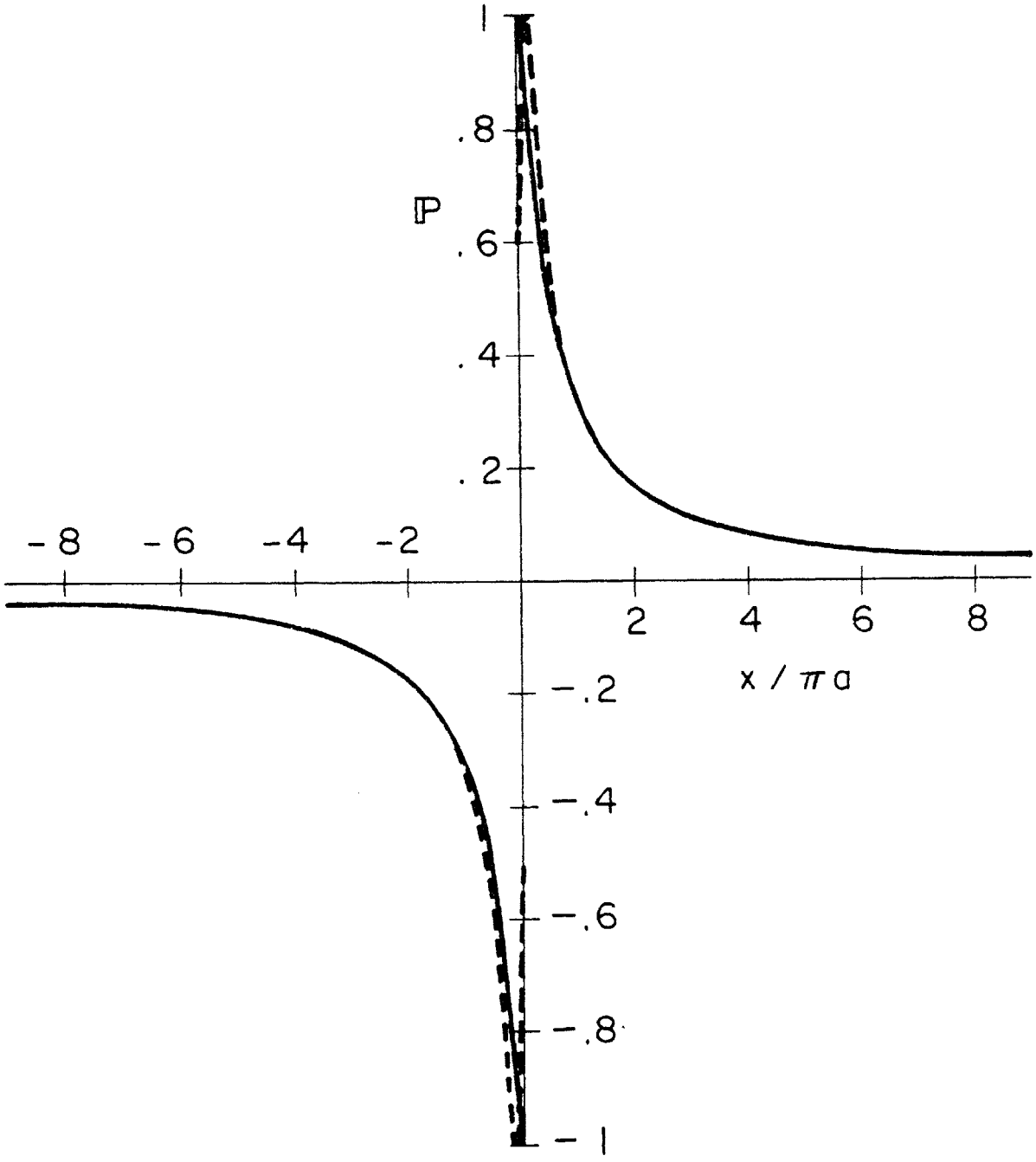

Figure (6.1)

Distribution of the sea bottom disturbance due to a pipe; _____ theoretical (Eq. 6.14), ---------- the two parameter approximation (Eq. 6.16).

with $\xi = 3x/\pi a$, $\eta = 3y/\pi a$. All the stresses are normalized by $i\pi KaP_o$. Note that the lines of constant p are circles which are centered on the horizontal line $y = b$ and are tangent to the y axis. The radius of $\tilde{p} =$ constant is $b[(1+m)\tilde{p}]^{-1}$. The effective stresses everywhere are given by:

$$\sigma_{11}/P_o = (\sigma_{11}^o + \sigma_{11}^b)/P_o = i\pi Ka(2b)\{-\frac{m}{1+m}\frac{\xi}{\xi^2 + (\eta-b)^2} - \frac{2\xi\eta(b-\eta)}{[\xi^2 + (\eta-b)^2]^2} + \frac{\nu}{1-\nu}\frac{m}{1+m}\frac{\xi}{\xi^2 + b^2}\exp\left(\frac{1-i}{\sqrt{2}}\frac{y}{\delta}\right)\}e^{-i\tau} \tag{6.19.a}$$

$$\sigma_{22}/P_o = (\sigma_{22}^o + \sigma_{22}^b)/P_o = i\pi Ka(2b)\{-\frac{m}{1+m}\frac{\xi}{\xi^2 + (\eta-b)^2} + \frac{2\xi\eta(b-\eta)}{[\xi^2 + (\eta-b)^2]^2} + \frac{m}{1+m}\frac{\xi}{\xi^2 + b^2}\exp\left(\frac{1-i}{\sqrt{2}}\frac{y}{\delta}\right)\}e^{-i\tau} \tag{6.19.b}$$

$$\sigma_{12}/P_o = (\sigma_{12}^o + \sigma_{12}^b)/P_o = i\pi Ka\tilde{\tau}_{12} \tag{6.19.c}$$

where in the boundary layer part y denotes the physical variable and δ is given by (3.37).

To get the total effective stress field under a pipe line in waves, Eqs. (4.14) must be added to (6.19). It should be recalled that different normalized outer variables ($\xi = Kx$, $\eta = Ky$) were used in §4. Note that for σ_{11}, contributions from the progressive wave and from the pipe are out of phase by $\pi/2$, whereas for σ_{12} the two contributions are in phase. In particular for $m = 0$ (incompressible fluid) the total effective stress field is, in the variables ξ,η of this section,

$$\text{Total}\quad \sigma_{11}/P_o = \pi Ka\{-\frac{1}{3}\eta e^{\pi Ka\eta/3} - \frac{i4b\xi\eta(b-\eta)}{[\xi^2 + (b-\eta)^2]^2}\}e^{-i\tau}$$

$$\text{Total}\quad \sigma_{22} = -\sigma_{11}$$

$$\text{Total} \quad \sigma_{12}/P_o = i(\pi Ka)\{\frac{1}{3}\eta e^{\pi Ka\eta/3} + \frac{2b\eta[\xi^2 - (\eta-b)^2]}{[\xi^2 + (\eta-b)^2]^2}\}e^{-i\tau}$$

$$\text{Total} \quad p/P_o = \{e^{\pi Ka\eta/3} + i\pi Ka \frac{2b\xi}{\xi^2 + (\eta-b)^2}\}e^{-i\tau}$$

(6.20.a-d)

Again the boundary layer is ineffective.

Sample contours of total stresses are shown in Figures 6.2 - 6.5 for the following input data:

wave period $T = 6$ sec

water depth $h = 10$ m

pipe diameter $2a = 1$ m

permeabilities $k = 10^2/\rho_w gG$

These imply: water wavelength = 50 m, $Kh = 1$, $Ka = 0.138$ and $\delta/2a = 0.1$. Three values of fluid bulk modulus have been examined:

$G/\beta = 0.0044$ $\quad G/\beta = 0.1$ $\quad G/\beta = 1$

The effective shear stress σ_{12} is independent of m (hence G/β). Also contributions from the progressive wave and from the pipe line are in phase and reinforce each other, Fig. 6.2.

From (6.20.d) or by comparing (4.14.a) with (6.18d) it is clear that the effect of the pipe line on the pore pressure is πKa times as large as the effect of the progressive wave. Hence the latter dominates for all $\vec{x}$ and no plot is given for p.

Figure 6.3 gives the normal stresses σ_{11} and σ_{22} for $G/\beta = 0.0044$ (no air entrainment). The deviations from the progressive wave background are not large and the two components are nearly equal in magnitude. Note that $\sigma_{11} \tilde{=} 0$ on the mud line $y = 0$ (cf. Eq. (6.20.a,b)).

For a lower bulk modulus ($G/\beta = 0.1$), the σ_{11} contours are

significantly different (Figure 6.4). For large x/a and immediately beneath the boundary layer, the wave induced σ_{11} is negative and then becomes positive as the depth increases (cf., 4.14.b). In Figure 6.5 σ_{22} contours are only quantitatively different from Figure 6.2.

For small values of G/β or m, the part of $\tilde{\sigma}_{11}$ and $\tilde{\sigma}_{22}$ due to the progressive wave is very small near the mud line and increases linearly with $|\eta|$ (cf., 4.14.b,c). Therefore near $\eta = 0$ the part of σ_{11} and σ_{22} contributed by the pipe line is relatively significant (though of order πKa). However, if m = O(1) (low fluid bulk modulus), the wave induced $\tilde{\sigma}_{11}$ is of O(1) near the mud line. Thus the disturbance by the pipe line $\tilde{\sigma}_{11}$ is much less by a factor πKa; the same is true for $\tilde{\sigma}_{22}$ outside the boundary layer. There is no need to present any plots here.

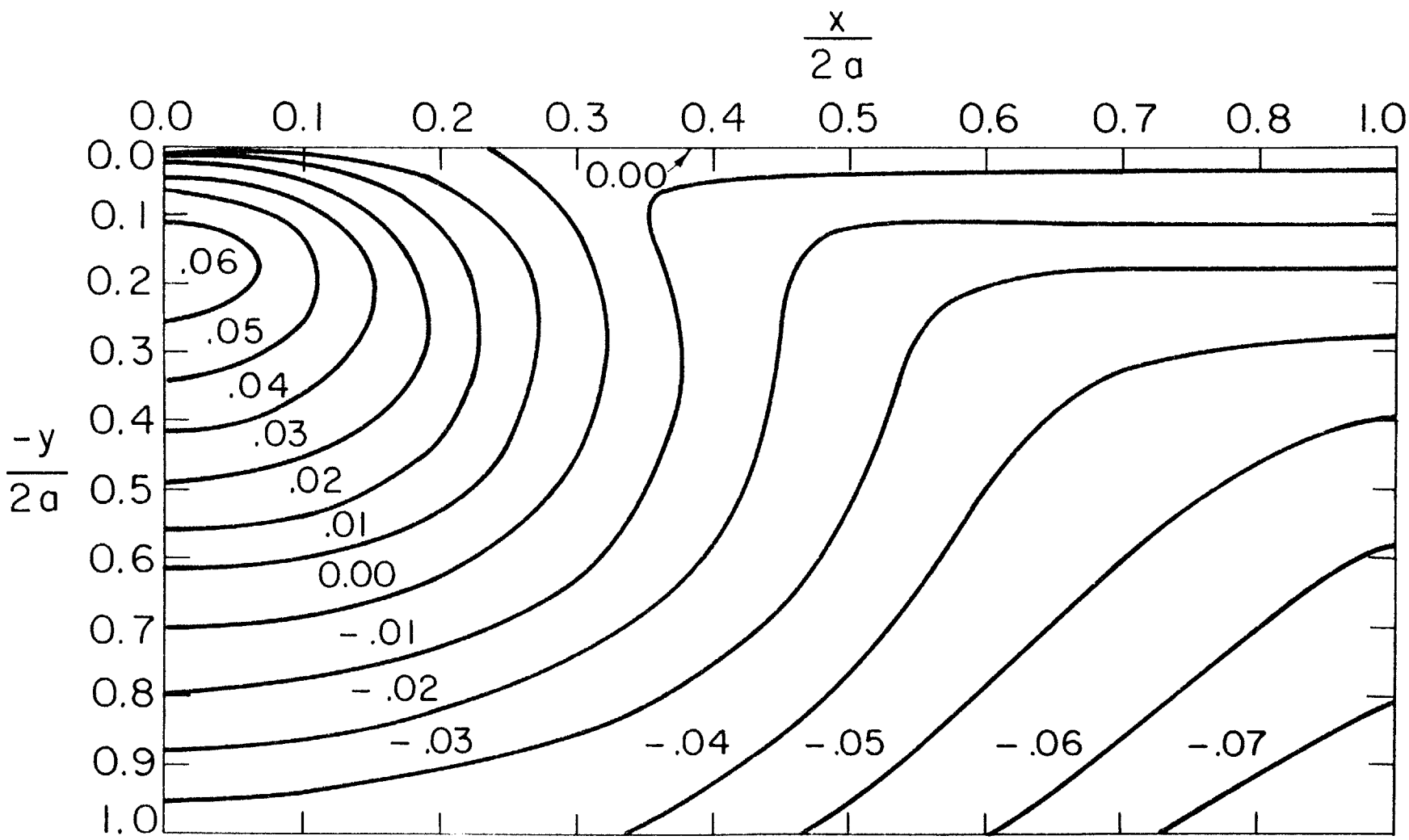

Figure (6.2)

Contour lines of the dimensionless shear stress amplitudes $\sigma'_{12}/\rho_w g A_o$, where A_o is the wave amplitude and $\sigma_{12} = i\sigma'_{12}$. $\exp[iKx-i\omega t)$ is the total shear stress, from both the progressive wave effect and the pipe line effect.

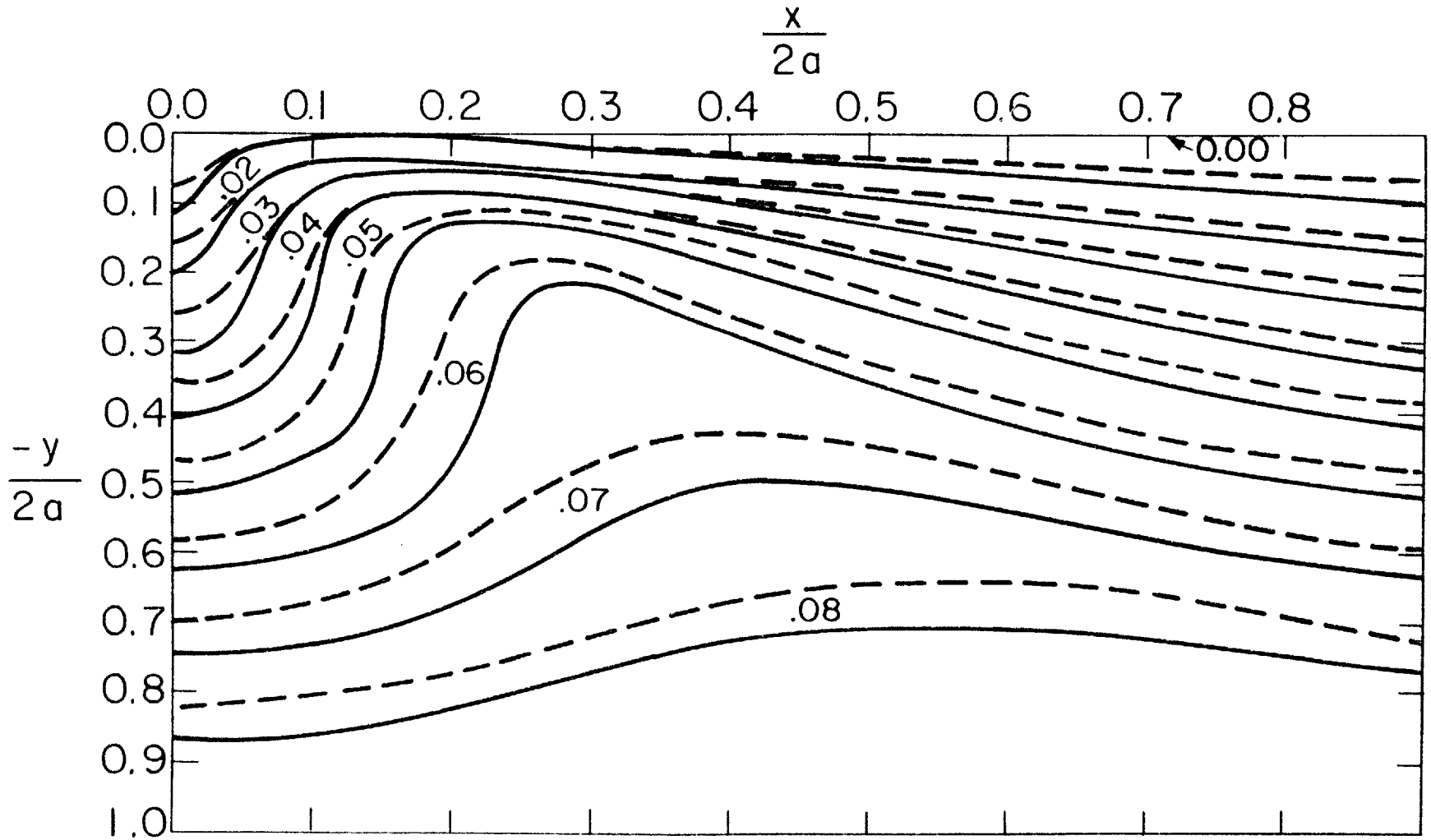

Figure (6.3)

Contour lines of the dimensionless total dynamic normal stresses; _____ $|\sigma_{11} / \rho_w g A_o$, ---------- $|\sigma_{22} / \rho_w g A_o$; for G/β = .0044 (no air entrainment).

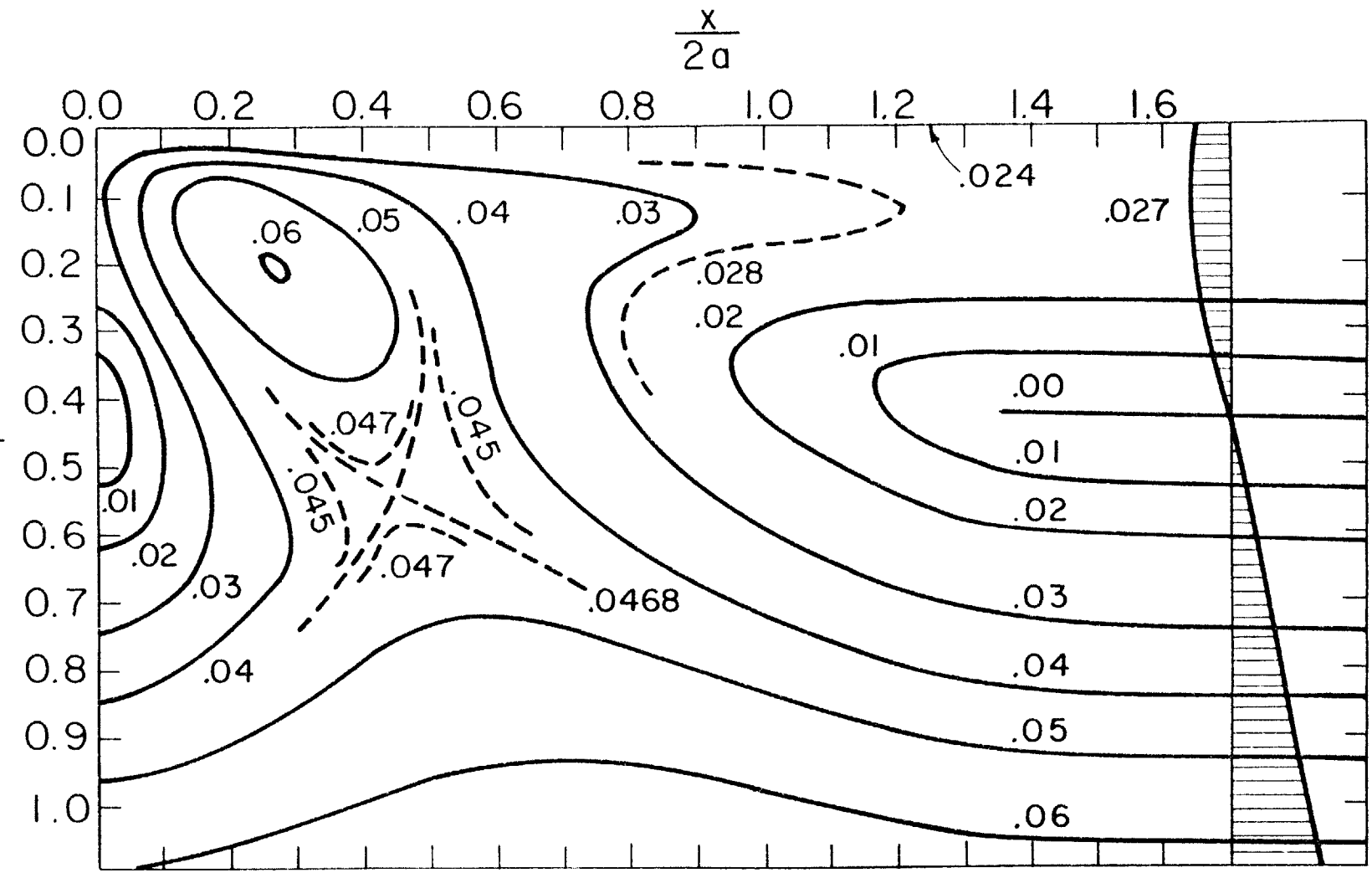

Figure (6.4)

Contour lines of the dimensionless total dynamic normal stress $|\sigma_{11}/\rho_w g A_o$ for $G/\beta = 0.1$ (smaller bulk modulus).

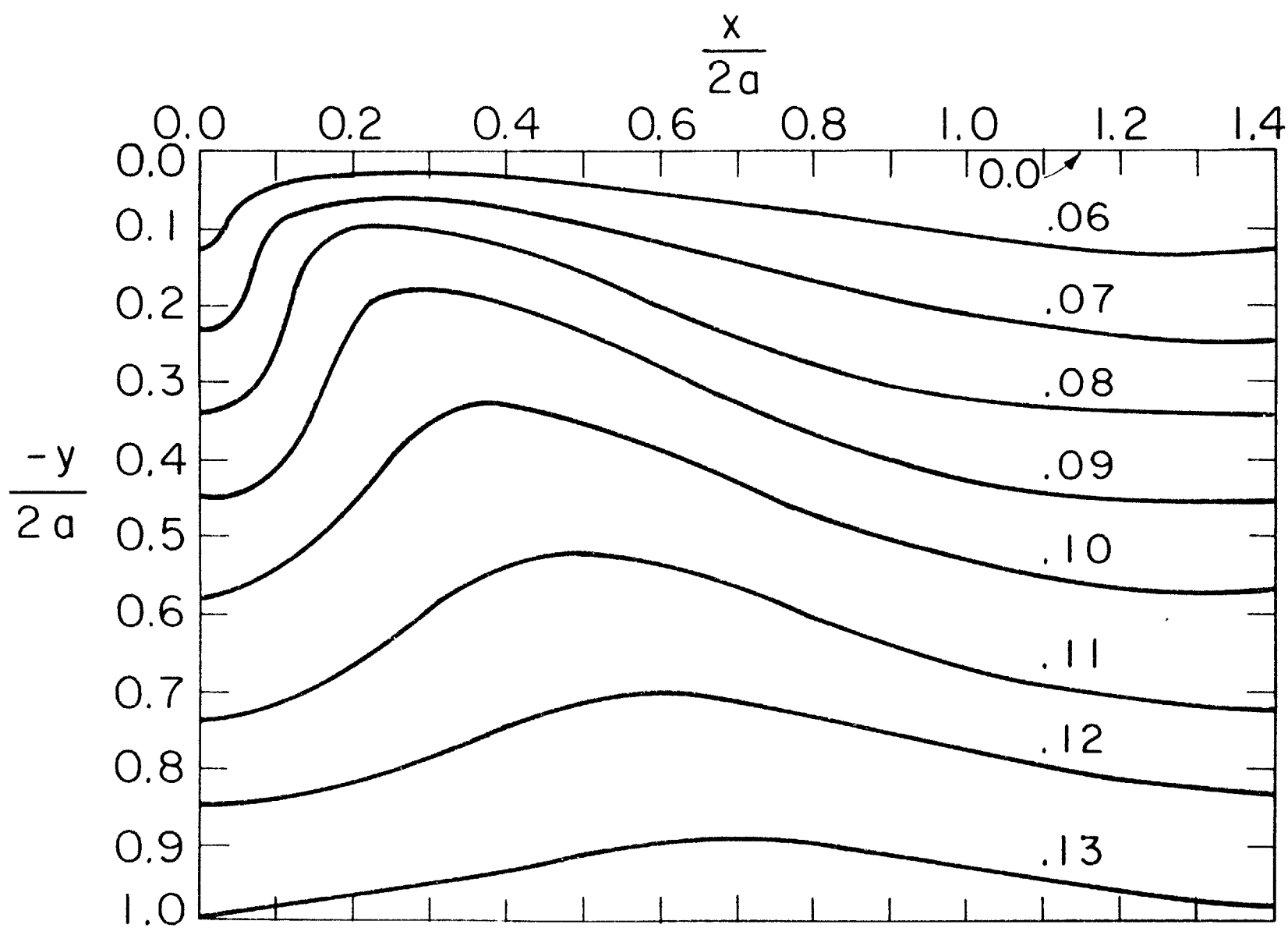

Figure (6.5)

Contour lines of the dimensionless total dynamic normal stress $|\sigma_{22}|/\sigma_w g A_o$ for $G/\beta = 0.1$.

7. P or SV Waves Incident on a Small Tunnel of Circular Cross-Section

Consider a circular cylindrical cavity of radius a in an infinite poro-elastic solid. For simplicity, the cavity surface is assumed to be directly exposed to atmospheric pressure. It is of obvious interest in tunnel engineering to know the stress field near the cavity surface. In a typical earthquake spectrum the peak period can be $0.5 \sim 1$ sec which corresponds to wavelength of 300 m or more. The diameter of ordinary tunnels are much less (< 30 m) so that the neighborhood of the tunnel $k_p r << 1$ is essentially elastostatic. For plane strain dynamic problems it is customary to introduce ϕ and ψ such that

$$v_1 = \frac{\partial \phi}{\partial x} + \frac{\partial \psi}{\partial y}$$

$$v_2 = \frac{\partial \phi}{\partial y} - \frac{\partial \psi}{\partial x} \tag{7.1}$$

If the incident wave is a plane P wave

$$\phi^{\infty} = \phi_o e^{i k_p x} \qquad \psi^{\infty} = 0 \qquad k_p = \omega/c_p \tag{7.2}$$

For brevity, the factor $e^{-i\omega t}$ is omitted everywhere, or equivalently considered to be absorbed in ϕ_o, ψ_o and P_o. The corresponding incident stress field in the region $k_p r << 1$ but $r/a >> 1$ is

$$\sigma_{11}^{\infty} = -(\lambda+2G) k_p^2 \phi_o$$

$$\sigma_{22}^{\infty} = -\lambda k_p^2 \phi_o \tag{7.3}$$

$$\sigma_{12}^{\infty} = 0$$

If instead the incident wave is a plane SV wave

$$\phi^{\infty} = 0 , \quad \psi^{\infty} = \psi_o e^{i k_s x} , \quad k_s = \omega/c_s \tag{7.4}$$

The corresponding stress field in $k_s r << 1$, $r/a >> 1$ is

$$\sigma_{11}^{\infty} = \sigma_{22}^{\infty} = 0 \ , \quad \sigma_{12}^{\infty} = Gk_s^2\psi_o \tag{7.5}$$

The associated pore pressure p^{∞} is constant in the P waves and zero in the S waves.

Without loss of generality, we shall consider the elastostatic outer* problem such that

$$\left.\begin{aligned} \tau_{11} &\to \tau_{11}^{\infty} = 2P_o S_1 \\ \tau_{22} &\to \tau_{22}^{\infty} = 2P_o S_2 \\ \tau_{12} &\to 0 \end{aligned}\right\} \quad r/a >> 1 \qquad kr << 1 \tag{7.6}$$

It is well known that a pure shear can be obtained by letting $S_2 = -S_1$ which corresponds to an SV wave incident at 45° with respect to the x-axis. The total stress field in the outer region is well known (Kirsch, 1946; Timoshenko, 1951). Assume that the radial coordinate r is already normalized by a, then

$$\tilde{\tau}_{rr} = (S_1 + S_2) - (S_2 - S_1)\cos 2\theta - \frac{1}{r^2}(S_1 + S_2) + \cos 2\theta\{-\frac{3}{r^4}(S_2 - S_1) + \frac{4}{r^2}(S_2 - S_1)\}$$

$$\tilde{\tau}_{\theta\theta} = (S_1 + S_2) + (S_2 - S_1)\cos 2\theta + \frac{1}{r^2}(S_1 + S_2) + \frac{3}{r^4}(S_2 - S_1)\cos 2\theta$$

$$\tilde{\tau}_{r\theta} = (S_2 - S_1)\sin 2\theta(1 + \frac{2}{r^2} - \frac{3}{r^4}) \tag{7.7.a-c}$$

(7.7.a-c)

The outer pore pressure is

*The word "outer" is relative to the boundary layer; it is actually the the inner field in terms of the wavelength.

$$-2(1 + m)\tilde{p} \cong 2(S_1 + S_2) + \frac{4}{r^2}(S_2 - S_1)\cos 2\theta \qquad (7.8)$$

This solution satisfies the conditions that the tunnel surface is traction-free:

$$\tilde{\tau}_{rr} = \tilde{\tau}_{r\theta} = 0 \qquad r = 1 \qquad (7.9)$$

The boundary layer analysis is as before. Under the assumptions that $\varepsilon = \delta/a << 1$, we have in outer coordinates the boundary layer correction

$$\begin{aligned} \hat{\sigma}_{rr} = \hat{p} &= \left\{ \begin{array}{c} 1 \\ \frac{\nu}{1-\nu} \\ 0 \end{array} \right\} (Q + R\cos 2\theta)\exp\left(\frac{-1+i}{\sqrt{2}}\frac{r-1}{\varepsilon}\right) \\ \hat{\sigma}_{\theta\theta} &= \\ \hat{\sigma}_{r\theta} &= \end{aligned} \qquad (7.10)$$

At the tunnel boundary we must have

$$\tilde{p} + \hat{p} = 0 \qquad r = 1 \qquad (7.11)$$

It follows that

$$Q = \frac{S_1 + S_2}{(1+m)} \qquad R = \frac{2}{1+m}(S_2 - S_1) \qquad (7.12)$$

which complete the correction in the boundary layer.

Consider P wave incidence. Let us first note that asymptotically

$$\frac{\sigma^{\infty}_{22}}{\sigma^{\infty}_{11}} = \frac{\lambda}{\lambda+2G} = \frac{\nu}{1-\nu} \qquad r \to \infty \qquad (7.13)$$

Now

$$\tau_{11}^{\infty} + \tau_{22}^{\infty} = \sigma_{11}^{\infty} + \sigma_{22}^{\infty} - 2p^{\infty} = \sigma_{11}^{\infty} + \sigma_{22}^{\infty} - 2\left(\frac{\tau_{11}^{\infty} + \tau_{22}^{\infty}}{-2(1+m)}\right) \tag{7.14}$$

In view of (7.6) we get

$$\sigma_{11}^{\infty} + \sigma_{22}^{\infty} = \frac{2m}{1+m}(S_1 + S_2)P_o \tag{7.15}$$

and

$$p^{\infty} = \frac{-1}{2m}(\sigma_{11}^{\infty} + \sigma_{22}^{\infty}) \tag{7.16}$$

Thus,

$$2P_oS_1 = \sigma_{11}^{\infty} - p^{\infty} = \sigma_{11}^{\infty} + \frac{\sigma_{11}^{\infty} + \sigma_{22}^{\infty}}{2m} \tag{7.17}$$

or

$$4mS_1P_o = (2m + 1)\sigma_{11}^{\infty} + \sigma_{22}^{\infty} \tag{7.18.a}$$

Similarly

$$4mS_2P_o = (2m + 1)\sigma_{22}^{\infty} + \sigma_{11}^{\infty} \tag{7.18.b}$$

It follows then

$$\frac{S_2}{S_1} = \frac{(2m+1)\ \sigma_{22}^{\infty} + \sigma_{11}^{\infty}}{(2m+1)\ \sigma_{11}^{\infty} + \sigma_{22}^{\infty}} = \frac{2m\nu + 1}{2m+1-2m\nu} \tag{7.19}$$

in view of (7.13).

This is so far a general relation for a plane P wave. In the limit of $m \to 0$, i.e., $G/\beta \to 0$

$$S_1 \to S_2 \tag{7.20}$$

In view of (7.7 - 7.12), the limiting solution is then independent of θ,

specifically,

$$\frac{p}{P_o S_1} = 2\left[-1 + \exp\left(\frac{-1+i}{\sqrt{2}}\,\frac{r-1}{\varepsilon}\right)\right]$$

$$\frac{\tau_{rr}}{P_o S_1} = 2\left(1 - \frac{1}{r^2}\right)$$

$$\frac{\tau_{\theta\theta}}{P_o S_1} = 2\left(1 + \frac{1}{r^2}\right)$$

$$\frac{\sigma_{rr}}{P_o S_1} = -\frac{2}{r^2} + 2\exp\left(-\frac{1+i}{\sqrt{2}}\,\frac{r-1}{\varepsilon}\right)$$

$$\frac{\sigma_{\theta\theta}}{P_o S_1} = \frac{2}{r^2} + \frac{2\nu}{1-\nu}\exp\left(-\frac{1+i}{\sqrt{2}}\,\frac{r-1}{\varepsilon}\right)$$

$$\sigma_{r\theta} = 0 \qquad (7.21)$$

Numerical results are shown for the following inputs: diameter 2a = 3 m, $\omega = 10\ \text{sec}^{-1}$ and Gk = 1, so that $\delta/a \tilde{\sim} 0.1$. Three values of G/β are considered, $G/\beta = 0.0044$, 1 and ∞.

Figure 7.1 shows Eq. (7.21). The effective stresses vanish several radii away from the tunnel, and the total stresses consist of the pore pressure only. This checks with Eq. (3.17) in that for $\beta \gg G$ it is the fluid elasticity alone which transmits P waves. It is nevertheless remarkable that in the neighborhood of the tunnel the solid stresses do not vanish; their isotropic character is of course due to the isotropy of the far field ($r/a \gg 0$, $r/\ell \ll 1$). Contrasting this with Figures 7.2 ($G/\beta = 1$) and 7.3 ($G/\beta \tilde{\sim} \infty$, pure solid with $\rho_w = 0$), the influence of pore fluid is evidently profound.

The results of S wave incidence is shown in Figures 7.4 to 7.6. The effects of different G/β are most pronounced near the tunnel.

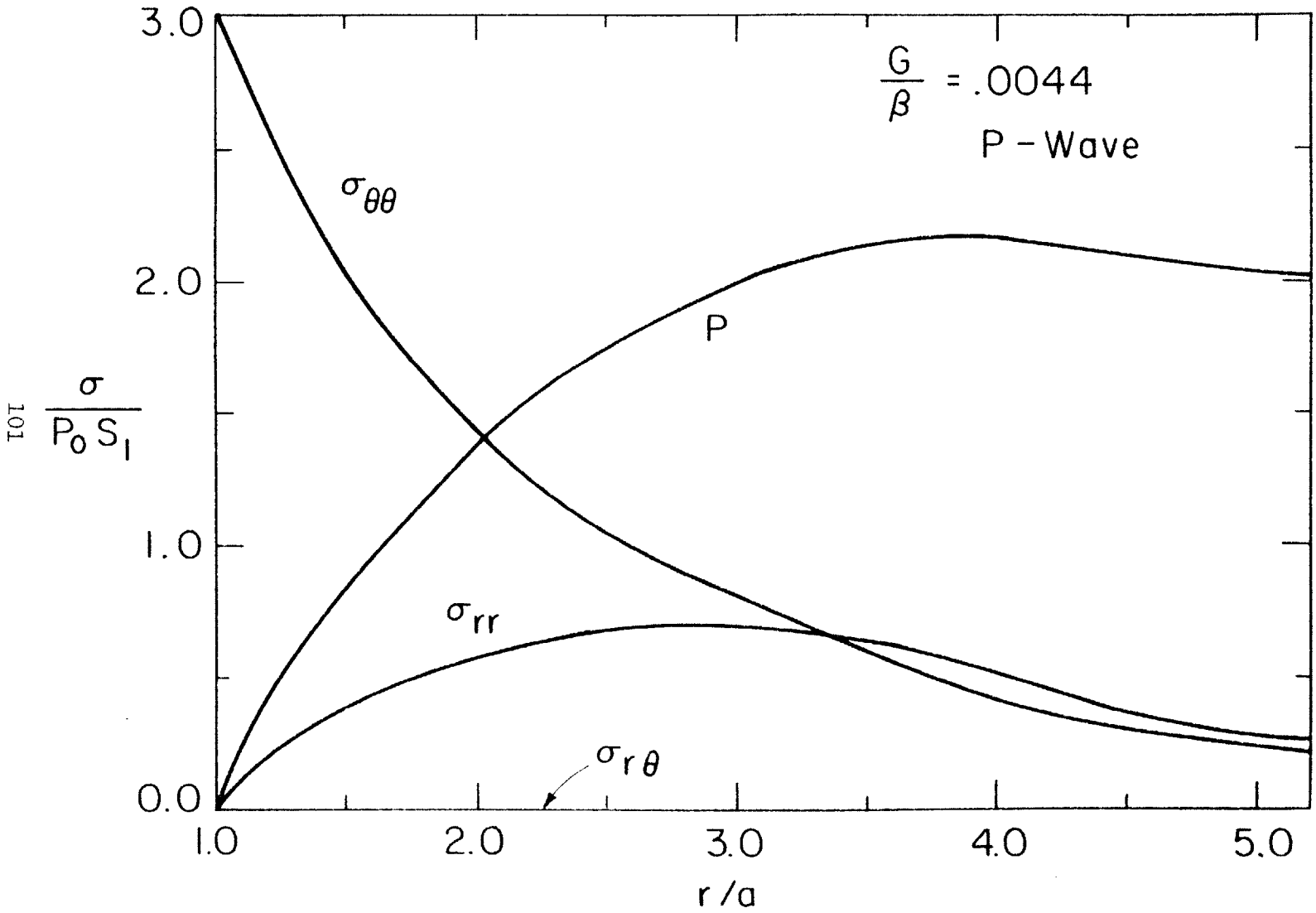

Figure (7.1)

Distribution of dimensionless effective stresses and pore pressure in response to P wave incidence on a small circular tunnel of radius as for $G/\beta=.0044$ and $Gk/\omega=0.1$. Distribution is axisymmetric.

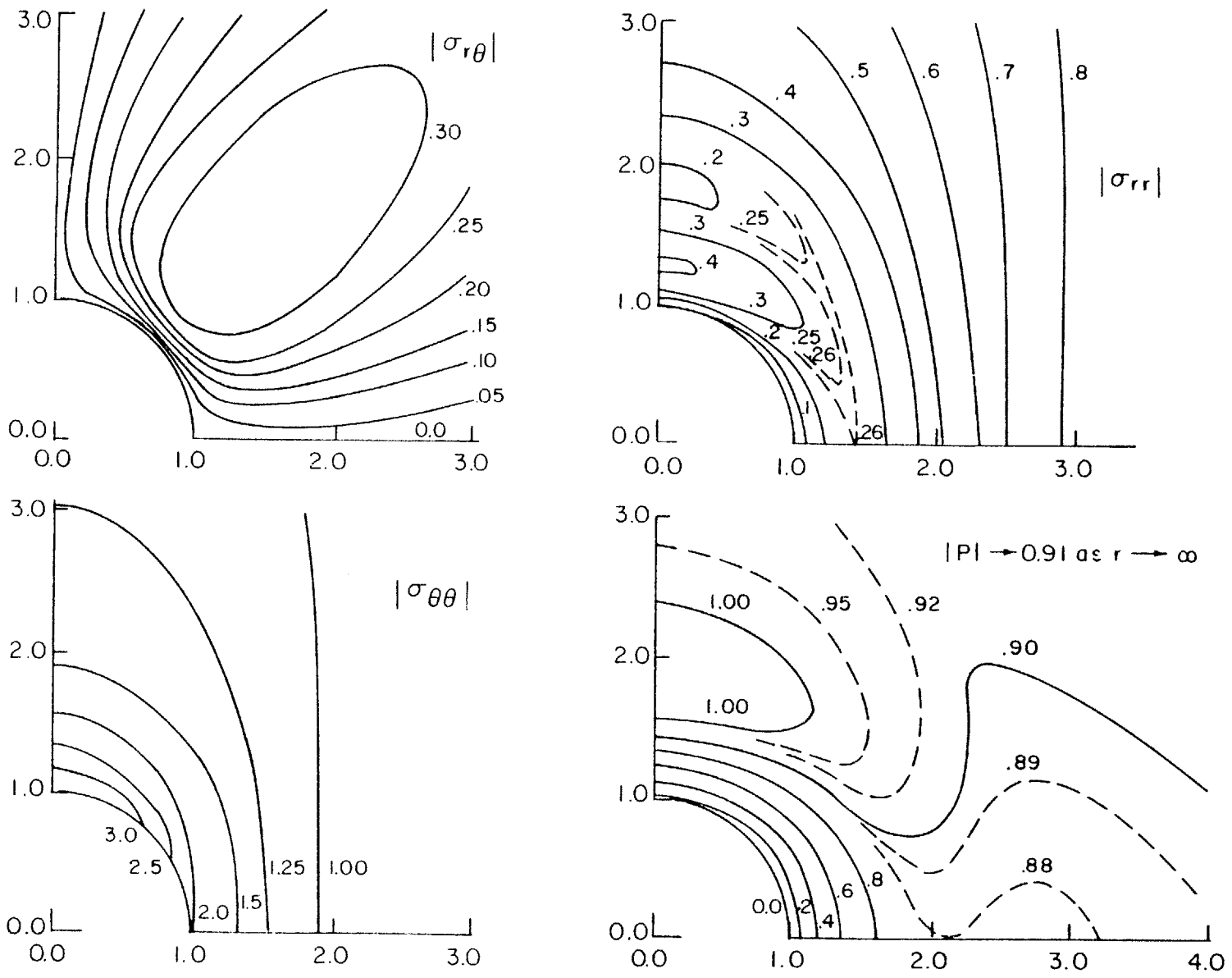

Figure (7.2)

Distribution of dimensionless effective stresses and pore pressure for P wave incidence, $G/\omega = 1.0$, $Ck/\omega = 0.1$. Normalizing scale is $P_o S_1$, cf. (7.6).

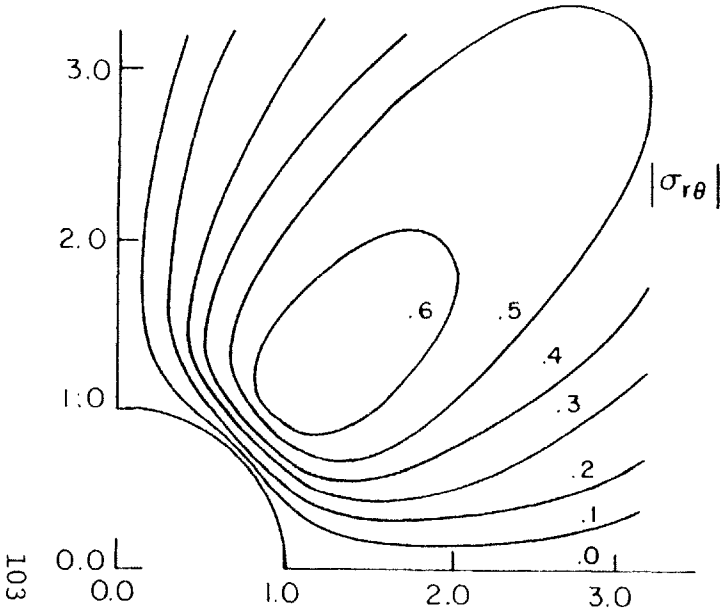

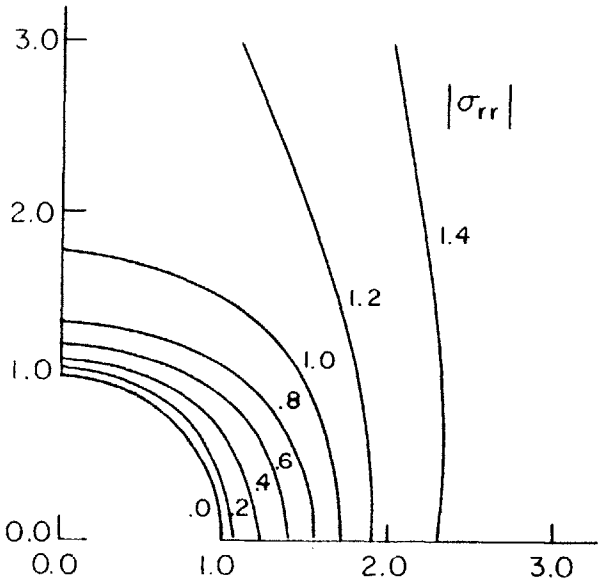

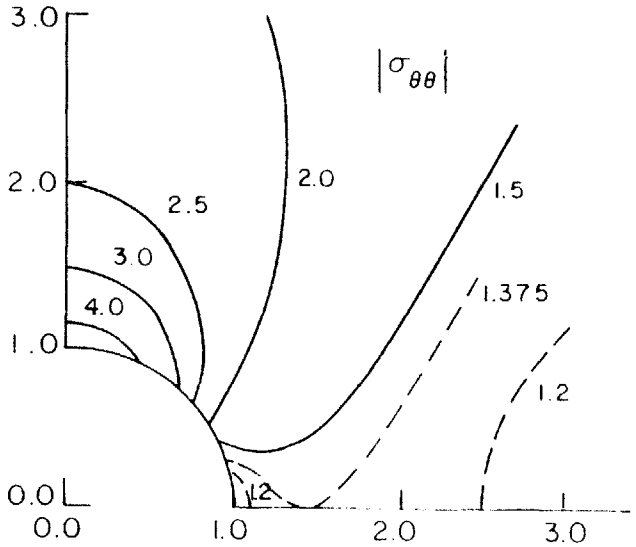

Figure (7.3)

Distribution of dimensionless effective stresses for P wave incidence, and dry soil ($G/ = \infty$, $\rho_w = 0.0$).

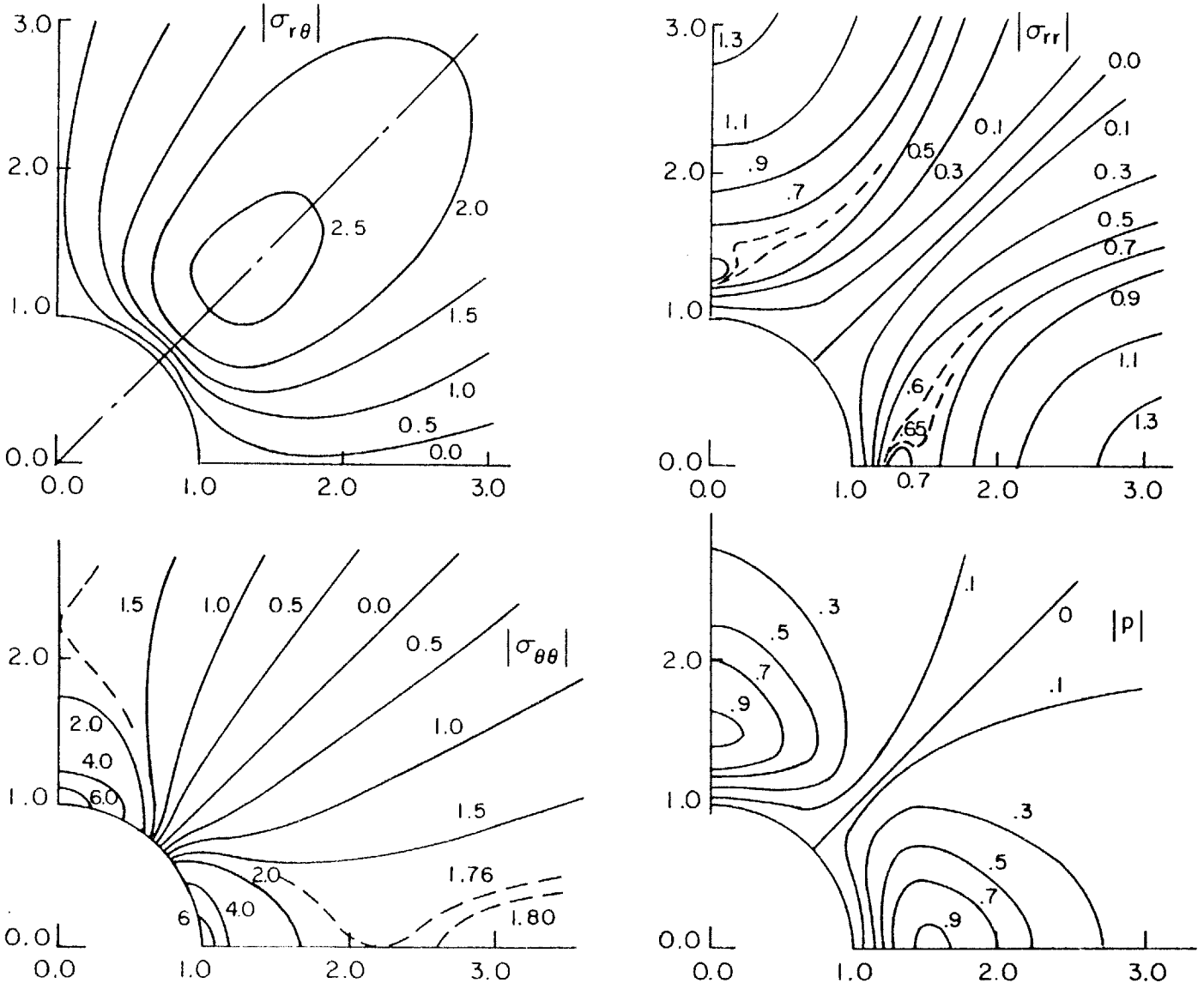

Figure (7.4)

Distribution of dimensionless effective stresses and pore pressure scaled by $P_o S_1$ for SV wave incidence, $G/\beta = 1.0$, $Gk/\omega = 0.1$.

Figure (7.5)

Distribution of dimensionless effective stresses and pore pressure for SV wave incidence, $G/\beta = .0044$, $Gk/\omega = 0.1$. Shear stresses same as in Figure 7.4.

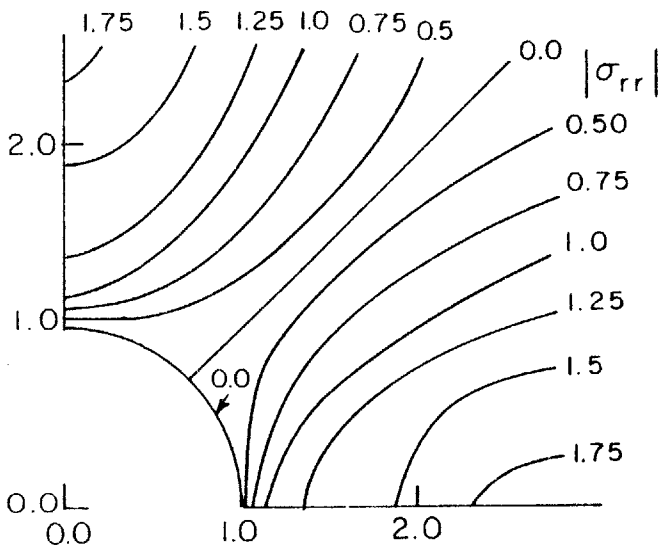

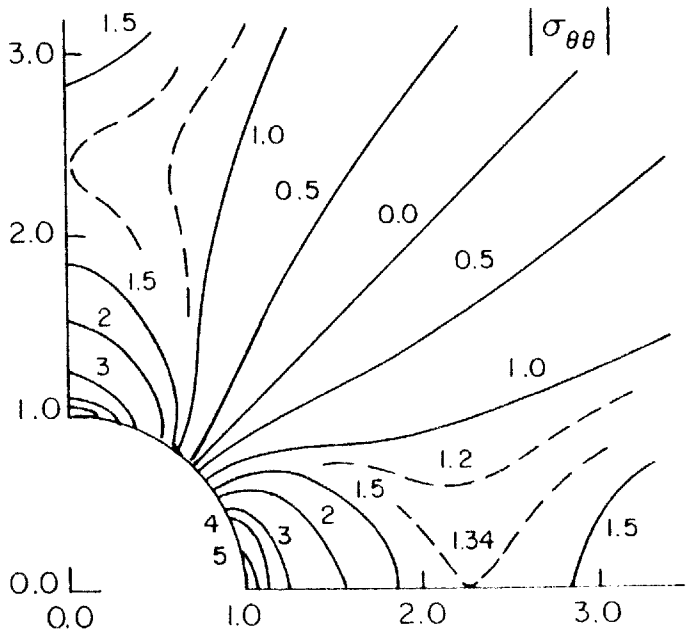

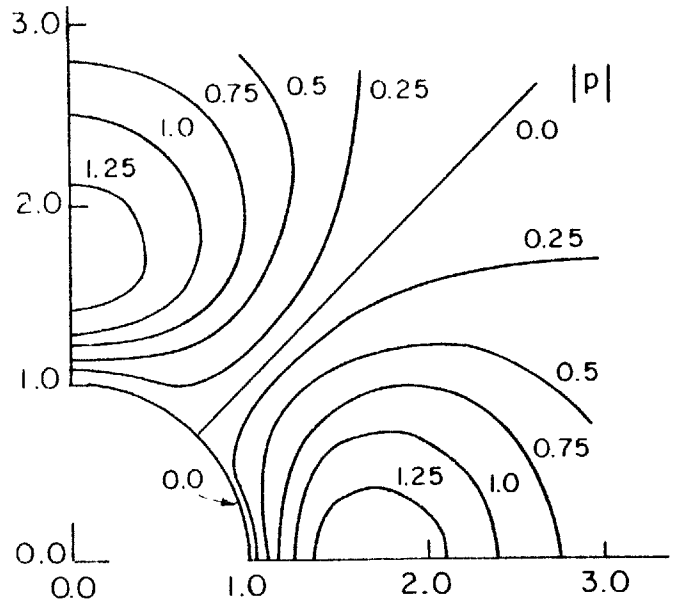

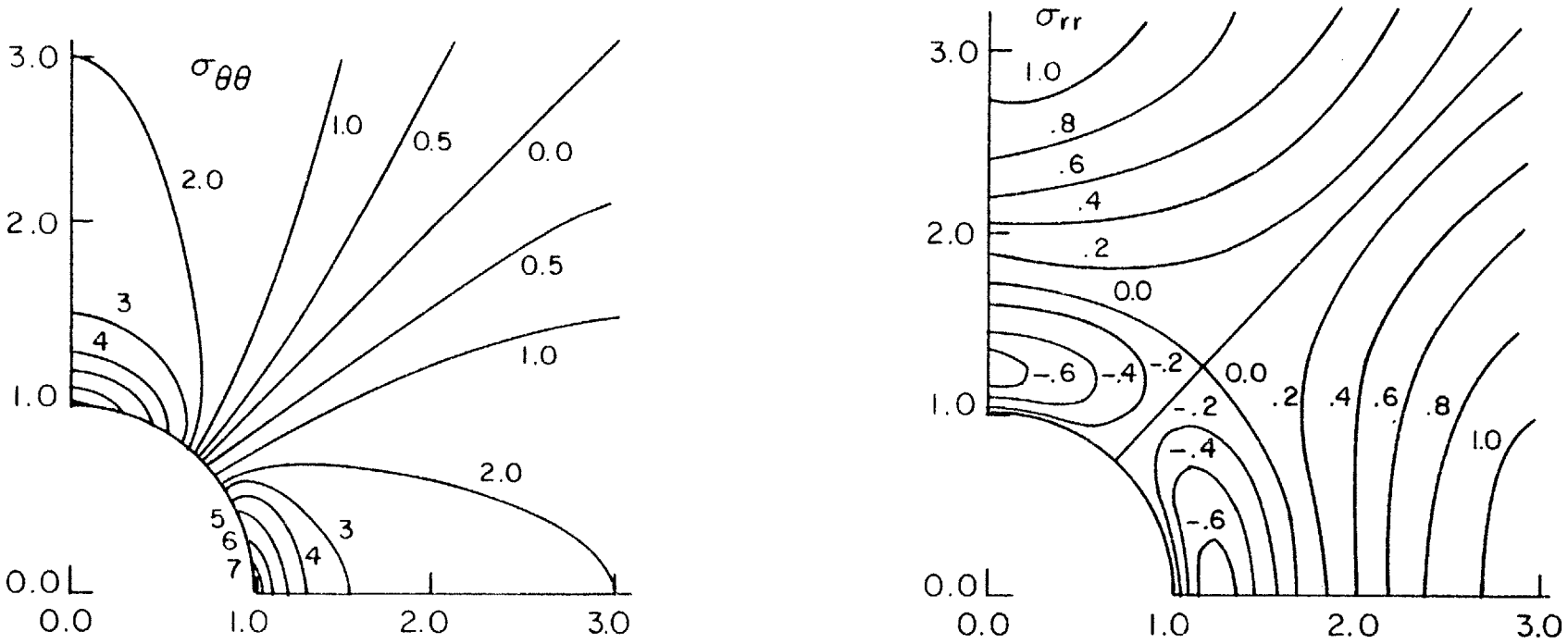

Figure (7.6)

Distribution of dimensionless effective stresses for SV wave incidence and ($G/\beta = \infty$, $\rho_w = 0$). Shear stresses same as in Figure 7.4.

8. RAYLEIGH WAVES IN A HALF SPACE

Consider a porous half space $y < 0$ with fluid saturated up to the free surface $y = 0$. A Rayleigh surface wave propagates along the free surface. What is the motion of the porous solid and of the fluid? Jones (1961) and Deresiewicz (1962) treated the full Biot equations and studied the complex speed which has a small imaginary part representing damping. To the leading order the damping effect can be ignored and the boundary layer approximation is especially simple.

Firstly, the governing equations (3.17) and (3.19) are formally the same as the classical elastodynamics of a pure solid when ρ_e and λ_e are used. On the free surface the traction-free conditions $\tau_{12} = \tau_{22} = 0$ further implies that the $\tilde{\tau}_{12} = \tilde{\tau}_{22} = 0$. Referring to Eq. (3.28) it is clear that the outer problem is formally identical to the classical case of pure solid without water. In particular, the wave speed, real to the first approximation, satisfies the Rayleigh relation as long as λ_e and ρ_e are used to replace the usual λ and ρ.

In terms of the customary potentials ϕ and ψ,

$$\tilde{v}_1 = \frac{\partial \phi}{\partial \xi} + \frac{\partial \psi}{\partial \eta}, \quad \tilde{v}_2 = \frac{\partial \phi}{\partial \eta} - \frac{\partial \psi}{\partial \xi} \tag{8.1}$$

We express the solution as follows

$$\phi = A_1 e^{q\eta} \tag{8.2.a}$$

$$\psi = \frac{2q}{i(1 + s^2)} A_1 e^{s\eta} \tag{8.2.b}$$

where the factor $\exp(i(\xi-\tau))$ is omitted in this section and

$$q^2 = 1 - \frac{\omega^2 K^2}{L^2 C_p^2} \qquad s^2 = 1 - \frac{\omega^2 K^2}{L^2 C_s^2} \tag{8.2.c,d}$$

where $K = 2\pi/\ell$ is the wave number of the Rayleigh wave. The outer stresses are

$$\tilde{p} = -iA_1 \frac{\beta}{nG} (q^2 - 1) e^{q\eta} \tag{8.3.a}$$

$$\tilde{\sigma}_{11} = iA_1 \{ [\frac{2\nu}{1-2\nu} q^2 - \frac{2(1-\nu)}{1-2\nu}] e^{q\eta} + \frac{4sq}{1+s^2} e^{s\eta} \} \tag{8.3.b}$$

$$\tilde{\sigma}_{22} = iA_1 \{ [\frac{2(1-\nu)}{1-2\nu} q^2 - \frac{2\nu}{1-2\nu}] e^{q\eta} - \frac{4sq}{1+s^2} e^{s\eta} \} \tag{8.3.c}$$

$$\tilde{\sigma}_{12} = A_1 2q(-e^{q\eta} + e^{s\eta}) \tag{8.3.d}$$

The solid velocity components are

$$\tilde{v}_1 = iA_1 (e^{q\eta} - \frac{2sq}{1+s^2} e^{s\eta}) \tag{8.4.a}$$

$$\tilde{v}_2 = A_1 (q\, e^{q\eta} - \frac{2q}{1+s^2} e^{s\eta}) \tag{8.4.b}$$

The boundary layer corrections are given by Eqs. (3.44) and (3.46) with

$$A = \frac{i\beta}{nG} (q^2 - 1) A_1 \tag{8.5}$$

In Figure 8.1 the pore pressure is plotted for various parameters. In Figure 8.2 the solid stresses for fully saturated solid are compared with those for the dry soil; the difference is particularly strong in shear σ_{12}. In these cases $s \ll q$ so that σ_{12} attenuates in depth very slowly.

Let us again study the maximum depth d for a fixed stress angle as in §5.3. The "stress angle" ϕ defined by (5.9) is calculated for the Rayleigh wave for a range of "earthquake intensity parameter" α defined by:

$$\alpha = \frac{|a|}{g} \tag{8.6}$$

where a is the amplitude of the verticle particle acceleration at the surface and g is the gravitational acceleration. Results are shown in Figure 8.3 giving the non-dimensional depth Kd for three different values of the ratio G/β, namely, $G/\beta = 0.0044$, 1.0 and ∞. In the last case, ρ_w is put equal to zero, and this corresponds to dry soil. The dashed curves are for $\phi = 30°$ at which slide failure would occur for some soil, while the solid lines are for $\phi = 90°$, at which tension would begin, at least for one instant of the wave period. In contrast to the gravity problem of §5, these depths are far greater than the boundary layer thickness.

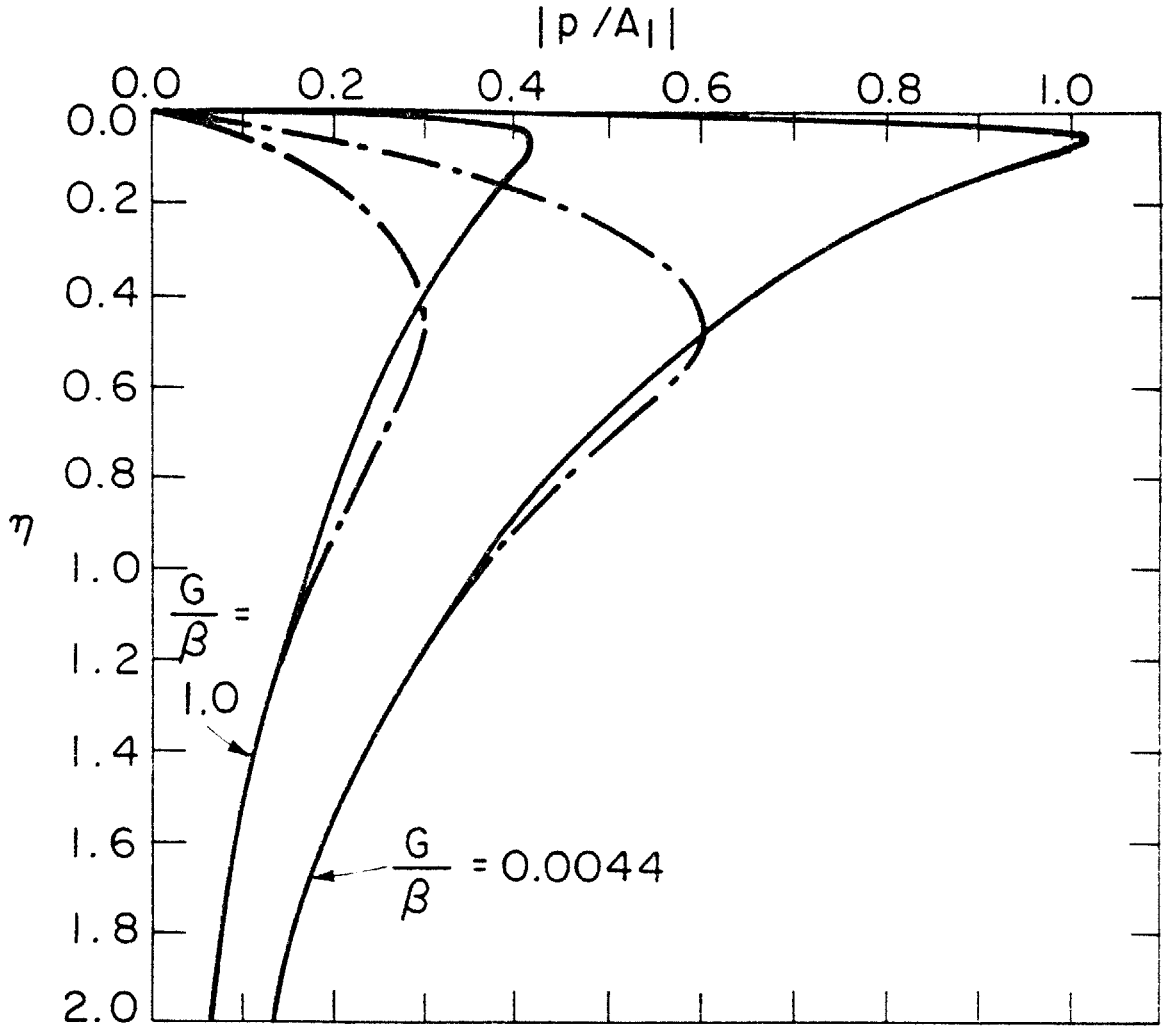

Figure (8.1)

Rayleigh wave in poro-elastic half-space. Distribution of dimensionless pore pressure with depth for both fine sand _____, $k=10^{-8}$ m^3sec/kg and coarse sand ——·——, $k=10^{-6}$ m^3 sec/kg. For each sand $G/\beta = .0044$ and $1(G=10^7$ $N/m^2)$. A_1 is defined by Eq. (8.2a).

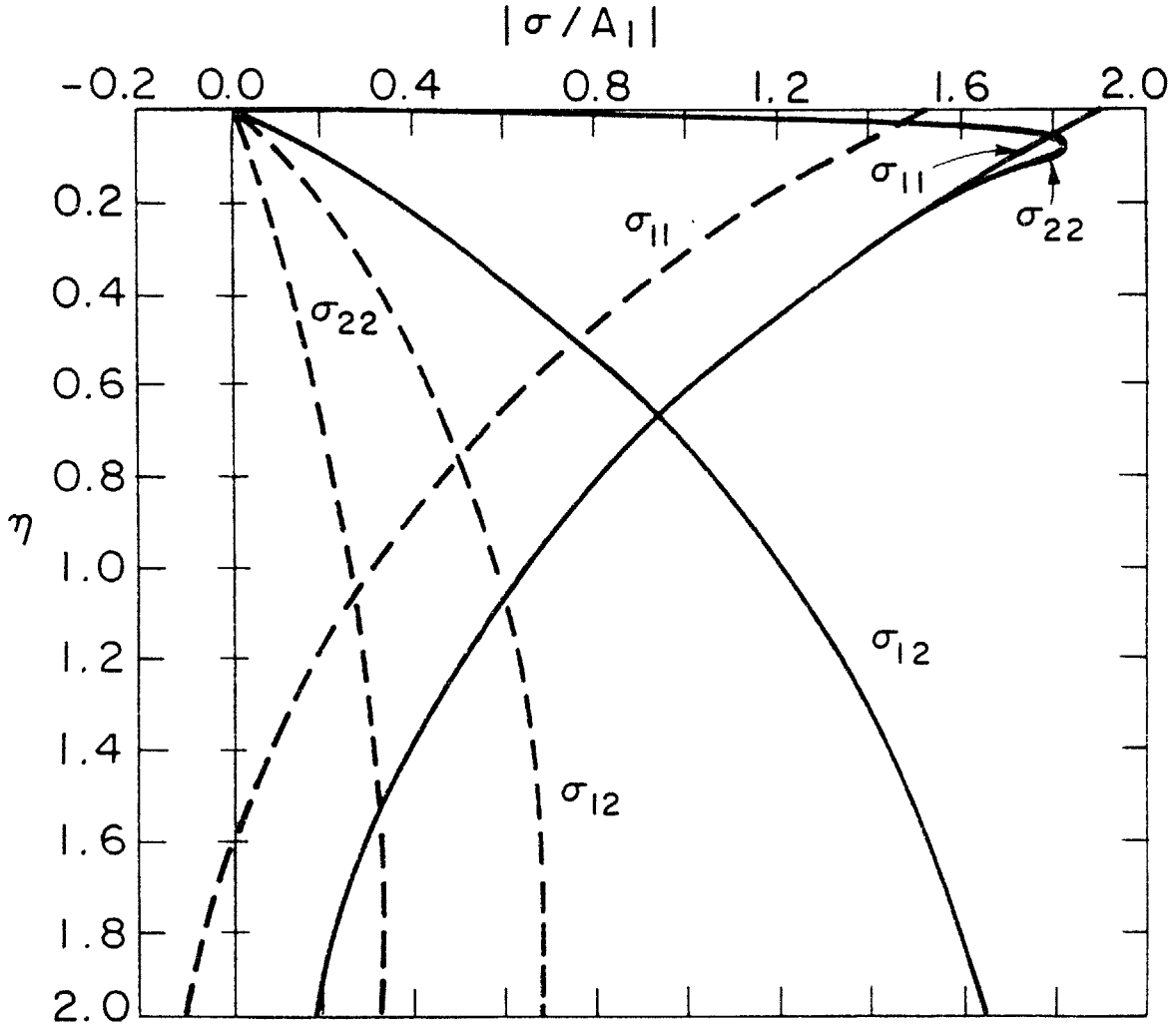

Figure (8.2)

Distribution of dimensionless effective stresses amplitude for Rayleigh wave in poro-elastic half-space. Two cases are shown for comparison, ------, dry soil and _____, saturated soil with $G/\beta = .0044$, $1 = 10^{-8}$ $m^3/sec\ kg$ (fine sand). $G=10^7$ N/m^2 for both cases.

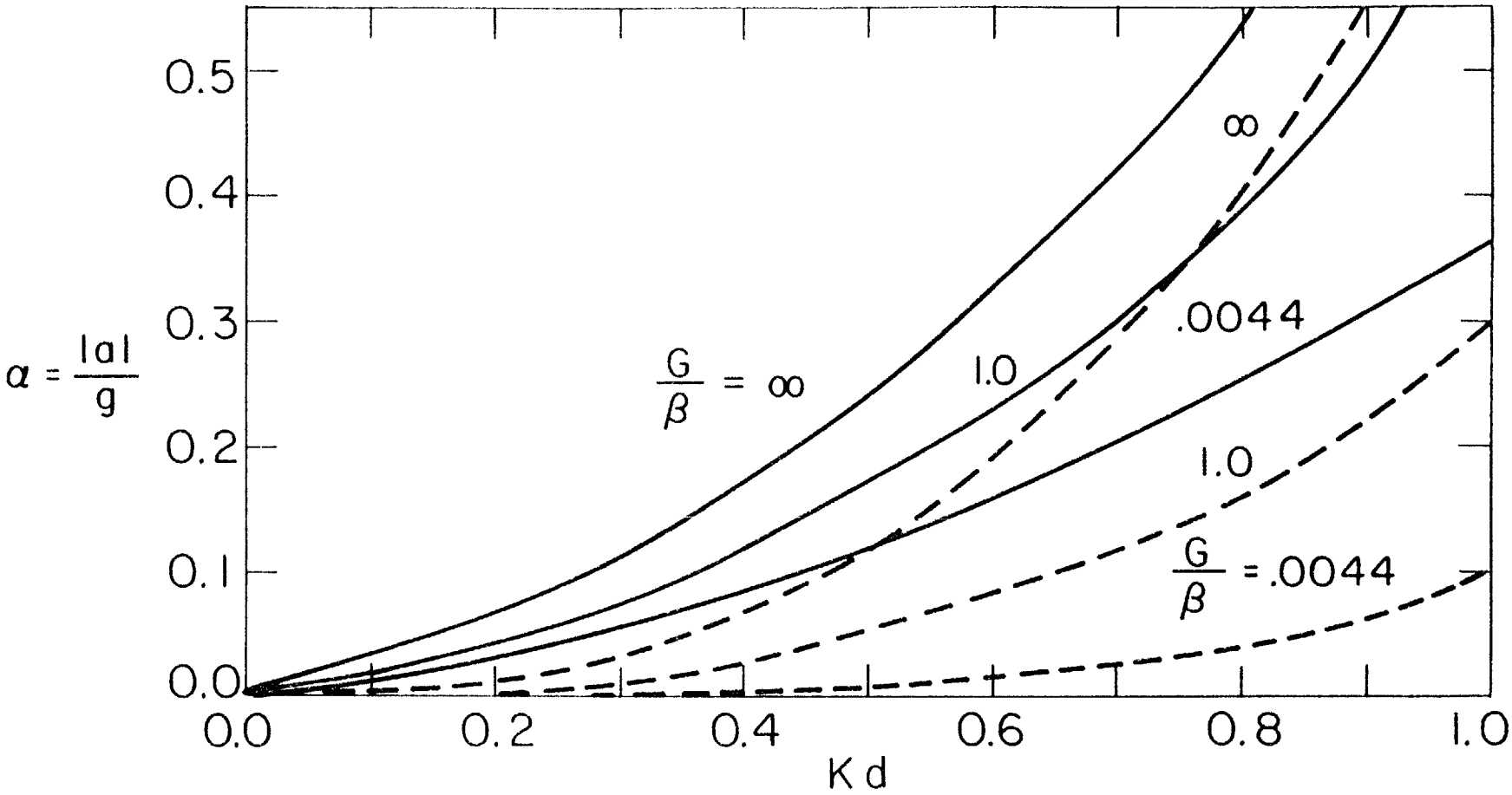

Figure (8.3)

Dimensionless depths above which there is momentary tension (———) or stress angle reaches 30° (------). The abscissa is the earthquake intensity factor $\alpha = |a|/g$; $|a|$ = amplitude of the vertical acceleration of a surface particle and g = gravitational acceleration. G/β = .0044, 1.0 and ∞. K is the Rayleigh wave number.

CONCLUDING REMARKS

From a physical view point, the boundary layer theory simply establishes in a quantitative manner the characteristics of the dynamical responses of low permeability porous media under wave action. For such low permeability porous media, the tendency of water flow relative to the solid under wave action is highly resisted so that such relative motion would be very small and water and soil would move essentially together. The only exception to such flow pattern is near a free surface where the water is more free to squeeze in and out of the free surface. Thus, away from the free surface, Darcian flow can be neglected and hence, the two phases would act as an equivalent one-phase media with properties obtained by averaging the solid and fluid properties (e.g. Equations (3.20a), (3.20b) etc.). However, this does not mean any decoupling of the pore pressure and the solid stress, but instead simply means that the coupling equations are simplified in such a way that enables us to cast it in terms of one specific combination of pore pressure and solid stress, that is the total stress τ_{ij}, and thus appear as a single phase equation. This reduction of the problem to single phase formualtion will not be possible near the free surface, and the more complicated two-phase nature of the media is essential in the analysis here. Therefore, the gross simplification, which is commonly done in the porous media literature, of assuming single phase formulation will be wrong near the free surface.

Another satisfying result of the analysis is that the general boundary layer solugion (§3.2) is obtained for arbitrary shape of the boundaries and with relative ease, because of the one-dimensional nature of the boundary layer.

It is remarkable that the boundary layer does not affect the traction on the free surface so that the outer solution may first be solved by ordinary methods of elasticity theory. Afterwards, the pore pressure can be calculated straightforwardly from the dilation of the solid matrix. By involving the free surface condition or the pore pressure, the boundary layer correction can be deduced which in turn introduces a correction in the diagonal stress along the free surface.

Of course, in the boundary layer, there is relative motion between the fluid and the solid and hence, viscous dissipation takes place only near free surfaces. This would be anticipated from physical grounds, because deep within low permeable soils, one would not expect significant dissipation to occur.

In this thesis, we have only studied the effect of pore fluid to the leading order. If one is interested in the attenuation of seismic waves in a porous media or of surface water waves by the porous sea bed, a Poincare type of perturbation method can be used to the order $O(\delta/L)$ in much the same way as one deals with fluid waves as damped by the viscous boundary layer. This method is again vastly simpler than the direct solution of the full poro-elastic equations.

A final point is to remark that the conceptual model represented here as a boundary layer theory is generic, and it is believed that it would work just as well if more realistic constitutive equations (e.g., non-linear stress-strain relation) were used instead of those used in the present study. Moreover, the significant simplification offered by using the boundary layer analysis would hopefully encourage the introduction of these more complicated but realistic soil constitutive relations into the analytical studies of porous media and still leave the problem tractable to analytical means. Also, there is the possible extension of the theory to the precisely analogous field of thermoelasticity (e.g., Nowaki, 1978).

REFERENCES

Atkin, R.T. and Craine, R.E. (1976a) " Continuum Theories of Mixtures: Gasic Theories and Historical Development," Q. Jl. Mech. Appl. Math. 29, 209-244.

Atkin, R.T. and Craine, R.E. (1976b) "Continuum Theories of Mixtures: Applications," J. Inst. Maths. Applics 17, 153-207.

BIOT, M.A. (1941) "General Theory of Three-Dimensional Consolidation," J. Appl. Physics, 12, 155-164.

Biot, M.A. (1956) "Theory of Propagation of Elastic Waves in a Fluid-Saturated Porous Solid, Part I: Low Frequency Range and Part II: Higher Frequency Range," J. Acoust. Soc. Am., Vol. 28, 168-191.

Bioley, B.A. and Weiner, J.H. (1960) "Theory of Thermal Stresses," John Wiley, New York.

Bowen, R.M. (1976) "Theory of Mixtures", in Continuum Physics, Vol. II, ed. Eringen, Academic Press, New York.

De Josselin de Jong, G. (1956) "What happens in the soil during Pile-driving," de Ingenieur, No. 25, pp. B.77-B.88.

Deresiewicz, H. (1962) "The Effect of Boundaries on Wave Propagation in a Liquid Filled Porous Solid: Part IV, Surface Waves in a Half Space," Bull. Seismol. Soc. Am., 52, 627-638.

Geertsma, J. (1976) "Numerical Treatment of Some Geomechanical Problem Areas in Oil and Natural Gas Production," Num. Methods in Geomechanics, Vol. II, ed. C.S. Desai, ASCE, 759-772.

Geertsma, J. and D.C. Smit (1961), "Some Aspects of Elastic Wave Propagation in Fluid-Saturated Porous Solids," Geophysics, 26, 169-181.

Jager, J.C. and N.C.W. Cook (1976), Fundamentals of Rock Mechanics, Halsted Press, New York.

Jones, J.P. (1961), "Rayleigh Waves in a Porous Elastic Fluid Saturated Solid," J. Acoustical Soc. Am., 33, 959-962.

Lambe, T.W. and R.V. Whitman (1969), Soil Mechanics, John Wiley & Sons.

Liu, P.L-F. and R.A. Dalrymple (1979) "Water Waves Propagated over Elastic Porous Sea Beds," to appear in ASCE, W.W. Division.

Longuet-Higgins, M.S. (1950) "A Theory of the Origin of Microseisms," Phil. Trans. Roy. Soc. Lond. A, 243, 1-35.

Love, A.E.H. (1927) A Treatise on the Mathematical Theory of Elasticity, 4th edition, Cambridge University Press, New York, pp. 205.

McNamee, J. andGibson, R.E. (1960) "Displacement Functions and Linear Transforms Applied to Diffusion through Porous Media," Quart, J. Mech. Appl. Math. 13, 210-227.

Madsen, O.S. (1978) "Wave Induced Pore Pressures and Effective Stresses in a Porous Bed," Geotechnique 28, no. 4, 377-393.

Milne-Thomson, L.M. (1967) Theoretical Hydrodynamics, 5th ed., Macmillan.

Nikolaeviskii, V.N., K.S. Vasniev, A.T. Gordbunov and G.A. Zotov (1970) "Mechanics of Saturated Porous Media," 335 pp., Nedra, Moscow.

Nowacki, W. (1978) Dynamic Problems of Thermoelasticity, Noordhoff.

Prevost, A. (1980) "Theory of Mixtures and Porous Media Dynamics," to appear in J. Inst. Maths. Applics.

Rice, J.R. and M.P. Clearly (1976) "Some Basic Stress Diffusion Solution for Fluid-Saturated Porous Media with Compressible Constituents," Rev. Geoph. Space Physics 14, No. 2, 227-241.

Simons, D.A. (1977) "Boundary-Layer Analysis of Propagating Mode II Cracks in Porous Elastic Media," Mech. Phys. Solids Vol. 25, pp. 99-115.

Terzaghi, K. (1925) "Principle of Soil Mechanics," (Leinpzig F. Deuticke, 1925), Eng. News Record (1925), a series of articles.

Terzaghi, K. and R.B. Peck (1948) Soil Mechanics in Engineering Practice, Wiley, New York.

Timoshenko, S. and J.N. Goodier (1951), Theory of Elasticity, McGraw-Hill, New York.

Truesdell, C. and Toupin, R. (1960) "The Classical Field Theories," Handbuch der Physik, Ed. S. Flügge, Vol. III/1, p. 226, Springer-Verlag, Berlin

Van der Kogel, H. (1977) "Wave Propagation in Saturated Porous Media," Ph.D. Thesis, Cal. Inst. Tech., Pasadena, Calif., U.S.A.

Verruijt, A. (1969) "Elastic Storage of Aquifers," in Flow Through Porous Media, R.J.M. DeWiest ed., Academic Press.

Yamamoto, T. (1977), "Wave Induced Instability in Sea Beds," ASCE Symposium on Coastal Sediments '77, Charleston, S.C.

Yamamoto, T., H.L. Koning, H. Sellmeiher and E.V. Hijum (1978) "On the Response of a Poro-elastic Bed to Water Waves," J. Fluid Mechanics, Vol. 78, part 1, 193-206.

APPENDIX I

EXTENSION OF LOVE'S RELATIONS TO SATURATED PORO-ELASTIC MEDIA

In one phase elastic media, displacement components may be related to Airy's stress function F by the relations of Love (1930, pp. 205). We will extend these relations to our case of saturated porous media as follows.

The effective stresses σ_{ij} and solid displacements V_i are related through Hook's Law (1.18) or (1.19). In plane strains, the relations can be written also in the form:

$$\sigma_{11} = \lambda\Theta + 2G\frac{\partial V_1}{\partial x} \tag{I.1a}$$

$$\sigma_{22} = \lambda\Theta + 2G\frac{\partial V_2}{\partial y} \tag{I.1b}$$

$$\sigma_{12} = G\left(\frac{\partial V_1}{\partial y} + \frac{\partial V_2}{\partial x}\right) \tag{I.1c}$$

where

$$\Theta = \frac{\partial V_1}{\partial x} + \frac{\partial V_2}{\partial y} \; ; \quad \lambda = \frac{2G\nu}{1-2\nu} \equiv \text{Lamé constant.}$$

We further introduce Airy's stress function F which is related to the total stresses τ_{ij} by

$$\tau_{11} = \sigma_{11} - p = \frac{\partial^2 F}{\partial y^2}$$

$$\tau_{22} = \sigma_{22} - p = \frac{\partial^2 F}{\partial x^2}$$

$$\tau_{12} = \sigma_{12} = -\frac{\partial^2 F}{\partial x \partial y} \qquad \text{(I.2)}$$

Now, adding (I.1a) and (I.1b) we get

$$2(\lambda + G)\Theta = \sigma_{11} + \sigma_{22} = (\tau_{11} + \tau_{22}) + 2p \qquad \text{(I.3)}$$

Outside the boundary layer, p is given by the outer solution (4.9b)

$$p = \frac{-1}{2(1+m)} \quad (\tau_{11} + \tau_{22}) \qquad \text{(I.4)}$$

Thus, substituting into (I.3) and using (I.2),

$$\Theta = \frac{m}{2(\lambda+G)(1+m)} \quad \nabla^2 F \ ; \text{ (outside the boundary layer)} \qquad \text{(I.5)}$$

Therefore, I.1a) becomes

$$\sigma_{11} = \frac{\partial^2 F}{\partial y^2} + p = \frac{\lambda m}{2(\lambda+G)(1+m)} \quad \nabla^2 F + 2G \frac{\partial V_1}{\partial x}$$

which, after using (I.4), gives

$$2G \frac{\partial V_1}{\partial x} = \frac{\partial^2 F}{\partial y^2} - \frac{1}{2(1+m)} \left[\frac{(1+m)\lambda+G}{\lambda+G}\right] \nabla^2 F$$

or,

$$2G \frac{\partial V_1}{\partial x} = - \frac{\partial^2 F}{\partial x^2} + \frac{\lambda+2G-G/(1+m)}{2(\lambda+G)} \nabla^2 F \qquad (1.6)$$

Similarly, from (I.1b) we get,

$$2G \frac{\partial V_2}{\partial y} = - \frac{\partial^2 F}{\partial y^2} + \frac{\lambda+2G-G/(1+m)}{2(\lambda+G)} \nabla^2 F \qquad (I.7)$$

Integrating (I.6) with respect to x and (I.7) with respect to y we get the extended Love relations

$$2GV_1 = - \frac{\partial F}{\partial x} + \Gamma \int \nabla^2 F \, dx \qquad (I.8a)$$

$$2GV_2 = - \frac{\partial F}{\partial y} + \Gamma \int \nabla^2 F \, dy \qquad (I.8b)$$

with

$$\Gamma = \frac{\lambda+2G-G/(1+m)}{2(\lambda+G)} \qquad (I.8c)$$

APPENDIX II

COMPARISON BETWEEN EXACT AND BOUNDARY LAYER SOLUTIONS FOR PROPAGATING SEA WAVES OVER INFINITELY THICK SEA BED

The problem is treated by Yamamoto et.al. (1978) and Madsen (1978), and the exact solution of Biot's equations is obtained. From Yamamoto (1978, Equations (3.8) to (3.15)), the exact solution for the pore pressure p, the horizontal displacement V_1 and the vertical displacement V_2 in the sea bed are, in dimensional variables:

$$p = \{1 - \frac{im\omega''}{-\lambda''+i(1+m)\omega''}]\exp(Ky) + \frac{im\omega''}{-\lambda''+i(1+m)\omega''}\exp(\lambda' y)\}p_o \exp[i(Kx-\omega t)]. \tag{II.1}$$

$$V_1 = i\{m\frac{-[1+2(1-\nu)\lambda'']+i(1-2\nu)\omega''}{-\lambda''+i(1+m)\omega''}\exp(Ky)[1-\frac{m\lambda''}{-\lambda''+i(1+m)\omega''}]Ky\exp(Ky)$$

$$+\frac{m}{-\lambda''+i(1+m)\omega''}\exp(\lambda' y)\}\frac{P_o}{2KG}\exp[i(Kx-\omega t)] \tag{II.2}$$

$$V_2 = -\{[1+m\frac{1+(1-2\nu)(-\lambda''+i\omega'')}{-\lambda''+i(1+m)\omega''}]\exp(Ky) - [1-\frac{m\lambda''}{-\lambda''+i(1+m)\omega''}]Ky\exp(Ky)$$

$$-\frac{m(1+\lambda'')}{\lambda''+i(1+m)\omega''}\exp(\lambda' y)\}\frac{P_o}{2KG}\exp[i(Kx-\omega t)] \tag{III.3}$$

where

$$\lambda'^2 = K^2 - i\,\frac{\omega}{k}\left[\frac{n}{\beta} + \frac{(1-2\nu)}{2(1-\nu)G}\right. \tag{II.4}$$

$$\lambda'' = (\lambda'-K)/K \tag{II.5}$$

$$\omega'' = \frac{-(1-\nu)}{(1-2\nu)K^2}\left[\frac{\omega}{k}\left(\frac{n}{\beta} + \frac{(1-2\nu)}{2(1-\nu)G}\right)\right] \tag{II.6}$$

$$m = \frac{nG/\beta}{1-2\nu} \tag{II.7}$$

We will now prove that the leading order approximation of this exact solution, for small k, (i.e., for δ defined in (3.37) much less than K^{-1}), is in complete agreement with the boundary layer solution obtained in §4 (Equations 4.14).

From (II.4) and (3.37)

$$\lambda'^2 = K^2 - \frac{i}{\delta^2}$$

But, as $\delta \ll K^{-1}$, then to the leading order

$$\lambda'^2 \simeq \frac{-i}{\delta^2} \qquad \text{or} \qquad \lambda' \simeq -\frac{\sqrt{-i}}{\delta} \tag{II.8}$$

so that the solution is bounded as $y \to -\infty$.

Also, from (II.5)

$$\lambda'' = \frac{\lambda'-K}{K} \simeq \frac{\lambda'}{K} \simeq -\frac{\sqrt{-i}}{K\delta} \tag{II.9}$$

to the leading order.

And from (II.6):

$$\omega'' = \frac{-(1-\nu)}{(1-2\nu)} \quad \frac{1}{(K\delta)^2} \tag{II.10}$$

Hence, we may neglect λ'' with respect to ω''. Applying this to (II.1) we get:

$$p \simeq [\frac{1}{1+m}\exp(Ky) + \frac{m}{1+m}\exp(\frac{1-i}{\sqrt{2}\,\delta}\, y)]p_o \exp[i(Kx-\omega t)] \tag{II.11}$$

which agrees with the first equation of (4.14).

In order to complete the comparison, we need to deduce the displacements V_1 and V_2 for the approximate boundary layer solution. In Appendix I, the relations of Love which relates the displacement components to Airy's stress function F for one-phase elastic media, is extended to our case of saturated porous media. Outside the boundary layer, these relations are [Equation (I.8)].

$$2GV_1 = -\frac{\partial F}{\partial x} + \Gamma \int \nabla^2 F \, dx \tag{II.12a}$$

$$2GV_2 = -\frac{\partial F}{\partial y} + \Gamma \int \nabla^2 F \, dy \tag{II.12a}$$

with

$$\Gamma = \frac{\lambda+2G-G/(1+m)}{2(\lambda+G)} \tag{II.12c}$$

From (4.4) and (4.8), the boundary layer solution for F, in dimensional variables, is

$$F = \frac{P_o}{K^2}(1-Ky)e^{Ky}\exp[i(Kx-\omega t)] \tag{II.13}$$

Substituting (II.13) into (II.12a,b) we get

$$V_1 = i\{\frac{(1-2\nu)m}{1+m} + Ky\}e^{Ky}\frac{P_o}{2KG}\exp[i(Kx-\omega t)] \tag{II.14}$$

$$V_2 = -\{(1 + \frac{(1-2\nu)m}{1+m} - Ky\}e^{Ky}\frac{P_o}{2KG}\exp[i(Kx-\omega t)] \tag{II.15}$$

Equations (II.14) and (II.15) are the outer region solution for the displacements. But, from (3.44), it is seen that the boundary layer correction to the displacements are $O(K\delta)$. Then, (II.14) and (II.15) are the leading order solution in the whole domain. Ignoring the terms of $O(K\delta)$ or smaller in the exact expressions for V_1 and V_2 (e.g., (II.2) and (II.3) respectively), they reduce exactly to the boundary layer solution (II.14) and (II.15).

APPENDIX III

THE APPROXIMATE SOLUTION FOR GRAVITY WAVES OVER A POROUS MEDIA OF FINITE THICKNESS

The outer problem is casted in terms of Airy's function F which satisfies:

$$\nabla^2\nabla^2 F=0 \qquad \text{in the porous layer} \qquad \text{(III.1)}$$

with the boundary conditions:

$$\tau_{22} = \frac{\partial^2 F}{\partial \xi^2} = -e^{i\theta} \; ; \; \theta=\xi-\tau$$

$$\tau_{12} = -\frac{\partial^2 F}{\partial \xi \partial \eta} = 0 \qquad \text{at mud line } \eta=0 \qquad \text{(III.2)}$$

and,

$$2V_1 = -\frac{\partial F}{\partial \xi} + \Gamma \int \nabla^2 F \, d\eta = 0$$

$$\text{at bottom } \eta=-H \qquad \text{(III.3)}$$

$$2V_2 = -\frac{\partial F}{\partial \eta} + \Gamma \int \nabla^2 F \, d\eta = 0$$

The solution to (III.1) is

$$F = [A_1 e^{\eta} + A_2 e^{-\eta} + A_3 \eta e^{\eta} + A_4 \eta e^{-\eta}]e^{i\theta} \qquad \text{(III.4)}$$

The condition $\tau_{12}=0$ at $\eta=0$ gives

$$A_1-A_2+A_3+A_4 = 0 \tag{III.5}$$

while the condition $\tau_{22}= -e^{i\theta}$ at $\eta=0$ gives

$$A_1+A_2 = 1 \tag{III.6}$$

We now turn to the bottom boundary conditions. But first we have

$$\int \nabla^2 F d\xi = -2i[A_3 e^{\eta} - A_4 e^{-\eta}]e^{i\theta}$$

$$\int \nabla^2 F d\eta = 2[A_3 e^{\eta} + A_4 e^{-\eta}]e^{i\theta}$$

$$-\frac{\partial F}{\partial \xi} = -i[A_1 e^{\eta} + A_2 e^{-\eta} + A_3 \eta e^{\eta} + A_4 \eta e^{-\eta}]e^{i\theta}$$

$$-\frac{\partial F}{\partial \eta} = -[A_1 e^{\eta} - A_2 e^{-\eta} + A_3(1+\eta)e^{\eta} + A_4(1-\eta)e^{-\eta}]e^{i\theta}$$

Therefore, substituting into (III.3) we get

$$A_1 e^{-H} + A_2 e^{H} + (2\Gamma-H)e^{-H}A_3 - (2\Gamma+H)e^{H}A_4 = 0 \tag{III.7}$$

$$A_1 e^{-H} - A_2 e^{H} + (1-H-2\Gamma)e^{-H}A_3 + (1+H-2\Gamma)e^{H}A_4 = 0 \qquad \text{(III.8)}$$

By adding and subtracting (III.5) and (III.6) we get

$$A_1 = \frac{1}{2}[1-(A_3 + A_4)] \qquad \text{(III.9)}$$

$$A_2 = \frac{1}{2}[1 + (A_3 + A_4)] \qquad \text{(III.10)}$$

Further, by adding and subtracting (III.7) and (III.8) we get

$$2A_1 e^{-H} = -(1-2H)e^{-H}A_3 - (1-4\Gamma)e^{H}A_4 \qquad \text{(III.11)}$$

$$2A_2 e^{H} = (1-4\Gamma)e^{-H}A_3 + (1+2H)e^{H}A_4 \qquad \text{(III.12)}$$

Then, substituting (III.9) and (III.10) into (III.11) and (III.12) respectively we get,

$$[-2He^{-2H}]A_3 + [-e^{-2H} + (1-4\Gamma)]A_4 = -e^{-2H} \qquad \text{(III.13)}$$

$$[1-(1-4\Gamma)e^{-2H}]A_3 + [-2H]\ A_4 = -1 \qquad \text{(III.14)}$$

which can be solved for A_3 and A_4 using Cramer's rule to get:

$$A_3 = \frac{-1}{\Lambda'}\,[(1-4\Gamma)-(1-2H)e^{-2H}] \tag{III.15}$$

$$A_4 = \frac{-1}{\Lambda'}[(1+2H)e^{-2H} - (1-4\Gamma)e^{-4H}] \tag{III.16}$$

where

$$\Lambda' = (1-4\Gamma)(1+4e^{-4H})-[1+4H^2+(1-4\Gamma)^2]e^{-2H} \tag{III.17}$$

Thus, from (III.4), (III.9) and (III.10), we have

$$F=[\cosh\eta -(A_3+A_4)\sinh\eta + A_3\eta e^{\eta} + A_4\eta e^{\eta}]e^{i\theta}$$

Then, substituting from (III.15) and (III.16) with little rearrangement we get finally

$$F=[\cosh\eta + \alpha_1 \sinh\eta + \eta(\alpha_2\sinh\eta- \alpha_1\cosh\eta)]e^{i(\xi-\eta)} \tag{III.18}$$

where

$$\alpha_1 = \Lambda^{-1}[4H+2(1-4\Gamma)\sinh 2H]$$

$$\alpha_2 = \Lambda^{-1}[2-2(1-4\Gamma)\cosh 2H]$$

$$\Lambda = 2(1-4\Gamma)\cosh 2H-[1+4H^2+(1-4\Gamma)^2] \tag{III.19}$$

Part II

EXCITATION OF SURF-BEATS IN THE OCEAN

1. INTRODUCTION

1.1 General

The impingement of water waves on seashores is a phenomenon of great interest to coastal engineers as it is their task to address the important problems of beaches stability, nearshore dynamics and sedimentology. These problems are becoming of growing practical importance as increasing number of offshore engineering activities are taking place in the environment of the nearshore region of the ocean, and a necessary first step for satisfactory performance of such activities is to establish a thorough understanding of this new environment. More specifically, it is necessary to understand the structure of natural beaches, the various flow patterns (e.g. wave modes, currents, etc.) that exist there, the distribution of wave energy, the interaction of beaches with these forms of motion and the resulting formation of the various coastal patterns (e.g. caps, cusps, cresentic bars, etc.).

The near-shore

The nearshore region of the ocean may be divided into two main zones, separated by the surf or the breaker line, which is the line at which the incoming waves first break as they propagate shorewards. The motion seawards

of this line is essentially irrotational and in most cases, the potential theory is used adequately to describe most of its features. Due to wave breaking turbulence occurs in the zone shorewards of the surf line, called the surf zone, and therefore turbulent dissipation of the incoming wave energy. Thus it is evident that, dynamically, these two zones are drastically different.

The position of the boundary between these two zones, the surf line, depends on the certain beach and incident wave conditions and may move with time as conditions change. It may be very close to the shoreline or even disappear so that eventually there is no wave breaking and the incoming wave energy is mostly reflected, creating a standing wave pattern on the beach; which may be called reflective beach. On the other hand, the surf line may be far seawards, creating a large enough surf zone so that all the incoming wave energy is destroyed with no wave reflection; the beach may be called dissipative. The dynamics and sedimentology of the nearshore region would evidently change drastically according to whether the beach is dissipative or reflective. This in turn depends on the relative importance of the surf zone. The distinction between reflective and dissipative systems is of course not a sharp one. On some beaches, waves may break on a series of bars, re-form as smaller non-breaking waves and reflect off the beach face. Thus, on the

largest scale with a wide surf zone, the nearshore system is dissipative, but may behave as a reflective system on the much smaller scale of the beach face (Guza and Inman, 1975).

Besides dissipation and reflection, the energy of the incident wave may be routed to generate or interact with other flow patterns in the nearshore region. Among the most important of such flow patterns are water currents and edge waves. For example, in the surf zone, rip currents are known and feared by many bathers and it has long been obvious that rip currents must form the return flow for water thrown ashore by breaking waves, (however, a thorough study of their dynamics is quite recent as will be shown later).

Edge waves are waves periodic in the longshore direction, sometimes called transverse waves, and exist only in the shallow regions of the ocean. For a long time, edge waves were regarded as a mere curiosity in hydrodynamics. Accordingly, in his discussion of Stokes' edge wave solution, Lamb (1945, p. 447) states that "it does not appear that the type of motion here referred to is very important." However, there is now considerable evidence which indicates that edge waves are common in occurence and of fundamental importance in the dynamics and sedimentology of the nearshore region through their interaction with incident wave and surf.

Indeed, edge waves may be related to beach scouring and formation of coastal patterns (e.g. caps, cusps, crescentic bars, etc.) which are rythmical in the longshore direction (Bowen and Inman, 1969).

Rythmical longshore patterns which are often observed in shorelines and nearshore bathymetry are essentially of two types, cuspate and crescentic. Cuspate features are usually formed at the shoreline, the cusps being concave seawards, that is, the points of the cusps point seaward. These occur over a wide range of sizes from beach cusps of a few meters wavelength to major shoreline features ($\sim$ 1 km or more) [Dolan and Ferm, 1968].

The second type of feature, the crescentic or lunate bar, is essentially a submerged sand bar, concave shorewards. These can be found within a bay of a finite width (Bowen and Inman, 1971), or off long straight beaches (Shepard, 1952; Homma and Sonu, 1963). Wavelengths of crescentic bars vary from 500 meters to 3 km (Sonu, 1972).

Edge Waves and Shelf Waves

Edge waves which are relevant to many of the above mentioned coastal patterns have characteristic length scale much larger than a typical incident wavelength ($\sim$ 100 ms.). Edge waves of such length scale are usually called "surf beats". The term was introduced by Munk (1949) who first

recognized and recorded such waves in the ocean, having periods of several minutes. Thus, with respect to the ocean waves frequency spectrum, surf beats lie between ocean tides and swells. Munk, Snodgrass and Gilbert (1964) showed from wave records that at this range of the spectrum, the ocean wave energy is almost exclusively in the form of edge wave modes, (except in the rare occurence of tsunamis).

Interest in such waves is derived also from various other reasons. For example, in studying energy trapping into a continental shelf wave-guide (Munk, Snodgrass and Gilbert, 1964), in studying the nearshore energy budget and in determining waves run-up on beach face (beach flooding).

Edge waves of such frequency range can also be of importance with regard to many offshore and harbor engineering practice. For example, many man-made or natural harbors have natural frequencies of the order of several minutes. Thus, one would expect a constructive interference between "surf beats" modes and such harbors. For the same reason, large vessels, tankers, etc. who are moored in the open sea may be resonated at this frequency range by "surf beats".

1.2 Incident vs. Edge Waves

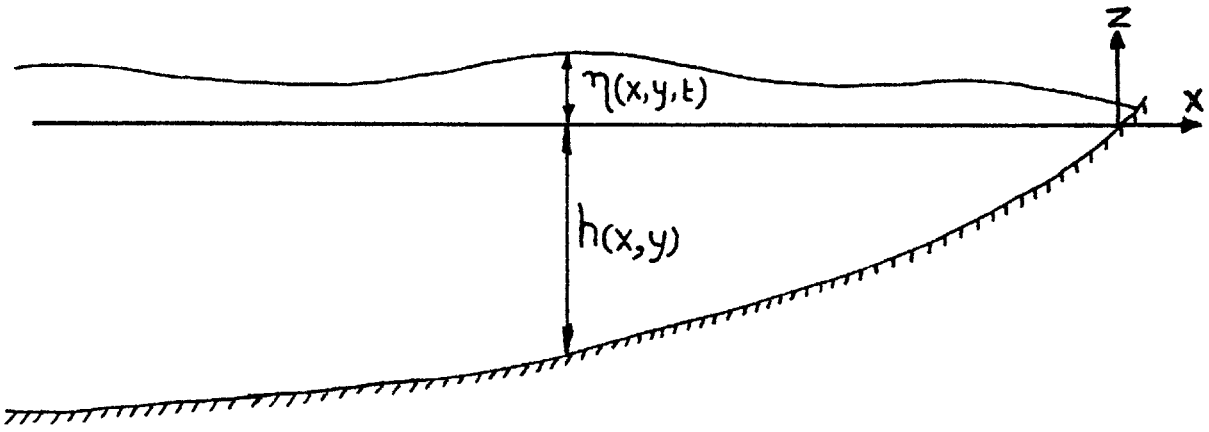

Figure (1.1)

The physical situation is indicated in Figure (1.1) to represent a general ocean beach.

In the inviscid theory, the Laplace equation should be satisfied

$$\nabla^2 \Phi = 0 \tag{1.1}$$

by the velocity potential Φ with the boundary conditions

$$\begin{aligned} &\Phi_n = 0 && \text{at } z = -h(x,y) \\ &\Phi_x \eta_x + \Phi_y \eta_y - \Phi_z + \eta_t = 0 && \text{at } z = \eta(x,y,t) \\ &g\eta + \Phi_t + \tfrac{1}{2}(\Phi_x^2 + \Phi_y^2 + \Phi_z^2) = 0 && \text{at } z = \eta(x,y,t) \end{aligned} \tag{1.2}$$

Solution to the linearized version of the problem in deep water zone ($h \to \infty$) is the plane progressive wave

$$\Phi = Ae^{kz} \exp[i(k_x x + k_y y - \omega t)] \tag{1.3}$$

with the dispersion relation

$$\omega^2 = gk \tag{1.4}$$

where $k = \sqrt{k_x^2 + k_y^2}$.

We note first that for this case, there is a continuous spectrum of frequencies defined by the dispersion relation for all real values of ω, and free motion could hence be expressed in terms of Fourier integral in time (t) for fixed, x, y and z. Therefore, the integral vanishes as $t \to \infty$ at all finite points so that the whole energy is ultimately transferred to infinity by radiation and only the forced periodic motion remains as $t \to \infty$.

We notice secondly from the dispersion relation that

$$\omega^2 > g|k_y| \tag{1.5}$$

where k_y is the wave number measured in the longshore direction. When $\omega^2 < g|k_y|$, it follows from the dispersion relation that waves cannot propagate in deep water and can only be confined (trapped) to near the shallow water. In fact, the frequencies of such waves (usually called edge or trapped waves) form a discrete spectrum out of the range of the continuous spectrum defined by (1.4). Consequently we have a mixed spectrum for surface waves in the ocean.

There are two main differences between continuous and discrete spectra. First, resonance is usually associated

with the discrete spectrum when a forced periodic motion of frequency ω approaches one of the spectral frequencies ω_n, and the singularity associated with it, in the linear theory, is of the order of $|\omega - \omega_n|^{-1}$. However, resonance in a continuous spectrum occurs only at the so-called cut-off frequencies (real, lower limits of the continuous spectrum) if they exist (Ursell, 1952). As can be seen from Green's function, the singularity at a cut-off frequency is of the order of $|\omega - \omega_1|^{-1/2}$.

Secondly, unlike the discrete spectrum, the motion in the continuous spectrum could be determined uniquely from the motion of the boundaries together with the radiation condition of Sommerfeld (e.g., incident wave from infinity, as in (1.3)).

1.3 Edge Waves in the Ocean (Historical Background)

The analytical development of the edge wave theory was initiated by Stokes (1846) who first noted a solution of the linear water wave equations that represents edge waves ($\omega^2 < g|k_y|$) on a beach of constant slope ($h = -\tan\beta\, x$)

$$\phi = D\, e^{[K\cos\beta x + K\sin\beta z]} e^{i(Ky - \omega t)} \qquad (1.6)$$

with

$$\omega^2 = gK\sin\beta \; ; \quad K \equiv |k_y| \qquad (1.6a)$$

These waves propagate along the beach with their crests perpendicular to the shoreline and with amplitude

decaying exponentially out to the sea. Ursell (1952) showed that Stokes solution is only the lowest of the possible edge wave modes with the dispersion relation given by

$$\omega^2 = gK \sin [(2n+1)\beta] \qquad (1.6b)$$

for $n = 0,1,2,\ldots$. Ursell also confirmed experimentally the existance of such modes.

For arbitrary bottom shape, the edge wave modes and dispersion relations can be found numerically [see for example Bowen and Chapman, 1979], but they all have the same feature of being periodic in the longshore direction, vanish in deepwater and $\omega^2 < gK$. Aside from beaches, trapped waves may exist on a shelf or a submerged ridge (Munk, Snodgrass and Gilbert, 1964) and nearly trapped waves on submerged sills (Longuet-Higgins, 1967).

There are various theories of edge wave generation in the ocean, offering various mechanisms through which energy can be fed to such trapped modes, under various physical situations.

Munk, Snodgrass and Carrier (1956) have shown from wave records that edge waves are important components in the disturbances produced by storms moving along the coastline. Such direct transfer of energy from the wind field to the wave system do occur as the wind blows at a speed close to the phase velocity, of a progressive edge

wave whose wavelength is determined by the spatial extent of the driving wind. The typical period of this kind of edge wave is several hours and the wavelength $\sim$ 10 km. Details of this theory were first given by Munk, Snodgrass and Carrier (1956) and by Greenspan (1957).

On the other end of the scale, Bowen & Inman (1969) found field evidence of standing edge waves of periods comparable in order of magnitudes to the period of the incoming swells (i.e., of several seconds). Their experimental study shows that rip currents (which are steady and have longshore periodicity) can result from the interaction of edge waves and normally incident breaking waves of equal frequencies. Galvin (1965) reported experiments in which very low amplitude incident waves excited subharmonic edge waves having a frequency one-half that of the incident wave. Motivated by these findings, Guza and Davis (1974) and Guza and Bowen (1976) developed a theory of subharmonic generation of standing edge wave of frequency ω via non-linear interaction with a normally incoming and reflected wave of frequency 2ω. Using the shallow water theory and accounting for cubic nonlinearity and radiation damping, they were able to predict both initial resonant growth and the final equilibrium amplitude. The theory was further extended by Minzoni and Whitham (1977) who formulated the problem in the full water wave theory (Equations (1.1) and (.12)) without making the

shallow water approximation in order to solve for more steep beach angle β. Their theory confirms the shallow water results in the limit of small β.

Surf Beats

Edge waves of intermediate periods of several minutes, i.e., in the frequency band between wind-generated waves and oceanic tides, are also commonly observed on natural beaches. It is thus of interest to consider how such standing edge waves are generated. The subharmonic generation of Guza and Davis (1974) is irrelevant here, as it requires periods of the incident waves of 15-30 seconds or higher, but, typically there is not much surface wave energy at such long periods (Sonu, 1972).

Gallagher (1967) gave a non-linear resonance theory for the generation of surf beat. Using a standard pertubation expansion for the velocity potential Φ, and expressing the incident wind waves as a Fourier-Stieltjes expansion in frequency ω, and longshore wave number K, he formulated the second order response in terms of the solution to an inhomogeneous Laguerre differential equation (Abramowitz and Stegun, 1965). The forcing terms are quadratic products of the incident wave components. Hence, each pair of incident swell trains, (K_1,ω_1) and (K_2,ω_2) may be thought of as a "group" which contribute one particular low amplitude wave

$(K_1 + K_2, \omega_1 + \omega_2)$, to the total second order response. The homogeneous solution of the Laguerre equation gives the discrete modes of the free edge wave on the constant sloping beach, and therefore, for some combination of $(K_1 + K_2, \omega_1 + \omega_2)$ in the driving function which coincides with those of the free waves, resonances occur. Gallagher empirically inserted a linear friction coefficient in the equation, in order to obtain a finite edge wave amplitude at resonance. Theory along this line has been pursued further by King and Smith (197). However, in these works, two more simplifying assumptions were made: Processes inside the surf zone are totally ignored, (b) Incident wind-generated waves do not change their wavelength as they shoal, and their amplitude grow exponentially towards shore. These assumptions, along with the uncertainties of linear friction coefficient are over simplified in our view.

1.4 Outline of the Present Thesis

Our aim here is to construct a consistent theory which will demonstrate that nonlinear interactions among wind-generated, incident wave group can excit shelf waves and surf beats. So, beside the beach geometry as in Figure (1.1), which is relevant to surf beats excitation, we will consider as well shelf wave excitation over submarine ridges, as depicted in Figure (1.2).

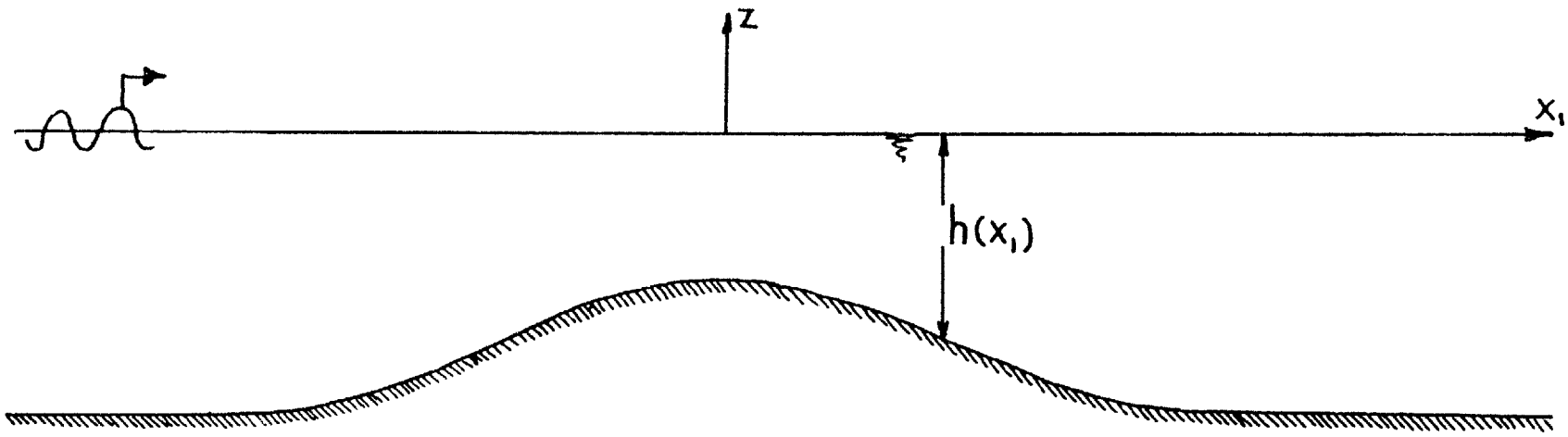

Figure (1.2)

Definition Sketch for the Submerged Ridge Problem.

In our analysis, we consider a wavefield consisting of a relatively short scale incident wave, the dominant Fourier component of which is characterized by (ω,k) and a long scale edge wave characterized by (Ω,K). The wavelength of the long scale motion is taken to be much greater than that of the short scale motion, i.e., $|k| >> |K|$. Now, if the short swells are modulated slowly over length and time scale commensurate with one of the edge wave discrete modes, resonance excitation can certainly occur at the second order response. This is essentially Gallagher (1971) resonance mechanism. However, when the edge wave is resonated for a sufficient time, its amplitude will grow so that cubic nonlinearity can become important, and hence we shall go to the third order response. The cubic nonlinear interaction between the incident wave Φ_i and the edge wave Φ_e can give rise to various harmonics. In particular, the possible combination (Φ_i,Φ_i,Φ_e) and (Φ_e,Φ_e,Φ_e) will give rise to the harmonics $(\omega\pm\omega\pm\Omega,\ k\pm k\pm K)$ and $(\Omega\pm\Omega\pm\Omega,\ K\pm K\pm K)$ respectively. Hence, these combinations will produce terms having the resonant edge wave harmonic (Ω,K). One or both of these terms can offset the resonant growth of edge wave and hence, a certain dynamical balance can be established. The most interesting situation is when all relevant terms, i.e., the two different cubic contributions denoted by (Φ_i,Φ_i,Φ_e) and $(\Phi_e\cdot\Phi_e,\Phi_e)$, and the resonant forcing, come to the dynamical

balance equation at the same level. It will be shown that this can be established by developing *a significant interaction theory* between the large scale edge wave and the short scale incident wave.

From the energy balance standpoint, the two cubic terms (Φ_i,Φ_i,Φ_e) and (Φ_e,Φ_e,Φ_e) in the dynamical balance equation can be interpreted as representing possible energy transfer between incident and edge waves, and radiation damping effects, respectively. Hence, in the present theory the dynamical balance is attained without resorting to empirical bottom friction (as in Gallagher (1971) and King and Smith, 1978). The obtained nonlinear equation will enable us to trace the evolution of these growing edge waves, from their initial resonant growth till their equilibrium amplitude is reached, if such an equilibrium state exists.

Following a systematic perturbation scheme, a nonlinear evolution equation will be obtained for the trapped wave and solved for some given initial conditions. In the process, some subtle aspects of the problem will be elucidated, such as: (a) In what way does the short (incident) wave interact with the long (edge) wave? (b) How is energy transferred between them? (c) What feed back effect is there on the incident wave as the edge wave grows? (d) What is the nature of the edge wave growth (is it an instability mechanism or a nonlinear forced resonance? (e) What mechanism(s) causes the growth of edge waves and what mechanism(s) limits its growth?

2. FORMULATION AND SOLUTION PROCEDURE

The problem is formulated as follows

$$\nabla^2\Phi = 0 \qquad \text{(in the fluid)} \qquad (2.1)$$

$$\Phi_n = 0 \qquad z = -h(x,y) \qquad (2.2)$$

$$\Phi_x\eta_x + \Phi_y\eta_y - \Phi_z + \eta_t = 0 \qquad z = \eta(x,y,t) \qquad (2.3)$$

$$g\eta + \Phi_t + \frac{1}{2}(\Phi_x^2 + \Phi_y^2 + \Phi_z^2) = 0 \qquad z = \eta(x,y,t) \qquad (2.3a)$$

Assuming the motion to be weakly nonlinear, one may expand the velocity potential Φ, and the water elevation η as follows:

$$\Phi = \sum_{n=1}^{\infty} \varepsilon^n \sum_{m=-n}^{n} \phi_{nm}\, e^{im\Psi/\varepsilon} \qquad (2.4a)$$

$$\eta = \sum_{n=1}^{\infty} \varepsilon^n \sum_{m=-n}^{n} \eta_{nm}\, e^{im\Psi/\varepsilon} \qquad (2.4b)$$

where $\varepsilon << 1$ characterizes the bottom slope and introduces the "slow variables":

$$x_1 = \varepsilon x\ ,\quad x_2 = \varepsilon^2 x\ ,\ldots\rightarrow \frac{\partial}{\partial x} = \frac{\partial}{\partial x} + \varepsilon\frac{\partial}{\partial x_1} + \ldots \qquad (2.5a)$$

$$y_1 = \varepsilon y\ ,\quad y_2 = \varepsilon^2 y\ ,\ldots\rightarrow \frac{\partial}{\partial y} = \frac{\partial}{\partial y} + \varepsilon\frac{\partial}{\partial y_1} + \ldots \qquad (2.5b)$$

$$t_1 = \varepsilon t\ ,\quad t_2 = \varepsilon^2 t\ ,\ldots\rightarrow \frac{\partial}{\partial t} = \frac{\partial}{\partial t} + \varepsilon\frac{\partial}{\partial t_1} + \ldots \qquad (2.5c)$$

where the phase function Ψ/ε and all Φ_{nm}, η_{nm} are functions of these slow variables; (Φ_{nm} are also functions of z). For Φ and η to be real, we require

$$\phi_{nm} = \phi^*_{n,-m} \tag{2.6a}$$

$$\eta_{nm} = \eta^*_{n,-m} \tag{2.6b}$$

where * denotes complex conjugate. The phase function Ψ/ε is defined by:

$$\nabla_1 \Psi = \left(\frac{\partial \Psi}{\partial x_1}, \frac{\partial \Psi}{\partial y_1}\right) = \vec{k} \tag{2.7a}$$

and

$$\frac{\partial \Psi}{\partial t_1} = -\omega \equiv \text{constant} \tag{2.7b}$$

where $\vec{k}$ and ω are respectively the wave-number vector and wave frequency of the incident swell.

The slope of the wave surface is assumed to be $O(\varepsilon)$ also. These expansions, which are essentially Stokes perturbation series (Wehuasen and Laitone, 1960, p. 654) with the idea of multiple scaling also incorporated, were used by many (for example, Benney and Roskes, 1969; Chu and Mei, 1970). In these works, the large scale motion (m=0) were always kept small compared to the shorter waves (m=1). This is inherent, by construction, in the expansions (2.4), where the ratio of the large scale to the small scale motion is of the order of ε. Thus, all these works, based on (2.4), may be

categorized as "weak interaction theories".

In the present work, we relax this constraint and allow for a significant interaction between the two scales by using the following expansion instead of (2.4):

$$\Phi = \sum_{n=0}^{\infty} \varepsilon^n \sum_{m=-n}^{n} \phi_{nm} e^{im\Psi/\varepsilon} \tag{2.8a}$$

$$\eta = \sum_{n=1}^{\infty} \varepsilon^n \sum_{m=-n}^{n} \eta_{nm} e^{im\Psi/\varepsilon} \tag{2.8b}$$

The difference between the two expansions, (2.4) and (2.8), is that in (2.8) we added the function Φ_{oo}, which is missing in the weak interaction theory. Indeed, corresponding to Φ_{oo} the long wave amplitude can be as large as the short wave amplitide, i.e., $O(\varepsilon)$.

The solution procedure starts by substituting the expansions (2.8) into the governing equation (2.1) and the boundary conditions (2.2) and (2.3). But, before the substitution, we will put the free surface boundary conditions (2.3a,b) in a more convenient form:

First, we can eliminate the water elevation η from the two boundary conditions (2.3a,b) to yield a single boundary condition in terms of Φ alone. Then, using Taylor Expansion to transfer the boundary condition from being applied at $z=\eta$ to being applied at the still water level $z=0$. We omit the algegraic details, which can be found in many references

(e.g Whitham, 1976) and give the end result:

$$\Phi_{tt} + g\Phi_z = [-\frac{1}{2}(\nabla\Phi)^2 + \frac{1}{2}\Phi_t\Phi_{zt}]_t - [\Phi_x\Phi_t]_x - [\Phi_y\Phi_t]_y$$

$$+ [\frac{1}{2g}(\Phi_t(\nabla\Phi^2))_z - \frac{1}{g^2}\Phi_t\Phi^2_{zt} - \frac{1}{2g^2}\Phi_{zzt}\Phi^2_t]_t$$

$$+ [\frac{-1}{2}\Phi_x(\nabla\Phi)^2 + \frac{1}{g}\Phi_x\Phi_t\Phi_{zt} + \frac{1}{2g}\Phi^2_t\Phi_{xz}]_x$$

$$+ [\frac{-1}{2}\Phi_y(\nabla\Phi)^2 + \frac{1}{g}\Phi_y\Phi_t\Phi_{zt} + \frac{1}{2g}\Phi^2_t\Phi_{yz}]_y + O(\Phi^4)$$

$$\text{at } z=0 \qquad (2.9)$$

This particular form of the boundary conditions was also used by Benney (1962) and Roskes (1969) among others.

Furthermore, the ocean bottom will be assumed here to be two-dimensional and slowly varying in the x-direction, i.e., $h=h(x_1)$. Thus, the bottom boundary condition (2.2) can be re-written as:

$$\Phi_z = -\varepsilon \frac{\partial h}{\partial x_1}\Phi_x \qquad \text{at } z=-h(x_1) \qquad (2.10)$$

Finally, we will assume that the swell is normally incident so that (2.7a) becomes:

$$\nabla_1\Psi = (\frac{\partial\Psi}{\partial x_1}, \frac{\partial\Psi}{\partial y_1}) = (k,0) \qquad (2.7c)$$

Now, substituting (2.8) into (2.1) and the boundary conditions (2.9) and (2.10), and separating the various orders of magnitude and harmonics, we end up with a set of differential equations for each set of (n,m):

$$\left(\frac{\partial^2}{\partial z^2} - m^2k^2\right) \phi_{nm} = F_{nm} \qquad -h < z < 0 \qquad (2.11a)$$

with

$$\left(g \frac{\partial}{\partial z} - m^2\omega^2\right) \phi_{nm} = G_{nm} \qquad z=0 \qquad (2.11b)$$

and

$$\frac{\partial}{\partial z} \phi_{nm} = H_{nm} \qquad z=-h \qquad (2.11c)$$

Equation (2.11a) replaces Laplace's Equation (2.1) while (2.11b) replaces (2.9) and (2.11c) replaces (2.10). The functions F_{nm}, H_{nm} are derived in detail in Appendix I while the functions G_{nm} are derived in Appendix II. The problem sets (2.11) are solved by starting with n=m=0, solving for ϕ_{oo}, then proceeding with higher values of n and m. At specific values of (n,m), the inhomogeneous terms F_{nm}, G_{nm} and H_{nm} in the problem for ϕ_{nm}, are functions of the previously obtained solutions. This can be seen in Appendices I and II.

However, the homogeneous version of (2.11), (i.e., (2.11) with $F_{nm} = G_{nm} = H_{nm} = 0$), for m=0 (zeroth harmonic) and m=1 (first harmonic) has nontrivial solution. Hence, the given non-homogeneous problems for m=0,1 are solvable

only if certain solvability conditions, which follows from the application of Green's formula, is satisfied:

If the homogeneous solution of (2.11) is denoted by Φ^h, then by integration by parts:

$$\int_{-h}^{0} (\phi^h \phi_{nm_{zz}} - \phi_{nm}\phi^h_{zz})dz = [\phi^h \phi_{nm_z} - \phi_{nm}\phi^h_z]_{-h}^{0} \quad (2.12)$$

For m=0, ϕ^h is constant with respect to z. Thus, using (2.11) Equation (2.12) will be:

$$\int_{-h}^{0} F_{no}dz + H_{no} = \frac{1}{g} G_{no} \quad (2.13)$$

From (I.6) and (I.7) [Appendix I]

$$H_{no} = - \frac{\partial h}{\partial x_1} \frac{\partial}{\partial x_1} (\Phi_{(n-2),0})_{z=-h} \quad (2.14a)$$

$$F_{no} = -\nabla_1^2 \phi_{(n-2),0} = -(\frac{\partial^2}{\partial x_1^2} + \frac{\partial^2}{\partial y_1^2}) \phi_{(n-2),0} \quad (2.14b)$$

Thus, substituting (2.14a,b) into (2.13) and using Leibniz rule, (2.13) becomes

$$\nabla_1 \cdot \int_{-h}^{0} \nabla_1 \phi_{(n-2),0} \, dz = \frac{-1}{g} G_{no} \; ; \; \nabla_1 = (\frac{\partial}{\partial x_1} , \frac{\partial}{\partial y_1}) \quad (2.15)$$

For m=1, $\phi^h = \cosh[k(z+h)]$ so that (2.12) becomes

$$H_{n1} + \int_{-h}^{0} F_{n1} \cosh[k(z+h)]dz = \frac{1}{g} \cosh(kh)\ G_{n1} \qquad (2.16)$$

In the following chapter, it will be shown how the functions ϕ_{nm} are determined using (2.11), (2.15) and (2.16).

3. SOLUTION OF THE INTERACTION PROBLEM

3.1 Main Wave Field

The main wave field consists of the large-scale edge wave, represented by ϕ_{oo}, and the short scale incident wave, represented by $(\phi_{11}e^{i\psi/\varepsilon} + *)$.

As for ϕ_{oo}, it is seen from Appendix I [(I.6a) and (I.7a)] that $F_{oo} = H_{oo} = 0$. Thus, ϕ_{oo} does not vary with depth, z. From Appendix II (II.4), $G_{20} = -\frac{\partial^2\phi_{oo}}{\partial t_1^2}$. Thus, the solvability condition (2.15) for n=2 will take the form:

$$\frac{\partial^2\phi_{oo}}{\partial t_1^2} - g\,\nabla_1 . h\nabla_1\,\phi_{oo} = 0 \tag{3.1}$$

which is an homogeneous equation for ϕ_{oo}. The corresponding free surface displacement is from Bernoulli's Equation

$$\varepsilon g\eta_{10} + \varepsilon\frac{\partial\phi_{oo}}{\partial t_1} = 0$$

$$\eta_{10} = -\frac{1}{g}\frac{\partial\phi_{oo}}{\partial t_1} \tag{3.1a}$$

We now take a standing edge wave as the solution for ϕ_{oo}, having the form

$$\phi_{oo} = \left(\frac{-igD_o}{2\Omega}\right) L_n(x_1)\,\cos Ky_1 e^{-i\Omega t_1} + * \tag{3.2}$$

where

D_o = edge wave amplitude

$L_n(x_1)$ = the nth modal shape

K, Ω = the longshore wavenumber and wave frequency, respectively, that satisfy the nth mode's dispersion relation

Thus, L_n satisfies

$$g(h\, L_n')' + (\Omega^2 - ghK^2)L_n = 0 \qquad (3.3)$$

where primes denote differentiation with respect to x_1, with the boundary conditions $L_n \to 0$ at infinity (deep water), which requires that

$$\Omega^2 - ghK^2 < 0 \quad \text{at } x_1 \sim \pm \infty \qquad (3.3a)$$

and we further require L_n bounded everywhere.

For general bottom profile, $h(x_1)$, the eigenvalue problem (3.3) is to be solved numerically for the dispersion relations $\Omega(K)$ and the corresponding modal shapes $L_n(x_1)$. The numerical scheme used here to solve (3.3) is a variation of the "Hybrid Element Method", developed for water waves problems by Chen and Mei (1974) and is discussed in details in Appendix V.

For the special case of a closed beach with a constant slope (i.e., $h=-\beta x_1$; β=constant), as depicted in Figure (3.1), there is a closed form analytical solution to (3.3).

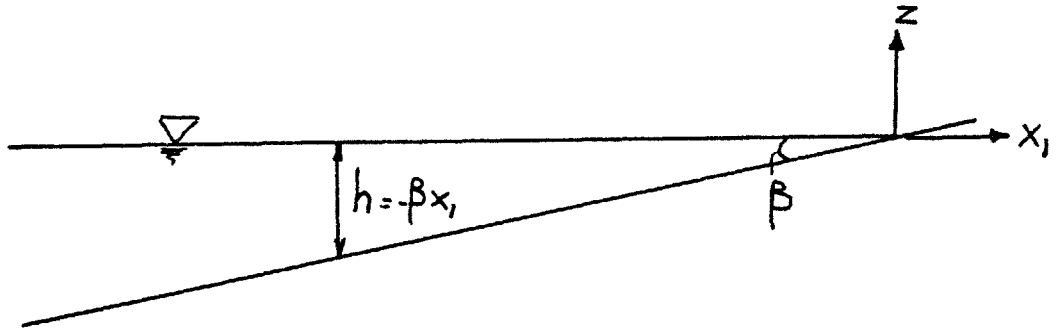

Figure (3.1)

$$L_n(x_1) = e^{Kx_1}\,\mathcal{L}_n(-2Kx_1) \qquad (3.4)$$

with

$$\Omega^2 = gK\beta(2n+1) \qquad n=0,1,... \qquad (3.5)$$

where $\mathcal{L}_n(-2Kx_1)$ is the n^{th} Laguerre polynomial of argument $(-2Kx_1)$ [Abramowitz & Stegun (1965)].

For D_o, it is in general a function of the slower variables,

$$D_o = D_o(x_2,x_3,...,y_2,y_3,...,t_2,t_3,...) \qquad (3.6)$$

yet to be determined. In fact, one of the main objectives of the analysis is to determine D_o. Because of the fact that ϕ_{oo} is an edge wave in the x_1-scale, it may be argued

that the variations of D_o with respect to the slower variables $x_2, x_3, \ldots$ are not relevant, because ϕ_{oo} is appreciable only along the x_1 scale ($L_n \to 0$ at $|x_1| \to \infty$). However, for the sake of completeness, the general form (3.6), which includes such variations for D_o will be maintained here.

As for the incident wave, the function ϕ_{11} is determined first by solving (2.11). From (I.6d), (I.7d) and (II.3) we have

$$F_{11} = H_{11} = G_{11} = 0 \tag{3.7}$$

and the solution is the homogeneous Stokes incident wave:

$$\phi_{11} = \frac{-ig\ chQ}{2\omega\ chq} A_o \tag{3.8}$$

where,

$$chQ \equiv coshQ = \cosh[k(z+h)]$$

$$chq \equiv coshq = \cosh(kh)$$

with the linear dispersion relation,

$$\omega^2 = gk\ thq \tag{3.9}$$

The abbreviation

$$ch \equiv \cosh, \quad sh \equiv \sinh \quad \text{and} \quad th \equiv \tanh$$

will be used, for convenience, throughout the text.

The incident wave amplitude A_o is yet free, and is, in general, a function of the slow variables:

$$A_o = A_o(x_1, x_2, \ldots, y_1, y_2, \ldots, t_1, t_2, \ldots) \tag{3.10}$$

Again, the assumed general form for A_o, (3.10) includes its spatial variations along the scales $x_2, x_3, \ldots$, which is outside the range of the trapped wave ϕ_{oo}. It will be shown however that such spatial variations do not directly affect the interaction between the incident and the trapped waves* [see for example Appendix III, Equation (III.2); Appendix IV, item (vii), etc.] and is included here for completeness.

The equation that governs A_o is the solvability condition (2.16) for n=2. From (I.6c), (I.7c) and (II.5a),

$$F_{21} = -i(k\,\phi_{11})_{x_1} - ik\,\phi_{11_{x_1}} \tag{3.11a}$$

$$H_{21} = -\frac{\partial h}{\partial x_1}(ik\,\phi_{11})_{z=-h} \tag{3.11b}$$

$$G_{21} = (i2\omega\phi_{11_{t_1}})_{z=0} + G_{21}^E \tag{3.11c}$$

where

$$G_{21}^E = ig[k\frac{\partial\phi_{oo}}{\partial x_1} - \frac{k^2}{2\omega\,ch^2q}\frac{\partial\phi_{oo}}{\partial t_1}]A_o \tag{3.11d}$$

Substituting into (2.16) we get:

---

*Only the temporal variations of A_o along $t_2, t_3, \ldots$ at the trapped wave location which resulted from such spatial variations that will play a role in the interaction problem.

$$(-\frac{\partial h}{\partial x_1})(ik\phi_{11})_{z=-h} + \int_{-h}^{0} [-i(k\phi_{11})_{x_1} - ik\phi_{11_{X_1}}]ch\ Q\ dz =$$

$$\frac{ch\ q}{g}\ [i2\omega\phi_{11_{t_1}} + G_{21}^{E}]_{z=0} \qquad (3.12)$$

Now, multiplying (3.12) by $\frac{g\ A_o^*}{2\omega\ ch\ q}$ we get,

$$(-\frac{\partial h}{\partial x_1})[k|\phi_{11}|^2]_{z=-h} - \int_{-h}^{0} [(k\phi_{11})_{x_1} + k\phi_{11_{x_1}}]\phi_{11}^* dz =$$

$$\frac{1}{g}[2\omega\phi_{11}^*\ \phi_{11_t} + \frac{gA_o^*}{2\omega}\ G_{21}^{E}]_{z=0} \qquad (3.13)$$

Further, taking the complex conjugate of (3.12) and multiplying it by $\frac{g\ A_o}{2\omega\ chq}$

$$(-\frac{\partial h}{\partial x_1})[k|\phi_{11}|^2]_{z=-h} - \int_{-h}^{0} [(k\phi_{11}^*)_{x_1} + k\phi_{11_x}^*]\ \phi_{11} dz =$$

$$\frac{1}{g}\ [2\omega\phi_{11}\ \phi_{11_t}^* + \frac{gA_o}{2\omega}\ G_{21}^{E*}]_{z=0} \qquad (3.14)$$

Adding (3.13) and (3.14), and noting from (3.11d) that $(A_o^* G_{21}^{E} + *)$ = zero, we get:

$$(-\frac{\partial h}{\partial x_1})[2k|\phi_{11}|^2]_{z=-h} - \int_{-h}^{0} \frac{\partial}{\partial x_1}(2k|\phi_{11}|^2) dz =$$

$$\frac{2\omega}{g}\ \frac{\partial}{\partial t_1}\ (|\phi_{11}|^2)_{z=0}$$

Applying Leibniz rule and using (3.8), this becomes

$$\frac{\partial}{\partial t_1}\left(\frac{|A_o|^2}{\omega}\right) + \frac{\partial}{\partial x_1}\left(Cg\ \frac{|A_o|^2}{\omega}\right) = 0 \qquad (3.15)$$

where Cg is the group velocity of the incident wave,

$$Cg = \frac{\partial \omega}{\partial k} = \frac{1}{2}\frac{\omega}{k}\left[\frac{\text{sh } 2q + 2q}{\text{sh } 2q}\right] \qquad (3.16)$$

Thus, (3.15) implies that the incident wave action is conserved up to this order, i.e., there is no energy exchange between the incident and the edge wave yet. In general, the amplitude $|A_o|$ is a function of the slow scales as in (3.10). However, a simple order of magnitude calculation shows that for a characteristic bottom slope represented by ε=0.05 and a typical wave period $\frac{2\pi}{\omega}$ = 10 secs, the scale t_1 is O (200 sec $\simeq$ 3.3 mins.) (typical of surf beats periods), t_2=O (1 hr), t_3=O (20 hr), etc. Thus, it is reasonable to assume that t_1 is not long enough for a significant change in usual ocean swells amplitudes. Therefore, we will allow such changes to be small, only up to $O(\varepsilon)$, along the t_1 scale, but can be significant, O(1) in general, along the slower scales $t_2, t_3, \ldots$ This amounts to assuming $|A_o|$ not a function of t_1, i.e.,

$$|A_o| = |A_o|\ (x_1, x_2, \ldots, y_1, y_2, \ldots, t_2, t_3, \ldots) \qquad (3.17)$$

while the small amplitude changes along the t_1 scale will be introduced later when solving for the second order-first harmonic potential ϕ_{21}. Invoking (3.17) and (2.7b), the solution of (3.15) is therefore the linear shoaling formula,

$$\left|A_o\right| = \sqrt{\frac{Cg_\infty}{Cg}}\ \left|A_{o\infty}\right| \tag{3.18}$$

where,

$$A_{o_\infty} = A_{o\infty}\ (x_2, x_3, \ldots, y_1, y_2, \ldots, t_2, t_3, \ldots);$$

$$Cg = Cg_\infty \qquad \text{at } x_1 \sim -\infty \tag{3.19}$$

Here, $A_{o\infty}$ represents incident wave amplitude in deep water outside the range of the trapped waves.

To complete the solution, we proceed to solve for the phase of A_o by first multiplying (3.12) by $\frac{gA_o}{2\omega\ chq}$ to get

$$\frac{\omega}{g}\frac{\partial}{\partial t_1}[\phi_{11}^2\Big|_{z=0}] + \frac{\partial}{\partial x_1}\int_{-h}^{0}(k\phi_{11}^2)dz = \frac{A_o}{2\omega}\,G_{21}^E \tag{3.20}$$

after using Leibniz rule as above. Then, substituting (3.8) to get:

$$\frac{\partial A_o^2}{\partial t_1} + \frac{\partial}{\partial x_1}\,(Cg\ A_o^2) = -2i[k\,\frac{\partial \phi_{oo}}{\partial x_1} - \frac{k^2}{2\omega\ ch^2 g}\,\frac{\partial \phi_{oo}}{\partial t_1}]A_o^2 \tag{3.21}$$

Writing

$$A_o = |A_o|\ e^{i\Theta} \tag{3.22}$$

where Θ is real and $|A_o|$ given by (3.18), we get from (3.20) the following governing equation for the phase Θ,

$$\left(\frac{\partial}{\partial t_1} + Cg\ \frac{\partial}{\partial x_1}\right)\Theta = -\left[k\ \frac{\partial}{\partial x_1} - \frac{k^2}{2\omega\ ch^2 q}\ \frac{\partial}{\partial t_1}\right] \left(\frac{-igD_o}{2\Omega}\ L_n(x_1)\cos Ky_1 e^{-i\Omega t_1} + *\right) \tag{3.23}$$

Thus, Θ must have the form

$$\Theta = \frac{-igD_o}{2\Omega} \cdot \textcircled{H}(x_1)\cdot \cos Ky_1 e^{-i\Omega t_1} + * \tag{3.24}$$

so that $\textcircled{H}(x_1)$ satisfies,

$$\left(\frac{\partial}{\partial x_1} - \frac{i\Omega}{Cg}\right)\ \textcircled{H} = \frac{-1}{Cg}\left[kL_n' + \frac{i\Omega k^2}{2\omega\ ch^2 q}\ L_n\right] \tag{3.25}$$

The solution for $\textcircled{H}$ is [Hildebrand, 1962, p. 7]:

$$\textcircled{H} = -e^{i\Omega\int^{x_1}\frac{d\zeta}{Cg}} \int_{-\infty}^{x_1} \frac{e^{-i\Omega\int^{\tilde{x}}\frac{d\zeta}{Cg}}}{Cg}\left[kL_n' + \frac{i\Omega k^2}{2\omega ch^2 q}L_n\right]d\tilde{x} \tag{3.26}$$

This completes the solution for A_o which is given by

$$A_o = \sqrt{\frac{Cg_\infty}{Cg}}\ A_{o\infty} e^{i\Theta} \tag{3.27}$$

and for ϕ_{11},

$$\phi_{11} = \frac{-ig\ ch\mathcal{Q}}{2\omega\ chq} \left(\sqrt{\frac{Cg_\infty}{Cg}}\, A_{o\infty}\right) e^{i\Theta} \tag{3.28}$$

The potential (3.28) represents the leading order solution for the incident wave. From (3.26) and (3.24) we see that $\Theta = 0$ at $x_1 \sim -\infty$ and the solution is merely the Stokes linear wave with a prescribed amplitude $A_{o\infty}$. Progressing towards the shallow region, the incident wave will evolve due to shoaling and due to the edge wave presence.

The edge wave will affect the phase of the incident wave as seen from (3.28) so that a two-dimensional normally incident wave from deep water onto a shallow region where edge waves (3.2) exist, will not remain two dimensional, i.e., its crests will not be straight, but oscillate in a sinusoidal fashion as they propagate, with the amplitude of oscillation growing with decreasing depth. By expanding the exponential $e^{i\Theta}$ in the power series $e^{i\Theta} = 1 + i\Theta - \Theta^2 + \ldots$, it is seen that the oscillation modes are those of the edge wave and all its higher harmonics, i.e., $(\pm K, \pm\Omega)$, $2(\pm K, \pm\Omega)$, $3(\pm K, \pm\Omega), \ldots$

So far it is the edge wave that affects the incident wave and not the reverse, with no energy transfer between the two. However, one would expect a mutual interaction at the higher orders with possible exchange of energy. This

may be anticipated mathematically as follows: When solving for the induced large scale motions ($\phi_{10}, \phi_{20}, \ldots$), using (2.11) and (2.15), one might expect governing equations similar to Equation (3.1), for ϕ_{oo}, with the right-hand side not equal to zero, but instead, a function of ϕ_{oo} and ϕ_{11}. We further, require that solutions $\phi_{10}, \phi_{20}, \ldots$ are bounded everywhere in order that expansion (2.8) is still valid. However, just like Equations (2.11), these inhomogeneous equations are only solvable if a certain solvability condition is satisfied. These conditions will be imposed on the inhomogeneous forcings and thus provide us with the desired conditions on the yet free amplitude D_o of the edge wave and hence, show how the edge wave evolves in the presence of the incident wave.

3.2 Higher Order Large Scale Motions

We proceed now to solve for the large scale motion (m=0) at higher order, i.e., $\phi_{10}, \phi_{20}, \ldots$

From (I.6b) and (I.7b), $F_{10}=H_{10}=0$, so that ϕ_{10} does not vary with depth z. Thus, ϕ_{10} will be determined from the solvability condition (2.15); n=3, which with G_{30} given by (II.10), takes the form:

$$\frac{\partial^2 \phi_{10}}{\partial t_1^2} - g\nabla_1 \cdot (h\nabla_1 \phi_{10}) = -2 \frac{\partial^2 \phi_{oo}}{\partial t_1 \partial t_2} + \frac{g^2}{2\omega} \frac{\partial}{\partial x_1} (k|A_o|^2)$$

$$- \frac{1}{2}[(\nabla_1 \phi_{oo})^2]_{t_1} - [\phi_{oo_{x_1}} \phi_{oo_{t_1}}]_{x_1} - [\phi_{oo_{y_1}} \phi_{oo_{t_1}}]_{y_1} \qquad (3.29)$$

Similarly, we may proceed to get the equations for n=2, m=0 (ϕ_{20}) as well.

From (I.6c) and (I.7c) we have:

$$F_{20} = -\left(\frac{\partial^2 \phi_{oo}}{\partial x_1^2} + \frac{\partial^2 \phi_{oo}}{\partial y_1^2}\right) \tag{3.30a}$$

$$H_{20} = -\frac{\partial h}{\partial x_1}\frac{\partial \phi_{oo}}{\partial x_1} \tag{3.30b}$$

Thus, from (2.11a):

$$\frac{\partial^2 \phi_{20}}{\partial z^2} = F_{20}$$

Integrating twice with respect to z:

$$\phi_{20} = \frac{1}{2} F_{20}\, z^2 + \ell_1 z + \ell_2 \tag{3.31}$$

where ℓ_1 and ℓ_2 are functions of the slow variables $(x_1, x_2, x_3, \ldots y_1, y_2, y_2, \ldots, t_1, t_2, \ldots)$. Using the bottom boundary condition (2.11c), we get ℓ_1:

$$\ell_1 = -\frac{\partial h}{\partial x_1}\frac{\partial \phi_{oo}}{\partial x_1} - h\left(\frac{\partial^2 \phi_{oo}}{\partial x_1^2} + \frac{\partial^2 \phi_{oo}}{\partial y_1^2}\right)$$

$$= -\nabla_1 \cdot (h \nabla_1 \phi_{oo}) = \frac{-1}{g}\frac{\partial^2 \phi_{oo}}{\partial t_1^2} \tag{3.32}$$

after using (3.1).

The function ℓ_2, i.e., the homogeneous part of ϕ_{20}, will be determined from the solvability condition (2.15); n=4:

$$-g\nabla_1 \cdot \int_{-h}^{0} \nabla_1 \phi_{20} dz = G_{40} \tag{3.33}$$

where G_{40} is given by (II.11) in Appendix II.

Substituting (3.31) into (3.33) and performing the z-integration we get:

$$-g\nabla_1 \cdot (h\nabla_1 \ell_2) = g\nabla_1 \cdot (\frac{h^3}{6} \nabla_1 F_{20} - \frac{h^2}{2} \nabla_1 \ell_1) + G_{40} \tag{3.34}$$

The only term in G_{40} that contains ϕ_{20} is the term

$$- \frac{\partial^2 \phi_{20}}{\partial t_1^2}\bigg|_{z=0} .$$

Turning this term to the left-hand side of (3.34), we get:

$$\frac{\partial^2}{\partial t_1^2} \ell_2 - g\nabla_1 \cdot (h\nabla_1 \ell_2) = g\nabla_1 \cdot (\frac{h^3}{6} \nabla_1 F_{20} - \frac{h^2}{2} \nabla_1 \ell_1) + \hat{G_{40}} \tag{3.35}$$

where $\hat{G_{40}}$ is the remainder of G_{40}. We further require that ℓ_2, as well as ϕ_{10}, is bounded everywhere. Equations for ϕ_{10} and ℓ_2 [(3.29) and (3.35), respectively], are similar inhomogeneous differential equations in the horizontal slow variables x_1, y_1 and slow time t_1. Thus, just like Equations (2.11), they are only solvable if a certain solvability condition is satisfied since ϕ_{oo} is a homogeneous solution. However, here, the integration in the Green's formula is with respect to the horizontal variable x_1, (instead of z in (2.15) and (2.16)).

3.3 Solvability Condition for the Higher Order Large Scale Motions

If we let S to represent the secular (resonance forcing) part of the right-hand side of (3.29) or (3.35) which is of the form:

$$S = S_1(x_1, D_o)\cos Ky_1 e^{-i\Omega t_1} \tag{3.36}$$

where K and Ω are those of ϕ_{oo} (3.2), and let R represents this part of the solution ϕ_{10} or ℓ_2 that is forced by S, i.e.,

$$\left(\frac{\partial^2}{\partial t_1^2} - g\nabla_1\cdot(h\nabla_1)\right)R = S \tag{3.36a}$$

then R, must be of the form:

$$R = R_1(x_1, D_o)\cos Ky_1 e^{-i\Omega t_1}$$

so that R satisfies

$$(hR_1')' + \frac{1}{g}(\Omega^2 - ghK^2)R_1 = \frac{-1}{g} S_1 \tag{3.37}$$

Consider first the submerged ridge (Figure 1.2). Application of Green's formula to R and the homogeneous mode L_n leads to

$$\frac{-1}{g}\int_{-\infty}^{\infty} S_1 L_n(x_1)dx_1 = [hL_nR_1' - hR_1L_n']_{-\infty}^{\infty} = 0 \tag{3.38}$$

because $L_n \to 0$ at infinity.

For a closed beach, however, the progressive Stokes wave solution (3.8) is singular at the shoreline ($x_1=0$). This is because breaking of waves is not accounted for. In reality a surf-zone occupies the region between the shoreline ($x_1=0$) and the breaker line ($x_1=x_b$). The inviscid theory (2.1-2.3) is not valid in the surf zone, because the motion there is turbulent due to wave breaking. However, breaking is associated only with the short-scale incident swell, and the resultant eddies of turbulence are of even shorter scale. One may argue that as far as the large scale edge wave is concerned, the inviscid motion assumption is still valid, even within the surf zone. However, short wave potentials ϕ_{ij} with $j\neq 0$ are only applicable outside the surf zone ($|x_1|>|x_b|$). The governing equations for the large scale edge wave, i.e., (3.1) for ϕ_{oo} and the part of Equations (3.29) for ϕ_{10} and (3.35) for ϕ_{20} that is of the form (3.36a), will therefore be extended to cover the whole domain ($-\infty < x_1 \leq 0$). However, in these equations, the inhomogeneous terms in G_{40} contain forcings from the short scale incident swell, which are defined only in the off-surf zone area ($|x_1|>|x_b|$). Therefore, in order to be able to use Equation (3.35) in the entire region ($x_1 \leq 0$), empirical hypothesis will be invoked for the short scale forcing from $x_1=x_b$ to $x=0$. Then, applying the Green's formula to (3.37), we get:

$$\frac{-1}{g}\int_{-\infty}^{0} S_1 L_n(x_1)\,dx_1=[hL_nR_1'-hR_1L_n']_{-\infty}^{0} = 0 \qquad (3.39)$$

because $L_n \to 0$ at infinity, and h=0 at x_1=0. Thus, (3.39) is the desired solvability condition for (3.29) and (3.35) in the case of a closed beach, with S_1 contains the empirically extended short scale forcing in the region $-x_b<x_1<0$. A detailed discussion concerning the empirical extension of S, as well as other features of the solvability condition (3.3a), will be given in Chapter 4.

For Equation (3.29), $S = -2\frac{\partial^2\phi_{oo}}{\partial t_1 \partial t_2}$, which does not contain any short scale forcing, so that for either problem (submerged or closed beach), i.e., from (3.38) or (3.39), we get,

$$\frac{\partial\phi_{oo}}{\partial t_2} = 0$$

which, from (3.2) implies

$$\frac{\partial D_o}{\partial t_2} = 0 \qquad (3.40)$$

For Equation (3.35), however, the function S, (i.e., the secular terms of R.H.S. of (3.35)) is much more complicated (see Equation (II.11) for G_{40}] and requires first solving for ϕ_{10} and ϕ_{21}. In fact, the remainder of this Chapter is devoted to finding this function S and then finding the corresponding solvability condition [(3.38) or (3.39)] which evenaually will give us the desired evolution equation. We first start by solving for the potential ϕ_{10}.

3.4 The Potential ϕ_{10}

Equation (3.40) guarantees that (3.29) is solvable:

$$\frac{\partial^2 \phi_{10}}{\partial t_1^2} - g\nabla_1 \cdot (h\nabla_1 \phi_{10}) = \frac{g^2}{2\omega} \frac{\partial}{\partial x_1}(k|A_o|^2) - [\tfrac{1}{2}(\nabla \phi_{oo})^2]_{t_1} -$$

$$- [\phi_{oo_{x_1}} \phi_{oo_{t_1}}]_{x_1} - [\phi_{oo_{y_1}} \phi_{oo_{t_1}}]_{y_1} \tag{3.41}$$

The harmonics in the right-hand side of (3.41) are 0, $\pm 2i\Omega t_1$. Thus, ϕ_{10} has the harmonics 0, and $\pm 2i\Omega t_1$, i.e., $\phi_{10} = \phi_{10}^{(0)} + \phi_{10}^{(2)} + \phi_{10}^{(2)*} + \phi_{10}^{h}$ where ϕ_{10}^{h} is an homogeneous solution.

(i) $\phi_{10}^{(0)}$ (no time dependence):

$$-g(h\phi_{10}^{(0)}{}_{x_1})_{x_1} = \frac{g^2}{2\omega} \frac{\partial}{\partial x_1}(k|A_o|^2)$$

Integrating,

$$\phi_{10}^{(0)}{}_{x_1} = \frac{-gk|A_o|^2}{2\omega h} = \frac{-gk}{2\omega h} \frac{Cg_\infty}{Cg} A_{o\infty}^2 \tag{3.42}$$

after using (3.27).

This is the usual mass transport current associated with progressive Stokes waves in finite water depth (Whitham, 1962).

(ii) $$\phi_{10}^{(2)} \sim e^{-2i\Omega t_1} \tag{3.43}$$

$$\left[\frac{\partial^2}{\partial t_1^2} - g\nabla_1(h\nabla_1)\right]\phi_{10}^{(2)} = \left(\frac{-igD_o}{2\Omega}\right)^2\left\{\frac{-1}{2}(-2i\Omega)\left[L_n'^2\cos^2 Ky_1 + K^2L_n^2\sin^2 Ky_1\right]\right.$$

$$+i\Omega\cos^2 Ky_1 (L_nL_n')' - i\Omega KL_n^2(\sin Ky_1\cos Ky_1)_{y_1}\Big\}e^{-2i\Omega t_1}$$

$$= \frac{-ig^2D_o^2}{8\Omega}\left\{\left[L_n'^2 + K^2L_n^2 + \frac{1}{2}(L_n^2)''\right]e^{-2i\Omega t_1}\right.$$

$$\left.+\left[L_n'^2 - 3K^2L_n^2 + \frac{1}{2}(L_n^2)''\right]\cos 2Ky_1 e^{-2i\Omega t_1}\right\} \tag{3.43a}$$

Thus, $\phi_{10}^{(2)}$ must have the form:

$$\phi_{10}^{(2)} = \left(\frac{-igD_o}{2\Omega}\right)^2\left[\psi_1(x_1)e^{-2i\Omega t_1} + \psi_2(x_1)\cos 2Ky_1 e^{-2i\Omega t_1}\right]$$

so that ψ_1 and ψ_2 satisfy:

$$-g(h\psi_1')' - 4\Omega^2\psi_1 = \frac{i\Omega}{2}\left[L_n'^2 + K^2L_n^2 + \frac{1}{2}(L_n^2)''\right] \tag{3.44}$$

$$-g(h\psi_2')' + 4(ghK^2 - \Omega^2)\psi_2 = \frac{i\Omega}{2}\left[L_n'^2 - 3K^2L_n^2 + \frac{1}{2}(L_n^2)''\right] \tag{3.45}$$

The condition of boundness is not sufficient to solve (3.44), as it has two oscillatory homogeneous solutions at infinity. This can be seen most readily by letting $h \to$ constant at infinity, then the homogeneous solutions are

$$\psi_1 \sim e^{\pm i\frac{2\Omega}{\sqrt{gh}}x} \tag{3.45a}$$

Thus, we further invoke the radiation condition of Sommerfeld, i.e., ψ_1 behaves as an outgoint wave at infinity. This will fix the appropriate sign in (3.45a) and will give us a unique solution for (3.44). On the other hand, because of the condition (3.3a), there is no radiating wave solution for ψ_2 according to (3.45). Thus, the boundness condition is sufficient for obtaining the localized motion ψ_2. The need for the radiation condition for ψ_1 implies that edge waves leaks energy to the deep water in the form of outgoing wave propagating away from the shallow region. A similar mechanism was first found by Guza and Bowen (1976) in their studies of subharmonic generation of edge waves in reflective beaches. Because of the energy leakage, there is radiation damping which limits the growth of the trapped wave. This will be more evident when obtaining the complete equation of the trapped wave.

For general profile, $h(x_1)$, Equations (3.44) and (3.45) are to be solved numerically for ψ_1 and ψ_2. However, closed form analytical solutions can be found for the important special case of uniformly sloping beach [Figure 3.1), where

$$h = -\beta x_1$$

and where the edge wave modes are explicitly given by (3.4a,b). For simplicity, we consider only the lowest (Stokes) mode, n=0, but the procedure is applicable for higher modes. For n=0, the Laguerre polynomial $\mathcal{L}_o = 1$ so that we have

$$L_o = e^{Kx_1} \; ; \; \Omega^2 = gK\beta \tag{3.46}$$

Then, (3.44) becomes

$$g\beta(x_1\psi_1')' - 4\Omega^2\psi_1 = 2i\Omega K^2 e^{2Kx_1} \tag{3.47}$$

with the boundary conditions

$$\psi_1 \sim \text{outgoing wave solution} \quad \text{as} \quad x_1 \to -\infty \tag{3.48a}$$

$$\psi_1 \text{ is finite} \qquad \text{at } x_1 = 0 \tag{3.48b}$$

The homogeneous solutions of (3.47) are the Bessel functions

$$J_o(4\sqrt{-Kx_1}) \text{ and } Y_o(4\sqrt{-Kx_1}) \tag{3.49}$$

Thus, as the time factor is $e^{-2i\Omega t_1}$ [c.f. (3.43)], an outgoing wave solution at infinity implies that

$$\psi_1 \sim H_0^{(1)}(4\sqrt{-Kx_1}) = J_o + iY_1 \quad \text{as } x_1 \to -\infty \tag{3.50}$$

Using the method of variation of parameters and the two homogeneous solutions (3.49), one gets the solution

$$\psi_1 = \frac{-2i\pi\Omega K}{g\beta} \{(E_2(\infty) - iE_1(\infty))J_o(4\sqrt{-Kx_1}) - E_2(4\sqrt{-Kx_1})$$

$$J_o(4\sqrt{-Kx_1}) + E_1(4\sqrt{-Kx_1})Y_o(4\sqrt{-Kx_1}) \qquad (3.51)$$

where,

$$E_1(4\sqrt{-Kx_1}) = \int_{Kx_1}^{0} e^{2\zeta} J_o(4\sqrt{-\zeta})d\zeta \qquad (3.52)$$

$$E_2(4\sqrt{-Ky_1}) = \int_{Kx_1}^{0} e^{2\zeta} Y_o(4\sqrt{-\zeta})d\zeta \qquad (3.53)$$

As for ψ_2, substitution of (3.46) into (3.45) yields the right-hand-side identically zero. Thus, $\psi_2 = 0$ for this special case, since (3.45) does not have any nontrivial homogeneous solutions.

On the other hand, the numerical scheme for the solution of (3.44) and (3.45), for general bottom profile $h(x_1)$ is outlined in Appendix V, where the idea of the Hybrid Element Method (Chen and Mei, 1974) is again used.

(iii) In addition to the above particular solution, ϕ_{10} may have the homogeneous solution

$$\phi_{10}^h = \frac{-igD_1}{2\Omega} L_n(x_1)\cos Ky_1 e^{-i\Omega t_1} + * \qquad (3.54)$$

with D_1 yet undetermined. ϕ_{10} is then the summation of $\phi_{10}^{(0)}$, $\phi_{10}^{(2)}$, $\phi_{10}^{(2)*}$ and ϕ_{10}^h.

3.5 The Potential ϕ_{21}

The solvability condition (3.12) guarantees a solution for ϕ_{21}. With the non-homogeneous terms in (2.11) given by (3.11), the solution for ϕ_{21} is formally the same as that given by Chu and Mei, (1970)*

$$\phi_{21} = \underbrace{\frac{-gchQ}{2\omega chq}\, iA_1}_{\phi_{21}^h} - \underbrace{\frac{gA_o}{2\omega chq}(\alpha_1 QchQ + \alpha_2 QshQ + \alpha_3 Q^2 chQ)}_{\phi_{21}^P} \tag{3.55}$$

where,

$$\alpha_1 = h_{x_1} \; ; \; \alpha_2 = \frac{\frac{\partial}{\partial x_1}[\frac{A_o}{2\omega chq}]^2}{2k[\frac{A_o}{2\omega chq}]^2} \; ; \quad \alpha_3 = \frac{k_{x_1}}{2k^2} \tag{3.55a}$$

and where the first term in R.H.S. of (3.47) represents the homogeneous solution (ϕ_{21}^h), with the amplitude A_1 yet free, while the rest of R.H.S. of (3.47) represents the particular solution (ϕ_{21}^P) which depends on A_o only. The amplitude A_1 is governed by the solvability condition (2.16); n=3.

From (I.6f), (I.7f) in Appendix I and (II.9a) in Appendix II)

$$F_{31} = -[(\frac{\partial^2}{\partial x_1^2} + \frac{\partial^2}{\partial y_1^2})\phi_{11} + i\frac{\partial}{\partial x_1}(k\phi_{21}) + ik\frac{\partial \phi_{21}}{\partial x_1}$$

$$+ i\frac{\partial}{\partial x_2}(k\phi_{11}) + ik\frac{\partial \phi_{11}}{\partial x_2}] \tag{3.56a}$$

$$H_{31} = -\frac{\partial h}{\partial x_1}(ik\phi_{21} + \frac{\partial \phi_{11}}{\partial x_1})_{z=-h} \tag{3.56b}$$

---

*We emphasize that A_o is not the same as in Chu and Mei because of the phase of A_o (3.27).

$$G_{31} = i2\omega\left[\frac{\partial\phi^h_{21}}{\partial t_1} + \frac{\partial\phi_{11}}{\partial t_2}\right]_{z=0} + ig\left(k\,\frac{\partial\phi_{oo}}{\partial x_1} - \frac{k^2}{2\omega ch^2q}\,\frac{\partial\phi_{oo}}{\partial t_1}\right)A_1 +$$

$$+ P_1(\phi_{oo},\, A_o) \qquad (3.56c)$$

where the lengthy expression for P_1 is given in Appendix II, (II.9b).

Substituting (3.56) into (2.16) and writing $\phi_{21}=\phi^h_{21}+\phi^p_{21}$, we get

$$\left(-\frac{\partial h}{\partial x_1}\right)\left[ik(\phi^h_{21}+\phi^p_{21}) + \frac{\partial\phi_{11}}{\partial x_1}\right]_{z=-h} + \int_{-h}^{0}\left[-i(k\phi^h_{21})_{x_1} - ik(\phi^h_{21})_{x_1} - i(k\phi_{11})_{x_2} - ik\phi_{11_{x_2}}\right]chQdz$$

$$+ \int_{-h}^{0}\left[-\phi_{11_{x_1x_1}} - \phi_{11_{y_1y_1}} - i(k\phi^p_{21})_{x_1} - ik(\phi^p_{21})_{x_1}\right]chQdz$$

$$= \frac{chq}{g}\left\{i2\omega\left[\frac{\partial\phi^h_{21}}{\partial t_1} + \frac{\partial\phi_{11}}{\partial t_2}\right]_{z=0}\right.$$

$$\left. + ig\left(k\,\frac{\partial\phi_{oo}}{\partial x_1} - \frac{k^2}{2\omega ch^2q}\,\frac{\partial\phi_{oo}}{\partial t_1}\right)A_1 + P_1\right\} \qquad (3.57)$$

Calling,

$$P_2(A_o)=(-\frac{\partial h}{\partial x_1})[ik\phi^p_{21}+\frac{\partial \phi_{11}}{\partial x_1}]_{z=-h}+\int_{-h}^{0}[-\phi_{11_{x_1x_1}}-\phi_{11_{y_1y_1}}$$

$$-i(k\phi^p_{21})_{x_1}-ik(\phi^p_{21})_{x_1}]chQdz \qquad (3.58)$$

and multiplying (3.57) by $\frac{gA_1}{2\omega chq}$, we get

$$\frac{\partial h}{\partial x_1}[k(\phi^h_{21})^2]_{z=-h}+\int_{-h}^{0}\frac{\partial}{\partial x_1}[k(\phi^h_{21})^2]dz+\frac{A_1}{A_o}\frac{\partial}{\partial x_2}\int_{-h}^{0}k\phi^2_{11}\,dz$$

$$=\{\frac{-\omega}{g}\frac{\partial}{\partial t_1}(\phi^h_{21})^2-\frac{\omega A_1}{gA_o}\frac{\partial \phi^2_{11}}{\partial t_2}\}_{z=0}+\frac{ig}{2\omega}(k\frac{\partial \phi_{oo}}{\partial x_1}-\frac{k^2}{2\omega ch^2q}\frac{\partial \phi_{oo}}{\partial t_1})A_1^2$$

$$+\frac{A_1}{2\omega}P_1(A_o,\phi_{oo})-\frac{gA_1}{2\omega chq}P_2(A_o) \qquad (3.59)$$

Applying Leibniz rule, and using (3.8) and (3.55), then, (3.59) becomes

$$\{\frac{\partial A_1^2}{\partial t_1}+\frac{\partial}{\partial x_1}(CgA_1^2)+2i(k\frac{\partial \phi_{oo}}{\partial x_1}-\frac{k^2}{2\omega ch^2q}\frac{\partial \phi_{oo}}{\partial t_1})A_1^2\}+$$

$$\frac{A_1}{A_o}\{\frac{\partial A_o^2}{\partial t_2}+\frac{\partial}{\partial x_2}(CgA_o^2)\}=2A_1[\frac{1}{chq}P_2(A_o)-\frac{1}{g}P_1(A_o,\phi_{oo})] \qquad (3.60)$$

Notice the similarity between the homogeneous part of Equation (3.60) for A_1 (i.e., the first curly bracket), and Equation (3.21) for A_o. Thus, similar to (3.27), we let

$$A_1 = A_1^{(1)} \sqrt{\frac{Cg_\infty}{Cg}}\, e^{i\theta} \tag{3.61}$$

where θ is given by (3.24). Substituting (3.61) into (3.60), we get,

$$\{\frac{2}{Cg} A_1^{(1)} \frac{\partial}{\partial t_1} A_1^{(1)} + 2A_1^{(1)} \frac{\partial}{\partial x_1} A_1^{(1)} + \frac{2i}{Cg} A_1^{(1)2} [\theta_{t_1} + Cg\theta_{x_1}$$

$$+ k \frac{\partial \phi_{oo}}{\partial x_1} - \frac{k^2}{2\omega ch^2 q} \frac{\partial \phi_{oo}}{\partial t_1}]\}Cg_\infty e^{2i\theta} =$$

$$-2\sqrt{\frac{Cg_\infty}{Cg}} A_1^{(1)} e^{i\theta} \{(\frac{\partial A_o}{\partial t_2} + Cg \frac{\partial A_o}{\partial x_2}) + \frac{1}{g} P_1 - \frac{1}{chq} P_2\} \tag{3.62}$$

But, from (3.23), the square bracket in the left-hand side of (3.62) is identically zero. Multiplying (3.62) by

$$\frac{Cg\, e^{-2i\theta}}{2Cg_\infty A_1^{(1)}}$$

we get the linear equation,

$$\frac{\partial}{\partial t_1} A_1^{(1)} + Cg \frac{\partial}{\partial x_1} A_1^{(1)} =$$

$$-\sqrt{\frac{C_g}{Cg_\infty}} \{(\frac{\partial A_o}{\partial t_2} + Cg \frac{\partial A_o}{\partial x_2}) + \frac{1}{g} P_1 - \frac{1}{chq} P_2\} e^{-i\theta} \tag{3.63}$$

Thus, we write the solution for $A_1^{(1)}$ as the sum of the homogeneous solution A_1^h (with the R.H.S. of (3.63) equal

to zero) and the particular solution A_1^p, so that from (3.61) we have

$$A_{1_{homog.}} = A_1^h \sqrt{\frac{\overline{Cg}_\infty}{Cg}}\, e^{i\theta}$$ representing the homogeneous solution for A_1 (3.63a)

and

$$A_{1_{part.}} = A_1^p \sqrt{\frac{\overline{Cg}_\infty}{Cg}}\, e^{i\theta}$$ the particular solution for A_1 (3.63b)

Before proceeding further with the solution of (3.63), we recall from the discussion at the end of Section (3.3) that the main objective of the analysis now is finding the secular forcings in Equation (3.35), i.e., the function S , which will lead eventually to the desired evolution equation for D_o. Thus, we will only be concerned here with obtaining this part of the solution A_1^h and A_1^p that contributes to the function S. The only place where the amplitude A_1 (or potential ϕ_{21}) appears in Equation (3.35) is in the components of the complicated function G_{40}, given by (II.11). From (II.11), the terms involving the potential ϕ_{21} are:

$$I = \{- \frac{\partial}{\partial t_1}[(k^2 \phi_{21}\phi_{11}^* + \phi_{21_z}\phi_{11_z}^*) + *]$$

$$+ \frac{1}{g}\frac{\partial}{\partial t_1}[(\omega^2 \phi_{11}\phi_{21_z}^* + \omega^2 \phi_{21}\phi_{11_z}^*) + *]$$

$$- 2\frac{\partial}{\partial x_1}[-\omega k\, \phi_{21}\phi_{11}^* + *]\}_{z=0} \qquad (3.64)$$

Factoring out the terms involving the amplitude A_1, using (3.55), we get

$$I = \frac{\partial}{\partial t_1}\{(A_o A_1^* + A_o^* A_1)[-(\frac{gk}{2\omega})^2 - (\frac{gkthq}{2\omega})^2 + \frac{1}{2} gkthq]\}$$

$$+ \frac{g^2}{2\omega} \frac{\partial}{\partial x_1} k(A_o A_1^* + *) + I'(\phi_{11}, \phi_{21}^p)$$

$$= - \frac{\omega^2}{4sh^2q} \frac{\partial}{\partial t_1}(A_o A_1^* + *) + \frac{g^2}{2\omega} \frac{\partial}{\partial x_1} k(A_o A_1^* + *)$$

$$+ I'(\phi_{11}, \phi_{21}^p) \qquad (3.65)$$

after using (3.8) and the linear dispersion relation (3.9).

Substituting (3.27) and (3.61), for A_o and A_1 respectively, into (3.65) we have,

$$I = - \frac{\omega^2}{5sh^2q} \frac{Cg_\infty A_{o\infty}}{Cg} \frac{\partial}{\partial t_1} [(A_1^h + A_1^p) + *]$$

$$+ \frac{g^2}{2\omega} (Cg_\infty A_{o\infty}) \frac{\partial}{\partial x_1}[\frac{k}{Cg}(A_1^h + A_1^p) + *] + I'(\phi_{11}, \phi_{21}^p) \qquad (3.66)$$

where $I'(\phi_{11}, \phi_{21}^p)$ depends only on A_o and not on A_1^h or A_1^p and its secular terms will be worked out in Appendix IV. Therefore, as far as ϕ_{21}^h is concerned, it is only the real parts of A_1^h and A_1^p that matter in the determination of the function S. Further, from (3.36), it is the

components of these real parts which are proportional to $\cos Ky_1 e^{-i\Omega t_1}$ that will contribute to S. These secular parts of A_1^h and A_1^p instead of the full A_1 will now be obtained from (3.63). As for the homogeneous solution A_1^h, (with R.H.S. equal to zero), its secular part is clearly

$$A_1^h \sim \cos Ky_1 e^{i\Omega[\int \frac{dx_1}{Cg} - t_1]} \tag{3.67}$$

so that the homogeneous solution of the amplitude A_1 (3.63a) is

$$A_{1_{homog.}} = \sqrt{\frac{\overline{Cg}_\infty}{Cg}} A_{1_\infty} \cos Ky_1 e^{i\Omega[\int \frac{dx_1}{Cg} - t_1]} e^{i\theta} \tag{3.68}$$

At $x_1 \sim -\infty$, $\theta = 0$ from (3.26) and (3.24), so that

$$A_{1_{homog}} \to A_{1\infty} \cos Ky_1 e^{i\Omega[\int \frac{dx_1}{Cg} - t_1]} \tag{3.68a}$$

and

$$A_{1\infty} = A_{1\infty}(x_2, x_3, y_2, t_2, t_3, \ldots) \tag{3.68b}$$

Therefore $A_{1\infty}$ represents physically the prescribed amplitude of the small modulation to the incident wave envelope at deep water (3.68a). These small modulations, having prescribed amplitude $|A_{1\infty}|$ at deep water (3.68b), will evolve due to shoaling effects and due to the presence of the edge wave, as in (3.68).

As for the particular solution A_1^p, its secular part is forced by the real part of the right-hand-side of Eq. (3.63 which is proportional to $\cos Ky_1 e^{-i\Omega t_1} + *$. This secular forcing is derived in detail in Appendix (III) and is given, after lengthy algebra, by

$$P = (A_{o\infty})\Big\{\frac{\omega}{k}\,\theta_{x_1}\Big[\frac{3k}{4k^2}x_1(2q^2-4q\coth 2q+2+\frac{4q^3}{3\sin 2q})$$

$$-\frac{h}{2}x_1(2q+\coth 2q+\frac{1+2q}{\cosh 2q})\Big]-\omega\Big[\frac{\theta_{x_1x_1}}{k^2}+\frac{2\theta_{x_1}}{k^2}(\ell n\,\frac{1}{\sqrt{Cg}\,\cosh q})x_1\Big]$$

$$\Big[\frac{q}{2\sin 2q}+\frac{1}{2}\,q\,\coth\,2q\Big]-\omega\,\frac{\theta_{y_1y_1}}{2k^2}(\frac{1}{2}+\frac{q}{\sin 2q})+\frac{1}{2\omega}\,\theta_{t_1t_1}$$

$$-\theta_{t_1}[\alpha_1 q+\tilde{\alpha}_2 q\tanh q+\alpha_3 q^2]-\frac{1}{k}\,\theta_{x_1t_1}q\,\tanh q+\frac{1}{2\omega}(\alpha_1 q+\tilde{\alpha}_2 q\,\tanh q$$

$$+\alpha_3 q^2)(-2k\omega\,\frac{\partial\phi_{oo}}{\partial x_1}+k^2\,\frac{\partial\phi_{oo}}{\partial t_1})+\frac{k}{2\omega}[\alpha_1(1+q\tanh q)+\tilde{\alpha}_2(\tanh q+q)$$

$$+\alpha_3(2q+q^2\tanh q](\frac{-\omega^2}{g}\,\frac{\partial\phi_{oo}}{\partial t_1})+\frac{k}{2\omega}\,\frac{\partial^2\phi_{oo}}{\partial x_1\partial t_1}-\frac{1}{2}(\ell n\,\frac{1}{\sqrt{Cg}})x_1\,\frac{\partial\phi_{oo}}{\partial x_1}$$

$$+\frac{\omega^2}{2g}\,\frac{\partial^2\phi_{oo}}{\partial t_1^2}+\frac{k}{2\omega}\,(\ell n\,\frac{1}{\sqrt{Cg}})x_1\,\frac{\partial\phi_{oo}}{\partial t_1}+\sqrt{Cg}\,[\frac{\partial\phi_{oo}}{\partial x_1}(\frac{-1}{2\sqrt{Cg}})$$

$$+\frac{\partial\phi_{oo}}{\partial t_1}\,(\frac{k}{2\omega\sqrt{Cg}})]x_1-\frac{1}{2}\,\frac{\partial^2\phi_{oo}}{\partial y_1^2}\Big\} \qquad (3.69)$$

where

$$\tilde{\alpha}_2 = \mathrm{Re}(\alpha_2) = \frac{1}{2k}\,(\ell n\,\frac{1}{Cg\,\cosh^2 q})x_1 \qquad (3.70)$$

From (3.2) and (3.24) it is seen indeed that the secular forcing P is of the form

$$P = \left(\frac{-igD_o}{2\Omega}\right) A_{o\infty} \mathcal{P}(x_1) \cos Ky_1 e^{-i\Omega t_1} + * \qquad (3.71)$$

Thus, the secular part of A_1^p must have the form

$$A_1^p = \left(\frac{-igD_o}{2\Omega}\right) A_{o\infty} a_1^p(x_1) \cos Ky_1 e^{-i\Omega t_1} + * \qquad (3.72)$$

with $a_1^p(x_1)$ satisfying, (from (3.63)),

$$\left(\frac{\partial}{\partial x_1} - \frac{i\Omega}{Cg}\right) a_1^p = \frac{1}{Cg} \mathcal{P}(x_1) \qquad (3.73)$$

The solution for a_1^p is therefore given by

$$a_1^p = e^{i\Omega\int^{x_1} \frac{d\zeta}{Cg}} \int_{-\infty}^{x_1} \frac{e^{-i\Omega\int^{x_1} \frac{d\zeta}{Cg}}}{Cg} \mathcal{P}(\tilde{x}_1) d\tilde{x}_1 \qquad (3.74)$$

where $\mathcal{P}(x_1)$ is obtained from (3.69) and (3.71).

Now, with the secular part of I' derived from Appendix IV, all the ingredients for evaluating (3.66), i.e., the contribution to S involving ϕ_{21} is obtained, and finally we may proceed to find the solvability condition for Equation (3.35).

3.6 The Evolution Equation for the Trapped Wave

Now, after solving for ϕ_{10} and ϕ_{21}, it is possible to obtain the solvability condition for ϕ_{20}, using either (3.38) for the submerged ridge problem, or (3.39) for the closed beach problem. This will provide us, like the solvability condition for ϕ_{10}, (3.40) with the desired information on the trapped wave amplitude evolution.

The equation for the homogeneous part of ϕ_{20} is (3.35), which is solvable only if (3.38) or (3.39) is satisfied

$$\int_{-\infty}^{\infty} \text{or} \int_{-\infty}^{0} S_1 L_n(x_1)\,dx_1 = 0 \tag{3.75}$$

where S_1 is defined by (3.36). The function S_1 is derived in Appendix IV (IV.4) and has the form

$$S_1 = \left(\frac{\partial D_o}{\partial t_3} + \frac{\partial D_1}{\partial t_2}\right)\tilde{\gamma}_o + (\tilde{\gamma}_{11} + A_{o\infty}^2\tilde{\gamma}_{12})D_o + \tilde{\gamma}_2|D_o|^2 D_o + A_{1\infty}A_{o\infty}\tilde{\gamma}_3 \tag{3.76}$$

where

$$\tilde{\gamma}_o = \left(\frac{-ig}{2\Omega}\right)[2i\Omega\, L_n(x_1)] \tag{3.77a}$$

$$\tilde{\gamma}_{11}(x_1) = \left(\frac{-ig}{4\Omega}\right)\left\{\frac{gh^3K^2}{3}(L_n'' - K^2L_n) + \Omega^2h^2K^2L_n + \left(\frac{gh^3}{3}[-L_n''' + K^2L_n'] - \Omega^2h^2L_n'\right)'\right\} \tag{3.77b}$$

$$\tilde{\gamma}_{12}(x_1) = \frac{-igCg_\infty}{4\Omega Cg}\{i\Omega g(\frac{q}{ch^2q} + \frac{1}{thq})\textcircled{H}' + (2\omega^2\Omega^2 - g^2K^2)\frac{\textcircled{H}}{\omega}$$

$$+ \frac{i\Omega\omega^2 a_1^p}{sh^2q} - \frac{i\Omega gKL_n'}{\omega h} + 2i\Omega\omega kL_n' + \frac{\omega^4\Omega^2 L_n}{g^2} - k^2\Omega^2 L_n$$

$$+ (\frac{g^2k^2}{2\omega^2} - \frac{\omega^2}{2})K^2L_n\} - \frac{igCg_\infty}{4\Omega}\{\frac{1}{Cg}[\frac{g}{\omega}(g+2\omega^2 h)\textcircled{H}'$$

$$+ \frac{i\Omega g^2 k\textcircled{H}}{\omega^2} + \frac{2g^2 ka_1^p}{\omega} - \frac{i\Omega gkL_n}{\omega h} - (\frac{3g^2k^2}{2\omega^2} - \frac{\omega^2}{2})L_n']\}' \tag{3.77c}$$

$$\tilde{\gamma}_2(x_1) = \frac{-ig^3}{8\Omega^3}\{i\Omega[K^2L_n(3\psi_2 - 2\psi_1) + \psi_1'L_n' + \frac{1}{2}\psi_2'L_2' + (2L_n'(\psi_1 + \frac{1}{2}\psi_2)$$

$$-L_n(\psi_1' + \frac{1}{2}\psi_2'))']' + \frac{K^2}{4}(L_nL_n'^2 + 3K^2L_n^2) - \frac{1}{4}(3L_n'^3 + K^2L_n'L_n^2)'\} \tag{3.77d}$$

$$\tilde{\gamma}_3(x_1) = \frac{i\Omega\omega^2 Cg_\infty}{4sh^2qCg}\, e^{i\Omega\int^{x1}\frac{d\zeta}{Cg}} + \frac{g^2Cg_\infty}{2\omega}[\frac{k}{Cg}\, e^{i\Omega\int^{x1}\frac{d}{Cg}}]'. \tag{3.77e}$$

and where primes denote differentiation with respect to x_1.

Recall, from the paragraph after (3.53), that $\psi_2 = 0$ for the losest edge wave mode on a plane beach. Recall also from (3.27) and (3.68) that $A_{o\infty}$ and $A_{1\infty}$ are, respectively, the prescribed values of the leading order incident wave amplitude $|A_o|$, and its second order resonant modulation amplitude A_1, at deep water.

The two are in general functions of the slow scales $x_2, x_3, \ldots y_1, y_2, \ldots, t_2, t_3, \ldots$

Now, applying the solvability condition (3.38) or (3.39), we get

$$\frac{\partial D_o}{\partial t_3} + \frac{\partial D_1}{\partial t_2} + (\gamma_{11}+A_{o\infty}^2\gamma_{12})D_o+\gamma_2|D_o|^2D_o+A_{1\infty}A_{o\infty}\gamma_3=0 \qquad (3.78)^*$$

where the constant coefficients γ_{11}, γ_{12}, γ_2 and γ_3 are given by

$$\gamma_j = \frac{1}{\gamma_o}\int_{-\infty}^{x_o} \tilde{\gamma}_j(x_1)\ L_n(X_1)dx_1 \ ;\ j=11,12,2 \text{ and } 3 \qquad (3.78a)$$

and

$$\gamma_o = \int_{-\infty}^{x_o} \tilde{\gamma}_o(x_1)\ L_n(x_1)dx_1 \qquad (3.78b)$$

with $x_o=+\infty$ in the submerged ridge case, or $x_o=0$ in the closed beach case. Equation (3.78) is the desired evolution equation that will enable us to determine the yet free amplitudes D_o and D_1 and thus, enables us to trace the evolution of the edge wave from its initial growth, along the t_2, and t_3 scales. The equation is nonlinear and it will be solved numerically for some given initial values and forcings, $A_{1\infty}$ and $A_{o\infty}$. However, first it is more convenient to cast the Equation in a non-dimensional form, which is done in the following section.

---

*As shown in Appendix III (Eq. III.2) and Appendix IV (item vii), there is no derivative with respect to $x_2, x_3, \ldots y_1, y_2, \ldots$ in the secular terms, hence only time derivatives appear in (3.78).

3.7 Non-dimensional Evolution Equation

We will use $1/k_o$ as a length scale, and $1/\omega$ as a time scale, where k_o and ω are, respectively, the incident wave wavenumber and frequency at some reference depth h_o. Then, from the dispersion relation (3.9),

$$k_o = \frac{\omega^2}{g\ th(k_o h_o)} \tag{3.79}$$

Thus, we let

$$(x_1,h) = \frac{1}{k_o}(\bar{x}_1,\bar{h}) \ ; \ (k,K) = k_o(\bar{k},\bar{K})$$

$$\Omega = \omega\bar{\Omega} \ ; \ t_{\substack{2\\3}} = \frac{1}{\omega}\,\bar{t}_{\substack{2\\3}} \quad \text{and} \quad Cg = \frac{\omega}{k_o}\,\bar{C}g \tag{3.80}$$

where the overbars denote the non-dimensional variables. From (3.74) to (3.77), we also need to non-dimensionalize $L_n(x_1)$, $\psi_1(x_1)$, $\psi_2(x_1)$, $\Theta(x_1)$ and $a_1^p(x_1)$. In Appendix V the non-dimensional functions $L_n(\bar{x}_1)$, $\bar{\psi}_1(\bar{x}_1)$ and $\bar{\psi}_2(\bar{x}_1)$ are obtained numerically, where

$$(\psi_1\ ,\ \psi_2) = \frac{\omega k_o}{g}\ (\bar{\psi}_1\ ,\ \bar{\psi}_2) \tag{3.81}$$

Recall that ψ_1 and ψ_2 are solutions of (3.44) and (3.45). From (3.26), we may let:

$$\Theta = \frac{k_0^2}{\omega}\ \bar{\Theta} \tag{3.82a}$$

$$\bar{\Theta} = -e^{i\bar{\Omega}\int^{\bar{x}_1}\frac{d\zeta}{\bar{C}g}} \int_{-\infty}^{\bar{x}_1} \frac{e^{-i\bar{\Omega}\int^{x_1}\frac{d\zeta}{\bar{C}g}}}{\bar{C}g} [\bar{k}L_n' + \frac{i\bar{k}^2\bar{\Omega}}{2\ ch^2 q} L_n] d\tilde{\bar{x}}_1 \tag{3.82b}$$

where primes now denote differentiation with respect to the non-dimensional $\bar{x}_1$ scale.

Similarly, for a_1^p (3.74)

$$a_1^p = \frac{k_o^2}{\omega} \overline{a_1^p} \tag{3.83a}$$

where

$$\overline{a_1^p} = e^{i\bar{\Omega}\int^{\bar{x}_1}\frac{d\zeta}{\bar{C}g}} \int_{-\infty}^{\bar{x}_1} e^{-i\bar{\Omega}\int^{\bar{x}_1}\frac{d\zeta}{\bar{C}g}} \frac{\bar{\wp}(\tilde{\bar{x}}_1)}{\bar{C}g} d\tilde{\bar{x}}_1 \tag{3.83b}$$

and where $\bar{\wp}$ is given by [See (3.69)]

$$\bar{\wp}(\bar{x}_1) = \frac{\bar{\Theta}'}{\bar{k}} \{\frac{3\bar{k}'}{4\bar{k}^2}[q^2 - 2q\coth 2q + 1 + \frac{2q^3}{3sh^2 q}]$$

$$- \frac{\bar{h}'}{2} [2q + \coth 2q + \frac{1+2q^2}{sh^2 q}]\}$$

$$- [\frac{\bar{\Theta}''}{\bar{k}^2} + \frac{2\bar{\Theta}'}{\bar{k}^2}(\ell n \frac{1}{\sqrt{Cg}\ chq})'](\frac{q}{2sh2q} + \frac{q}{2}\coth 2q)$$

$$+ \frac{\bar{K}^2\bar{\Theta}}{2\bar{k}^2}(\frac{1}{2} + \frac{q}{sh2q}) + [-\frac{\bar{\Omega}^2}{2} + i\bar{\Omega}(\alpha_1 q + \tilde{\alpha}_2 qthq + \alpha_3 q^2)]\bar{\Theta}$$

$$+ \frac{i\bar{\Omega}}{\bar{k}} qthq\ \bar{\Theta}' - q(\alpha_1 + \tilde{\alpha}_2 thq + \alpha_3 q)(\bar{k}L_n' + \frac{i}{2}\bar{k}^2\bar{\Omega}L_n)$$

$$+ \frac{iT}{2} \bar{k}\,\bar{\Omega}\, L_n[\alpha_1(1+qthq) + \tilde{\alpha}_2(thq+q) + \alpha_3(2q + q^2 thq)]$$

$$- \frac{1}{2}(L_n' + i\bar{\Omega}\bar{k}L_n)\left(\ell n \frac{1}{\sqrt{Cg}}\right)' + \frac{1}{2}(\bar{K}^2 L_n - \bar{\Omega}^2 T^2 L_n - i\bar{\Omega}\bar{k}L_n')$$

$$- \frac{\sqrt{\bar{C}g}}{2}\left[\frac{1}{\sqrt{\bar{C}g}}(L_n' + i\bar{\Omega}\bar{k}L_n)\right]' \qquad (3.83c)$$

where $T = thq_o = thk_o h_o = th\bar{h}_o$ and where primes denote differentiation with respect to $\bar{x}_1$.

Using the above scalings, (3.78) can be put in the following non-dimensional form,

$$\frac{\partial \bar{D}_o}{\partial \bar{t}_3} + \frac{\partial \bar{D}_1}{\partial \bar{t}_2} + (\bar{\gamma}_{11} + \bar{\mathcal{A}}_o^2\,\bar{\gamma}_{12})\bar{D}_o + \bar{\gamma}_2|\bar{D}_o|^2\bar{D}_o = \bar{\mathcal{A}}_o^2\,\bar{\mathcal{A}}_1\,\bar{\gamma}_3 \qquad (3.84)$$

where

$\bar{\mathcal{A}}_o = \frac{k_o}{\varepsilon} A_{o\infty}$ nondimensional, leading order incident wave amplitude prescribed at $x_1 \sim -\infty$

$\bar{\mathcal{A}}_1 = \frac{A_{1\infty}}{A_{o\infty}}$ nondimensional, second order modulation amplitude prescribed at $x_1 \sim -\infty$

$\bar{D}_o = \frac{k_o}{\varepsilon} D_o$ nondimensional, leading order edge wave amplitude

$\bar{D}_1 = \frac{k_o}{\varepsilon} D_1$ nondimensional, second order homogeneous edge wave amplitude

where ε represents the characteristic bottom slope [c,f, (2.10)] and the constant coefficients $\bar{\gamma}_{11}$, $\bar{\gamma}_{12}$, $\bar{\gamma}_2$ and $\bar{\gamma}_3$ are given by

$$\bar{\gamma}_{11} = \frac{i}{\bar{\gamma}_o}\int L_n\{\frac{\bar{h}^3\bar{K}^2}{12\bar{\Omega}}(\bar{K}^2L_n - L_n'') - \frac{1}{4}\bar{\Omega}\bar{h}^2\bar{K}^2L_n - (\frac{\bar{h}^3}{12\bar{\Omega}}[\bar{K}^2L_n' - L_n'''] - \frac{\bar{\Omega}}{4}\bar{h}^2L_n')'\}d\bar{x}_1 \tag{3.84a}$$

$$\bar{\gamma}_{12} = \frac{1}{\bar{\gamma}_o}\int L_n\{\frac{\bar{C}g_\infty}{\bar{C}g}[(\frac{q}{4ch^2q} + \frac{1}{4thq})\bar{\Theta}' - \frac{i}{2}(T\bar{\Omega} - \frac{\bar{K}^2}{2T\bar{\Omega}})\bar{\Theta} + \frac{\bar{T}\,\overline{a_1^p}}{4sh^2q} - \frac{\bar{k}L_n'}{4\bar{h}} + \frac{T}{2}\bar{k}L_n' + \frac{i}{4}\bar{\Omega}\bar{k}^2TL_n - \frac{i}{4}T^3\bar{\Omega}L_n - \frac{i\bar{K}^2}{4\bar{\Omega}}L_n(\frac{\bar{k}^2}{2T} - \frac{T}{2})] + [\frac{\bar{C}g_\infty}{\bar{C}g}(\frac{-i\bar{\Theta}'}{2\bar{\Omega}}[\frac{1}{2T} + \bar{h}] + \frac{\bar{k}\bar{\Theta}}{4T} - \frac{\bar{k}L_n}{4\bar{h}} - \frac{i\bar{k}\overline{a_1^p}}{2\bar{\Omega}T} + \frac{iL_n'}{4\bar{\Omega}}[\frac{3\bar{k}^2}{2T} - \frac{T}{2}])]'\}d\bar{x}_1 \tag{3.84b}$$

$$\bar{\gamma}_2 = \frac{1}{4\bar{\Omega}^2\bar{\gamma}_o}\int L_n\{\bar{K}^2L_n(\frac{3}{2}\bar{\psi}_2 - \bar{\psi}_1) + \frac{1}{2}L_n'\bar{\psi}_1' + \frac{1}{4}L_n'\bar{\psi}_2' + [L_n'(\bar{\psi}_1 + \frac{1}{2}\bar{\psi}_2) - \frac{L_n}{2}(\bar{\psi}_1' + \frac{1}{2}\bar{\psi}_2')]' + \frac{i}{8\bar{\Omega}T}(3L_n'^3 + \bar{K}^2L_n'L_n^2)' - \frac{i\bar{K}^2}{8\bar{\Omega}T}(L_nL_n'^2 + 3\bar{K}^2L_n^3)\}d\bar{x}_1 \tag{3.84c}$$

$$\bar{\gamma}_3 = \frac{-1}{\bar{\gamma}_o}\int L_n\{\frac{\bar{C}g_\infty}{\bar{C}g}\frac{i\bar{\Omega}T^2}{4sh^2q}\, e^{i\bar{\Omega}\int^{\bar{x}_1}\frac{d\zeta}{\bar{C}g}} + (\frac{\bar{C}g_\infty}{\bar{C}g}\frac{\bar{k}}{2}\, e^{i\bar{\Omega}\int^{\bar{x}_1}\frac{d\zeta}{\bar{C}g}})'\}d\bar{x}_1 \tag{3.84d}$$

where

$$\bar{\gamma}_o = T\int L_n^2(\bar{x}_1)d\bar{x} \;;\; T = th\,\bar{h}_o$$

$$\bar{C}g_\infty = \bar{C}g \quad (\bar{x}_1 = -\infty) \tag{3.84e}$$

For the submerged case, the integration limits are $(-\infty$ to $+\infty)$, while for the closed beach case, they are $(-\infty$ to $0)$.

From (3.21a), the amplitude $\bar{\mathcal{A}}_o = k_o A_{o\infty}/\varepsilon$ is in general a function of the slow scales $t_2, t_3, \ldots x_2, x_3, \ldots y_2, y_3, \ldots$ due to amplitude changes in the incident wave at infinity. Likewise, the small modulation amplitude $\bar{\mathcal{A}}_1$ is in general a function of $t_2, t_3, \ldots y_2, y_3, \ldots$. The trapped wave amplitude D_o however is not a function of t_2, (from (3.40)). The second order trapped wave amplitude correction D_1 will thus account for the edge wave response to such changes in $\bar{\mathcal{A}}_o$ or $\bar{\mathcal{A}}_1$ along the t_2 scale.

By averaging along the t_2 scale, we can always write,

$$\bar{\mathcal{A}}_o^2\,(t_2, t_3, \ldots y_1, y_2, \ldots) = \bar{A}_o^2(t_3, \ldots, y_2, y_3, \ldots) + \Delta\bar{\mathcal{A}}_o^2(t_2) \tag{3.85a}$$

$$\bar{\mathcal{A}}_1\,(t_2, t_3, \ldots) = \bar{A}_1(t_3, \ldots, y_1, y_2, \ldots) + \tilde{A}_1(t_2) \tag{3.85b}$$

so that,

$$\{\frac{\partial \bar{D}_o}{\partial \bar{t}_3} + (\bar{\gamma}_{11} + \bar{A}_o^2\,\bar{\gamma}_{12})\bar{D}_o + \bar{\gamma}_2|\bar{D}_o|^2\bar{D}_o - \bar{A}_o^2\bar{A}_1\bar{\gamma}_3\}$$

$$+\{\frac{\partial \bar{D}_1}{\partial \bar{t}_2} + \tilde{A}_o^2\,\bar{\gamma}_{12}\bar{D}_o - (\bar{A}_o^2\tilde{A}_1 + \Delta\bar{A}_o^2\bar{A}_1 + \Delta\bar{A}_o^2\tilde{A}_1)\bar{\gamma}_3\} = 0 \tag{3.86}$$

We require then that each curly bracket, by itself, is identically zero, i.e.,

$$\{\frac{\partial \bar{D}_o}{\partial \bar{t}_3} + (\bar{\gamma}_{11} + \bar{A}_o^2\,\bar{\gamma}_{12})\bar{D}_o + \bar{\gamma}_2|\bar{D}_o|^2\bar{D}_o = \bar{A}_o^2\bar{A}_1\bar{\gamma}_3 \tag{3.87a}$$

$$\frac{\partial \bar{D}_1}{\partial \bar{t}_2} + \tilde{A}_o^2\bar{\gamma}_{12}\bar{D}_o - (\bar{A}_o^2\tilde{A}_1 + \Delta\bar{A}_o^2\bar{A}_1 + \Delta\bar{A}_o^2\tilde{A}_1)\bar{\gamma}_3 = 0 \tag{3.87b}$$

Equations (3.87a,b) can then be integrated successively to get $\bar{D}_o$ and $\bar{D}_1$, hence the edge wave amplitude $\bar{D}_o + \varepsilon\bar{D}_1$.

4. EXCITATION MECHANISMS OF TRAPPED WAVES IN THE SURF BEATS FREQUENCY RANGE

Based on the evolution equation (3.87) we will investigate now the various mechanisms and possibilities of the excitation of trapped waves, in the surf beats frequency range, through their interaction with incident wave groups in the ocean. The incident wave group considered here has an envelope given by

$$A = A_o + \varepsilon A_1 + O(\varepsilon^2)$$

which from (3.18) and (3.68a) gives outside the range of the trapped wave, i.e., at $x_1 \sim -\infty$,

$$A = A_{o\infty} + \varepsilon(A_{1\infty} \cos Ky_1 e^{i\Omega[\int \frac{dx_1}{Cg_\infty} - t]} + *) + O(\varepsilon^2)$$

as $x_1 \to -\infty$

where $A_{o\infty}$ and $A_{1\infty}$ are prescribed functions of $x_2, x_3, \ldots, y_2, y_3, \ldots, t_2, t_3, \ldots$. Figure (4.1a) shows a profile of the envelope along the x-axis. This profile will be stationary for an observer moving with the group velocity. Such a three-dimensional envelope for the incident wave can be constructed by the grouping of a number of plane wave trains as shown in Figure (4.1b). First, most of the incident wave energy is carried by the normally incident, fundamental wave of frequency ω and amplitude $A_{o\infty}$. Then, added to it are two small wave groups. Each has an amplitude $\sim \varepsilon A_{1\infty}$, and is composed by the superposition of two wave trains of slightly

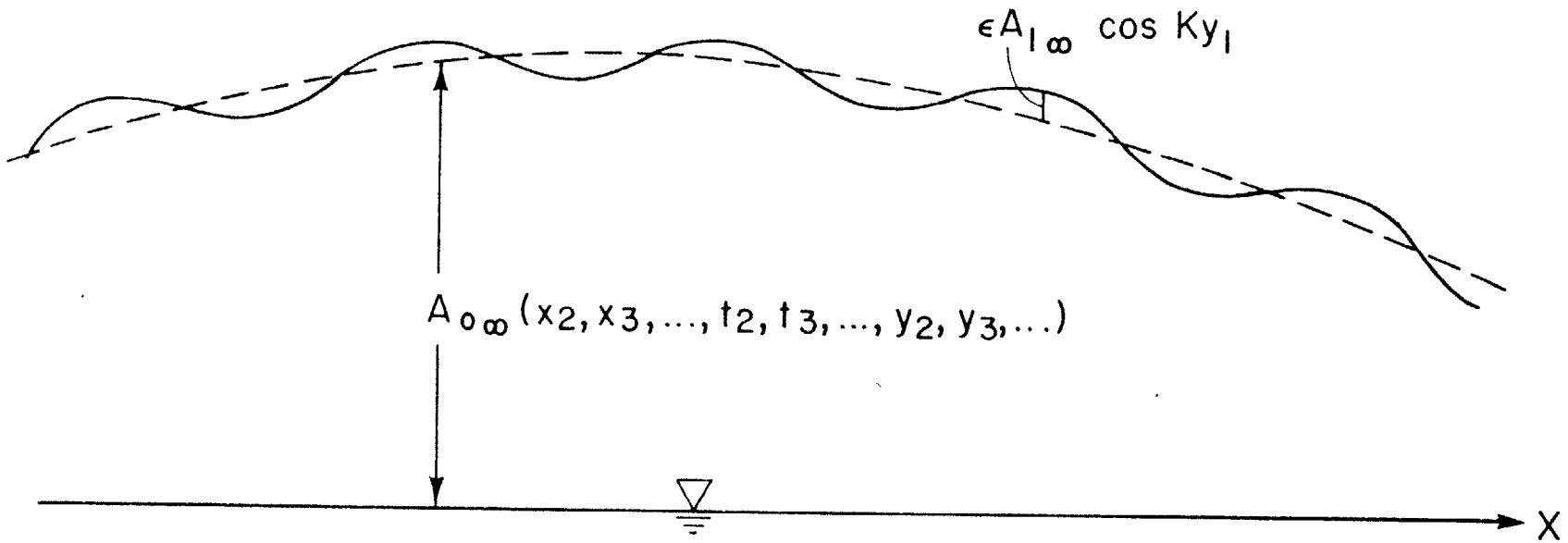

Figure (4.1a)

Incident wave envelope outside the range of the trapped wave ϕ_{oo}. The amplitude of the small modulation is sinusoidal along the lateral y_1 direction. $A_{1\infty}$ itself is in general a function of $x_2, x_3, \ldots t_2, t_3, \ldots y_2, y_3 \ldots$

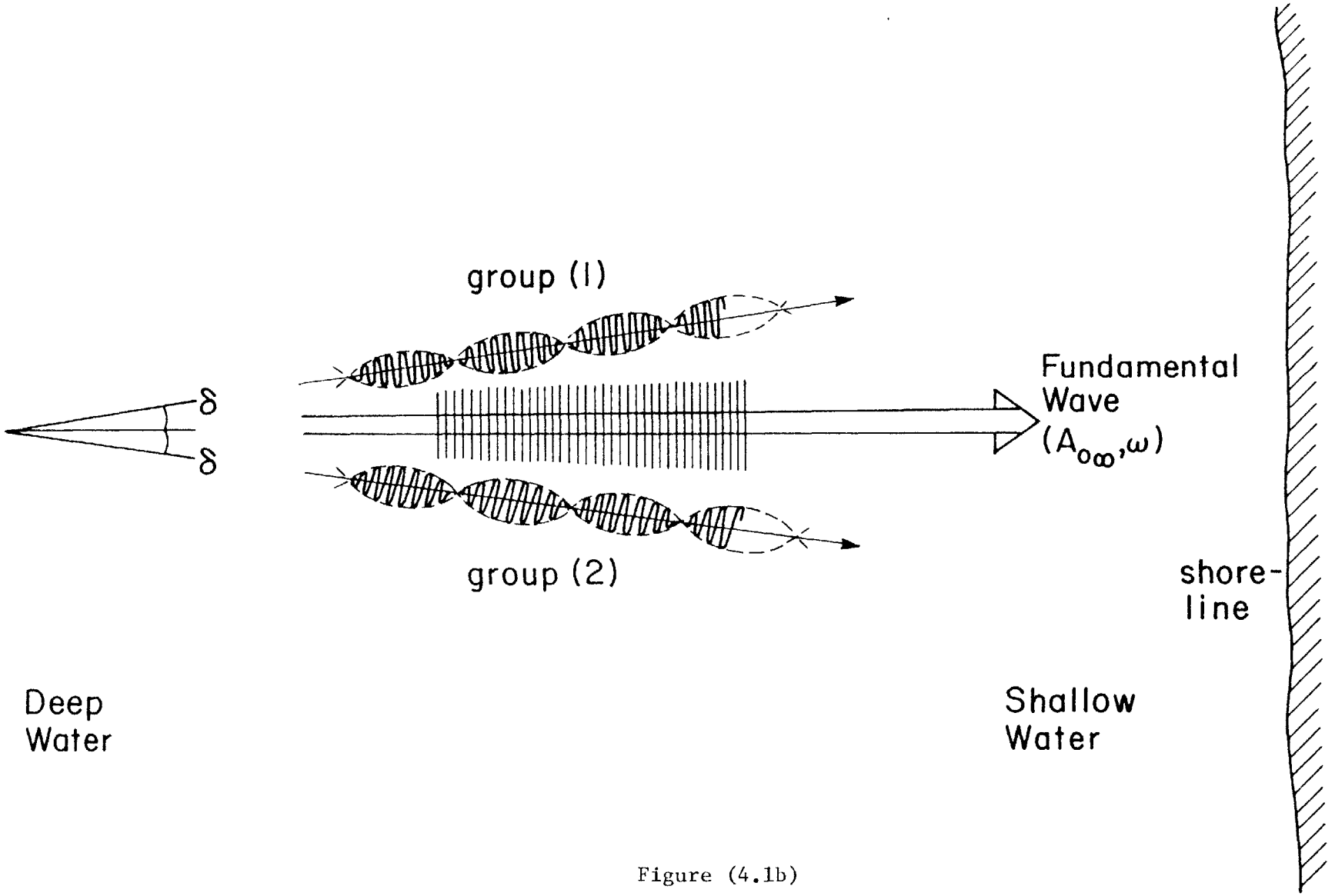

Figure (4.1b)

Incident wave pattern in deep water that develops envelope similar to the one in Figure (4.1a).

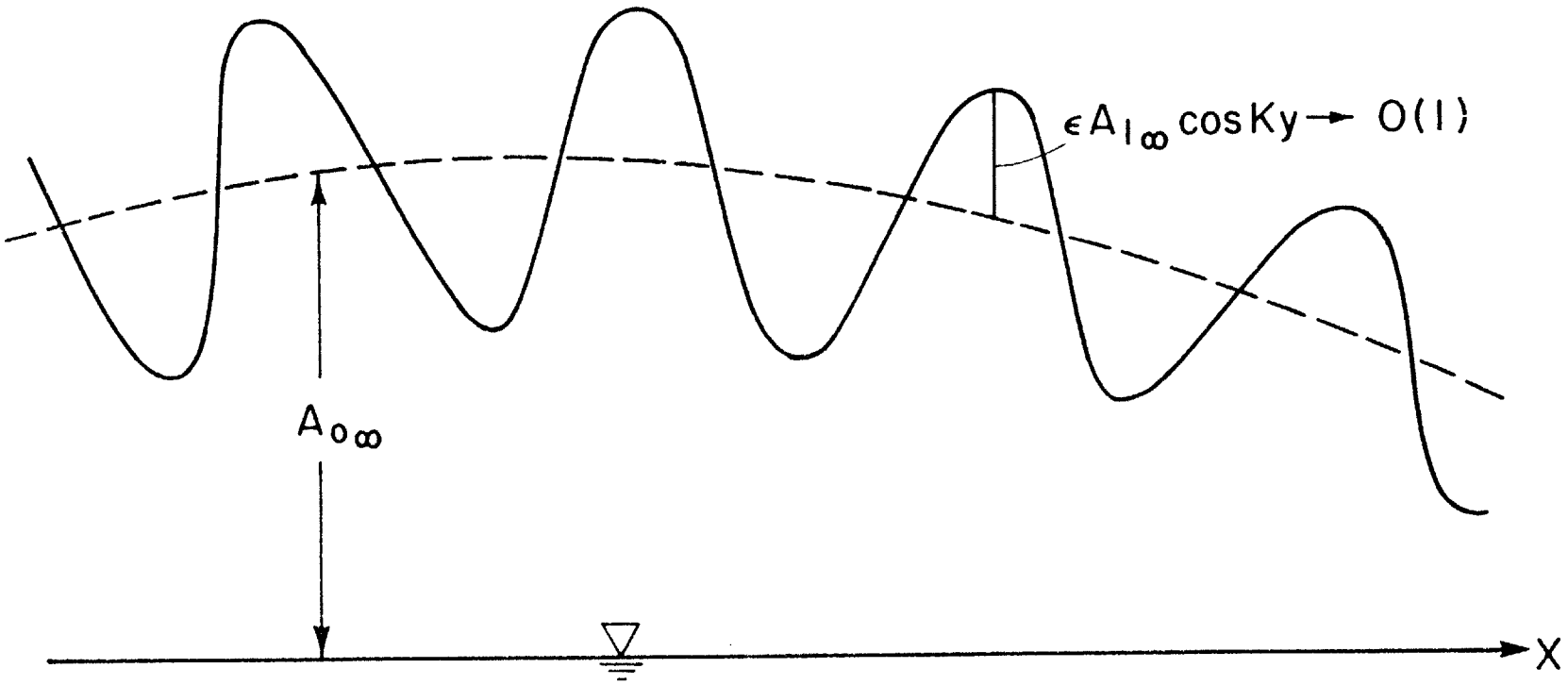

Figure (4.1c)

Strong resonant modulation to the incident wave.

different frequencies $\omega_1 = \omega + \varepsilon\Omega$ and $\omega_2 = \omega - \varepsilon\Omega$, with angle of incidence $=+\delta$ for one group; $=-\delta$ for the other. The angle δ is clearly given by,

$$\delta \simeq \tan^{-1} \frac{\varepsilon K}{k_o} \simeq \frac{\varepsilon K}{k_o} << 1.$$

where both Ω and K are those of the trapped wave ϕ_{oo} [Eq. (3.2)].

The small modulation, represented by the two small wave groups, has therefore zero propagation speed in the y-direction and the whole incident wave packet forms a narrow banded spectrum of waves with central frequency ω and bandwidth $\sim\varepsilon 2\Omega$, that is normally approaching the shallow waters with directional bandwidth, or a "beam" of $\sim \frac{2\varepsilon K}{k_o}$. This packet's structure has two main features that is commonly observed in wind-generated waves, (i) The incident waves are long crested, [its directional bandwidth $2\delta << 1$] and (ii) Its amplitude at a given station does not change significantly over a typical surf beats period; say 1-5 minutes period [see for example Munk (1949) and Tucker (1950); Figure (4.12)].

Turning now to the evolution equation (3.87), let us first enumerate the different parameters that appear in the equation. First, $\bar{\mathcal{A}}_o = \frac{k_o A_{o\infty}}{\varepsilon}$, i.e., the ratio of the leading order incident wave steepness at $x_1 \sim -\infty$ to the characteristic

sea bed slope ε, and it represents the relative importance of nonlinearity. Secondly, the relative modulation amplitude $\bar{\mathcal{A}}_1 = \frac{A_{1\infty}}{A_{o\infty}}$. Third, the constant frequency ratio $\bar{\Omega} = \frac{\Omega}{\omega}$, where Ω is measured along the slow time scale t_1. Lastly, the effect of the incident wave number k_o as well as the bottom topography appears in the nondimensional bottom profile $\bar{h} = k_o h = \bar{h}(x_1)$.

It is seen from (3.87) that the existance of small modulation, described by $\bar{\mathcal{A}}_1$, will always generate trapped waves over the submerged ridge. However, how large the resonated trapped wave will be, depends on the life span of such modulation. For example, if the resonant modulation is short lived, i.e., if

$$\bar{\mathcal{A}}_1 = \tilde{A}_1(\bar{t}_2) \; ; \quad \bar{A}_1(t_3,\ldots) = 0$$

then, there is no forcing in (3.87a) and the excited trapped wave will consist only of D_1 and hence of $O(\varepsilon)$ relative to the incident wave amplitude [no ϕ_{oo}].

On the other hand, if $\bar{\mathcal{A}}_1$ is extended over the longer $\bar{t}_3$ scale, the amplitude of the resulted trapped wave will be comparable to the incident wave amplitude.

Trapped waves which are generated due to the presence of such resonant modulations in the incident wave will eventually die away as the forcing vanishes. To see what

agents cause the eventual decay of the trapped wave, we let $\bar{A}_1 = 0$ in (3.87a), multiply the equation by $\bar{D}_o^*$, then add the resulted equation to its complex conjugate to get the following energy equation for $|\bar{D}_o|^2$,

$$\frac{\partial |\bar{D}_o|^2}{\partial \bar{t}_3} + 2\,\bar{A}_o^2\,\mathrm{Re}(\bar{\gamma}_{12})\,|\bar{D}_o|^2 + 2\mathrm{Re}(\bar{\gamma}_2)\,|\bar{D}_o|^4 = 0 \qquad (4.1)$$

where Re denotes the real part of.

For the coefficient $\mathrm{Re}(\bar{\gamma}_2)$, it is seen from (3.45) that ψ_2, representing the higher order forced trapped wave, is pure imaginary and hence, not contributing to $\mathrm{Re}(\bar{\gamma}_2)$ [See (3.84c)]. In fact, the only contribution to $\mathrm{Re}(\bar{\gamma}_2)$ comes from ψ_1 (Equation (3.44)) which represents the energy leakage from the trapped wave ϕ_{oo} in the form of outgoing long wave, propagating to infinity. Thus, it can be asserted that $\mathrm{Re}(\bar{\gamma}_2)$ is positive definite, representing the radiation damping of the trapped wave in (4.1). Another possible damping agent that can cause the decaying of the trapped wave is through losing energy to the incident wave group. The coefficient $\mathrm{Re}(\bar{\gamma}_{12})$ [see (3.84b)] does in fact represent the possible energy exchange between incident and trapped waves. Thus, if

$$\mathrm{Re}(\bar{\gamma}_{12}) > 0 \qquad (4.2)$$

direct transfer of energy from the trapped wave to the incident wave will take place, i.e., the incident wave will

work to damp out the trapped wave. A steady state condition can then be established when there is a dynamical balance between the resonant forcing $\bar{A}_1$ on one hand and the two damping agents on the other. The situation is analogous to the response of a one-dimensional weakly damped, weakly nonlinear oscillator to resonant sinuosidal forcings (Collinge and Ockenden, 1979).

If, on the other hand,

$$\mathrm{Re}(\bar{\gamma}_{12}) < 0 \tag{4.3}$$

energy will be transferred from the incident wave to the trapped wave, making the latter unstable. Hence, the conditions (4.2) and (4.3) define different physical mechanisms. It is evident initially that when D_o is small, instability prevails over the nonlinear radiation damping. Therefore, the incident wave need not have any $\bar{A}_1$ modulation for the generation of the trapped waves. Instead, the energy would directly be transferred from the incident wave itself to small existing trapped wave perturbations in the surf beats frequency range. Consequently, the homogeneous Equation (4.1) can be integrated for a given small initial value of $|\bar{D}_o|$, and given enough time will yield under steady state condition the nontrivial solution,

$$|\bar{D}_o|_s^2 = (\bar{A}_o)_s^2 \left(\frac{-\mathrm{Re}\ \bar{\gamma}_{12}}{\mathrm{Re}\ \bar{\gamma}_2} \right) \tag{4.4}$$

where $|\bar{D}_o|_s$ and $(\bar{A}_o)_s$ are the nondimensional steady state amplitudes for the trapped and the incident wave respectively.

It is seen also that the time scale for this instability mechanism is $\bar{t}_3$ and hence, the incident group life span has to be $O(\bar{t}_3)$, i.e., O (20 hours) for this mechanism to actively work in generating trapped waves of significant amplitude. Of course, as the group disappears, the trapped wave will decay with time due to radiation damping.

Therefore, incident wave groups can excite trapped waves in the ocean through two possible generation mechanisms, (i) Forced nonlinear resonance, with the forcing being the resonant, small modulation to the incident wave, (ii) Instability mechanism, with the condition (4.3) satisfied. The two mechanisms will be studied further in detail, investigating the occurance possibilities as well as the characteristics of the generated edge waves for each mechanism.

4.1 Solution of the Evolution Equation

As $\bar{D}_o$ is not a function of $\bar{t}_2$, Equation (3.87b) can easily be integrated for $\bar{D}_1$,

$$\bar{D}_1 = -\bar{\gamma}_{12}\,\bar{D}_o \int_0^{\bar{t}_2} \tilde{A}_o^2\, d\bar{t}_2 + \bar{\gamma}_3 \int_0^{\bar{t}_2} \Delta\bar{\sigma}\bar{A}_o^2\tilde{A}_1 + \bar{A}_o^2\tilde{A}_1^* + \Delta\bar{\sigma}\bar{A}_o^{2*}\tilde{A}_1\, d\bar{t}_2 \tag{4.5}$$

where we have assumed the initial condition that $\bar{D}_1 = 0$ at $\bar{t}_2=0$. Since by definition, (3.85a,b), $\Delta\bar{A}_o^2$ and $\tilde{A}_1$ have zero averages, theintegrals in (4.5) is always convergent.

Equation (3.87a) is on the other hand a nonlinear differential equation which lies within the realm of the theory of nonlinear oscillations [see for example Bogolinbov and Mitropolsky (1961); Minorsky (1962); Stoker (1950)] where various solution techniques are proposed to treat nonlinear differential equations. For small nonlinearity, there exist some analytical methods, such as the perturbation and iteration methods, [Cole, 1968; Nayfeh, 1973], that can be used to get the solution. Nonlinear systems can also be analyzed qualitatively using topological methods, e.g. the phase plane or phase space representation. Numerical methods are however, the most extensively used methods in solving nonlinear differential equations arising from actual physical systems.

A solution obtained using any of the above methods merely represents a state of equilibrium; its actual existance must then be confirmed by stability investigation. The question of stability is relatively simple in a linear system in which a single equilibrium condition exists. If the system is nonlinear, more than a single equilibrium condition may appear. A stable equilibrium can be maintained in practice, whereas an unstable one cannot. Hence, the question of

stability is particularly important in the study of nonlinear systems.

One simple stability criterion that can be applied to our case is the Routh-Hurwitz Criterion (Hayashi, 1964) which states that "In order to investigate the stability of a system near a chosen equilibrium point, we apply a sufficient small disturbance to the system by changing the solution from its equilibrium values. If, as the time $\bar{t}_3$ increases indefinitely, the solution returns to its original equilibrium values, the system is asymptotically stable at this point. On the other hand, if all or some of the solution values depart further from their original equilibrium values with increasing $\bar{t}_3$, the system is unstable".

Under the Instability Mechanism, there is only one unique steady state solution (4.4). For the Forced Excitation Mechanism, condition (4.2), the steady state solution can similarly be found as follows,

$$\bar{\gamma}_1 \bar{D}_{o_s} + \bar{\gamma}_2 |\bar{D}_o|_s^2 \bar{D}_{o_s} = \bar{A}_o^2 \bar{A}_1 \bar{\gamma}_3 \qquad (4.6)$$

where $\frac{\partial}{\partial \bar{t}_3} = 0$; $\bar{A}_o$, $\bar{A}_1$ = constants for steady state and $\bar{\gamma}_1 = \bar{\gamma}_{11} + \bar{A}_o^2 \bar{\gamma}_{12}$. Writing

$$\bar{\gamma}_1 = \gamma_1' + i\gamma_1'' \ , \ \bar{\gamma}_2 = \gamma_2' + i\gamma_2'' \quad \text{and} \quad \bar{A}_1 \bar{\gamma}_3 = |\bar{A}_1 \bar{\gamma}_3| e^{i\alpha}$$

where γ_1', γ_1'', γ_2', γ_2'' and α are real, we get from (4.6)

$$[(\gamma_1' + \gamma_2' |\bar{D}_o|_s^2) + i(\gamma_1'' + \gamma_2'' |\bar{D}_o|_s^2)]\bar{D}_{o_s} = \bar{A}_o^2 |\bar{A}_1 \bar{\gamma}_3| e^{i\alpha} \tag{4.7}$$

Letting $\bar{D}_{o_s} = |\bar{D}_o|_s e^{i(\alpha+\delta)}$

then,

$$\tan\delta = - \frac{(\gamma_1'' + \gamma_2'' |\bar{D}_o|_s^2)}{(\gamma_1' + \gamma_2' |\bar{D}_o|_s^2)}$$

so that (4.7) reduces to,

$$[(\gamma_1' + \gamma_2' |\bar{D}_o|_s^2)^2 + (\gamma_1'' + \gamma_2'' |\bar{D}_o|_s^2)^2]^{1/2} |\bar{D}_o|_s =$$

$$= \bar{A}_o^2 |\bar{A}_1 \bar{\gamma}_3| \tag{4.8}$$

or, by taking the square of (4.8) and letting $\mathcal{E} = |\bar{D}_o|_s^2$

$$|\bar{\gamma}_2|^2 \mathcal{E}^3 + 2[\bar{\gamma}_1 \cdot \bar{\gamma}_2]\mathcal{E}^2 + |\bar{\gamma}_1|^2 \mathcal{E} = \bar{A}_0^4 |\bar{A}_1 \bar{\gamma}_3|^2 \tag{4.9}$$

where

$\bar{\gamma}_1 \cdot \bar{\gamma}_2$ is the dot product of the two vectors $\bar{\gamma}_1$ and $\bar{\gamma}_2$ in the complex plane.

We will only take the real positive roots of the cubic equation (4.9) as our steady state equilibrium conditions, then determine the stable equilibrium conditions from the obtained solutions.

Equations similar to (3.87a) are derived in the literature when studying the Duffing's Equation for a hard

spring oscillation. Collinge and Ockendon (1979) derived this equation, with $Re(\bar{\gamma}_2)=0$, when studying the transition through resonance of a weakly damped, weakly nonlinear oscillator as the forcing frequency increases slowly. Ablowitz, Funk and Newell (1973) derived the same equation, with both $Re(\bar{\gamma}_1)$ and $Re(\bar{\gamma}_2)$ equal to zero, when studying semi-resonant interactions.

4.2 Trapped Waves over Submerged Ridge, by Forced Resonance

As our first example, we consider the excitation of Trapped waves over submerged ridges (Figure 1.2]. A wave packet is incident from $x \sim -\infty$, propagating in the positive x-direction over the bottom profile $\bar{h}(\bar{x}_1)$. The wave packet is assumed to suffer no wave breaking or reflection as it passes by the ridge to $x \sim +\infty$. The ridge shape is assumed here to be Gaussian so that,

$$\bar{h} = \bar{h}_o \left[1-(1-r)e^{-\beta \bar{x}_1^2}\right] \qquad (4.10)$$

where $\bar{h}_o$ is the non-dimensional constant water depth at infinity, r is the ratio between the minimum water depth at the ridge's top ($\bar{x}_1=0$), to the maximum water depth at infinity. The coefficient β is chosen to be,

$$\beta = \frac{e}{2[(1-r)\bar{h}_o]^2}$$

so that the bottom slope, characterized by its maximum value, is

$$\left.\frac{dh}{dx}\right|_{max} = \varepsilon \left.\frac{dh}{dx_1}\right|_{max} = \varepsilon \left.\frac{d\bar{h}}{d\bar{x}_1}\right|_{max} = \varepsilon$$

for any value of $\bar{h}_o$ and r.

For given values of $\bar{h}_o$, r and $\bar{\Omega}$, the values of the coefficients $\bar{\gamma}_{11}$, $\bar{\gamma}_{12}$, $\bar{\gamma}_2$ and $\bar{\gamma}_3$ of (3.87) can be evaluated for a certain trapped wave mode n, from (3.84a,...,e) and by following the general procedure of Chaper 3. The amplitudes $\bar{\mathcal{A}}_o$ and $\bar{\mathcal{A}}_1$ are prescribed for a given incident wave packet [see Figures (4.1a,b)]. Equation (3.87a) can be integrated numerically for the amplitude $\bar{D}_o$, then the variation of $\bar{D}_1$ in $\bar{t}_2$ is determined from (4.5). The numerical scheme is based on an algorithm written by Krogh (1969) using the Adams-Moulton numerical integration method. The numerical program adjusts the order of the integration formula to maximize step size without introducing estimated errors larger than a given specified bound, [see Krogh (1969) for further details].

A broad range of the relevant parameters was considered in the calculation; $0.1 \leq r \leq 0.5$, $1.0 \leq \bar{h}_o \leq 5.0$ and $1.0 \leq \bar{\Omega} \leq 3.0$. As for the trapped wave modes, we considered both the excitation of the lowest even mode (n=0) and the lowest odd mode (n=1). Then, for a given combination of parameters and specified wave mode, the first important task, before integrating (3.87), was to evaluate the

coefficient $\bar{\gamma}_{12}$ from (3.84b) and determine whether $\mathrm{Re}(\bar{\gamma}_{12} \gtrless 0$ [Condition (4.2) ir (4.3)] in order to identify the possible trapped wave generation mechanism for the particular case considered. The evolution of the integral in (3.84b) for $\bar{\gamma}_{12}$, as well as the coefficients defined in (3.84a-e), was carried out numerically using Simpson's Rule.

In all the cases investigated, it was found that Condition (4.2) always prevails, i.e.,

$$\mathrm{Re}(\bar{\gamma}_{12}) > 0$$

meaning that the trapped wave modes are always damped in the presence of unmodulated incident waves. Thus, for the generation of these trapped modes, they must be forced by non-zero $\bar{A}_1$.

The second task is then to investigate the possible equilibrium solutions of the nonlinear equations (3.87) and carry out stability analysis on them to select the most stable solution as our actual solution. This is necessary if more than one equilibrium solution of (3.87) is possible. At steady state equilibrium (3.87) reduces to the cubic equation (4.9). However, it is known [Abramowitz and Stegun, 1965] that when solving for (4.9), if the following condition is satisfied

$$q_c = \frac{1}{3}\frac{|\bar{\gamma}_1|^2}{|\bar{\gamma}_2|^2} - \frac{1}{9}\left[\frac{2(\bar{\gamma}_1\cdot\bar{\gamma}_2)}{|\bar{\gamma}_2|^2}\right]^2$$

$$= \frac{|\bar{\gamma}_1|^2}{|\bar{\gamma}_2|^2}\left(\frac{1}{3} - \frac{4}{9}\cos^2\sigma\right) > 0$$

i.e., if

$$|\sigma| > \frac{\pi}{6}$$

where σ is the phase angle between $\bar{\gamma}_1$ and $\bar{\gamma}_2$ in the complex plane, then there is only one real root to (4.9). In all the calculation carried out, the above condition was well satisfied. Consequently, the question of stability of the nonlinear solutions never came in.

The final task is then to integrate (3.87) numerically for the given parameter range. Sample results of the integration, are shown in Figures (4.2) to (4.8) displaying some characteristics of the generated trapped waves. Figures (4.2) to (4.7) show the results for the gravest even mode (n=0), while Figure (4.8) shows a comparison between the results for this gravest even mode and those obtained for the first odd mode (n=1).

Figure (4.2) shows the transient response of the trapped wave amplitude $|\bar{D}_o|$ $(\bar{t}_3)$ in the case of a step-function loading, i.e.,

$$\left.\begin{matrix}\bar{\mathcal{A}}_o \\ \bar{\mathcal{A}}_1\end{matrix}\right\} = \begin{cases} 0 & \text{for } \bar{t}_3 \leq 0 \\ \text{constant} & \text{for } \bar{t}_3 \geq 0 \end{cases}$$

That is, a uniform wave train with constant modulation is suddenly introduced at $\bar{t}_3=0$. From the Figure, the general behavior is seen to be first, a rapid shoot from zero initial-value, then oscillation around the steady-state value which is reached asymptotically as $\bar{t}_3 \sim \infty$. Figure (4.3) is for the case of a finite extent wave packet $\bar{\mathcal{A}}_o = \bar{A}_o(\bar{t}_3)$ with constant relative modulation $\bar{\mathcal{A}}_1 = \frac{A_{1\infty}}{A_{o\infty}} = 1.0$ (case 1), while Figure (4.4) is for the case of a uniform wave train $\bar{\mathcal{A}}_o = 1$ (i.e., $A_{o\infty}$ = constant) which suffers modulation as in (3.68a) for a finite length of time, i.e., $\bar{\mathcal{A}}_1 = \bar{A}_1(\bar{t}_3)$ (Case 2). Although in the two cases the generated amplitude reaches roughly the same peak value, it is seen from the Figures that the decay rate afterward is much lower in case 1 than in case 2. The reason is condition (4.11) which implies that the incident wave acts to damp out the trapped wave, as seen from Equation (4.1). Hence, in case 2, the trapped wave decay is due to both the incident wave damping (the term $2\bar{A}_o^2$ Re $\bar{\gamma}_{12}\,|\bar{D}_o|^2$ in (4.1)) and the radiation damping (the term 2Re $\bar{\gamma}_2|\bar{D}_o|^4$ in (4.1)). But, in case 1, because $\bar{A}_o$ has finite extent, the trapped wave decay is mainly due to just the radiation damping.

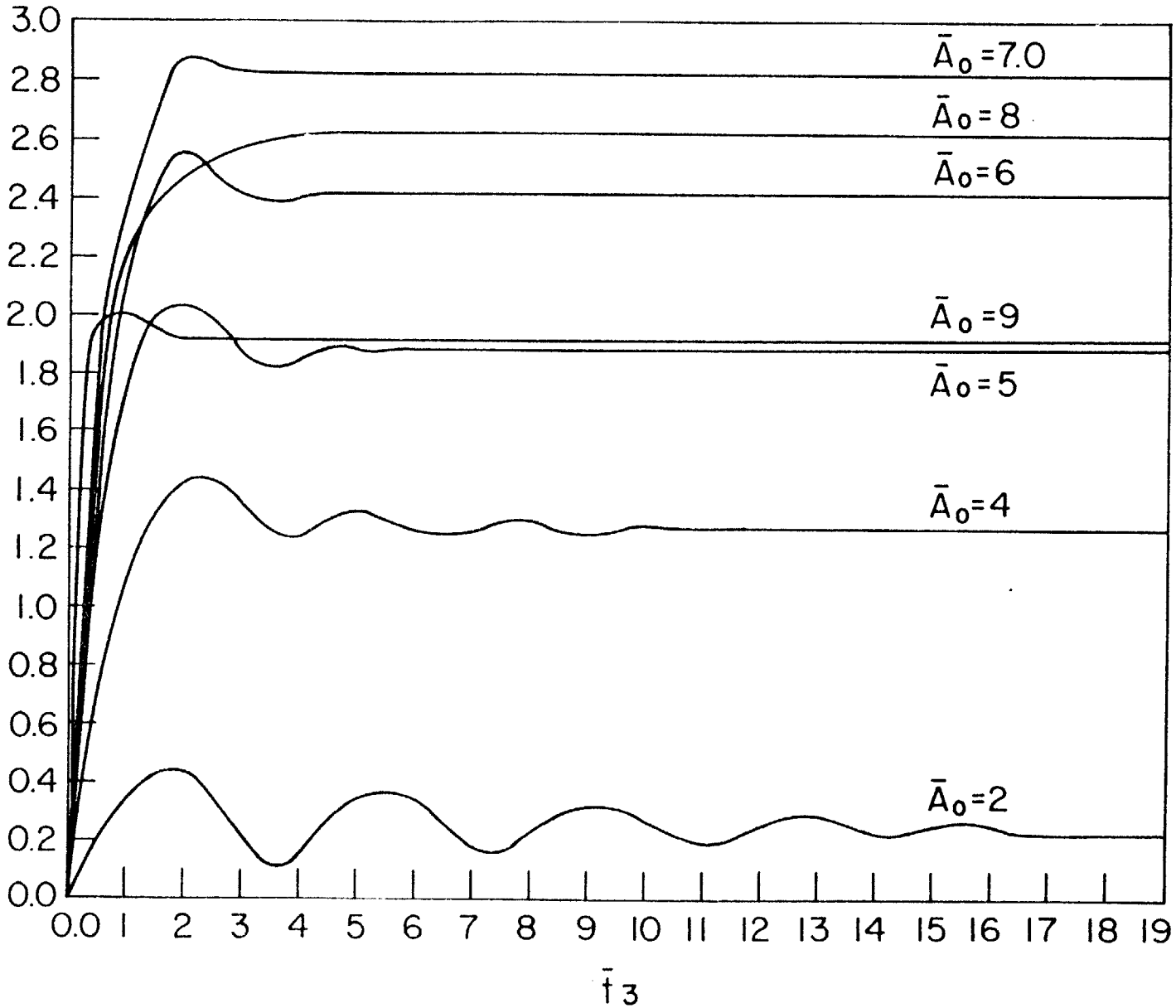

Figure (4.2)

Transient response of the trapped wave amplitude due to a step-function loading of the incident wave at $\bar{t}_3=0$, for various constant values of $\bar{}_o$ and $\bar{}_1 = 1.0$.

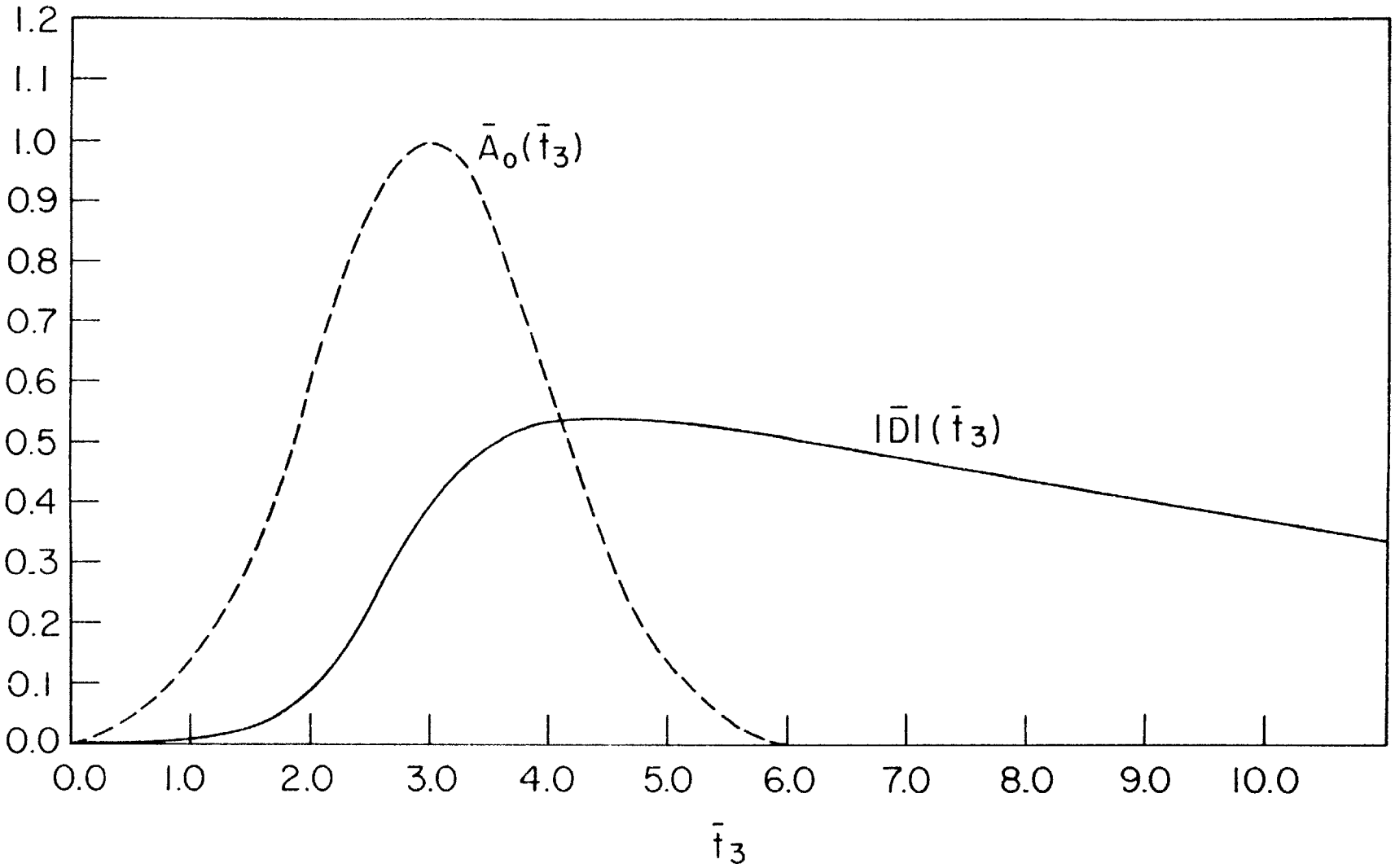

Figure (4.3)

Transient response of the trapped wave amplutide for the case of a finite extent wave packet $\bar{}_o$ = exp[=0.5($\bar{t}_3$-e)^2] and constant relative modulation $\bar{}_1$ = 1.0.

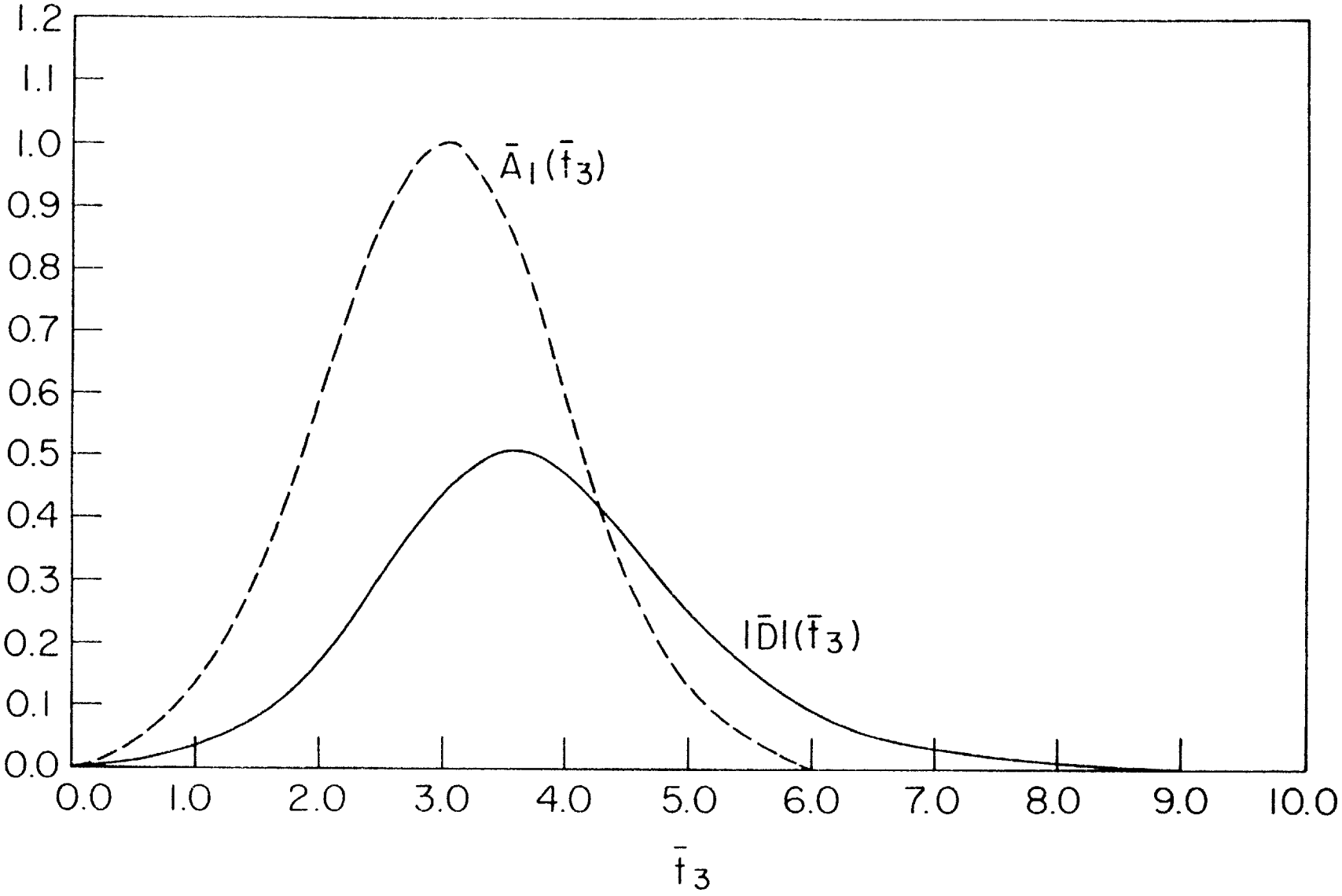

Figure (4.4)

Transient response of the trapped wave amplitude for the case of a uniform wave train $\bar{}_o$ = 1.0 and a relative modulation $\bar{}_1 = \exp[-0.5(\bar{t}_3-3)^2]$.

Beside integrating (3.87) to get the transient response, teh cubic equation (4.9) was solved for the steady state amplitude $|\bar{D}_o|_s$ for a wide range of parameters. The results are shown in Figures (4.5) to (4.7). It is seen from the figures that the effect of nonlinearity, presented by $\bar{A}_o$ is important in the generation of the trapped waves.

Effect of Nonlinearity on Steady State Amplitude

For negligible nonlinearity, i.e., $\bar{A}_o \sim 0$, the forcing in the right-hand-side of (3.87a) is negligible and so will the trapped wave amplitude. Hence, we may neglect the nonlinear term in (3.87a), (i.e., $\bar{\gamma}_2 |\bar{D}|^2 \bar{D}$), at this limit to get the approximate solution

$$\bar{D}_o = \frac{\bar{A}_o^2 \bar{A}_1 \bar{\gamma}_3}{\bar{\gamma}_{11} + \bar{A}_o^2 \bar{\gamma}_{12}} \{1-\exp[-(\bar{\gamma}_{11} + \bar{A}_o^2 \bar{\gamma}_{12})\bar{t}_3]\} \text{ for } \bar{A}_o << 1$$

which satisfies the initial condition $\bar{D}_o = 0$ at $\bar{t}_3=0$. Notice that the steady state solution gives

$$\bar{D}_o \sim \bar{A}_o^2$$

or

$$\frac{D}{A_{o\infty}} \to 0 \quad \text{as} \quad A_{o\infty} \text{ (or } \bar{A}_o) \to 0$$

i.e., the trapped wave is even more negligible than the swells.

At the other limit of strong nonlinearity, $\bar{A}_o >> 1$,

it is seen from the figures, as well as (3.87a), that $|\bar{D}_o|_s$ no longer changes with $\bar{\mathcal{A}}_o$, as it reaches a limit given by

$$\lim_{\bar{\mathcal{A}}_o \to \infty} |\bar{D}_o|_s = \frac{|\bar{\mathcal{A}}_1 \bar{\gamma}_3|}{|\bar{\gamma}_{12}|}$$

Notice from Figures (4.5) to (4.7) that the maximum $|\bar{D}_o|_s$ is not in general reached at the limit $\bar{\mathcal{A}}_o \to \infty$, but instead at some finite $\bar{\mathcal{A}}_o$.

For all these values of $\bar{\mathcal{A}}_o$, it is important to investigate their relevance in real ocean conditions. First, a typical value of wind wave steepness ($k_o A_{o\infty}$) in the ocean is 0.05. Then, for $\bar{\mathcal{A}}_o \sim 0(1)$ [i.e., bottom slope $\varepsilon \sim 0.05$] the generation time scale $\bar{t}_3$ corresponds to 0(20 hrs), which is relevant for typical wind-wave-group life span. However, $\bar{}_o >> 1$ implies a much milder bottom slope for the same wave steepness, and hence a much longer generation time, rendering the mechanism of generation very weak. Hence, even if the steady state solution for $\bar{\mathcal{A}}_o >> 1$ is large, the results are impractical as it requires an unusually long duration of the forcings (e.g., for $\bar{\mathcal{A}}_o \sim 10$, that required generation time will be of the order 0(100 hrs)).

The effects of the incident wave number k_o and the topography (represented by the coefficient $r = \frac{h_{min}}{h_{max}}$) on the steady state $|\bar{D}_o|_s$ are also shown in Figures (4.5) to (4.7). For the incident wave, $\bar{h} = k_o h \geq \pi$ implies short wave compared to depth and hence deep water condition, while $\bar{h} \leq \pi/10$

implies long waves compared to depth, i.e., shallow water conditions. For the shorter waves, for example Figure (4.5) [r=0.5 and $\bar{h}_o$=2,3] and Figure (4.6) [r=0.3 and $\bar{h}_o$=3], it is seen that the maximum value for $|\bar{D}_o|_s$ is attainable for large values of $\bar{\mathcal{A}}_o$, implying longer generation time or weaker growth rate. As the waves get longer, for example Figure (4.7) [r=0.1 and $\bar{h}_o$=1,2,3] and Figure (4.6) [r=0.3 and $\bar{h}_o$=1,2], the curves $|\bar{D}_o|_s$ ($\bar{\mathcal{A}}_o$) reaches their peaks at much smaller values of $\bar{\mathcal{A}}_o$. From Figures (4.5) to (4.7) it is also seen that increasing $\bar{\Omega}$, with $\bar{h}_o$ fixed, has similar effect on the curves $|\bar{D}_o|_s$ ($\bar{\mathcal{A}}_o$) as when decreasing $\bar{h}_o$ at the same $\bar{\Omega}$.

The Lowest Odd Mode

The results for the lowest odd mode (n=1) (see Fig. (4.8a) for modal profile) is qualitatively similar to those just discussed for the even mode (n=0). Some of the quantitative differences between the two modes are shown in Figure (4.8) which shows $|\bar{D}_o|_s$ for each mode for selected input parameters. It is seen from the Figure that the peaks of the steady-state curves tend to migrate to regions of higher nonlinearity (larger $\bar{\mathcal{A}}_o$) for the higher mode (n=1). More specifically, it is seen that for moderate to low values of $\bar{\mathcal{A}}_o$, $|\bar{D}_o|_s$ for n=0 is larger than for n=1, and the reverse is true for larger values of $\bar{\mathcal{A}}_o$.

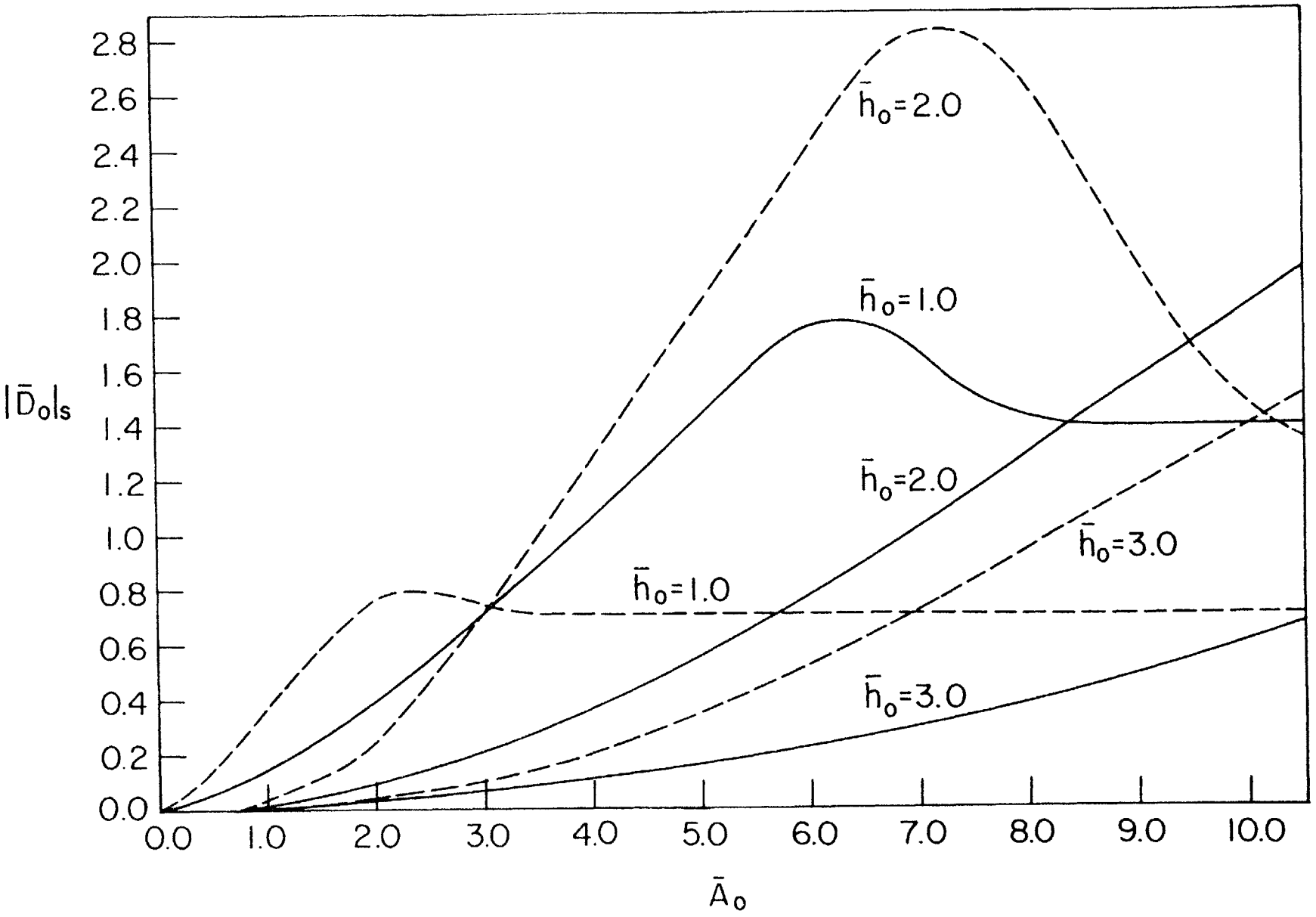

Figure (4.5)

Trapped wave steady state amplitude vs. $\bar{}_o$ for relative modulation $\bar{}_1 = 1$, $r=h_{min}/h_{max}=0.5$ and $\bar{h}_o$=1,2 and 3. _____ $\bar{\Omega} = 1$; ---------- $\bar{\Omega} = 2$.

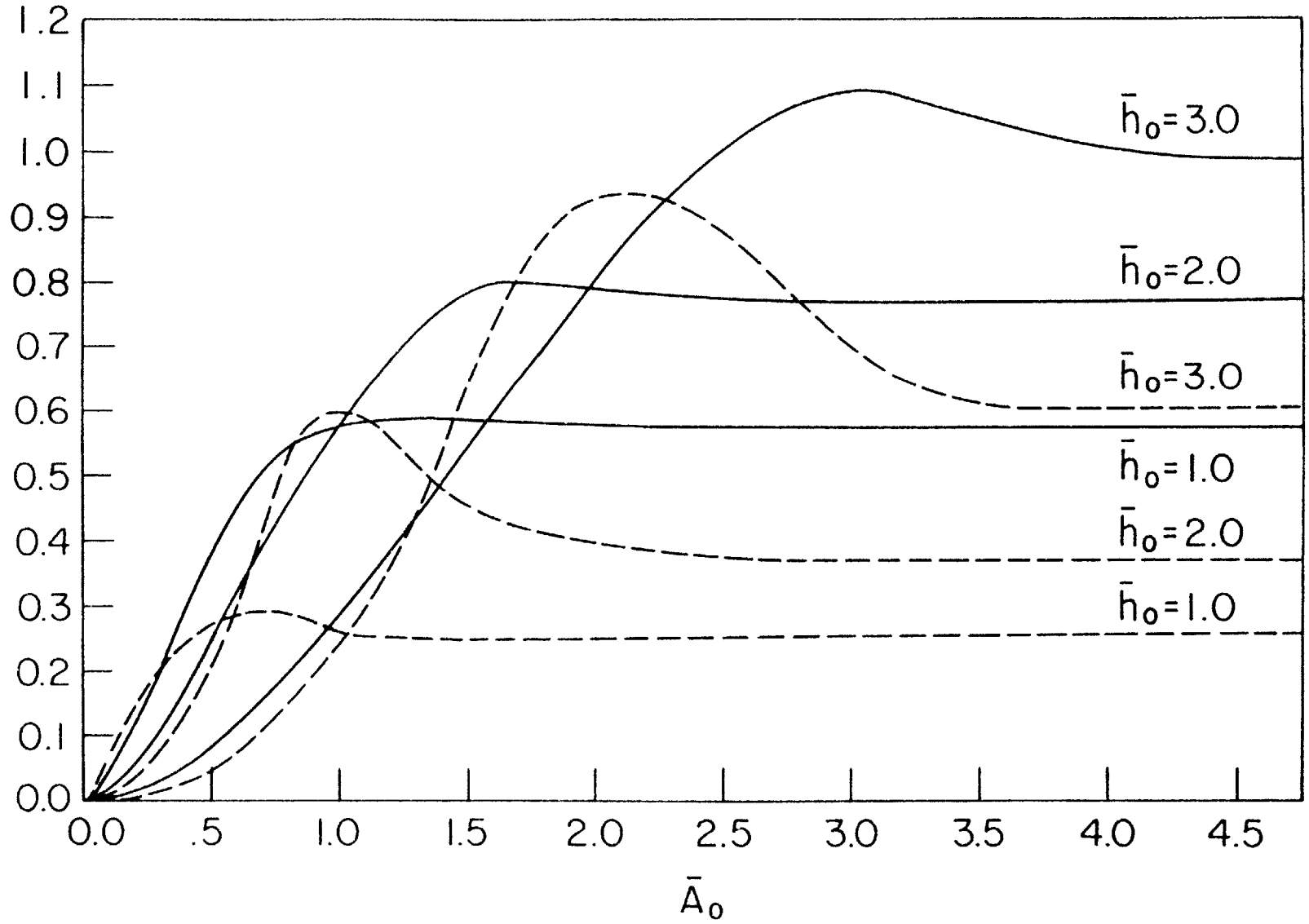

Figure (4.6)

Trapped wave steady state amplitude vs. $\bar{A}_o$ for relative modulation $\bar{h}_1 = 1$, r=0.3 and $\bar{h}_o$=1,2 and 3. _____ $\bar{\Omega} = 1$' _____ $\bar{\Omega} = {}^{o}2$.

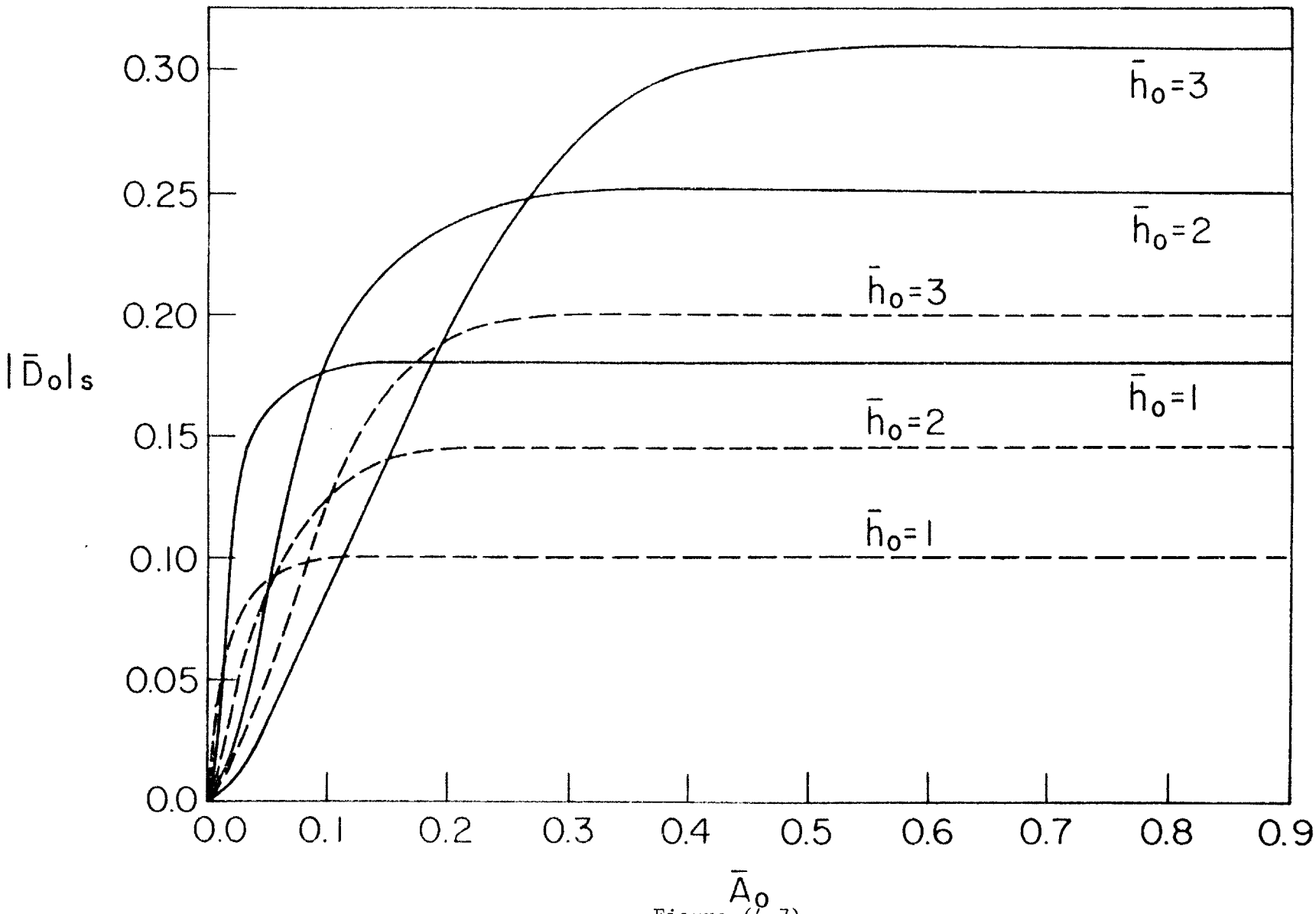

Figure (4.7)

Trapped wave steady state amplitude vs. $\bar{A}_o$ for relative modulation $\bar{h}_1$=1, R=0.1 and $\bar{h}_1$ = 1,2 and 3. _____ $\bar{\Omega}_1$=1; ---------- $\bar{\Omega}$ = 2.

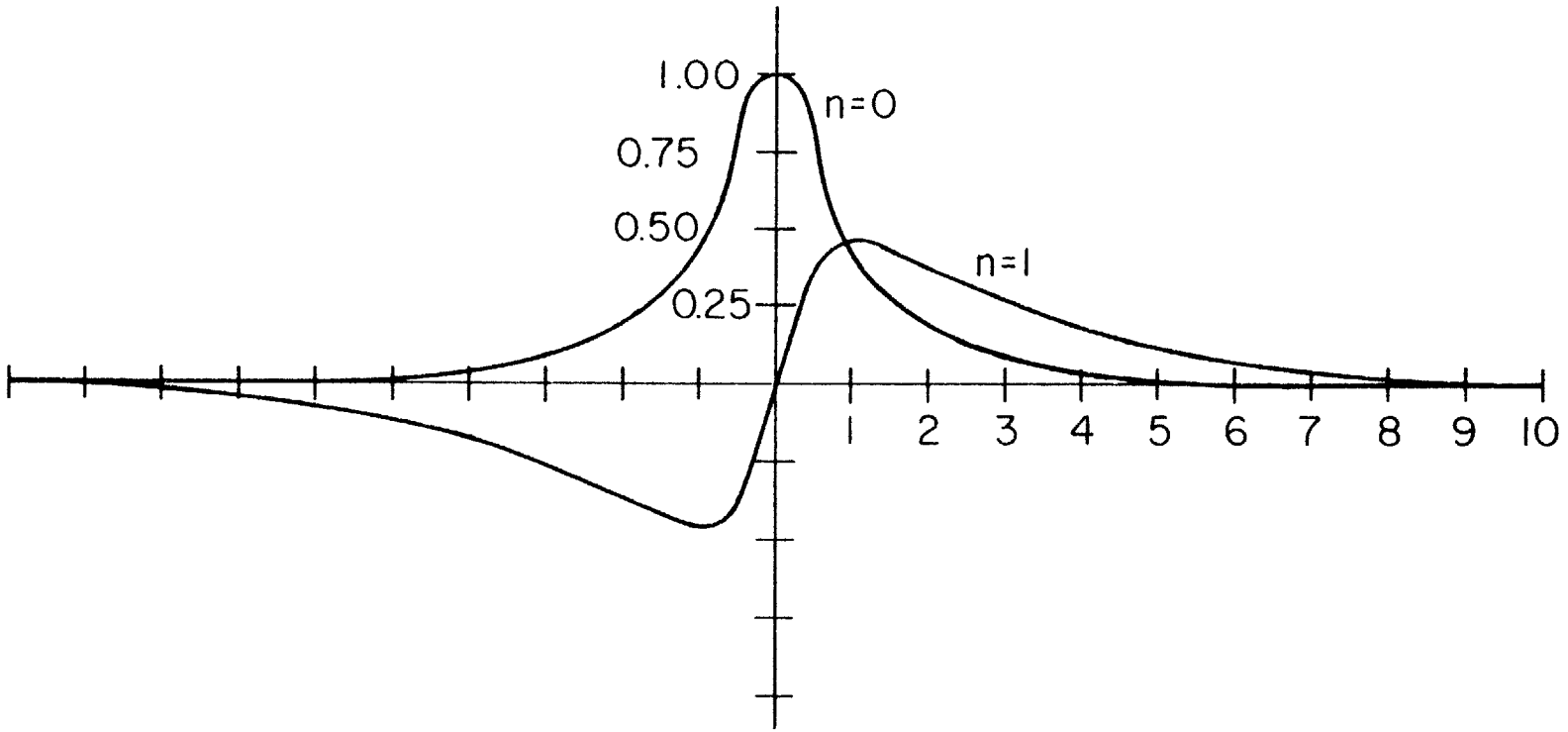

Figure (4.8a)

Modal shapes for the lowest even mode (n=0), and the lowest odd mode (n-1) for r=0.3, $\bar{h}_o$=2 and $\bar{\Omega}$=2.

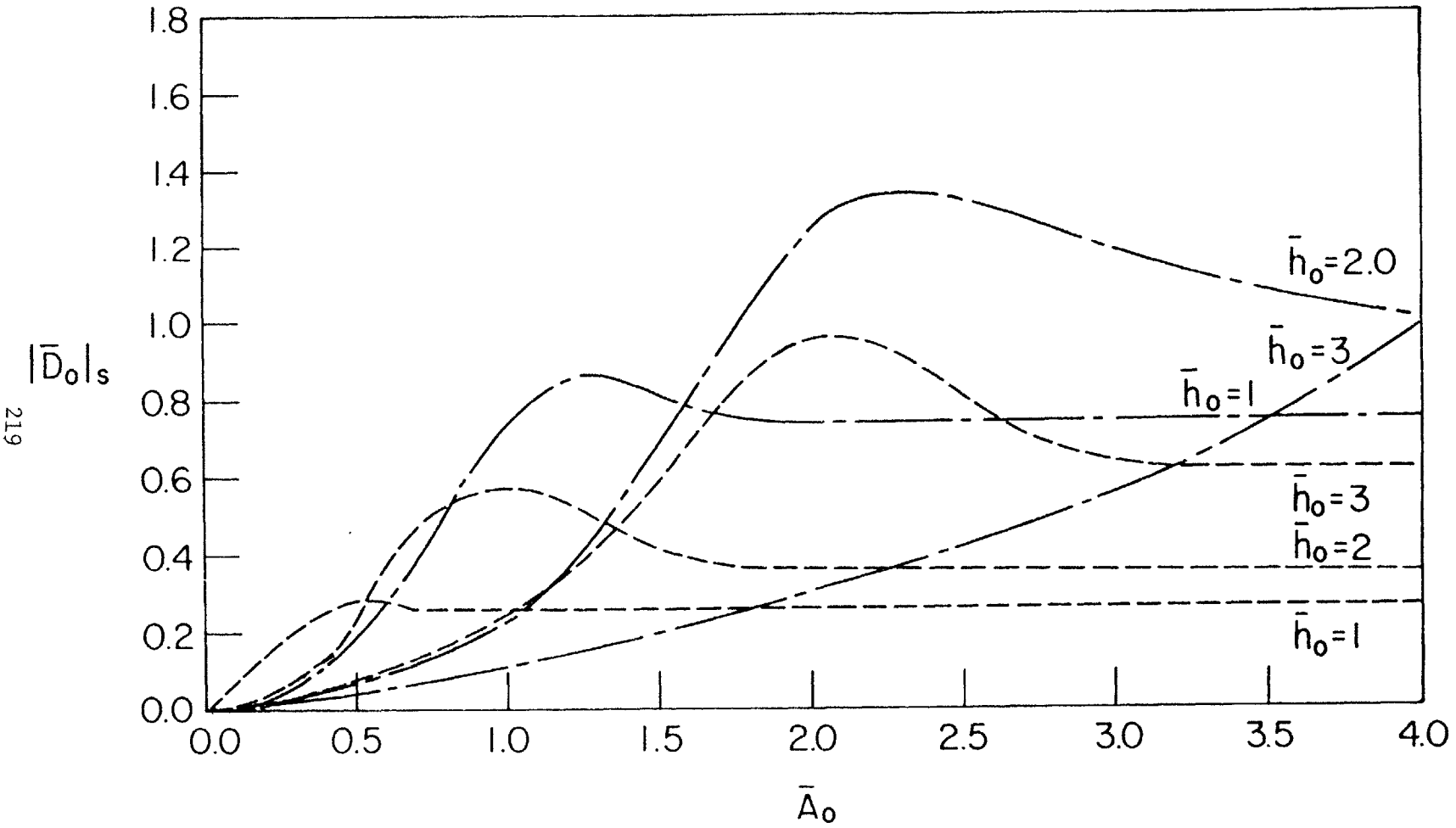

Figure (4.8)

Trapped wave steady state amplitude vs. $\bar{A}_o$ for relative modulation $\bar{h}_1=1$, r=0.3, $\bar{h}_o=1,2$ and 3 and $\Omega=2$. _____losest even mode; _____ lowest odd mode.

Remarks on Strong Resonant Modulation

Since by definition, (2.5c), we have

$$\frac{\partial}{\partial \bar{t}_2} = \frac{\partial}{\partial \bar{t}_2} + \varepsilon \frac{\partial}{\partial \bar{t}_3}$$

we may get from (3.84)

$$\frac{\partial \bar{D}_o}{\partial \bar{t}_2} = -\varepsilon\{\frac{\partial \bar{D}_1}{\partial \bar{t}_2} + (\bar{\gamma}_{11} + \bar{\mathcal{A}}_o^2\ \bar{\gamma}_{12})\bar{D}_o + \bar{\gamma}_2|\bar{D}_o|^2\bar{D}_o - \bar{\mathcal{A}}_o\bar{\mathcal{A}}_1\ \bar{\gamma}_3\} \tag{4.11}$$

In the analysis here, we have considered only small resonant modulation to the incident wave amplitude [Figure 4.1a,b] which means that $\bar{\mathcal{A}}_1 \sim 0(1)$. In the more severe situation of strong resonant modulation [Figure 4.1c], i.e., $\varepsilon\bar{\mathcal{A}}_1 \sim 0(1)$, it is seen from (4.11) that, (i) Initially, we have stronger resonant growth rate,

$$\frac{\partial \bar{D}_o}{\partial \bar{t}_2} \simeq \varepsilon\bar{\mathcal{A}}_o\bar{\mathcal{A}}_1\ \bar{\gamma}_3 \sim 0(1) \tag{4.12}$$

as it is along the $\bar{t}_2$ scale, instead of the slower t_3 scale for the small modulation case, and (ii) The steady state amplitude $|\bar{D}_o|_s >> 1$, i.e., much larger than the incident wave amplitude. Therefore, the expansion (2.8) for the velocity potential ϕ may need to be modified for this particular case in order to accomodate for the fact that the

resulted trapped wave amplitude may be much larger than the incident wave amplitude. However, the case of strong resonant modulation requires significant changes in the incident wave amplitude over periods of say 1-5 minutes as shown in Figure (4.1c). This does not agree with the observations of Munk (1949) and Tucker (1950) [Figure (4.12)] which shows such significant changes to occur over much longer periods of time. Unfortunately, observations similar to those of Munk and Tucker, and in general available information about the actual incident wave spectrum in the ocean is indeed very limited (Barnett and Kenyon, 1975), especially with regard to the incident wave directional spread, and further observational evidence is needed in order to decide whether envelopes similar to that in Figure (4.1a), or that in Figure (4.1c) are more effective in generating low frequency trapped waves in the real ocean conditions.

4.3 Surf Beats on a Beach (Instability Excitation)

The second example we consider is the excitation of surf beats on dissipative closed beaches, with the surf zone occupying the region between the shoreline $\bar{x}_1=0$ and the breaker line $\bar{x}_1 = \bar{x}_b$. It is assumed that all incident swells break so that there is no wave reflection to deep water. The geometry is depicted in Fig. (3.1) where the beach, extended along the negative x-axis, is assumed plane, with the slope given by $\varepsilon << 1.$, i.e.,

$$h = -\varepsilon x = -x_1 \tag{4.13}$$

or,

$$\bar{h} = -\bar{x}_1 \tag{4.13a}$$

where the scaling k_{2o} (3.79) is replaced by the deep water wave number $k_\infty = \frac{\omega^2}{g}$. The wave packet is incident from deep water $x \sim -\infty$. Once inside the surf zone, turbulence prevails so that the breaking wave crest diminishes in amplitude until the shore is reached where the amplitude is zero. Kinematically however, the wave rays proceed in the surf zone roughly in the same direction as if they were no breaking.

Although the flow in breaking waves is highly complex and does not lend itself to a detailed deterministic treatment, there exist in the literature a number of

empirical relations between some flow parameters that have been verified repeatedly by many field observations and laboratory experiments, leaving little doubt about their validity. A succinct summary of such experimental works as well as a servey of our empirical knowledge on wave breaking is given in Battjes (1974) and Galvin (1972).

The first of such empirical formulae gives the ratio, at the breaking point, of wave height $H_b = 2A_b$ to the local water depth h_b,

$$\gamma_b = \frac{H_b}{b} = \frac{2A_b}{h_b} = 0.7 \sim 1.2 \tag{4.14}$$

with γ_b close to the lower limit ($\sim$0.7) for the spilling breaker, close to the higher limit ($\sim$1.2) for the collapsing breaker and inbetween for the plunging breaker.

Another important parameter that is found to play a significant role in defining the characteristics of the flow in the surf zone is the dimensionless parameter

$$\xi = \frac{\varepsilon}{\sqrt{H_b/\lambda_\infty}} = \frac{\sqrt{\pi}\ \varepsilon}{\sqrt{A_b\ k_\infty}} \tag{4.15}$$

where $\lambda_\infty = 2\pi/k_\infty$ is the deep water wave length, ε the beach slope.

It was found by Irribaren and Nogales (1949) and others that

$$\xi = \xi_c \simeq 2.3 \tag{4.16}$$

marks the critical state between wave breaking and non-breaking on slope beach. If $\xi < 2.3$, waves break and the reflection coefficient reduces to below unity. Carrier and Greenspan (1958) used Airy's nonlinear approximation, with the criterion that the free surface is vertical at the breaking point and showed analytically that the condition for wave breaking indeed depends solely on the parameter ξ. However, their critical value $\xi_c = 1.77$ is different from the experimental one.

Battjes (1974) showed also that the parameter ξ dictates, among other things, the breaker type, and hence determines more closely the value of γ_b in (4.14), and the reflection coefficient. Based on experiments by Galvin (1968), it is found that the ranges of ξ and the associated breaker types are

$\xi < 0.4$	spilling
$0.4 < \xi < 2.0$	plunging
$\xi < 2.0$	collapsing

(4.17)

Galvin (1968), originally presented his criterion regarding breaker type in terms of an "offshore parameter" $H_\infty/(\lambda_\infty \varepsilon^2)$ in which H_∞ is the deep-water wave height. Galvin's offshore parameter can be written as ξ_o^{-2}, where

$$\xi_o = \frac{\varepsilon}{\sqrt{H_\infty}/\lambda_\infty} = \frac{\sqrt{\pi}\ \varepsilon}{\sqrt{k_\infty\ A_{o\infty}}} \tag{4.18}$$

in which the index "O" refer to deep water (wave height). In terms of ξ_o, Galvin results give

$$\begin{aligned} &\xi_o < 0.5 && \text{spilling} \\ &0.5 < \xi_o < 3.3 && \text{plunging} \\ &\xi_o > 3.3 && \text{collapsing} \end{aligned} \tag{4.19}$$

Also, it has been suggested by Bowen et al (1968) that the parameter γ_b (4.14) may be a function of ξ_o only.

Munk in 1949 first introduced the hypothesis that throughout the surf zone, the breaking wave height H=2A is related to the local depth h_ℓ by the relation

$$\frac{2A}{h_\ell} = \gamma_b \tag{4.20}$$

where γ_b is given by (4.14). It is significant that no new empirical coefficient is introduced. With some scatter, Equation (4.20) has been extensively verified experimentally for normally incident waves on a plane veach (e.g. Bowen et al 1968).

Based on these empirical relations, we will try now to extend the functions $\tilde{\gamma}_{0,2,3,4}(x_1)$, given by (3.74 - 77) over the surf zone so that we can perform the integrations in (3.84a-e) to get the coefficients, $\bar{\gamma}_{11}$, $\bar{\gamma}_{12}$, $\bar{\gamma}_2$, $\bar{\gamma}_3$, and $\bar{\gamma}_o$, of the evolution equation (3.87).

First, the location of the breaker line will be determined using (4.14) and the linear shoaling formula (3.27), which gives

$$|A_o| = \sqrt{\frac{Cg_\infty}{Cg}}\, A_{o\infty} = \frac{A_{o\infty}}{\sqrt{2\ \bar{C}g}}$$

Assuming that wave breaking occurs in very shallow water so that the linear dispersion relation (3.9) is reduced to

$$\omega^2 = gk^2h \tag{4.22}$$

or, in non dimensional variables

$$k_\infty k = \bar{k} = \frac{1}{\sqrt{\bar{h}}} = \frac{1}{\sqrt{-\bar{x}_1}} \tag{4.23}$$

we have,

$$\bar{C}g = \frac{1}{\bar{k}} = \sqrt{-\bar{x}_1} \tag{4.24}$$

Hence, from (4.14), (4.21) and (4.24) we have

$$-\bar{x}_b = \frac{2}{\gamma_b}\,(k_\infty |A_b|) = \left[\frac{\sqrt{2}}{\gamma_b}\, k_\infty\, A_{o\infty}\right]^{0.8} \tag{4.25}$$

note that $k_\infty A_\infty << 1.0$ for ocean swells, so that $\bar{x}_b$ is a small quantity.

From observed data, Komar and Gaughan (1972) found that the best fitting value for γ_b in (4.25) to be

$$\gamma_b = 1.42 \tag{4.26}$$

which is larger than that of Equation (4.14) where h_b is the measured wave height. This discrepancy is of course due to a inadequacy of the linear theory at the breaker line.

Now, we will assume that the results obtained for the short incident wave potentials (ϕ_{m1}, m=1,2,...) are valid up to the breaker line ($\bar{x}_b$). We then assume that inside the surf zone, the amplitude of the incident wave will satisfy (4.20), i.e., will decay linearly from A_b at the breaking point to zero at the shoreline $\bar{x}_1=0$. However, the kinematics of the incident wave will be assumed unaffected by breaking. Hence, inside the surf zone we have instead of (3.27), the incident wave amplitude A given by

$$\frac{A}{A_{o\infty}} = (-s\bar{x}_1)e^{i\theta} \quad , \text{ for } |\bar{x}_1| < |\bar{x}_b| \tag{4.27}$$

where, by matching at the break point $\bar{x}_b$,

$$s = \frac{1}{(-\bar{x}_b)\sqrt{2\bar{C}g_b}} = \frac{1}{\sqrt{2}}(-\bar{x}_b)^{-5/4} \tag{4.28}$$

On the other hand, as was argued earlier, the long edge wave motion is assumed to be inviscid and suffer no breaking itself, even within the surf zone. Hence, the coefficients $\bar{\gamma}_{11}$, $\bar{\gamma}_2$ and $\bar{\gamma}_o$ are readily found and given by (3.84a,c,e) respectively. As for $\bar{\gamma}_{12}$, we split the

integral in (3.84b) into two parts. The first is in the inviscid, shoaling zone from $-\infty$ to $\bar{x}_b$ with the integrand as given in (3.84b) unaltered. The second is in the surf zone from $\bar{x}_b$ to zero with the integrand modified to incorporate the above empirical relations. We now proceed to get the contribution to $\bar{\gamma}_{12}$ from the integral over the surf zone.

For plane beaches, the edge wave modes and dispersion relations are given by (3.4a,b). For simplicity, we will consider here only the zeroth edge wave mode, for which the Laguerre Polynomial $\mathcal{L}_o = 1$ so that, in nondimentional form

$$L_o = e^{\bar{K}\,\bar{x}_1} \; ; \; \bar{\Omega}^2 = \bar{K} \tag{4.29}$$

The phase function θ in the surf zone is unchanged from the inviscid calculation. Thus, from (3.82b) we write

$$\overline{\textcircled{H}} = -e^{i\bar{\Omega}\int^{\bar{x}_1}\frac{d\varsigma}{\bar{C}_g}}\left\{\int_{\bar{x}_b}^{\bar{x}_1}\frac{e^{-i\bar{\Omega}\int^{\tilde{x}_1}\frac{d\varsigma}{\bar{C}_g}}}{\bar{C}_g}\left[\bar{k}\bar{K}+\frac{i\bar{k}\bar{\Omega}}{2ch^2q}\right]e^{\bar{K}\tilde{x}_1}d\tilde{x}_1+\Lambda_\theta\right\} \tag{4.30}$$

where $\bar{x}_1$ is any point inside the surf zone, Λ_θ is a constant given by,

$$\Lambda_\theta = \int_{-\infty}^{\bar{x}_b} \frac{e^{-i\bar{\Omega}\int_{\tilde{x}_1}^{\tilde{x}_1} \frac{d\zeta}{\bar{c}_g}}}{\bar{c}_g} \cdot \left(\bar{k}\bar{K} + \frac{i\bar{k}^2\bar{\Omega}}{2ch^2q} \right) e^{\bar{K}\tilde{x}_1} \cdot d\tilde{x}_1 \tag{4.31}$$

Using the shallow water approximation, we get

$$\bar{\Theta} \simeq -e^{-2i\bar{\Omega}\sqrt{-\bar{x}_1}} \left\{ \int_{\bar{x}_b}^{\bar{x}_1} e^{2i\bar{\Omega}\sqrt{-\bar{x}_1} + \bar{K}\bar{x}_1} \left[\frac{\bar{K}}{-\bar{x}_1} + \frac{i\bar{\Omega}}{2(-\bar{x}_1)^{3/2}} \right] d\bar{x}_1 + \Lambda_\theta \right\}$$

$$\bar{\Theta} = -e^{-2i\bar{\Omega}\sqrt{-\bar{x}_1}} \left\{ \int_{-\bar{x}_b}^{\bar{x}_1} \left[1 + 2i\bar{\Omega}\sqrt{-\bar{x}_1} + \bar{K}\bar{x}_1 + \frac{1}{2}(4\bar{\Omega}^2\bar{x}_1 - 4i\bar{\Omega}\bar{K}(-\bar{x}_1)^{3/2}) \right.\right.$$

$$\left.\left. + \cdots \right] \cdot \left[\frac{\bar{K}}{-\bar{x}_1} + \frac{i\bar{\Omega}}{2(-\bar{x}_1)^{3/2}} \right] dx_1 + \Lambda_\theta \right\} \tag{4.32}$$

Then, after invoking (4.2a), we get to the leading order,

$$\bar{\Theta} = -e^{-2i\bar{\Omega}\sqrt{-\bar{x}_1}} \left\{ \frac{i\bar{\Omega}}{\sqrt{-\bar{x}_1}} - \frac{i\bar{\Omega}}{\sqrt{-\bar{x}_b}} + 2i\bar{\Omega}^3(\sqrt{-\bar{x}_b} - \sqrt{-\bar{x}_1}) + \cdots + \Lambda_\theta \right\} \tag{4.33}$$

Therefore $\bar{\Theta}$ is singular at the shoreline $\bar{x}_1=0$. We may write (4.33) alternatively as the sum of a singular part plus a regular part, i.e.,

$$\bar{\Theta} = \frac{-i\bar{\Omega}}{\sqrt{-\bar{x}_1}} + \bar{\Theta}_{\text{regular}}\ (\bar{x}_1, \bar{x}_b) \tag{4.33a}$$

where $\bar{\Theta}_{\text{regular}}$ is the remainder of $\bar{\Theta}$ from (4.33) which is regular for $0 > \bar{x}_1 > \bar{x}_b$ and is easily evaluated numerically.

We need further to get the modified expression for $\overline{a_1}^P$ [c.f. (3.83b)] in the surf zone, after invoking (4.27) instead of (3.27). First, Equation (3.69) for P is modified in the surf zone to,

$$P = \sqrt{\frac{C_g}{C_{g\infty}}}(-s\bar{x}_1)A_{o\infty}\Big\{\omega\frac{\Theta_{x_1}}{k}\Big[\frac{3k_{x_1}}{4k^2}\Big(2q^2 - 4q\coth 2q + 2 + \frac{4q^3}{3\sinh 2q}\Big) + \frac{1}{2}\Big(2q + \coth 2q + \frac{1+2q}{\cosh 2q}\Big)\Big]$$

$$-\omega\Big[\frac{\Theta_{x_1x_1}}{k^2} + \frac{2\Theta_{x_1}}{k^2}\Big(\ln\frac{1}{C_q\cosh q}\Big)_{x_1}\Big]\Big[\frac{q}{2\sinh 2q} + \frac{1}{2}q\coth 2q\Big]$$

$$-\omega\frac{\Theta_{y_1y_1}}{2k^2}\Big(\frac{1}{2} + \frac{q}{\sinh 2q}\Big) + \frac{1}{2\omega}\Theta_{t_1t_1} - \Theta_{t_1}\Big[\alpha_1 q + \tilde{\alpha}_2 q\tanh q + \alpha_3 q^2\Big] - \frac{\Theta_{x_1t_1}}{k}q\tanh q$$

$$+\frac{1}{2\omega}\left(\alpha_1 q+\tilde{\alpha}_2\, q\,\text{th}\,q+\alpha_3 q^2\right)\cdot\left(-2k\omega\frac{\partial\phi_{00}}{\partial x_1}+k^2\frac{\partial\phi_{00}}{\partial t_1}\right)$$

$$+\frac{k}{2\omega}\left(\alpha_1[1+q\,\text{th}\,q]+\tilde{\alpha}_2[\text{th}\,q+q]+\alpha_3[2q+q^2\,\text{th}\,q]\right)\cdot\left(\frac{-\omega^2}{g}\frac{\partial\phi_{00}}{\partial t_1}\right)$$

$$+\frac{k}{2\omega}\frac{\partial^2\phi_{00}}{\partial x_1\partial t_1}+\frac{\omega^2}{2g}\frac{\partial^2\phi_{00}}{\partial t_1^2}-\frac{1}{2}\frac{\partial^2\phi_{00}}{\partial y_1^2}\Big\}+\sqrt{\frac{G}{G_\infty}}\,A_{0\infty}\Big\{-\frac{k}{2}(-S)\frac{\partial\phi_{00}}{\partial x_1}$$

$$+\frac{kk_0}{2\omega}(-S)\frac{\partial\phi_{00}}{\partial t_1}+\left[\frac{S\bar{x}_1}{2}\frac{\partial\phi_{00}}{\partial x_1}+(-S\bar{x}_1)\frac{k}{2\omega}\frac{\partial\phi_{00}}{\partial t_1}\right]\Big\} \qquad (4.34)$$

Notice that P is still of the form of Equation (3.71) so that the solution for A_1^P is still of the form (3.72). Thus,

$$A_1^P = \left(\frac{-igD}{\sqrt{2}\,\Omega}\right) A_{0\infty}\, a_1^P(x_1)\,\cos Ky_1\, e^{-i\Omega t_1} + *$$

Then, we nondimensionalize a_1^P as in (3.83a):

$$a_1^P = \frac{k_\infty^2}{\omega}\,\bar{a}_1^P$$

with $\bar{a}_1^P$ given by (3.83b)

$$\bar{a}_1^P = e^{i\bar{\Omega}\int^{\bar{x}_1}\frac{d\xi}{\bar{G}}}\int_{-\infty}^{\bar{x}_1} e^{-i\bar{\Omega}\int^{\tilde{x}_1}\frac{d\xi}{\bar{G}}}\,\frac{\bar{P}(\tilde{x}_1)}{\bar{G}}\,d\tilde{x}_1$$

but now, the function $\bar{P}(\bar{x}_1)$ is discontinuous at the breaker line ($\bar{x}_b$), being given by (3.83c) in the shoaling zone ($-\infty$ to $\bar{x}_b$), and by (4.34) in the surf zone ($\bar{x}_b$ to $\bar{x}_1$). Thus, we write

$$\bar{a}_1^P = e^{i\bar{\Omega}\int^{\bar{x}_1}\frac{d\varsigma}{\bar{c}_g}}\left[\int_{\bar{x}_b}^{\bar{x}_1} e^{-i\bar{\Omega}\int^{\bar{x}_1}\frac{d\varsigma}{\bar{c}_g}}\frac{\bar{\rho}}{\bar{c}_g}\,d\bar{x}_1 + \int_{-\infty}^{\bar{x}_b} e^{-i\bar{\Omega}\int^{\bar{x}_1}\frac{d\varsigma}{\bar{c}_g}}\frac{\sqrt{2}\,\bar{\rho}}{\bar{c}_g}\,d\bar{x}_1\right] \tag{4.35}$$

and for the first integral $\int_{\bar{x}_b}^{\bar{x}_1}$ we again write the integrand as the sum of a singular part and a regular part, i.e.,

$$I = e^{-i\bar{\Omega}\int^{\bar{x}_1}\frac{d\zeta}{\bar{c}_g}}\frac{\bar{\rho}}{\bar{c}_g} = I_{\text{singular}} + I_{\text{regular}} \tag{4.36}$$

For the singular part, we get from (4.34), (4.29) and (4.33a),

$$I_{\text{singular}} = e^{2i\bar{\Omega}\sqrt{-\bar{x}_1}}\left\{\frac{(-s\bar{x}_1)\sqrt{\bar{c}_g}}{\bar{c}_g}\left[\frac{1}{2}\left(\frac{-i\bar{\Omega}}{\sqrt{-\bar{x}_1}}\right)' - \frac{1}{2}\left[(-\bar{x}_1)\left(\frac{-i\bar{\Omega}}{\sqrt{-\bar{x}_1}}\right)''\right.\right.\right.$$
$$\left.\left.\left. + \frac{3}{2}\left(\frac{-i\bar{\Omega}}{\sqrt{-\bar{x}_1}}\right)'\right]\right] + \frac{(-s)\sqrt{\bar{c}_g}}{\bar{c}_g}\left[\frac{-1}{2}\left(\bar{K} + \frac{i\bar{\Omega}}{\sqrt{-\bar{x}_1}}\right)\right.$$
$$\left. - \frac{1}{2}\left(\bar{K} + \frac{i\bar{\Omega}}{\sqrt{-\bar{x}_1}}\right) + \frac{i\bar{\Omega}}{4\sqrt{-\bar{x}_1}}\right]\Bigg\}$$

$$= e^{2i\bar{\Omega}\sqrt{-\bar{x}_1}}\frac{(-s)}{(-\bar{x}_1)^{1/4}}\left[\frac{-10i\bar{\Omega}}{8\sqrt{-\bar{x}_1}} - \bar{\Omega}^2\right]\;;\; \bar{x}_b \leq \bar{x} \leq 0 \tag{4.37}$$

The regular part, $I_{regular}$, is then the remainder of I, hence is given by,

$$I_{regular} = e^{2i\bar{\Omega}\sqrt{-\bar{x}_1}} \frac{(-s\bar{x}_1)\sqrt{\bar{\varsigma}}}{\bar{\varsigma}} \left\{ \frac{\bar{\Theta}'}{\bar{k}} \left[\frac{3\bar{k}}{\bar{k}^2} \left(2q^2 - 4q \coth 2q \right.\right.\right.$$

$$\left. + 2 + \frac{4q^3}{3 \sinh 2q} \right) + \frac{1}{2} \left(2q + \frac{1+2q}{\cosh 2q} \right) \Big] + \frac{\bar{K}^2}{2\bar{k}^2} \bar{\Theta} \cdot$$

$$\left(\frac{1}{2} + \frac{q}{\sinh 2q} \right) - \frac{\bar{\Omega}^2}{2} \bar{\Theta} + i\bar{\Omega} \bar{\Theta} \left[\alpha_1 q + \tilde{\alpha}_2 q \tanh q \right.$$

$$\left. + \alpha_3 q^2 \right] + \frac{i\bar{\Omega}}{\bar{k}} \bar{\Theta}' q \tanh q + \frac{1}{2} \left(\alpha_1 q + \tilde{\alpha}_2 q \tanh q \right.$$

$$\left. + \alpha_3 q^2 \right) \cdot \left(-2\bar{k}\bar{K} - i\bar{\Omega}\bar{k}^2 \right) e^{\bar{K}\bar{x}_1} + \frac{\bar{k}}{2} \left[\alpha_1 (1 + q \tanh q) \right.$$

$$\left. + \tilde{\alpha}_2 (\tanh q + q) + \alpha_3 (2q + q^2 \tanh q) \right] (i\bar{\Omega} e^{\bar{K}\bar{x}_1})$$

$$- \frac{i}{2} \bar{\Omega} \bar{k} \bar{K} e^{\bar{K}\bar{x}_1} - \frac{1}{2} (\bar{\Omega} - \bar{K}^2) e^{\bar{K}\bar{x}_1} \Big\}$$

$$+ e^{2i\bar{\Omega}\sqrt{-\bar{x}_1}} \frac{(-s)\sqrt{\bar{\varsigma}}}{\bar{\varsigma}} \left\{ \frac{-\bar{x}_1}{2} (\bar{K}^2 + i\bar{\Omega}\bar{k}\bar{K}) e^{\bar{K}\bar{x}_1} \right\}$$

(3.38)

The expression for $I_{regular}$ is complicated but can be easily integrated numerically as it is regular for $0 \geq \bar{x}_1 \geq \bar{x}_b$. $I_{singular}$ is integrated analytically so that we finally get

$$\bar{a}_1^P = e^{-2i\bar{\Omega}\sqrt{-\bar{x}_1}} \left\{ S\left[5i\bar{\Omega}\left[(-\bar{x}_b)^{1/4} - (-\bar{x}_1)^{1/4}\right] - 2\bar{\Omega}^2 \cdot \left[(-\bar{x}_b)^{3/4} - (-\bar{x}_1)^{3/4}\right]\right] + \int_{\bar{x}_b}^{\bar{x}_1} I_{regular}\, d\bar{x}_1 \right\} \tag{4.39}$$

Using (4.33a) and (4.39) we may now evaluate the coefficient $\bar{\gamma}_{12}$ as follows,

$$\bar{\gamma}_{12} = \frac{1}{\bar{\gamma}_o} \int_{-\infty}^{\bar{x}_b} e^{\bar{K}\bar{x}_1} \left[f_1(\bar{x}_1) + f_2'(\bar{x}_1)\right] d\bar{x}_1 + \frac{1}{\bar{\gamma}_o} \int_{\bar{x}_b}^{0} e^{\bar{K}\bar{x}_1} \left[f_{1S}(\bar{x}_1) + f_{2S}'(\bar{x}_1)\right] d\bar{x}_1 \tag{4.40}$$

where, from (3.84b)

$$f_1(\bar{x}_1) = \frac{\bar{G}_\infty}{\bar{G}} \left\{ \left(\frac{q}{4ch^2q} + \frac{1}{4thq}\right)\bar{\Theta}^{1} + \frac{i}{2}\left(\bar{\Omega} - \frac{\bar{K}}{2\bar{\Omega}}\right)\bar{\Theta} \right.$$

$$+ \frac{\bar{a}_1^P}{4sh^2q} - \frac{\bar{k}\bar{K}}{4\bar{h}} e^{\bar{K}\bar{x}_1} + \frac{1}{2}\bar{k}\bar{K} e^{\bar{K}\bar{x}_1} + \frac{i}{4}\bar{\Omega}\bar{k}^2 e^{\bar{K}\bar{x}_1}$$

$$\left. - \frac{i}{4}\bar{\Omega} e^{\bar{K}\bar{x}_1} - \frac{i\bar{K}^2}{4\bar{\Omega}} e^{\bar{K}\bar{x}_1}\left(\frac{\bar{k}^2}{2} - \frac{1}{2}\right) \right\} \qquad (4.40a)$$

$$f_2(\bar{x}_1) = \frac{\bar{G}_\infty}{\bar{G}} \left\{ \frac{-i\bar{\Theta}^{1}}{2\bar{\Omega}}\left(\frac{1}{2} + \bar{h}\right) + \frac{\bar{k}\bar{\Theta}}{4} - \frac{\bar{k}e^{\bar{K}\bar{x}_1}}{4\bar{h}} - \frac{i\bar{k}\,\bar{a}_1^P}{2\bar{\Omega}} \right.$$

$$\left. + \frac{i\bar{K}e^{\bar{K}\bar{x}_1}}{4\bar{\Omega}}\left(\frac{3\bar{k}^2}{2} - \frac{1}{2}\right) \right\} \qquad (4.40b)$$

with $\bar{\Theta}$ and $\bar{a}_1^P$ given by (3.82b) and (3.83b) respectively while,

$$f_{1S}(\bar{x}_1) = (-s\bar{x}_1)^2 \left\{ \left(\frac{q}{4ch^2q} + \frac{1}{4thq}\right)\bar{\Theta}^{1} + \frac{i}{2}\left(\bar{\Omega} - \frac{\bar{K}^2}{2\bar{\Omega}}\right)\bar{\Theta} \right.$$

$$- \frac{\bar{k}\bar{K}}{4\bar{k}} e^{\bar{K}\bar{x}_1} + \frac{1}{2}\bar{k}\bar{K} e^{\bar{K}\bar{x}_1} + \frac{i}{2}\bar{\Omega}\bar{k}^2 e^{\bar{K}\bar{x}_1} - \frac{i}{4}\bar{\Omega} e^{\bar{K}\bar{x}_1}$$

$$\left. - \frac{i\bar{K}^2}{4\bar{\Omega}} e^{\bar{K}\bar{x}_1}\left(\frac{\bar{k}^2}{2} - \frac{1}{2}\right) \right\} + (-s\bar{x}_1)\frac{\bar{a}_1^P}{4\sqrt{\bar{G}}\,sh^2q} \qquad (4.40c)$$

$$f_{2S}(\bar{x}_1) = (-S\bar{x}_1)^2 \left\{ \frac{-i\bar{\omega}'}{2\bar{\Omega}} \left(\frac{1}{2} + \bar{h}\right) + \frac{\bar{k}\bar{\omega}}{4} - \frac{\bar{k}e^{\bar{K}\bar{x}_1}}{4\bar{h}} \right.$$

$$\left. + \frac{i\bar{K}e^{\bar{K}\bar{x}_1}}{4\bar{\Omega}} \left(\frac{3\bar{k}^2}{2} - \frac{1}{2} \right) \right\} + (-S\bar{x}_1) \left(\frac{-i\bar{k}\,\bar{q}_1^P}{2\sqrt{\bar{g}}\,\bar{\Omega}} \right) \qquad (4.40d)$$

It is seen from (4.33a) that $f_{2S} \sim (-\bar{x}_1)^{1/2}$ so that $f'_{2S} \sim (-\bar{x}_1)^{-1/2}$. Therefore, the integrand in the second integral in (4.40), i.e., $\int_{\bar{x}_b}^{0}$ has square-root singularity at the shoreline $\bar{x}_1=0$. Integrating by parts, we get

$$\bar{\gamma}_{12} = \frac{1}{\bar{\gamma}_o} \int_{-\infty}^{\bar{x}_b} e^{\bar{K}\bar{x}_1} \left[f_1(\bar{x}_1) - \bar{K} f_2(\bar{x}_1) \right] d\bar{x}_1$$

$$+ \frac{1}{\bar{\gamma}_o} \int_{\bar{x}_b}^{0} e^{\bar{K}\bar{x}_1} \left[f_{1S}(\bar{x}_1) - \bar{K} f_{2S}(\bar{x}_1) \right] d\bar{x}_1 \qquad (4.41)$$

because $f_{2S}(0) = 0$ [see (4.33a) and (4.3a)] and from matching, i.e., from (4.28), we have $f_2(\bar{x}_b) = f_{2S}(\bar{x}_b)$. Now, the integrand in (4.41) have no singularities and can be straightforwardly integrated numerically. There are only two parameters that can vary in the calculation for $\bar{\gamma}_{12}$ (4.41). These are the frequency ratio $\bar{\Omega}$ and the

wave steepness $k_\infty A_{c\infty}$, which determines $\bar{x}_b$ through (4.25). Figure (4.9) shows the real part of $\bar{\gamma}_{12}$, $\mathrm{Re}(\bar{\gamma}_{12})$, numerically obtained for a wide range of $\bar{\Omega}$ and $\bar{x}_b$ (or $k_\infty A_{o\infty}$). As shown in the figure, it is found that (i) $\mathrm{Re}(\bar{\gamma}_{12})$ is always negative, (ii) contribution to $\mathrm{Re}(\bar{\gamma}_{12})$ from the surf zone integral $\int_{\bar{x}_b}^{0}$ is always negative, while (iii) contribution from the shoaling zone integral $\int_{-\infty}^{\bar{x}_b}$ is always positive. Hence, we may conclude from this that it is the surf zone integral that rendered

$$\mathrm{Re}(\bar{\gamma}_{12}) < 0 \tag{4.42}$$

and therefore made the edge wave mode unstable in the presence of incident waves. This means that in the presence of the surf zone, edge wave mode perturbations will grow in time, and under steady state conditions its amplitude will be given by (4.4), which is of a comparable order of magnitude as that of the incident wave.

Figure (4.9) also shows the dependence of $\mathrm{Re}(\bar{\gamma}_{12})$ on $\bar{x}_b$ (or $k_\infty A_{o\infty}$), and it is seen from the Figure that for all $\bar{\Omega}$ considered, this dependence is closely represented by the relation:

$$\mathrm{Re}(\bar{\gamma}_{12}) = \frac{\tilde{\mathcal{F}}(\bar{\Omega})}{-\bar{x}_b} = \frac{\mathcal{F}(\bar{\Omega})}{(k_\infty A_{o\infty})^{0.8}} \tag{4.43}$$

where $\mathcal{F}(\bar{\Omega})$ is obtained from the numerical curves in Figure (4.9) and is given in Table (1).

Also shown in the Figure is the relative importance of the surf zone integral $\int_{\bar{x}_b}^{0}$ in the determination of $\mathrm{Re}(\bar{\gamma}_{12})$, and it is seen that for $\bar{\Omega} \geq 3$, $\mathrm{Re}(\bar{\gamma}_{12})$ is essentially given by the surf zone integral, with negligible contribution from the shoaling zone integral.

Now, we turn to determine $\mathrm{Re}(\bar{\gamma}_2)$ in order to solve (4.1) for $|\bar{D}_o|(\bar{t}_3)$. The analytical solution for ψ_1 is already obtained in (4.51). Thus, the non-dimensional $\bar{\psi}_1$ is given by,

$$\bar{\psi}_1 = \frac{g}{\omega k_\infty}\,\psi$$

$$= -2i\pi\bar{\Omega}\bar{K}\{[E_2(\infty)-iE_1(\infty)]J_o(4\sqrt{-\bar{K}\bar{x}_1})$$

$$- E_2(4\sqrt{-\bar{K}\bar{x}_1})\ J_o(4\sqrt{-\bar{K}\bar{x}_1})+E_1(4\sqrt{-\bar{K}\bar{x}_1})Y_o(4\sqrt{-\bar{K}\bar{x}_1})\} \qquad (4.44)$$

[N.B. beach slope $\beta = 1.0$ here, see (4.13)]

Then, from (3.84c) we have,

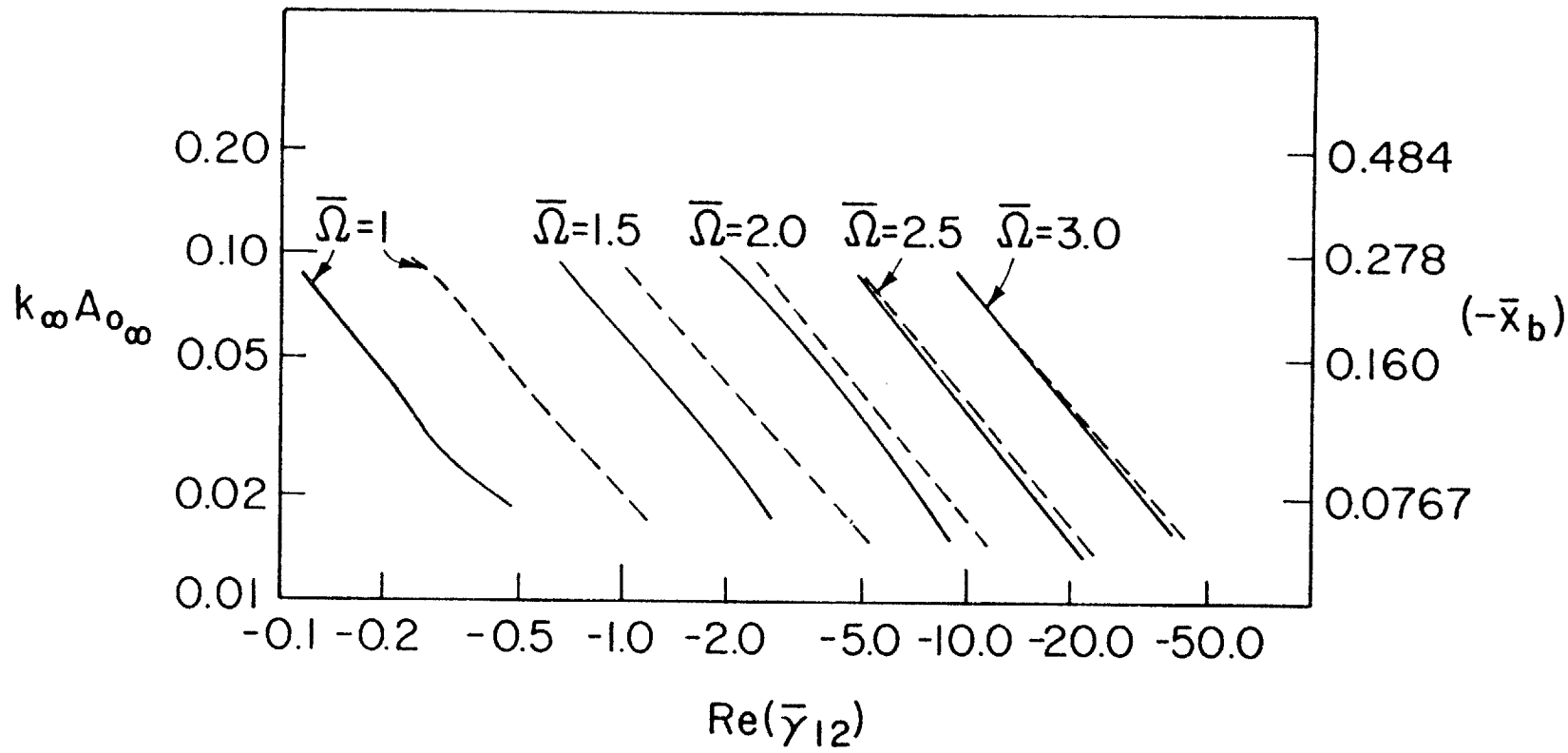

Figure (4.9)

Log-log plot of $Re(\bar{\gamma}_{12})$ vs. $k_\infty A_{o_\infty}$ (or $\bar{x}_b$) for different values of $\bar{\Omega}$. _____ $Re(\bar{\gamma}_{12})$; _ _ _ _ _ contribution to $Re(\bar{\gamma}_{12})$ from surf zone integral.

TABLE 1

$\bar{\Omega}$	1	1.5	2.0	2.5	3.0
$\mathcal{F}(\bar{\Omega})$	-0.016	-0.105	-0.328	-0.683	-1.365

$$\mathrm{Re}(\bar{\gamma}_2) = \frac{1}{4\bar{\Omega}^2\bar{\gamma}_o} \int_{-\infty}^{0} e^{\bar{K}\bar{x}_1} \mathrm{Re}\{-K^{-2}e^{\bar{K}\bar{x}_1}\,\bar{\psi}_1 +$$

$$+ \frac{\bar{K}}{2} e^{\bar{K}\bar{x}_1}\,\bar{\psi}_1' + (K^{-}e^{\bar{K}\bar{x}_1}\,\bar{\psi}_1 - \frac{1}{2}e^{\bar{K}\bar{x}_1}\,\bar{\psi}_1')'\}d\bar{x}_1$$

$$= \frac{1}{8\bar{\Omega}^2\bar{\gamma}_o} \int_{-\infty}^{0} e^{2\bar{K}\bar{x}_1} \mathrm{Re}[2\bar{K}\,\bar{\psi}_1' - \bar{\psi}_1'']d\bar{x}_1$$

Integrating by parts twice we get

$$\mathrm{Re}(\bar{\gamma}_2) = \frac{1}{8\bar{\Omega}^2\bar{\gamma}_o} \mathrm{Re}\{[4\bar{K}\,\bar{\psi}_1 - \bar{\psi}_1']_{\bar{x}_1=0} - 8\bar{K}^2\int_{-\infty}^{0} e^{2\bar{K}\bar{x}_1}\,\bar{\psi}_1 d\bar{x}_1\}$$

Substituting from (4.44), the first term above vanishes and the integral gives

$$\mathrm{Re}(\bar{\gamma}_2) = \frac{1}{8\bar{\Omega}^2\bar{\gamma}_o} \{16\,\pi\bar{\Omega}\bar{K}^2\,E_1^2(\infty)\} = \frac{2}{\bar{\gamma}_o}\,\pi\bar{\Omega}^3\,E_1^3(\infty) \qquad (4.45)$$

where,

$$E_1(\infty) = \int_{-\infty}^{0} e^{2\zeta}\,J_o(4\sqrt{-\zeta})d\zeta = 0.06767.$$

The Solution $\bar{D}_o(\bar{t}_3)$ for Unmodulated Incident Wave:

With the coefficients $Re(\bar{\gamma}_{12})$ and $Re(\bar{\gamma}_2)$ given by (4.43) and (4.45) respectively, Equation (4.1) may be integrated numerically with a given small initial value for $|\bar{D}_o|$ at $\bar{t}_3=0$, to get the transient response of the surf beats $|\bar{D}_o|(\bar{t}_3)$ for the case of unmodulated incident wave. Since $Re(\bar{\gamma}_{12})$ depends on the breaker location $\bar{x}_b$, which is a function of the incident wave steepness $k_\infty A_{o\infty}$, then for incident wave packets, e.g., $A_{o\infty} = A_{o\infty}(t_3,\ldots y_2,y_3,\ldots x_2,\ldots)$, the coefficient $Re(\bar{\gamma}_{12})$ will not be a constant, but instead a function of the same variables as $A_{o\infty}$. Substituting (4.43) into (4.1) we get,

$$\frac{\partial|\bar{D}_o|^2}{\partial\bar{t}_3} + 2\frac{\mathcal{F}(\bar{\Omega})}{\xi_e^2}|\bar{D}_o|^2 + 2\,Re(\bar{\gamma}_2)\,|\bar{D}_o|^4 = 0 \qquad (4.46)$$

where

$$\xi_e = \frac{\varepsilon}{(k_\infty A_{o\infty})^{0.6}} \qquad (4.47)$$

The parameter ξ_e is very close to "the offshore parameter" ξ_o (4.18) which was shown from experimental and observational studies to be of significant influence on the characteristics of the motion in the nearshore region of

the ocean, especially the surf zone. At steady state, $\frac{\partial}{\partial \bar{t}_3} = 0$, (4.51) gives

$$|\bar{D}_o|_s = \frac{1}{(\xi_e)_s} \sqrt{\frac{-\mathcal{F}(\bar{\Omega})}{Re(\bar{\gamma}_2)}} \tag{4.48}$$

Equations (4.1a) and (4.48) suggest that $|\bar{D}_o|_s$ is the largest in the case of spilling breaker. For this breaker type, the reflection coefficient for the incident wave energy is indeed negligibly small (Battjes 1974) as was assumed here apriori.

Transpient Response for Unmodulated Incident Wave Packet

Besides the steady state solutions, Equation (4.46) was integrated numerically to solve for the transient growth of the surf beats. Starting with a small edge wave perturbation on the beach, it will grow with time as the incident wave group hits the beach due to the instability mechanism. Then, as the incident wave dies away, so will the edge wave due to radiation damping effect. Results are shown in Figures (4.10) and (4.11) for the case of finite extent incident wave packet $A_{o\infty}(\bar{t}_3)$ hitting the beach of a constant slope ε=0.05. Unlike the steady state solutions, the transient solutions depend on the initial-value of the edge wave perturbation, i.e., $|\bar{D}_o|$ at $\bar{t}_3$=0, as well as the

incident wave packet profile. Figure (4.10) shows two transient responses $|\bar{D}_o|$ $(\bar{t}_3)$ for the same incident wave packet profile, but with two different initial values; 0.1% and 0.2% of the incident group amplitude. Of course, the perturbation with the larger initial value grows to larger peak values.

Figure (4.11) on the other hand shows the response $|\bar{D}_o|$ $(\bar{t}_3)$ for an incident wave packet having a longer life span than that in Figure (4.10), with initial value for $|\bar{D}_o|$ 0.1% of the group amplitude. From the two figures, it is seen that the two edge wave perturbations having the same initial value will initially grow in a similar fashion, then for the longer-lived incident group case, the edge wave will grow to a much larger peak value.

Also, it is seen from the figures that the response curves $|\bar{D}_o|(\bar{t}_3)$ have long tails, meaning that they persist long after the forcing storm is gone. This is because the radiation damping is not strong (see Equation (4.80)).

Figure (4.10) is consistent with the observations of Munk (1949), Figure (4.12), which shows the correlation between incident wave amplitude and surf beats amplitude, measured some 1000 feet from shore. Discrepancy at the tail is of course expected because we have not accounted for frictional damping at the sea bottom, which will greatly shorten the theoretical curve in (4.10). More detailed

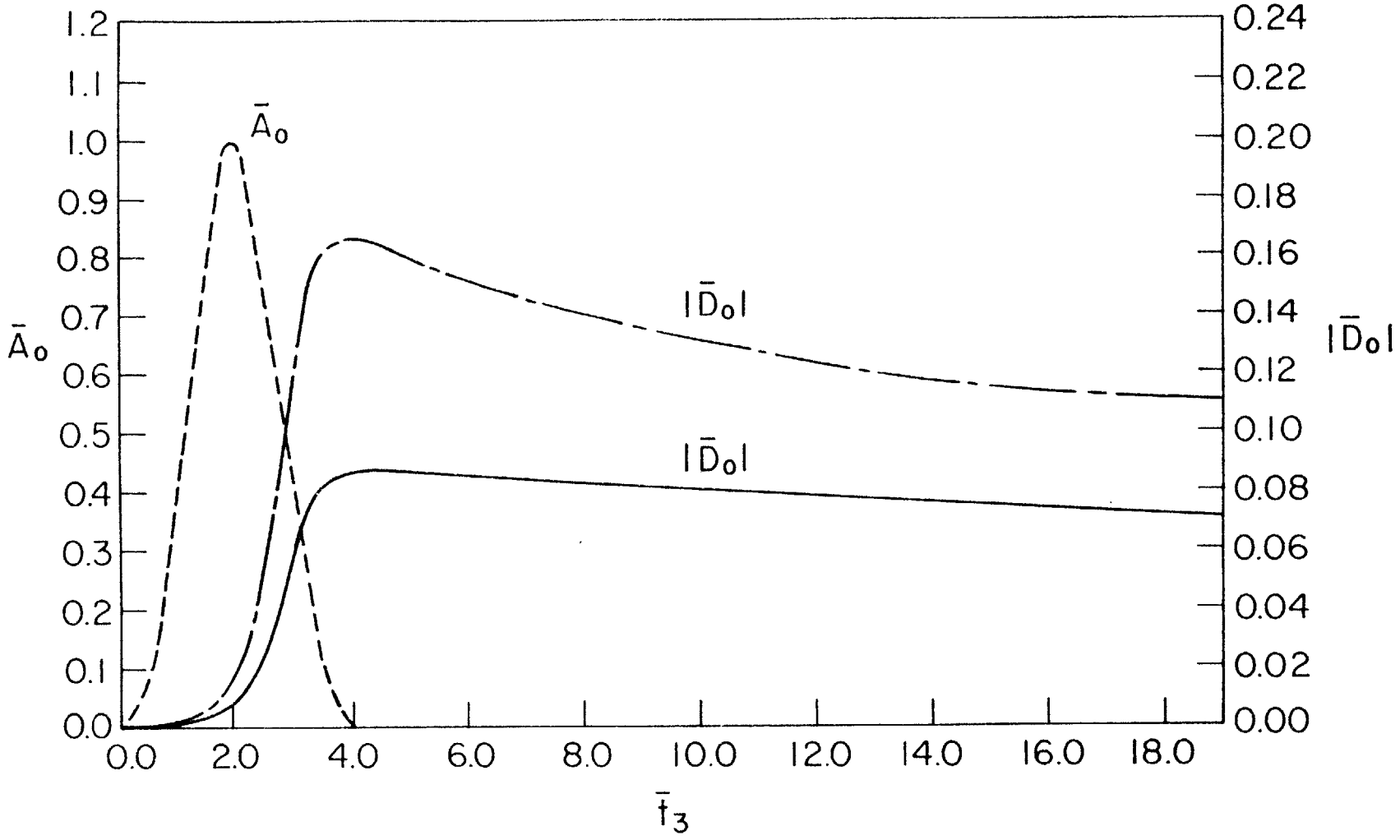

Figure (4.10)

Transient response of the trapped wave perturbation to finite extent unmodulated incident wave for two different initial values for $|\bar{D}_o|$; _____ 0.1% of incidenr group amplitude at $\bar{t}_3=0$ and _____ 0.2% of the incident group amplitude at $\bar{t}_3=0$.

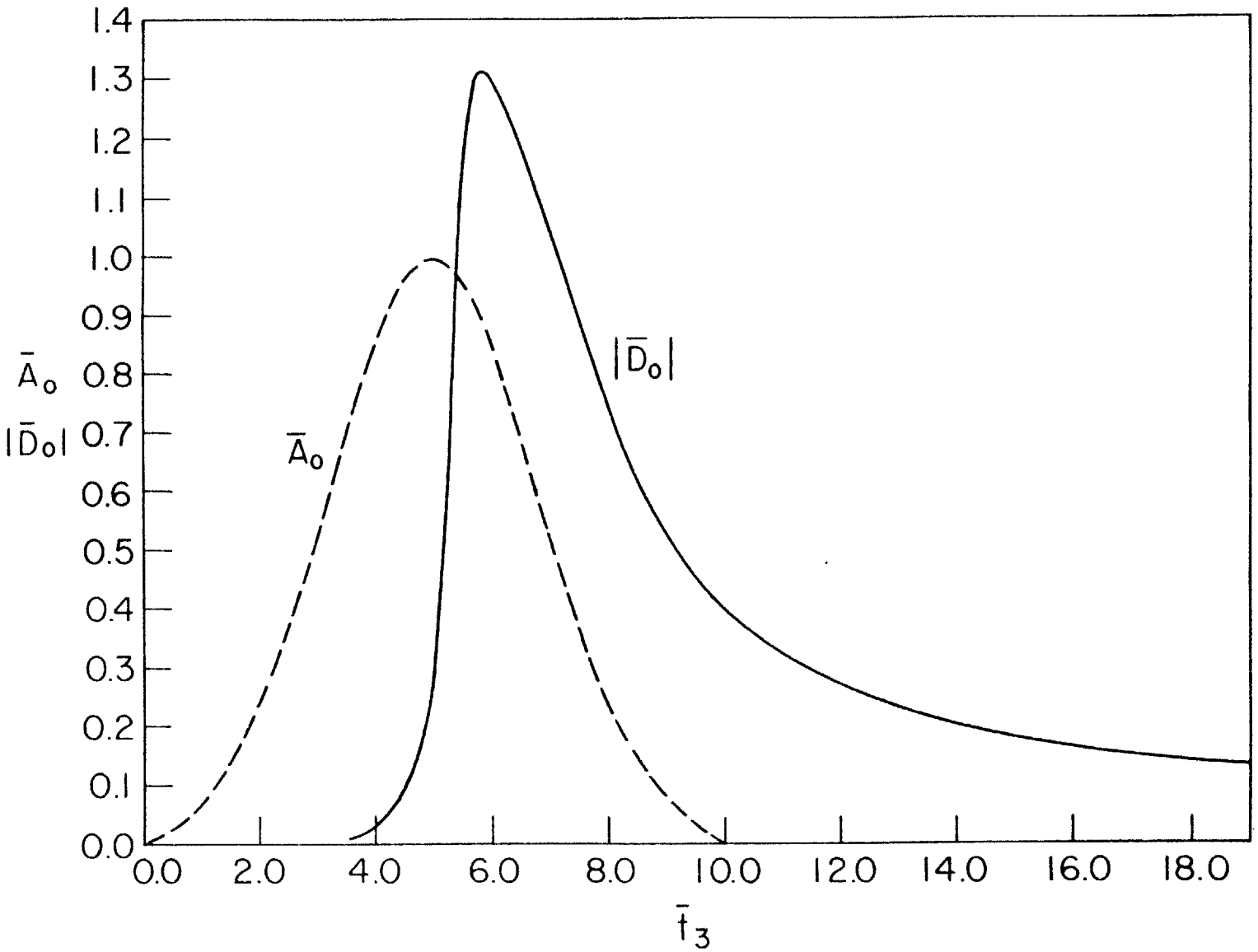

Figure (4.11)

Transient response of the trapped wave perturbation to unmodulated incident wave for initial value of the perturbation amplitude = 0.1% of the group amplitude. The life span of the incident group is longer than in Figure (4.10).

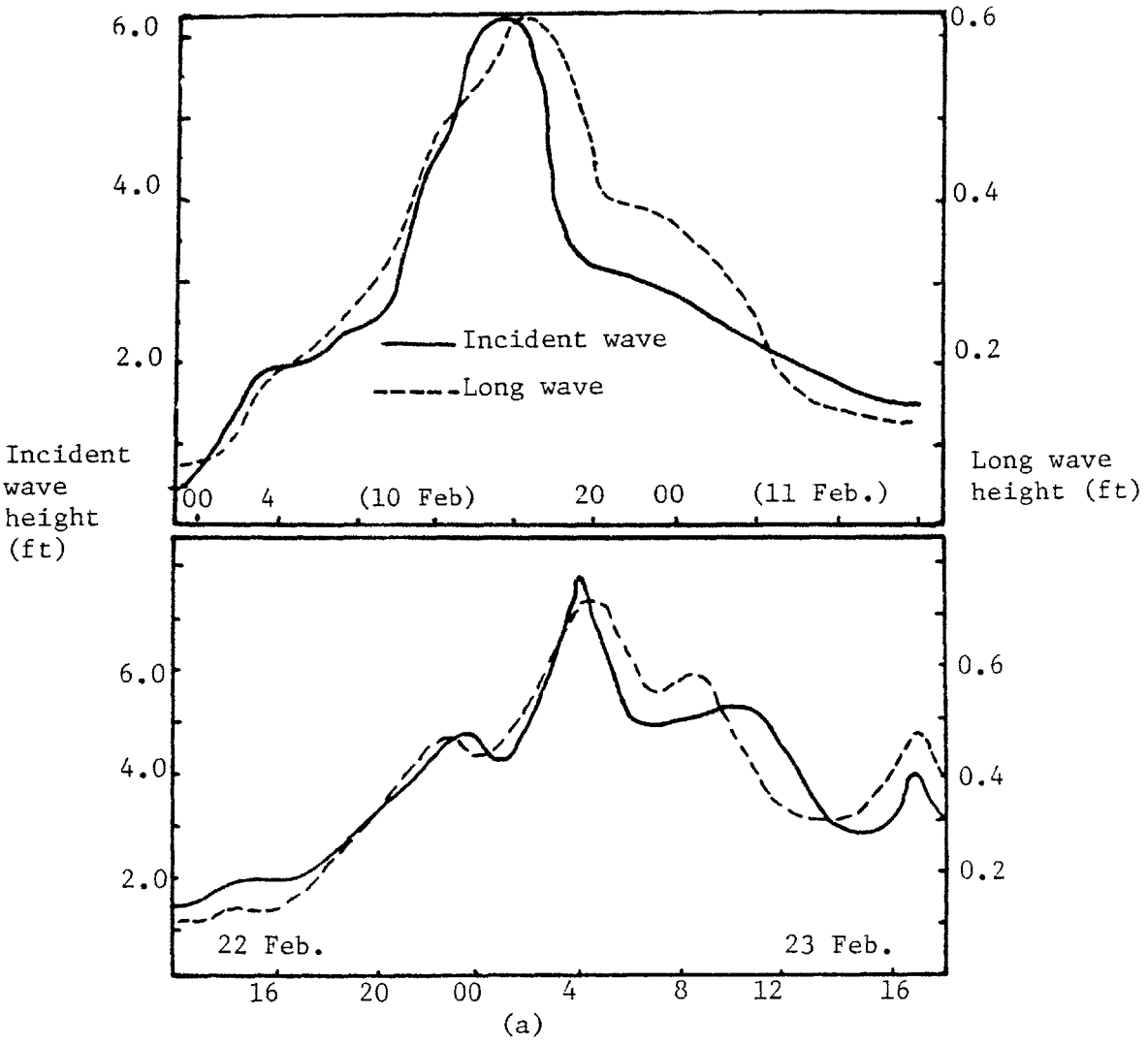

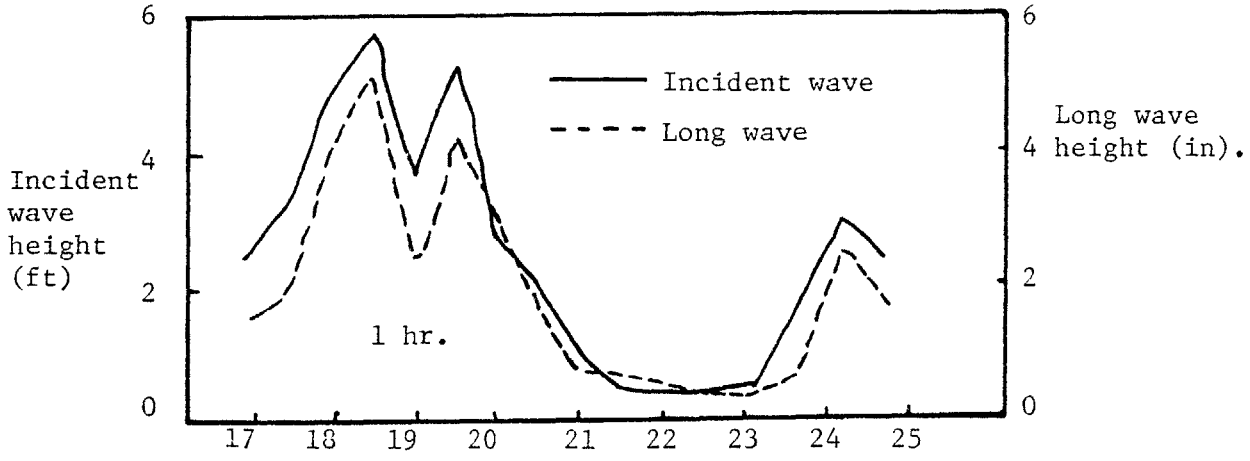

Figure (4.12)
Observations (a) from Munk (1949) and (b) Tucker (1950) showing themeasured heights of incident (short) waves and those of the low frequency motion.

comparison is not possible because some physical parameters, such as beach slope, is not available.

Surf Beats Response for Modulated Incident Wave Packet

If the incident wave is further modulated as in Figures (4.1a,b), then both nonlinear resonance, forced by non-zero $\bar{\mathcal{A}}_1$ [Equation (3.87), and the instability mechanism will act to generate surf beats. For the small modulation case, as in Figure (4.1a), both mechanisms are working along the $\bar{t}_3$-time-scale and the solution procedure is as for the submerged ridge case, except that now both the non-homogeneous term in (3.87a), i.e., $\bar{\mathcal{A}}_o^2 \cdot \bar{\mathcal{A}}_1 \cdot \bar{\gamma}_3$, and the linear term, i.e., $(\bar{\gamma}_{11} + \bar{A}_o^2 \bar{\gamma}_{12})\bar{D}_o$, are reinforcing each other in generating the surf beats, while there is only the nonlinear radiation damping, i.e., $\bar{\gamma}_2 |\bar{D}_o|^2 \bar{D}_o$, which acts to limit its growth. For the case of strong modulation, as in Figure (4.1c), the nonlinear resonance will overwhelm the instability mechanism, as the former is working along the faster $\bar{t}_2$ scale [Eqs. (4.11) and (4.12)].

Bowen and Guza (1978) performed laboratory experiments to study the generation of surf beats on beaches by obliquely incident groups, Figure (4.13a). The incident groups in their experiments are different from those considered here in that (i) their incident wave pattern is composed only of one of the obliquely incident groups in

Figure (4.1b). Therefore it has a velocity component in the y-direction and hence the generated edge wave they observed are progressive, with the same y-velocity, rather than a standing edge wave, (ii) As shown in Figure (4.13b), the incident wave amplitude is significantly changing over a surf beats period, not $O(\varepsilon)$ changes as in Figure (4.1a). Thus, their experiments may be compared with the case of strong modulation, Figure (4.1c) rather than Figure (4.1a).

Due to the finite extent of the wave tank, they were only able to show the initial growth of the long edge waves. Their results, as shown in Figure (4.13c), confirmed the nonlinear resonance mechanism, which was first proposed by Gallagher (1971). For the progressive edge wave case, resonance occurs when the longshore incident group velocity coincides with the phase velocity of an edge wave mode having the same wavelength as that of the group in the y-direction. This is equivalent to the resonant modulations in Figure (4.1a,c) for the standing edge wave case. When the resonance condition is satisfied, a significant increase in the observed low-frequency amplitude is noticed, Figure (4.13c), indicating resonance. Away from resonance condition, low-frequency motion was still observed, but Bowen and Guza attributed them to higher order forced responce.

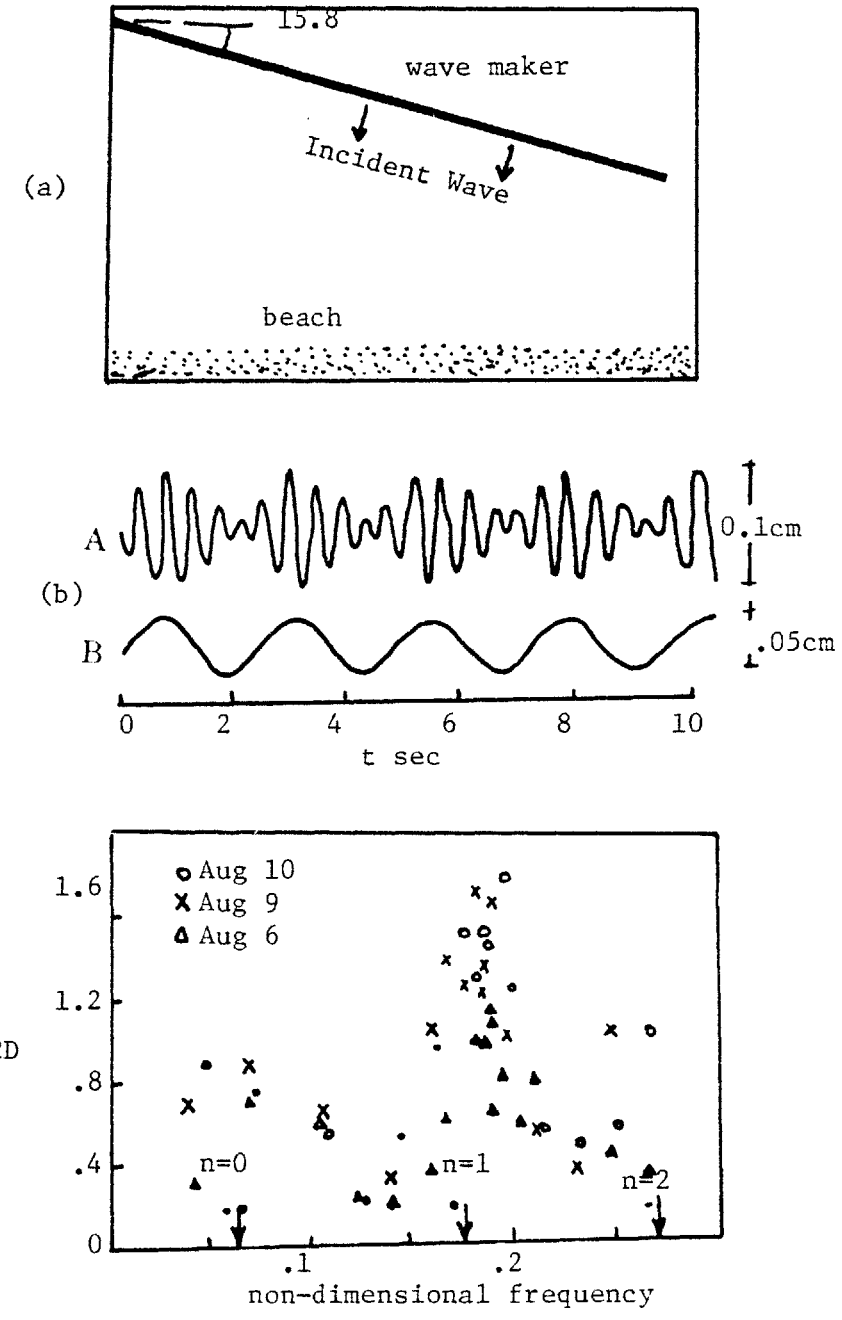

Figure (4.13)
Experimental results from Bowen and Guza (1978). (a) Experimental arrangement, (b) Typical data record of sea surface elevation, A-incident group B-low frequency beat wave at resonance, (c) Response curve showing excitation of resonant low-frequency trapped waves at specific location in the wave tank. Arrows indicate resonance condition.

Bowen and Guza also measured the offshore and the longshore structures of the low frequency motion at the resonance condition, confirming that ti is essentially an edge wave. Their results on the other hand seem not to confirm the instability mechanism, which would work even away from the resonance condition. However, from (4.12) it is seen that the growth rate for the case of nonlinear resonance due to strong modulation [Figure 4.1c], which is relevant to these experiments, is $O(\bar{t}_2)$, while for the instability mechanism is much weaker $O(\bar{t}_3)$ and hence would not generate edge waves of comparable amplitude initially, but much less. Further experimental investigations are therefore needed to test the proposed instability mechanism.

Reassessment

Certainly, the presence of the surf zone has complicated the problem considerably, and it was necessary to invoke some empirical relations between flow parameters in the surf-zone. However, we have introduced only one empirical parameter which is the well established γ_b in Equation (4.14).

Near the shoreline, a full nonlinear analysis is in principle needed but is not given here. If properly treated, the edge wave solution must be corrected. In addition, the excited edge wave having an amplitude comparable to that of the swells implies that the mean shoreline and the mean breaker line must be oscillating in time over the range

$(A_{o\infty}/\varepsilon)$ which is comparable to a wavelength of the swells. However, for sufficiently small edge wave amplitude, the excursion amplitude of the breaker and the shore lines will be small and may be neglected and hence assumed stationary. Under such circumstances [see for example the observations of Munk (1949) and Tucker (1950); Figure (4.12)] the present analysis is approximately valid.

The inadequate treatment of the shoreline also leads to a singularity at $\bar{x}_1=0$. This is readily seen from (4.40) and (4.40d) which shows that the function S', i.e., the secular part of the right-hand-side of Equation (3.35) is singular at the shoreline. This in turn means that the edge wave ϕ_{20} has local singularity at $\bar{x}_1=0$ implying that the perturbation expansion

$$\Phi_o = \phi_{oo} + \varepsilon\, \phi_{10} + \varepsilon^2 \phi_{20} + \cdots$$

breaks down there. However, it is seen from (4.40) and (4.40d) that the singularity of S is mile (square-root singularity) and is integrable. Therefore, the bad behavior of $_{20}$ is indeed localized to $\bar{x}_1=0$. It is hoped that this bad local behavior of the solution at $\bar{x}_1=0$ does not affect the global features.

Concluding Remarks

Following a systematic perturbation scheme, we have established a *significant interaction theory* between the short scale incident wave and the large scale trapped wave, and were able to trace the evolution of such trapped waves in the presence of the incident waves. The solution procedure is summarized in the flow charg shown in Figure (4.14), where the incident wave in deep water away from the trapped wave range is assumed a prescribed input to the problem. Once within the trapped wave range, mutual interaction between the two will take place as shown in the flow chart. Although the trapped wave has the first order effect on the incident wave of affecting its phase [Equation (3.27)], it is not until the third order that the large scale trapped wave is affected by the incident wave presence. At this order, mutual exchange of energy can occur between the two scales. Two generation mechanisms for trapped waves are identified as possible agents for feeding energy into such trapped modes in the ocean. One is a resonance mechanism, when the directional spread of the incident waves allows for a wave pattern such as the one shown in Figure (4.1b) so that the incident wave is slowly modulated over time and length scales commensurate to one of the discrete trapped wave modes. Such trapped modes are

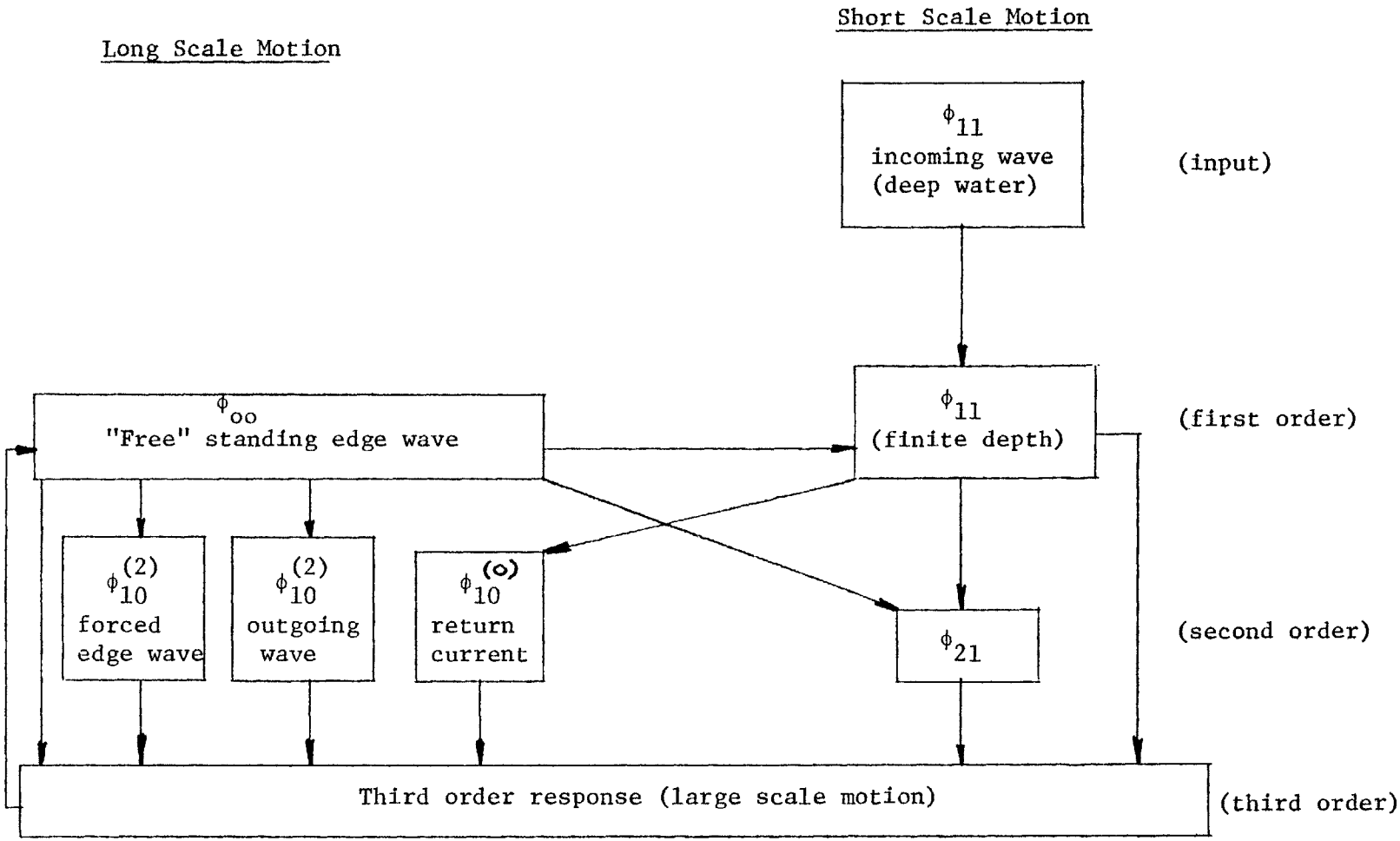

Fig. (4.14) Flow Chart of the Solution Procedure

then resonantely excited, as demonstrated in the submerged ridge exampel [§4.2]. The second generation mechanism for the large scale trapped waves is a side-band instability mechanism, when trapped wave perturbations having frequency $\varepsilon\Omega << \omega$ are unstable in the presence of incident waves. This was demonstrated by the second example of a closed beach with a surf zone. For both mechanisms, the evolution of the trapped waves were traced from the stage of initial growth up till the steady state is reached when a dynamical balance is established between the destabilizing mechanism on one hand and the damping effect [e.g. the nonlinear radiation damping] on the other.

When dealing with the closed beach, a number of difficulties were encountered, and we had to make various simplifying assumptions to solve the problem. For example, near the shoreline the perturbation scheme is inadequate and a full nonlinear theory is needed there, but this was not done here. Further, the fact that the breaker line as well as the shoreline willoscillate in the onshore-offshore direction due to the edge wave presence was ignored and instead assumed stationary in their mean location. Also, because of our very limited knowledge about wave breaking and the flow in the surf zone, we have resorted to empirical

relations between some flow parameters (e.g. Equation (4.14)). It is hoped that future investigations of this problem will address itself to some of the above mentioned difficulties so that a more concrete theory of surf beats could be established.

Experimental studies and field observations of surf beats and low frequency trapped waves in general are also very limited and further work is needed to supplement and verify the theoretical investigations. For the resonance mechanism, the directionality of incident waves is important, but directional information is not usually provided by the observations. For the side-band instability mechanism, it is hoped that the present theory might permit laboratory testing using apparatus of modest dimensions.

REFERENCES

Alblowitz, M.J., Funk, B.A. and Newell, A.C. (1973) Stud. Appl. Math., 52 pp. 51-74.

Abramowitz, M. and Stegun, I. (1965) Handbook of Mathematical Functions, Dover, New York

Battjes, J.A. (1974) Communication on Hydraulics, Dept. of Civil Engineering, Delft University of Technology, Report 74-2

Benney, D.J. (1962) J. Fluid Mech. 14, 577-584

Benney, D.J. and Roskes, G.J. (1969) Stud. Appl. Math., XLVII, 377-385

Bogoliubov, N.N. and Mitropolsky, Y.A. (1961) Asymptotic Methods in the Theory of Nonlinear Oscillations, Delhi, Hindustan

Bowen, A.J. and Guza, R.T. (1978) J. Geoph.Res.

Bowen, A.J. and Inman, D.L. (1971) J. Geoph. Res. 76, 8662-8671

Bowen, A.J. and Inman, D.L. (1969) J. Geoph. Res. 74, No. 23, 5479-5490

Bowen, A.J., Inman, D.L. and Simmons, V.P. (1968) J. Geoph. Res. 73, No. 8, 2569-2577

Carrier, G.F. and Greenspan, H.P. J. Fluid Mech. Vol. 4 pp. 1988-1997

Chen, H.S. and Mei, C.C. (1974) Proc. 10th Symp. Naval Hydrodyn., Cambridge, MA. pp. 573-596

Chu, V.H. and Mei, C.C. (1970) J. Fluid Mech. Vol. 41, pp. 873-887

Cole, J.D. (1968) Perturbation Methods in Applied Mathematics, Blaisdell, Waltham, MA

Collinge, I.R. and Ockendon, J.R. (1979) SIAM Vol. 37, No. 2, pp. 350-357

Dolan, R. and Ferm, J.C. (1968) Science 195, pp. 627-629

Gallagher, B. (1971) J. Fluid Mech., Vol. 49, pp. 1-20

Galvin, C.J. Jr. (1972) Wave Breaking in Shallow Water in Waves on Beaches, ed. R.E. Meyer, pp. 413-456 Academic Press, New York

Galvin, C.J. Jr. (1968) J. Geoph. Res. 73, No. 12, pp. 3651-3659

Galvin, C.J. Jr. (1965) EOS Trans., AGU, 46, p. 112-

Greenspan, H.P. (1957) J. Fluid Mech. Vol. 20, pp. 574-592

Guza, R.T. and Bowen, A.J. (1975) J. Marine Res. 34, pp. 269-293

Guza, R.T. and Davis, R.E. (1974) J. Geoph. Res. 79, pp. 1285-1291

Guza, R.T. and Inman, D. (1975) J. Geoph. Res. 80, pp, 2997-3011

Hayashi, C. (1964) Nonlinear Oscillation in Physical Systems, McGraw Hill, New York

Hildebrand, F.B. (1962) Advanced Calculus for Application, Prentice-Hall, New Jersey

Holman, R.A. and Bowen, A.J. (1979) J. Geoph. Res., 84, No. CIO, 6339-6346

Homma, M. and Sonu, C.J. (1963) Proc. 8th Conf. Coastal Eng. pp. 248-279, ASCE, New York

Irribarren, C.R. and Nogales, C. (1949) Comm. 4, 17th Internl. Navigation Cong. Lisbon, pp. 31-80

King, R. and Smith, R. (1978) Cambridge University, Technical Report

Komar, P.D. and Ganghan, N.K. (1972) Proc. 13th Conf. Coastal Eng., pp. 405-418

Krogh, F.T. (1968) Information Processing 1968: Proceedings of IFIP Congress 1968, A.J.H. Morrell, editor, North Holland Publishing Company, Amsterdam, 1969, Vol. 1, pp. 194-199.

Lamb, H. (1959) Hydrodynamics, Dover Publications, New York

Longuet-Higgins, M.S. (1967) J. Fluid Mech. Vol. 29, pp. 781-821

Minorsky, N. (1962) Nonlinear Oscillations D. Van Nostrand Company Inc. Princeton, N.J.

Minzoni, A.A. and Whitham, G.B. (1977), J. Fluid Mech. Vol. 79, pp. 273-287

Munk, W.H. (1949) Trans. Am. Geophys. Union 30, pp. 849-854

Munk, W.H., Snodgrass, F. and Carrier, G. (1956) Science 123, p. 127

Munk, W.H., Snodgrass, F. and Gilbert, F. (1964) J. Fluid Mech. Vol. 20, pp. 525-554

Nayleh, A.H. (1973) Perturbation Methods, John Wiley & Sons, New York

Roskes, G.J. (1969) Ph.D. Thesis, Dept. of Math., M.I.T. Cambridge, MA

Sonu, C.J. (1972) J. Geoph. Res. 77, No. 33, pp. 6629-6633.

Stoker, J.J. (1950) Nonlinear Vibrations, Interscience, New York

Stokes, G.G. (1846) 16th Meet. Brit. Assoc. Adv. Sci. Southampton, pp. 1-20, London, John Murray.

Tucker, M.J. (1950) Proc. Roy. Soc. London, A202, pp. 565-573

Ursell, F. (1952) Proc. Roy. Soc. London, A214, pp. 79-97

Wehausen, J.V. and Laiton, E.V. (1960) Surface Waves Handbuk der Physik, Sringer-Verlag, Berlin, 9, p. 654

Whitham, G.B. (1976) J. Fluid Mech. Vol. 74, pp. 353-368

Whitham, G.B. (1974) Linear and Nonlinear Waves John Wiley & Sons, New York.

Whitham, G.B. (1962) J. Fluid Mech., Vol. 12, pp. 135.

Wilkenson, J.H. (1965) The Algebraic Eigenvalue Problem, Clarendon Press, Oxford.

Appendix I

Determination of the functions F_{nm}, H_{nm}

a) The functions F_{nm}

The governing equation in the fluid is the Laplace's Equation:

$$\nabla^2 \Phi = \left(\frac{\partial^2}{\partial x^2} + \frac{\partial^2}{\partial y^2} + \frac{\partial^2}{\partial z^2} \right) \Phi = 0 \qquad \text{(I.1)}$$

From (2.5a):

$$\frac{\partial^2}{\partial x^2} = \frac{\partial^2}{\partial x^2} + 2\epsilon \frac{\partial^2}{\partial x \partial x_1} + \epsilon^2 \left[\frac{\partial^2}{\partial x_1^2} + 2 \frac{\partial^2}{\partial x \partial x_2} \right] + \cdots\cdots \qquad \text{(I.2)}$$

Similar expansion for $\frac{\partial^2}{\partial y^2}$ from (2.5b):

$$\frac{\partial^2}{\partial y^2} = \frac{\partial^2}{\partial y^2} + 2\epsilon \frac{\partial^2}{\partial y \partial y_1} + \epsilon^2 \left[\frac{\partial^2}{\partial y_1^2} + 2 \frac{\partial^2}{\partial y \partial y_1} \right] + \cdots\cdots \qquad \text{(I.3)}$$

But we are only concerned here with normal incidence of the swell (2.7c). Thus, derivatives with respect to the fast y scale in zero:

$$\frac{\partial^2}{\partial y^2} = \epsilon^2 \frac{\partial^2}{\partial y_1^2} + 2\epsilon^3 \frac{\partial^2}{\partial y_1 \partial y_2} + \cdots\cdots \qquad \text{(I.4)}$$

Now, substituting the expansion (2.8a) for Φ which can be re-written as:

$$\Phi = \phi_{00} + \epsilon \left(\phi_{10} + \left(\phi_{11} e^{i\psi/\epsilon} + * \right) \right) + \epsilon^2 \left(\phi_{20} + \right.$$

$$\left. \left(\phi_{21} e^{i\psi/\epsilon} + * \right) + \left(\phi_{22} e^{2i\psi/\epsilon} + * \right) \right) + \cdots\cdots \qquad \text{(I.5)}$$

and using (I.2) and (I.3), we can separate various orders of magnitudes and harmonics as follows:

$$\frac{\partial^2}{\partial z^2}\Phi_{00} = 0 \tag{I.6a}$$

$$\frac{\partial^2}{\partial z^2}\Phi_{10} = 0 \tag{I.6b}$$

$$\frac{\partial^2}{\partial z^2}\Phi_{20} = -\left(\frac{\partial^2\Phi_{00}}{\partial x_1^2} + \frac{\partial^2\Phi_{00}}{\partial y_1^2}\right) \tag{I.6c}$$

$$\left(\frac{\partial^2}{\partial z^2} - k^2\right)\Phi_{11} = 0 \tag{I.6d}$$

$$\left(\frac{\partial^2}{\partial z^2} - k^2\right)\Phi_{21} = -i\left[\frac{\partial}{\partial x_1}(k\Phi_{11}) + k\frac{\partial}{\partial x_1}(\Phi_{11})\right] \tag{I.6e}$$

$$\left(\frac{\partial^2}{\partial z^2} - k^2\right)\Phi_{31} = -\left[\left(\frac{\partial^2}{\partial x_1^2} + \frac{\partial^2}{\partial y_1^2}\right)\Phi_{11} + i\frac{\partial}{\partial x_1}(k\Phi_{21}) + ik\frac{\partial\Phi_{21}}{\partial x_1}\right. \tag{I.6f}$$

$$\left. + ik\frac{\partial\Phi_{11}}{\partial x_2} + i\frac{\partial}{\partial x_2}(k\Phi_{11})\right]$$

b) The Function H_{nm}

From (2.10), the bottom boundary condition is:

$$\frac{\partial}{\partial Z}\Phi = -\epsilon \frac{\partial h}{\partial x_1}\frac{\partial}{\partial x}\Phi \qquad \text{at } z=-h(x_1)$$

Now, substituting (2.5a) and (2.8a) into (2.10) and separating orders of magnitude and harmonics, we get:

$$\frac{\partial \Phi_{00}}{\partial Z} = 0 \qquad \text{at } z=-h(k_x) \qquad \text{(I.7a)}$$

$$\frac{\partial \Phi_{10}}{\partial Z} = 0 \qquad \text{"} \qquad \text{(I.7b)}$$

$$\frac{\partial \Phi_{20}}{\partial Z} = -\frac{\partial h}{\partial x_1}\frac{\partial \Phi_{00}}{\partial x_1} \qquad \text{"} \qquad \text{(I.7c)}$$

$$\frac{\partial \Phi_{11}}{\partial Z} = 0 \qquad \text{"} \qquad \text{(I.7d)}$$

$$\frac{\partial \Phi_{21}}{\partial Z} = -\frac{\partial h}{\partial x_1}(ik\Phi_{11}) \qquad \text{"} \qquad \text{(I.7e)}$$

$$\frac{\partial \Phi_{31}}{\partial Z} = -\frac{\partial h}{\partial x_1}\left[ik\Phi_{21} + \frac{\partial \Phi_{11}}{\partial x_1}\right] \qquad \text{"} \qquad \text{(I.7f)}$$

Appendix II

Determination of the Functions G_{nm}

By separating the various orders and harmonics, the free surface boundary condition (2.9) becomes of the form:

$$\left(g\frac{\partial}{\partial z} - m^2\omega^2\right)\Phi_{nm} = G_{nm} \qquad ; \quad z = 0 \qquad \text{(II.1)}$$

The contribution of G_{nm} comes from: (i) the linear operation $\frac{\partial^2}{\partial t^2}\Phi$ at theleft hand side of (2.9), and (ii) the nonlinear terms in (2.9).

We will take each of these terms one by one and separate various orders and harmonics to get G_{nm}. First the linear term:

$$\begin{aligned}
\frac{\partial^2}{\partial t^2}\Phi &= \left(\frac{\partial}{\partial t} + \epsilon\frac{\partial}{\partial t_1} + \cdots\right)\left(\frac{\partial}{\partial t} + \epsilon\frac{\partial}{\partial t_1} + \cdots\right)\left[\Phi_{00} + \epsilon\left(\Phi_{10} + \left(\Phi_{11}e^{i\psi/\epsilon} + *\right)\right) + \cdots\right] \\
&= -\omega^2\sum_{n=1}^{\infty}\sum_{m=1}^{\infty}\epsilon^n m^2 \Phi_{nm} e^{im\psi/\epsilon} \\
&+ \epsilon^2\left[\frac{\partial^2\Phi_{00}}{\partial t_1^2}\right] + \epsilon^2\left[-2i\omega\Phi_{11_{t_1}}\right]e^{i\psi/\epsilon} + \epsilon^3\left[2\frac{\partial^2\Phi_{00}}{\partial t_1\partial t_2} + \frac{\partial^2\Phi_{10}}{\partial t_1^2}\right] \\
&+ \epsilon^3\left[\Phi_{11_{t_1t_1}} - 2i\omega\left(\Phi_{11_{t_2}} + \Phi_{21_{t_1}}\right)\right]e^{i\psi/\epsilon} \\
&+ \epsilon^4\left[2\frac{\partial^2\Phi_{00}}{\partial t_1\partial t_3} + 2\frac{\partial^2\Phi_{10}}{\partial t_1\partial t_2} + \frac{\partial^2\Phi_{20}}{\partial t_1^2}\right] + \cdots\cdots
\end{aligned} \qquad \text{(II.2)}$$

Of course the first term (the double summation) goes to the left of (II.1). The rest of the terms give contributions to $G_{20}, G_{21}, G_{30}, G_{31}$ and G_{40}, respectively. In fact, these are the only functions needed in the analysis. Thus, it is only the contribution to these five functions that will be determined from the nonlinear terms in (2.9):

$$\left[-\frac{1}{2}(\nabla\Phi)^2\right]_t = -\frac{1}{2}\left(\frac{\partial}{\partial t}+\epsilon\frac{\partial}{\partial t_1}+\cdots\right)\left\{\left(\left(\frac{\partial}{\partial x}+\epsilon\frac{\partial}{\partial x_1}+\cdots\right)\left[\Phi_{00}+\epsilon\left(\Phi_{10}+\left(\Phi_{11}e^{i\Psi/\epsilon}+*\right)\right)+\cdots\right]\right)^2\right.$$

$$+\left(\left(\frac{\partial}{\partial y}+\epsilon\frac{\partial}{\partial y_1}+\cdots\right)\left[\Phi_{00}+\epsilon\left(\Phi_{10}+\left(\Phi_{11}e^{i\Psi/\epsilon}+*\right)\right)+\cdots\right]\right)^2$$

$$\left.+\left(\frac{\partial}{\partial z}\left[\Phi_{00}+\epsilon\left(\Phi_{10}+\left(\Phi_{11}e^{i\Psi/\epsilon}+*\right)\right)+\cdots\right]\right)^2\right\}$$

$$=\epsilon^2\left\{-\frac{\partial}{\partial t}\left[\frac{\partial\Phi_{00}}{\partial x_1}\cdot\frac{\partial}{\partial x}\left(\Phi_{11}e^{i\Psi/\epsilon}\right)\right]\right\}+\epsilon^3\left\{-\frac{1}{2}\frac{\partial}{\partial t_1}\left[\left(\frac{\partial\Phi_{00}}{\partial x_1}\right)^2\right.\right.$$

$$\left.+\left(\frac{\partial\Phi_{00}}{\partial y_1}\right)^2\right]-\frac{\partial}{\partial t_1}\left[\frac{\partial}{\partial x}\left(\Phi_{11}e^{i\Psi/\epsilon}\right)\frac{\partial}{\partial x}\left(\Phi_{11}^*e^{-i\Psi/\epsilon}\right)+\frac{\partial}{\partial z}\left(\Phi_{11}e^{i\Psi/\epsilon}\right)\cdot\right.$$

$$\left.\left.\frac{\partial}{\partial z}\left(\Phi_{11}^*e^{-i\Psi/\epsilon}\right)\right]\right\}+\epsilon^3\left\{-\frac{\partial}{\partial t_1}\left[\frac{\partial\Phi_{00}}{\partial x_1}\frac{\partial}{\partial x}\left(\Phi_{11}e^{i\Psi/\epsilon}\right)\right]-\frac{\partial}{\partial t}\left[\frac{\partial\Phi_{00}}{\partial x_2}\cdot\right.\right.$$

$$\frac{\partial}{\partial x}\left(\Phi_{11}e^{i\Psi/\epsilon}\right)+\frac{\partial\Phi_{00}}{\partial x_1}\cdot\frac{\partial}{\partial x_1}\left(\Phi_{11}e^{i\Psi/\epsilon}\right)+\frac{\partial\Phi_{00}}{\partial y_1}\frac{\partial}{\partial y_1}\left(\Phi_{11}e^{i\Psi/\epsilon}\right)+\frac{\partial\Phi_{00}}{\partial x_1}\cdot$$

$$\left.\left.\frac{\partial}{\partial x}\left(\Phi_{21}e^{i\Psi/\epsilon}\right)\right]\right\}+\epsilon^4\left\{-\frac{\partial}{\partial t_2}\left[\frac{\partial}{\partial x}\left(\Phi_{11}e^{i\Psi/\epsilon}\right)\cdot\frac{\partial}{\partial x}\left(\Phi_{11}^*e^{-i\Psi/\epsilon}\right)+\right.\right.$$

$$\left.\left.\frac{\partial}{\partial z}\left(\Phi_{11}e^{i\Psi/\epsilon}\right)\cdot\frac{\partial}{\partial z}\left(\Phi_{11}^*e^{-i\Psi/\epsilon}\right)\right]-\frac{\partial}{\partial t_1}\left(\left[\frac{\partial}{\partial x}\left(\Phi_{21}e^{i\Psi/\epsilon}\right)\frac{\partial}{\partial x}\left(\Phi_{11}^*e^{-i\Psi/\epsilon}\right)+\right.\right.\right.$$

$$\frac{\partial}{\partial z}\left(\Phi_{21}e^{i\psi/\epsilon}\right)\frac{\partial}{\partial z}\left(\Phi_{11}^{*}e^{-i\psi/\epsilon}\right)\Big]+*\Big)-\frac{\partial}{\partial t_1}\Big[\frac{\partial}{\partial x}\left(\Phi_{11}e^{i\psi/\epsilon}\right)\frac{\partial}{\partial x_1}\left(\Phi_{11}^{*}e^{-i\psi/\epsilon}\right)+*\Big]$$

$$-\frac{\partial}{\partial t_1}\Big[\frac{\partial\Phi_{00}}{\partial x_1}\frac{\partial\Phi_{10}}{\partial x_1}+\frac{\partial\Phi_{00}}{\partial y_1}\frac{\partial\Phi_{10}}{\partial y_1}\Big]-\frac{1}{2}\frac{\partial}{\partial t_2}\Big[\left(\frac{\partial\Phi_{00}}{\partial x_1}\right)^2+\left(\frac{\partial\Phi_{00}}{\partial y_1}\right)^2\Big]$$

$$-\frac{\partial}{\partial t_1}\Big[\frac{\partial\Phi_{00}}{\partial x_1}\frac{\partial\Phi_{00}}{\partial x_2}+\frac{\partial\Phi_{00}}{\partial y_1}\frac{\partial\Phi_{00}}{\partial y_2}\Big]\Big\}+\cdots$$

$$\frac{1}{g}\left(\Phi_t\Phi_{zt}\right)_t=\epsilon^2\Big\{\frac{1}{g}\frac{\partial\Phi_{00}}{\partial t_1}\frac{\partial^2}{\partial t^2}\left(\Phi_{11z}e^{i\psi/\epsilon}\right)\Big\}+\epsilon^3\Big\{\frac{1}{g}\frac{\partial}{\partial t_1}\Big[\frac{\partial}{\partial t}\left(\Phi_{11}e^{i\psi/\epsilon}\right)\cdot$$

$$\frac{\partial}{\partial t}\left(\Phi_{11z}^{*}e^{-i\psi/\epsilon}\right)+*\Big]\Big\}+\epsilon^3\Big\{\frac{1}{g}\frac{\partial}{\partial t_1}\Big[\frac{\partial\Phi_{00}}{\partial t_1}\frac{\partial}{\partial t}\left(\Phi_{11z}e^{i\psi/\epsilon}\right)\Big]+\frac{1}{g}\frac{\partial\Phi_{00}}{\partial t_2}\cdot$$

$$\frac{\partial^2}{\partial t^2}\left(\Phi_{11z}e^{i\psi/\epsilon}\right)+\frac{1}{g}\frac{\partial}{\partial t}\Big[\frac{\partial\Phi_{00}}{\partial t_1}\frac{\partial}{\partial t_1}\left(\Phi_{11z}e^{i\psi/\epsilon}\right)\Big]+\frac{1}{g}\frac{\partial\Phi_{00}}{\partial t_1}\frac{\partial^2}{\partial t^2}\left(\Phi_{21z}e^{i\psi/\epsilon}\right)\Big\}$$

$$+\epsilon^4\Big\{\frac{1}{g}\frac{\partial}{\partial t_2}\Big[\frac{\partial}{\partial t}\left(\Phi_{11}e^{i\psi/\epsilon}\right)\cdot\frac{\partial}{\partial t}\left(\Phi_{11z}e^{-i\psi/\epsilon}\right)+*\Big]+\frac{1}{g}\frac{\partial}{\partial t_1}\Big[\Big(\frac{\partial}{\partial t_1}$$

$$\left(\Phi_{11}e^{i\psi/\epsilon}\right)\cdot\frac{\partial}{\partial t}\left(\Phi_{11z}^{*}e^{-i\psi/\epsilon}\right)+\frac{\partial}{\partial t}\left(\Phi_{11}e^{i\psi/\epsilon}\right)\frac{\partial}{\partial t_1}\left(\Phi_{11z}^{*}e^{-i\psi/\epsilon}\right)\Big)+*\Big]$$

$$+\frac{1}{g}\frac{\partial}{\partial t_1}\Big[\Big(\frac{\partial}{\partial t}\left(\Phi_{11}e^{i\psi/\epsilon}\right)\frac{\partial}{\partial t}\left(\Phi_{21z}^{*}e^{-i\psi/\epsilon}\right)+\frac{\partial}{\partial t}\left(\Phi_{21}e^{i\psi/\epsilon}\right)\frac{\partial}{\partial t}\left(\Phi_{11z}^{*}e^{-i\psi/\epsilon}\right)\Big)+*\Big]\Big\}$$

$$+\cdots\cdot$$

$$-\left(\Phi_x\Phi_t\right)_x=\epsilon^2\Big\{-\frac{\partial\Phi_{00}}{\partial x_1}\frac{\partial^2}{\partial x\partial t}\left(\Phi_{11}e^{i\psi/\epsilon}\right)-\frac{\partial\Phi_{00}}{\partial t_1}\frac{\partial^2}{\partial x^2}\left(\Phi_{11}e^{i\psi/\epsilon}\right)\Big\}$$

$$+\epsilon^3\Big\{-\frac{\partial}{\partial x_1}\Big[\frac{\partial}{\partial x}\left(\Phi_{11}e^{i\psi/\epsilon}\right)\cdot\frac{\partial}{\partial t}\left(\Phi_{11}^{*}e^{-i\psi/\epsilon}\right)+*\Big]-\frac{\partial}{\partial x_1}\Big[\frac{\partial\Phi_{00}}{\partial x_1}\frac{\partial\Phi_{00}}{\partial t_1}\Big]\Big\}$$

$$+\epsilon^3\Big\{-\frac{\partial\Phi_{00}}{\partial x_1}\frac{\partial^2}{\partial x\partial t}\Big(\Phi_{21}e^{i\psi/\epsilon}\Big)-\frac{\partial\Phi_{00}}{\partial t_1}\frac{\partial^2}{\partial x^2}\Big(\Phi_{21}e^{i\psi/\epsilon}\Big)$$

$$-\frac{\partial\Phi_{00}}{\partial x_2}\frac{\partial^2}{\partial x\partial t}\Big(\Phi_{11}e^{i\psi/\epsilon}\Big)-\frac{\partial\Phi_{00}}{\partial t_2}\frac{\partial^2}{\partial x^2}\Big(\Phi_{11}e^{i\psi/\epsilon}\Big)-\frac{\partial\Phi_{00}}{\partial x_1}\frac{\partial^2}{\partial x\partial t_1}\Big(\Phi_{11}e^{i\psi/\epsilon}\Big)$$

$$-\frac{\partial\Phi_{00}}{\partial t_1}\frac{\partial^2}{\partial x\partial x_1}\Big(\Phi_{11}e^{i\psi/\epsilon}\Big)-\frac{\partial}{\partial x_1}\Big[\frac{\partial\Phi_{00}}{\partial x_1}\frac{\partial}{\partial t}\Big(\Phi_{11}e^{i\psi/\epsilon}\Big)+\frac{\partial\Phi_{00}}{\partial t_1}\frac{\partial}{\partial x}\Big(\Phi_{11}e^{i\psi/\epsilon}\Big)\Big]\Big\}$$

$$+\epsilon^4\Big\{-\frac{\partial}{\partial x_2}\Big[\frac{\partial}{\partial x}\Big(\Phi_{11}e^{i\psi/\epsilon}\Big)\cdot\frac{\partial}{\partial t}\Big(\Phi_{11}^{*}e^{-i\psi/\epsilon}\Big)+*\Big]-\frac{\partial}{\partial x_1}\Big[\Big(\frac{\partial}{\partial x_1}\Big(\Phi_{11}e^{i\psi/\epsilon}\Big)\cdot$$

$$\frac{\partial}{\partial t}\Big(\Phi_{11}^{*}e^{-i\psi/\epsilon}\Big)+\frac{\partial}{\partial t_1}\Big(\Phi_{11}e^{i\psi/\epsilon}\Big)\cdot\frac{\partial}{\partial x}\Big(\Phi_{11}^{*}e^{-i\psi/\epsilon}\Big)\Big)+*\Big]-\frac{\partial}{\partial x_1}\Big[\Big(\frac{\partial}{\partial x}$$

$$\Big(\Phi_{21}e^{i\psi/\epsilon}\Big)\cdot\frac{\partial}{\partial t}\Big(\Phi_{11}^{*}e^{-i\psi/\epsilon}\Big)+\frac{\partial}{\partial t}\Big(\Phi_{21}e^{i\psi/\epsilon}\Big)\cdot\frac{\partial}{\partial x}\Big(\Phi_{11}^{*}e^{-i\psi/\epsilon}\Big)\Big)+*\Big]$$

$$-\frac{\partial}{\partial x_1}\Big[\frac{\partial\Phi_{00}}{\partial x_1}\frac{\partial\Phi_{10}}{\partial t_1}+\frac{\partial\Phi_{00}}{\partial t_1}\frac{\partial\Phi_{10}}{\partial x_1}\Big]-\frac{\partial}{\partial x_2}\Big[\frac{\partial\Phi_{00}}{\partial x_1}\frac{\partial\Phi_{00}}{\partial t_1}\Big]$$

$$-\frac{\partial}{\partial x_1}\Big[\frac{\partial\Phi_{00}}{\partial x_2}\frac{\partial\Phi_{00}}{\partial t_1}+\frac{\partial\Phi_{00}}{\partial x_1}\frac{\partial\Phi_{00}}{\partial t_2}\Big]\Big\}+\cdots\cdots\cdots$$

$$-\Big[\Phi_y\Phi_t\Big]_y=\epsilon^3\Big\{-\frac{\partial}{\partial y_1}\Big(\frac{\partial\Phi_{00}}{\partial y_1}\frac{\partial\Phi_{00}}{\partial t_1}\Big)\Big\}+\epsilon^3\Big\{-\frac{\partial}{\partial y_1}\Big[\frac{\partial}{\partial t}\Big(\Phi_{11}e^{i\psi/\epsilon}\Big)\frac{\partial\Phi_{00}}{\partial y_1}\Big]\Big\}$$

$$+\epsilon^4\Big\{-\frac{\partial}{\partial y_1}\Big[\frac{\partial}{\partial t}\Big(\Phi_{11}e^{i\psi/\epsilon}\Big)\cdot\frac{\partial}{\partial y_1}\Big(\Phi_{11}^{*}e^{-i\psi/\epsilon}\Big)+*\Big]-\frac{\partial}{\partial y_1}\Big[\frac{\partial\Phi_{00}}{\partial y_1}\frac{\partial\Phi_{10}}{\partial t_1}$$

$$+\frac{\partial\Phi_{00}}{\partial t_1}\frac{\partial\Phi_{10}}{\partial y_1}\Big]-\frac{\partial}{\partial y_2}\Big[\frac{\partial\Phi_{00}}{\partial y_1}\frac{\partial\Phi_{00}}{\partial t_1}\Big]-\frac{\partial}{\partial y_1}\Big[\frac{\partial\Phi_{00}}{\partial y_1}\frac{\partial\Phi_{00}}{\partial t_2}+\frac{\partial\Phi_{00}}{\partial y_2}\frac{\partial\Phi_{00}}{\partial t_1}\Big]\Big\}+\cdots$$

$$\frac{1}{2g}\left[\Phi_t(\nabla\Phi)^2\right]_{zt} = \epsilon^3\left\{\frac{1}{2g}\frac{\partial^2}{\partial z\partial t}\left[\frac{\partial}{\partial t}(\phi_{11}e^{i\psi/\epsilon})\cdot\left(2\left[\frac{\partial}{\partial x}(\phi_{11}e^{i\psi/\epsilon})\cdot\right.\right.\right.\right.$$

$$\left.\frac{\partial}{\partial x}(\phi_{11}^* e^{-i\psi/\epsilon}) + \frac{\partial}{\partial z}(\phi_{11}e^{i\psi/\epsilon})\cdot\frac{\partial}{\partial z}(\phi_{11}^* e^{-i\psi/\epsilon})\right] + \left(\frac{\partial\phi_{00}}{\partial x_1}\right)^2 + \left(\frac{\partial\phi_{00}}{\partial y_1}\right)^2\Big)$$

$$+ 2\frac{\partial\phi_{00}}{\partial t_1}\frac{\partial\phi_{00}}{\partial x_1}\frac{\partial}{\partial x}(\phi_{11}e^{i\psi/\epsilon}) + \frac{\partial}{\partial t}(\phi_{11}^* e^{-i\psi/\epsilon})\cdot\left(2\left[\frac{\partial}{\partial x}(\phi_{11}e^{i\psi/\epsilon})\right]^2\right.$$

$$\left.\left.\left.\left.+ 2\left[\frac{\partial}{\partial z}(\phi_{11}e^{i\psi/\epsilon})\right]^2\right)\right]\right\} + \epsilon^4\left\{\frac{1}{2g}\frac{\partial^2}{\partial z\partial t_1}\left[2\frac{\partial\phi_{00}}{\partial t_1}\cdot\right.\right.$$

$$\left(\frac{\partial}{\partial x}(\phi_{11}e^{i\psi/\epsilon})\cdot\frac{\partial}{\partial x}(\phi_{11}^* e^{-i\psi/\epsilon}) + \frac{\partial}{\partial z}(\phi_{11}e^{i\psi/\epsilon})\cdot\frac{\partial}{\partial z}(\phi_{11}^* e^{-i\psi/\epsilon})\right)$$

$$\left.\left.+\left(2\frac{\partial}{\partial t}(\phi_{11}e^{i\psi/\epsilon})\cdot\frac{\partial}{\partial x}(\phi_{11}^* e^{-i\psi/\epsilon})\frac{\partial\phi_{00}}{\partial x_1} + *\right)\right]\right\} + \cdots\cdots$$

$$\frac{-1}{g^2}\left[\Phi_t\,\Phi_{zt}^2\right]_t = \epsilon^3\left\{\frac{-1}{g^2}\frac{\partial}{\partial t}\left[2\frac{\partial}{\partial t}(\phi_{11}e^{i\psi/\epsilon})\cdot\frac{\partial}{\partial t}(\phi_{11_z}e^{i\psi/\epsilon})\frac{\partial}{\partial t}(\phi_{11_z}^* e^{-i\psi/\epsilon})\right.\right.$$

$$\left.\left.+\frac{\partial}{\partial t}(\phi_{11}^* e^{-i\psi/\epsilon})\cdot\frac{\partial}{\partial t}(\phi_{11_z}e^{i\psi/\epsilon})\frac{\partial}{\partial t}(\phi_{11_z}e^{i\psi/\epsilon})\right]\right\} + \epsilon^4\left\{\frac{-1}{g^2}\frac{\partial}{\partial t_1}\right.$$

$$\left.\left[\frac{\partial\phi_{00}}{\partial t_1}\frac{\partial}{\partial t}(\phi_{11_z}e^{i\psi/\epsilon})\cdot\frac{\partial}{\partial t}(\phi_{11_z}^* e^{-i\psi/\epsilon})\right]\right\} + \cdots\cdots$$

$$\frac{-1}{2g^2}\left[\Phi_{zzt}\,\Phi_t^2\right]_t = \epsilon^3\left\{\frac{-1}{2g^2}\frac{\partial}{\partial t}\left[2\frac{\partial}{\partial t}(\phi_{11_{zz}}e^{i\psi/\epsilon})\cdot\left[\frac{\partial}{\partial t}(\phi_{11}e^{i\psi/\epsilon})\cdot\right.\right.\right.$$

$$\left.\left.\frac{\partial}{\partial t}(\phi_{11}^* e^{-i\psi/\epsilon}) + \frac{1}{2}\left(\frac{\partial\phi_{00}}{\partial t_1}\right)^2\right] + \frac{\partial}{\partial t}(\phi_{11_{zz}}^* e^{-i\psi/\epsilon})\cdot\left(\frac{\partial}{\partial t}\phi_{11}e^{i\psi/\epsilon}\right)^2\Big]\Big\}$$

$$+\epsilon^4\left\{\frac{-1}{2g^2}\frac{\partial}{\partial t_1}\left[2\frac{\partial \Phi_{00}}{\partial t_1}\cdot\frac{\partial}{\partial t}\left(\Phi_{11}e^{i\psi/\epsilon}\right)\cdot\frac{\partial}{\partial t}\left(\Phi^*_{11_{zz}}e^{-i\psi/\epsilon}\right)+*\right]\right\}+\cdots$$

$$\frac{-1}{2}\left[\Phi_x(\nabla\Phi)^2\right]_x=\epsilon^3\left\{\frac{-1}{2}\frac{\partial}{\partial x}\left[2\frac{\partial}{\partial x}\left(\Phi_{11}e^{i\psi/\epsilon}\right)\left[\frac{\partial}{\partial x}\left(\Phi_{11}e^{i\psi/\epsilon}\right)\cdot\right.\right.\right.$$

$$\frac{\partial}{\partial x}\left(\Phi^*_{11}e^{-i\psi/\epsilon}\right)+\frac{\partial}{\partial z}\left(\Phi_{11}e^{i\psi/\epsilon}\right)\cdot\frac{\partial}{\partial z}\left(\Phi^*_{11}e^{-i\psi/\epsilon}\right)\Big]+\frac{\partial}{\partial x}\left(\Phi^*_{11}e^{-i\psi/\epsilon}\right)\cdot$$

$$\left[\left(\frac{\partial}{\partial x}\Phi_{11}e^{i\psi/\epsilon}\right)^2+\left(\frac{\partial}{\partial z}\Phi_{11}e^{i\psi/\epsilon}\right)^2\right]+2\frac{\partial\Phi_{00}}{\partial x_1}\left[\frac{\partial\Phi_{00}}{\partial x_1}\frac{\partial}{\partial x}\left(\Phi_{11}e^{i\psi/\epsilon}\right)\right]$$

$$\left.\left.+\frac{\partial}{\partial x}\left(\Phi_{11}e^{i\psi/\epsilon}\right)\left[\left(\frac{\partial\Phi_{00}}{\partial x_1}\right)^2+\left(\frac{\partial\Phi_{00}}{\partial y_1}\right)^2\right]\right]\right\}$$

$$+\epsilon^4\left\{\frac{-1}{2}\frac{\partial}{\partial x_1}\left[\frac{\partial\Phi_{00}}{\partial x_1}\left[\left(\frac{\partial\Phi_{00}}{\partial x_1}\right)^2+\left(\frac{\partial\Phi_{00}}{\partial y_1}\right)^2\right]+2\frac{\partial\Phi_{00}}{\partial x_1}\left[\frac{\partial}{\partial x}\right.\right.\right.$$

$$\left(\Phi_{11}e^{i\psi/\epsilon}\right)\cdot\frac{\partial}{\partial x}\left(\Phi^*_{11}e^{-i\psi/\epsilon}\right)+\frac{\partial}{\partial z}\left(\Phi_{11}e^{i\psi/\epsilon}\right)\cdot\frac{\partial}{\partial z}\left(\Phi^*_{11}e^{-i\psi/\epsilon}\right)\Big]$$

$$\left.\left.+\left[2\frac{\partial}{\partial x}\left(\Phi_{11}e^{i\psi/\epsilon}\right)\frac{\partial}{\partial x}\left(\Phi^*_{11}e^{-i\psi/\epsilon}\right)\frac{\partial\Phi_{00}}{\partial x_1}+*\right]\right]\right\}+\cdots\cdots$$

$$\frac{1}{g}\left[\Phi_x\Phi_t\Phi_{zt}\right]_x=\epsilon^3\left\{\frac{1}{g}\frac{\partial}{\partial x}\left[\frac{\partial\Phi_{00}}{\partial x_1}\frac{\partial\Phi_{00}}{\partial t_1}\frac{\partial}{\partial t}\left(\Phi_{11_z}e^{i\psi/\epsilon}\right)\right.\right.$$

$$+\frac{\partial}{\partial x}\left(\Phi_{11}e^{i\psi/\epsilon}\right)\cdot\left[\frac{\partial}{\partial t}\left(\Phi_{11}e^{i\psi/\epsilon}\right)\cdot\frac{\partial}{\partial t}\left(\Phi^*_{11_z}e^{-i\psi/\epsilon}\right)+*\right]$$

$$\left.\left.+\frac{\partial}{\partial x}\left(\Phi^*_{11}e^{-i\psi/\epsilon}\right)\cdot\left[\frac{\partial}{\partial t}\left(\Phi_{11}e^{i\psi/\epsilon}\right)\cdot\frac{\partial}{\partial t}\left(\Phi_{11_z}e^{i\psi/\epsilon}\right)\right]\right]\right\}$$

$$+\epsilon^4\left\{\frac{1}{g}\frac{\partial}{\partial x_1}\left[\frac{\partial \Phi_{00}}{\partial x_1}\frac{\partial}{\partial t}\left(\Phi_{11}^{*}e^{-i\psi/\epsilon}\right)\cdot\frac{\partial}{\partial t}\left(\Phi_{11_z}e^{i\psi/\epsilon}\right)\right.\right.$$

$$\left.\left.+\frac{\partial \Phi_{00}}{\partial t_1}\frac{\partial}{\partial x}\left(\Phi_{11}^{*}e^{-i\psi/\epsilon}\right)\frac{\partial}{\partial t}\left(\Phi_{11_z}e^{i\psi/\epsilon}\right)\right]+*\right\}+\cdots$$

$$\frac{1}{2g}\left[\Phi_t^2\Phi_{xz}\right]_x=\epsilon^3\left\{\frac{1}{2g}\frac{\partial}{\partial x}\left[2\frac{\partial}{\partial x}\left(\Phi_{11_z}e^{i\psi/\epsilon}\right)\cdot\frac{\partial}{\partial t}\left(\Phi_{11}e^{i\psi/\epsilon}\right)\cdot\right.\right.$$

$$\frac{\partial}{\partial t}\left(\Phi_{11}^{*}e^{-i\psi/\epsilon}\right)+\frac{\partial}{\partial x}\left(\Phi_{11_z}e^{i\psi/\epsilon}\right)\left(\frac{\partial \Phi_{00}}{\partial t_1}\right)^2$$

$$\left.\left.+\frac{\partial}{\partial x}\left(\Phi_{11_z}^{*}e^{-i\psi/\epsilon}\right)\left(\frac{\partial}{\partial t}\Phi_{11}e^{i\psi/\epsilon}\right)^2\right]\right\}$$

$$+\epsilon^4\left\{\frac{1}{2g}\frac{\partial}{\partial x_1}\left[2\frac{\partial \Phi_{00}}{\partial t_1}\frac{\partial}{\partial t}\left(\Phi_{11}^{*}e^{-i\psi/\epsilon}\right)\frac{\partial}{\partial x}\left(\Phi_{11_z}e^{i\psi/\epsilon}\right)+*\right]\right\}+\cdots\cdots$$

$$\frac{-1}{2}\left[\Phi_y\left(\nabla\Phi\right)^2\right]_y=\epsilon^4\left\{\frac{-1}{2}\frac{\partial}{\partial y_1}\left[\frac{\partial \Phi_{00}}{\partial y_1}\left[\left(\frac{\partial \Phi_{00}}{\partial x_1}\right)^2+\left(\frac{\partial \Phi_{00}}{\partial y_1}\right)^2\right]\right.\right.$$

$$-2\frac{\partial \Phi_{00}}{\partial y_1}\left[\frac{\partial}{\partial x}\left(\Phi_{11}e^{i\psi/\epsilon}\right)\frac{\partial}{\partial x}\left(\Phi_{11}^{*}e^{-i\psi/\epsilon}\right)+\frac{\partial}{\partial z}\left(\Phi_{11}e^{i\psi/\epsilon}\right)\cdot\right.$$

$$\left.\left.\left.\frac{\partial}{\partial z}\left(\Phi_{11}^{*}e^{-i\psi/\epsilon}\right)\right]\right]\right\}+\cdots\cdots\cdots$$

$$\frac{1}{g}\left[\Phi_y\Phi_t\Phi_{zt}\right]_y=\epsilon^4\left\{\frac{1}{g}\frac{\partial}{\partial y_1}\left[\frac{\partial \Phi_{00}}{\partial y_1}\frac{\partial}{\partial t}\left(\Phi_{11}e^{i\psi/\epsilon}\right)\frac{\partial}{\partial t}\left(\Phi_{11_z}^{*}e^{-i\psi/\epsilon}\right)+*\right]\right\}+\cdots$$

$$\frac{1}{2g}\left[\Phi_t^2\Phi_{yz}\right]_y$$

Thus, by simply collecting these various contributions we get the desired functions:

$$G_{00} = G_{10} = G_{11} = 0 \tag{II.3}$$

$$G_{20} = -\frac{\partial^2 \phi_{00}}{\partial t_1^2} \tag{II.4}$$

$$G_{21} = 2i\omega \frac{\partial \phi_{11}}{\partial t_1} - \frac{\partial \phi_{00}}{\partial x_1}(k\omega \phi_{11}) + \frac{1}{g}\frac{\partial \phi_{00}}{\partial t_1}(-\omega^2 \phi_{11z}) - \left[\frac{\partial \phi_{00}}{\partial x_1}(k\omega \phi_{11}) + \frac{\partial \phi_{00}}{\partial t_1}(-k^2 \phi_{11})\right] \tag{II.5}$$

after suing (2.7b,c). But G_{nm} are evaluated at z=0. Thus, using (3.8), G_{21} is simplified to

$$G_{21} = (i2\omega \phi_{11t_1})_{z=0} + ig\left[k\frac{\partial \phi_{00}}{\partial x_1} - \frac{k^2}{2\omega_{ch}^2 q}\frac{\partial \phi_{00}}{\partial t_1}\right] A_0 \tag{II.5a}$$

where use has been made also of the dispersion relation (3.9). The function G_{31} is a lot more complicated than G_{21}. However, its components can be grouped as follows:

$$G_{31} = \left[i2\omega(\phi_{11t_2} + \phi_{21t_1}) - \phi_{11t_1t_1}\right]_{z=0} + P'(\phi_{00}, \phi_{21}) + P''(\phi_{00}, \phi_{11}) + P'''(\phi_{11}, \phi_{11}, \phi_{11}) \tag{II.6}$$

where

$$P^{III}(\phi_{II},\phi_{II},\phi_{II}) = \frac{1}{2g}(-i\omega)\frac{\partial}{\partial z}\Big\{(-i\omega\phi_{II})\big[2k^2|\phi_{II}|^2 +$$

$$2|\phi_{II_z}|^2\big] + (i\omega\phi_{II}^*)\big[-2k^2\phi_{II}^2 + 2\phi_{II_z}^2\big]\Big\}$$

$$\frac{-2}{g}(-i\omega)\Big\{(-i\omega\phi_{II})\big[\omega^2|\phi_{II_z}|^2\big] + (i\omega\phi_{II}^*)\cdot$$

$$(-\omega^2\phi_{II_z}^2)\Big\} - \frac{1}{g^2}(-i\omega)\Big\{(-i\omega\phi_{II_{zz}})(\omega^2|\phi_{II}|^2)$$

$$+ i\omega\phi_{II_{zz}}^*(-\omega^2\phi_{II}^2)\Big\} - ik\Big\{(ik\phi_{II})\big[k^2|\phi_{II}|^2$$

$$+|\phi_{II_z}|^2\big] + (-ik\phi_{II}^*)\big[-k^2\phi_{II}^2 + \phi_{II_z}^2\big]\Big\}$$

$$+\frac{1}{g}(ik)\Big\{(ik\phi_{II})(\omega^2\phi_{II}\phi_{II_z}^* + *) + (-ik\phi_{II}^*)\cdot$$

$$(-\omega^2\phi_{II}\phi_{II_z})\Big\} + \frac{1}{2g}(ik)\Big\{2ik\phi_{II_z}(\omega^2|\phi_{II}|^2)$$

$$-ik\phi_{II_z}(-\omega^2\phi_{II}^2)\Big\}$$

Then, using (3.8), and evaluating P''' at z=0, P''' will be simplified to:

$$P''' = iA_o\omega g\left[\frac{k^2|A_o|^2}{16}(9\coth^4 q - 10\coth^2 q + 9)\right] \qquad \text{(II.7)}$$

Similarly,

$$P' = -2\frac{\partial\phi_{00}}{\partial x_1}(k\omega)\phi_{21} + \frac{\partial\phi_{00}}{\partial t_1}\left[\frac{-\omega^2}{g}\phi_{21_z} + k^2\phi_{21}\right] \quad , z=0$$

But, from (3.29), $\phi_{21} = \phi_{21}^h + \phi_{21}^p$; where $\phi_{21}^h = \phi_{11}\frac{A_1}{A_o}$.
Thus, using (II.5a), P' can be rewritten as:

$$P' = ig\left[k\frac{\partial\phi_{00}}{\partial x_1} - \frac{k^2}{2\omega\cosh^2 q}\frac{\partial\phi_{00}}{\partial t_1}\right]A_1 +$$

$$\left\{-2\frac{\partial\phi_{00}}{\partial x_1}(k\omega)\phi_{21}^p + \frac{\partial\phi_{00}}{\partial t_1}\left[\frac{-\omega^2}{g}\phi_{21_z}^p + k^2\phi_{21}^p\right]\right\}_{z=0} \qquad \text{(II.8)}$$

Also, we collect the terms in P''(ϕ_{00},ϕ_{11}) to get:

$$P'' = \left\{-\frac{\partial}{\partial t_1}\left[\frac{\partial\phi_{00}}{\partial x_1}(ik\phi_{11})\right] - \frac{\partial\phi_{00}}{\partial x_2}(k\omega\phi_{11}) - \frac{\partial\phi_{00}}{\partial x_1}(-i\omega\frac{\partial\phi_{11}}{\partial x_1})\right.$$

$$-\frac{\partial\phi_{00}}{\partial y_1}(-i\omega\frac{\partial\phi_{11}}{\partial y_1}) + \frac{1}{g}\frac{\partial}{\partial t_1}\left[\frac{\partial\phi_{00}}{\partial t_1}(-i\omega\phi_{11_z})\right] +$$

$$\frac{1}{g}\frac{\partial\phi_{00}}{\partial t_2}(-\omega^2\phi_{11_z}) + \frac{1}{g}\frac{\partial\phi_{00}}{\partial t_1}(-i\omega\frac{\partial\phi_{11}}{\partial t_1}) - \frac{\partial\phi_{00}}{\partial x_2}(k\omega\phi_{11})$$

$$\left.-\frac{\partial\phi_{00}}{\partial t_2}(-k^2\phi_{11}) - \frac{\partial\phi_{00}}{\partial x_1}(ik\frac{\partial\phi_{11}}{\partial t_1}) - \frac{\partial\phi_{00}}{\partial t_1}(ik\frac{\partial\phi_{11}}{\partial x_1})\right.$$

$$-\frac{\partial}{\partial x_1}\left[\frac{\partial \phi_{00}}{\partial x_1}(-i\omega\phi_{11})+\frac{\partial \phi_{00}}{\partial t_1}(ik\phi_{11})\right]-\frac{\partial}{\partial y_1}\left[\frac{\partial \phi_{00}}{\partial y_1}\right.$$

$$\left.(-i\omega\phi_{11})\right]+\frac{1}{2g}(-i\omega)\left\{(-i\omega\phi_{11_Z})\left[\left(\frac{\partial \phi_{00}}{\partial x_1}\right)^2\right.\right.$$

$$\left.+\left(\frac{\partial \phi_{00}}{\partial y_1}\right)^2\right]+2(ik\phi_{11_Z})\frac{\partial \phi_{00}}{\partial t_1}\frac{\partial \phi_{00}}{\partial x_1}\Bigg\}$$

$$-\frac{1}{2g^2}(-\omega^2\phi_{11_{ZZ}})\left(\frac{\partial \phi_{00}}{\partial t_1}\right)^2-\frac{1}{2}(-k^2\phi_{11})\left[\left(\frac{\partial \phi_{00}}{\partial x_1}\right)^2\right.$$

$$\left.+\left(\frac{\partial \phi_{00}}{\partial y_1}\right)^2\right]-(-k^2\phi_{11})\left(\frac{\partial \phi_{00}}{\partial x_1}\right)^2+\frac{1}{g}(k\omega\phi_{11_Z})\cdot$$

$$\left.\frac{\partial \phi_{00}}{\partial x_1}\frac{\partial \phi_{00}}{\partial t_1}+(ik\phi_{11_Z})\left(\frac{\partial \phi_{00}}{\partial t_1}\right)^2\right\}_{Z=0}$$

(II.9)

Thus, the function G_{31} is given by

$$G_{31}=i2\omega\left(\frac{\partial \phi_{21}^{h}}{\partial t_1}+\frac{\partial \phi_{11}}{\partial t_2}\right)_{Z=0}+ig\left(k\frac{\partial \phi_{00}}{\partial x_1}\right.$$

$$\left.-\frac{k^2}{2\omega\,ch^2q}\frac{\partial \phi_{00}}{\partial t_1}\right)A_1+P_1(\phi_{00},A_0) \qquad \text{(II.9a)}$$

where

$$P_1(\phi_{00}, A_0) = \left(2i\omega \phi^P_{21 t_1} - \phi_{11 t_1 t_1}\right)_{Z=0} + \left[-2k\omega \phi^P_{21} \frac{\partial \phi_{00}}{\partial x_1} + \frac{\partial \phi_{00}}{\partial t_1}\left(\frac{-\omega^2}{g}\phi^P_{21 Z} + k^2 \phi^P_{21}\right)\right]_{Z=0} + P'' + P''' \qquad \text{(II.9b)}$$

with P" and P"' given by (II.9) and (II.7), respectively.

Turning to G_{30}, we find:

$$G_{30} = \left(-2\frac{\partial^2 \phi_{00}}{\partial t_1 \partial t_2} - \frac{\partial^2 \phi_{10}}{\partial t_1^2}\right) + \left\{-\frac{1}{2}\frac{\partial}{\partial t_1}\left[\left(\frac{\partial \phi_{00}}{\partial x_1}\right)^2 + \left(\frac{\partial \phi_{00}}{\partial y_1}\right)^2\right]\right.$$

$$\left. - \frac{\partial}{\partial x_1}\left[\frac{\partial \phi_{00}}{\partial x_1}\frac{\partial \phi_{00}}{\partial t_1}\right] - \frac{\partial}{\partial y_1}\left[\frac{\partial \phi_{00}}{\partial y_1}\frac{\partial \phi_{00}}{\partial t_1}\right]\right\} + \left\{-\frac{\partial}{\partial t_1}\left[k^2 |\phi_{11}|^2\right.\right.$$

$$\left.\left. + |\phi_{11 Z}|^2\right] + \frac{1}{g}\frac{\partial}{\partial t_1}\left[\omega^2 \phi_{11}\phi^*_{11 Z} + *\right] + \frac{\partial}{\partial x_1}\left[2k\omega |\phi_{11}|^2\right]\right\}_{Z=0}$$

Using (3.8), G_{30} can be simplified to:

$$G_{30} = -2\frac{\partial^2 \phi_{00}}{\partial t_1 \partial t_2} - \frac{\partial^2 \phi_{10}}{\partial t_1^2} + \frac{g^2}{2\omega}\frac{\partial}{\partial x_1}\left(k|A_0|^2\right)$$

$$- \frac{\omega^2}{4\sinh^2 q}\frac{\partial}{\partial t_1}|A_0|^2 + \left\{\left[-\frac{1}{2}\left(\nabla_1 \phi_{00}\right)^2\right]_{t_1} - \left[\phi_{00 x_1}\phi_{00 t_1}\right]_{x_1}\right.$$

$$\left. - \left[\phi_{00 y_1}\phi_{00 t_1}\right]_{y_1}\right\} \qquad \text{(II.10)}$$

where use has been made of the dispersion relation (3.9). The last function we need to determine is G_{40}. Collecting the various contributions to G_{40} we get:

$$G_{40} = \left(-2\frac{\partial^2\Phi_{00}}{\partial t_1\partial t_3} - 2\frac{\partial^2\Phi_{10}}{\partial t_1\partial t_2} - \frac{\partial^2\Phi_{20}}{\partial t_1^2}\right) - \frac{\partial}{\partial t_2}\left[k^2|\Phi_{11}|^2 + |\Phi_{11_Z}|^2\right]$$

$$-\frac{\partial}{\partial t_1}\left[\left(k^2\Phi_{21}\Phi_{11}^* + \Phi_{21_Z}\Phi_{11_Z}^*\right) + *\right] - \frac{\partial}{\partial t_1}\left[ik\Phi_{11}\frac{\partial\Phi_{11}^*}{\partial x_1} + *\right]$$

$$-\frac{\partial}{\partial t_1}\left[\frac{\partial\Phi_{00}}{\partial x_1}\frac{\partial\Phi_{10}}{\partial x_1} + \frac{\partial\Phi_{00}}{\partial y_1}\frac{\partial\Phi_{10}}{\partial y_1}\right] - \frac{1}{2}\frac{\partial}{\partial t_2}\left[\left(\frac{\partial\Phi_{00}}{\partial x_1}\right)^2 + \left(\frac{\partial\Phi_{00}}{\partial y_1}\right)^2\right]$$

$$-\frac{\partial}{\partial t_1}\left[\frac{\partial\Phi_{00}}{\partial x_1}\frac{\partial\Phi_{00}}{\partial x_2} + \frac{\partial\Phi_{00}}{\partial y_1}\frac{\partial\Phi_{00}}{\partial y_2}\right] + \frac{1}{g}\frac{\partial}{\partial t_2}\left[\omega^2\Phi_{11}\Phi_{11_Z}^* + *\right]$$

$$+\frac{1}{g}\frac{\partial}{\partial t_1}\left[\left(i\omega\Phi_{11_Z}^*\frac{\partial\Phi_{11}}{\partial t_1} - i\omega\Phi_{11}\frac{\partial^2\Phi_{11}^*}{\partial z\partial t_1}\right) + *\right] + \frac{1}{g}\frac{\partial}{\partial t_1}\left[\left(\omega^2\Phi_{11}\Phi_{21_Z}^*\right.\right.$$

$$\left.\left.+\omega^2\Phi_{21}\Phi_{11_Z}^*\right) + *\right] + \frac{\partial}{\partial x_2}\left(2\omega k|\Phi_{11}|^2\right) - \frac{\partial}{\partial x_1}\left[\left(i\omega\Phi_{11}^*\frac{\partial\Phi_{11}}{\partial x_1}\right.\right.$$

$$\left.\left.-ik\Phi_{11}^*\frac{\partial\Phi_{11}}{\partial t_1}\right) + *\right] - 2\frac{\partial}{\partial x_1}\left(-\omega k\Phi_{21}\Phi_{11}^* + *\right) - \frac{\partial}{\partial x_1}\left(\frac{\partial\Phi_{00}}{\partial x_1}\cdot\right.$$

$$\left.\frac{\partial\Phi_{10}}{\partial t_1} + \frac{\partial\Phi_{00}}{\partial t_1}\frac{\partial\Phi_{10}}{\partial x_1}\right) - \frac{\partial}{\partial x_2}\left(\frac{\partial\Phi_{00}}{\partial x_1}\frac{\partial\Phi_{00}}{\partial t_1}\right) - \frac{\partial}{\partial x_1}\left(\frac{\partial\Phi_{00}}{\partial x_2}\frac{\partial\Phi_{00}}{\partial t_1}\right.$$

$$\left.+\frac{\partial\Phi_{00}}{\partial x_1}\frac{\partial\Phi_{00}}{\partial t_2}\right) - \frac{\partial}{\partial y_1}\left(i\omega\Phi_{11}^*\frac{\partial\Phi_{11}}{\partial y_1} + *\right) - \frac{\partial}{\partial y_1}\left(\frac{\partial\Phi_{00}}{\partial y_1}\frac{\partial\Phi_{10}}{\partial t_1}\right.$$

$$+\frac{\partial\Phi_{00}}{\partial t_1}\frac{\partial\Phi_{10}}{\partial y_1}) - \frac{\partial}{\partial y_2}\left(\frac{\partial\Phi_{00}}{\partial y_1}\frac{\partial\Phi_{00}}{\partial t_1}\right) - \frac{\partial}{\partial y_1}\left(\frac{\partial\Phi_{00}}{\partial y_1}\frac{\partial\Phi_{00}}{\partial t_2}\right.$$

$$\left.+\frac{\partial\Phi_{00}}{\partial y_2}\frac{\partial\Phi_{00}}{\partial t_1}\right)+\frac{1}{2g}\frac{\partial^2}{\partial z\partial t_1}\left\{2\frac{\partial\Phi_{00}}{\partial t_1}\left(k^2|\Phi_{11}|^2+|\Phi_{11_z}|^2\right)\right.$$

$$\left.+2\frac{\partial\Phi_{00}}{\partial x_1}\left(-k\omega|\Phi_{11}|^2\right)+2\frac{\partial\Phi_{00}}{\partial x_1}\left(-k\omega|\Phi_{11}|^2\right)\right\}$$

$$-\frac{2}{g^2}\frac{\partial}{\partial t_1}\left[\frac{\partial\Phi_{00}}{\partial t_1}\left(\omega^2|\Phi_{11_z}|^2\right)\right]-\frac{1}{g^2}\frac{\partial}{\partial t_1}\left[\frac{\partial\Phi_{00}}{\partial t_1}\left(\omega^2\Phi_{11}\Phi^*_{11_{zz}}\right.\right.$$

$$\left.\left.+*\right)\right]-\frac{1}{2}\frac{\partial}{\partial x_1}\left[\frac{\partial\Phi_{00}}{\partial x_1}\left(\left(\frac{\partial\Phi_{00}}{\partial x_1}\right)^2+\left(\frac{\partial\Phi_{00}}{\partial y_1}\right)^2\right)\right]-\frac{\partial}{\partial x_1}\left[\frac{\partial\Phi_{00}}{\partial x_1}\right.$$

$$\left.\left(k^2|\Phi_{11}|^2+|\Phi_{11_z}|^2\right)+2\frac{\partial\Phi_{00}}{\partial x_1}\left(k^2|\Phi_{11}|^2\right)\right]+\frac{1}{g}\frac{\partial}{\partial x_1}\left[\frac{\partial\Phi_{00}}{\partial x_1}\right.$$

$$\left.\left(\omega^2\Phi^*_{11}\Phi_{11_z}+*\right)+\frac{\partial\Phi_{00}}{\partial t_1}\left(-k\omega\Phi^*_{11}\Phi_{11_z}+*\right)\right]$$

$$+\frac{1}{g}\frac{\partial}{\partial x_1}\left[\frac{\partial\Phi_{00}}{\partial t_1}\left(-k\omega\Phi^*_{11}\Phi_{11_z}+*\right)\right]-\frac{1}{2}\frac{\partial}{\partial y_1}\left[\frac{\partial\Phi_{00}}{\partial y_1}\right.$$

$$\left.\left[\left(\frac{\partial\Phi_{00}}{\partial x_1}\right)^2+\left(\frac{\partial\Phi_{00}}{\partial y_1}\right)\right]\right]-\frac{\partial}{\partial y_1}\left[\frac{\partial\Phi_{00}}{\partial y_1}\left(k^2|\Phi_{11}|^2+|\Phi_{11_z}|^2\right)\right]$$

$$+\frac{1}{g}\frac{\partial}{\partial y_1}\left[\frac{\partial\Phi_{00}}{\partial y_1}\left(\omega^2\Phi_{11}\Phi^*_{11_z}+*\right)\right]$$

There is no contribution to G_{40} from quartie terms, i.e., $O(\Phi^4)$ in (2.9), because $G_{40}\sim$zeroth harmonic, implying at least one differentiation with respect to slow scale variables hence, gives at least $O(\varepsilon^5)$ contributions [see contributions to G_{30} for example which involve only quadratic terms].

Appendix III

Determination of the Secular Forcing for the Second-order Incident-wave Amplitude

In this Appendix, we will derive that part of the forcing for the second-order incident wave amplitude (A_1^p) which will force secular contribution in the right-hand-side of Equation (3.35) for ϕ_{20}.

The complete forcing for the second-order incident-wave amplutide is given as the right-hand-side of Equation (3.63). Thus, we need to pick from this complete forcing, the real terms that are of the form,

$$P(x_1) \cos Ky_1 \, e^{-i\Omega t_1} + * \qquad \text{(III.1)}$$

(i) Contribution from $(\frac{\partial A_o}{\partial t_2} + Cg \frac{\partial A_o}{\partial x_2}) e^{-i\theta}$:

Substititing from (3.27), we get

$$I_1 = \sqrt{\frac{G_\infty}{G}} \left\{ A_{o\infty} \left[\frac{\partial i\theta}{\partial t_2} + G \frac{\partial i\theta}{\partial x_2} \right] + \left[\frac{\partial A_{o\infty}}{\partial t_2} + G \frac{\partial A_{o\infty}}{\partial x_2} \right] \right\} \qquad \text{(III.2)}$$

Therefore, it is seen that there is no contribution from these terms, simply because the first square bracket produce pure imaginary terms, and the second square bracket is not a function of t_1 (3.19).

(ii) Contribution from $P_2(A_o)$:

From (3.58), $P_2(A_o)$ is given by:

$$P_2 = \left\{ \left(-\frac{\partial h}{\partial x_1}\right)\left[ik\phi_{21}^P + \frac{\partial \phi_{11}}{\partial x_1}\right]_{Z=-h} + \int_{-h}^{o}\left[-\phi_{11}{}_{x_1x_1} - i(k\phi_{21}^P)_{x_1}\right.\right.$$

$$\left.\left. -ik(\phi_{21}^P)_{x_1}\right] ch\,Q\,dz \right\} - \int_{-h}^{o} \phi_{11}{}_{y_1y_1}\, ch\,Q\,dz \qquad \text{(III.3)}$$

Chu and Mei (1970), gave the explicit expression of the terms in the curly bracket after lengthy albegra. Using their results, and invoking (3.27) we get,

$$\frac{\sqrt{C_g}}{ch\,q} P_2\, e^{-i\theta} = -i\sqrt{C_{g_\infty}}\, A_{o_\infty}\, \omega \left\{ -\frac{\hat{\alpha}_1\hat{\alpha}_2}{sh\,2q} \right.$$

$$\left. -\frac{\beta_1}{4}\left(1 + \frac{2q}{sh\,2q}\right) - \frac{1}{4}\beta_2\left(coth\,2q - \frac{1}{sh\,2q}\right)\right.$$

$$-\frac{1}{8}\beta_3\left(2q - \coth 2q + \frac{1+2q^2}{\operatorname{ch} 2q}\right) - \frac{1}{8}\beta_4\left(2q\coth 2q - 1\right)$$

$$+\frac{1}{8}\beta_5\left(2q^2 - 2q\coth 2q + 1 + \frac{4q^3}{3\operatorname{sh} 2q}\right) - \frac{1}{8}\beta_6\left[\left(1+2q^2\right)\right.$$

$$\left.\coth 2q - 2q - \frac{1}{\operatorname{sh} 2q}\right] - \frac{1}{16}\beta_7\left[\left(4q^3+6q\right)\coth 2q - \left(6q^2+3\right)\right]\Bigg\}$$

$$+\frac{\sqrt{G}}{\operatorname{ch} q}\int_{-h}^{0} -\Phi_{111y_1y_1}\operatorname{ch} Q\, dz \cdot e^{-i\theta} \qquad \text{(III.4)}$$

where,

$$\hat{\alpha}_1 = \frac{\partial h}{\partial x_1} \quad ; \quad \hat{\alpha}_2 = \frac{\dfrac{\partial}{\partial x_1}\left[\dfrac{A_0}{2\omega \operatorname{ch} q}\right]}{k\left[\dfrac{A_0}{2\omega \operatorname{ch} q}\right]} \quad ; \quad \hat{\alpha}_3 = \frac{k_{x_1}}{2k^2}$$

$$\hat{\alpha}_4 = \frac{h_{x_1x_1}}{k} \quad ; \quad \hat{\alpha}_5 = \frac{k_{x_1x_1}}{2k^3} \quad ; \quad \hat{\alpha}_6 = \frac{\dfrac{\partial^2}{\partial x_1^2}\left[\dfrac{A_0}{2\omega \operatorname{ch} q}\right]}{k^2\left[\dfrac{A_0}{2\omega \operatorname{ch} q}\right]} \qquad \text{(III.5a-f)}$$

and,

$$\beta_1 = 3\hat{\alpha}_1^2 + \hat{\alpha}_6$$

$$\beta_2 = 4\hat{\alpha}_1\hat{\alpha}_2 + 4\hat{\alpha}_1\hat{\alpha}_3 + 4\hat{\alpha}_4$$

$$\beta_3 = 14\hat{\alpha}_1\hat{\alpha}_3 + 4\hat{\alpha}_1\hat{\alpha}_2 + 2\hat{\alpha}_4$$

$$\beta_4 = 6\hat{\alpha}_2\hat{\alpha}_3 + 2\hat{\alpha}_1^2 + 2\hat{\alpha}_5 + 2\hat{\alpha}_6$$

$$\beta_5 = 2\hat{\alpha}_5 + 6\hat{\alpha}_2\hat{\alpha}_3 + 6\hat{\alpha}_3^2$$

$$\beta_6 = 6\hat{\alpha}_1\hat{\alpha}_3$$

$$\beta_7 = 4\hat{\alpha}_3^2 \qquad \text{(III.5g-m)}$$

The coefficients $\hat{\alpha}_1$, $\hat{\alpha}_3$, $\hat{\alpha}_4$ and $_5$ are real, while the coefficients $\hat{\alpha}_2$ and $\hat{\alpha}_6$ are complex, and since we are interested in the real part of (III.4), the contribution then must involve $\hat{\alpha}_2$ and $\hat{\alpha}_6$. Substituting (3.27) into (III.5b) we get,

$$\hat{\alpha}_2 = \frac{1}{k}(\sqrt{G}\, ch q)\left(\frac{1}{ch q \sqrt{G}}\right) + i\frac{\Theta_{x_1}}{k} \qquad \text{(III.6)}$$

and into (III.5f) to get

$$\hat{\alpha}_6 = \left\{\frac{1}{k^2}(\sqrt{G}\, ch q)\left(\frac{1}{\sqrt{G}\, ch q}\right)_{x_1 x_1} - \left(\frac{\Theta_{x_1}}{k}\right)^2\right\}$$

$$+ i\left\{\frac{\Theta_{x_1 x_1}}{k^2} + \frac{2}{k^2}\Theta_{x_1}(\sqrt{G}\, ch q)\left(\frac{1}{\sqrt{G}\, ch q}\right)_{x_1}\right\} \qquad \text{(III.7)}$$

Also, the remaining z-integral in (III.4) will give,

$$W = \frac{-\sqrt{G}}{ch q}\int_{-h}^{0} \Phi_{11_{y_1 y_1}}\, ch Q\, dz$$

$$= \frac{i g \sqrt{G_\infty}\, A_{0\infty}}{2\omega\, ch^2 q}\frac{\partial^2 e^{i\Theta}}{\partial y_1^2}\int_{-h}^{0} ch^2 Q\, dz$$

$$= \frac{i g\sqrt{G_\infty}\, A_{o\infty}}{2\omega k\ ch^2 q}\left[i\,\theta_{y,y_1} - (\theta_y)^2\right] e^{i\theta} \int_0^q ch^2 Q\, dQ$$

$$= \frac{g\sqrt{G_\infty}\, A_{o\infty}}{2\omega k\ ch^2 q}\left(\tfrac{1}{2} q + \tfrac{1}{4} sh\,2q\right)\left[- \theta_{y,y_1} - i(\theta_y)^2\right] e^{i\theta}$$

(III.8)

Thus, the contribution for $P_2(A_o)$ is given by (from (III.4))

$$I_2 = \sqrt{G_\infty}\, A_{o\infty}\, \omega \left\{ -\frac{\hat{\alpha}_1 \delta_1}{sh\,2q} - \frac{\delta_2}{4}\left(1 + \frac{2q}{sh\,2q}\right) - \frac{4\hat{\alpha}_1\delta_1}{4}\left(\coth 2q - \frac{1}{sh\,2q}\right)\right.$$

$$- \frac{4\hat{\alpha}_1\delta_1}{8}\left(2q - \coth 2q + \frac{1+2q^2}{sh\,2q}\right) - \frac{6\hat{\alpha}_3\delta_1 + 2\delta_2}{8}\left(2q\coth 2q - 1\right)$$

$$\left. + \frac{6\hat{\alpha}_3\delta_1}{8}\left(2q - 2q\coth 2q + 1 + \frac{4q^3}{3\,sh\,2q}\right) - \frac{1}{2k^2}\left(\frac{1}{2} + \frac{q}{sh\,2q}\right)\theta_{y,y_1}\right\}$$

(III.9)

where

$$\delta_1 = Im(\hat{\alpha}_2) = \frac{\theta_{x_1}}{k}$$

$$\delta_2 = Im(\hat{\alpha}_6) = \frac{\theta_{x_1x_1}}{k^2} + \frac{2}{k^2}\,\theta_{x_1}\left(\sqrt{G}\, ch\,q\right)\left(\frac{1}{\sqrt{G}\, ch\,q}\right)_{x_1}$$

By re-arranging, (III.9) can be put in a more compact form:

$$I_2 = \sqrt{g_\infty}\, A_{o_\infty}\, \omega\, \delta_1 \left\{ \frac{6\hat{\alpha}_3}{8}\left(2q^2 - 4q\coth 2q + 2 + \frac{4q^3}{3\,\mathrm{sh}2q}\right) - \frac{\hat{\alpha}_1}{2}\left(2q + \coth 2q + \frac{1+2q}{\mathrm{sh}2q}\right)\right\} - \sqrt{g_\infty}\, A_{o_\infty}\, \omega\, \delta_2 \left\{ \frac{q}{2\,\mathrm{sh}2q} + \frac{1}{2} q \coth 2q \right\} - \sqrt{g_\infty}\, A_{o_\infty}\, \omega\, \Theta_{y_1 y_1} \left(\frac{1}{2} + \frac{q}{\mathrm{sh}2q}\right) \qquad \text{(III.10)}$$

(iii) Contribution from $P_1(\phi_{oo}, A_o)$

From (II.9b), P_1 is given by

$$P_1(\phi_{oo}, A_o) = \left\{ -\phi_{11_{t_1 t_1}} + 2i\omega \phi^P_{21_{t_1}} + \left[-2k\omega \phi^P_{21} \frac{\partial \phi_{oo}}{\partial x_1} + \frac{\partial \phi_{oo}}{\partial t_1}\left(\frac{-\omega^2}{g}\phi^P_{21_z} + k^2 \phi^P_{21}\right)\right] + P'' + P''' \right\}_{z=o} \qquad \text{(III.11)}$$

where ϕ^P_{21} is given, from (3.29), by:

$$\phi^P_{21} = -\frac{gA_o}{2\omega\, ch q}\left(\alpha_1 Q\, ch Q + \alpha_2 Q\, sh Q + \alpha_3 Q^2\, ch Q\right) \qquad \text{(III.12)}$$

with α_1, α_2 and α_3 given by (3.29a)

P"' given by (II.7) and P" given by (II.9)

We proceed to collect contributions from the terms of P_1:

$$\text{(i)} \quad -\left.\frac{\partial^2 \phi_{11}}{\partial t_1^2}\right|_{z=0} = \frac{igd}{2\omega\sqrt{G}}\left(i\theta_{t_1t_1} - (\theta_t)^2\right)e^{i\theta}$$

$$= \left\{\frac{-gd}{2\omega\sqrt{G}}\ \theta_{t_1t_1} + i(\cdots)\right\}e^{i\theta}$$

where for brevity, we write $d = \sqrt{Cg_\infty}\ A_{0\infty}$ (see (3.27)].

$$\text{(ii)} \quad i2\omega\, \phi^P_{21t_1}\Big|_{z=0}$$

The coefficients α_1 and α_3 in ϕ^P_{21} solution (3.29) are real, while α_2 is complex:

$$\alpha_2 = \frac{1}{2k}\left(G_g\, ch^2 q\right)\left(\frac{1}{G_g\, ch^2 q}\right)_{x_1} + i\frac{\theta_{x_1}}{k}$$

$$= \tilde{\alpha}_2 + i\,\tilde{\tilde{\alpha}}_2$$

where $\tilde{\alpha}_2$ and $\tilde{\tilde{\alpha}}_2$ are the real and imaginary parts of α_2. Thus,

$$i2\omega\, \phi^P_{21t_1}\Big|_{z=0} = \left\{\theta_{t_1}\frac{gd}{\sqrt{G}\,ch q}\left(\alpha_1 q\, ch q + \tilde{\alpha}_2 q\, sh q\right.\right.$$

$$\left.\left. + \alpha_3 q^2 ch q\right) + \theta_{x_1t_1}\frac{gd}{k\sqrt{G}\,ch q}\, q\, sh q + i(\cdots)\right\}e^{i\theta}$$

$$\text{(iii)} \; -2k\omega \Phi_{21}^{P} \frac{\partial \Phi_{00}}{\partial x_1} + \frac{\partial \Phi_{00}}{\partial t_1}\left(-\frac{\omega^2}{g}\Phi_{21_z}^{P} + k^2 \Phi_{21}^{P}\right) =$$

$$\left\{\left(-2k\omega \frac{\partial \Phi_{00}}{\partial x_1} + k^2 \frac{\partial \Phi_{00}}{\partial t_1}\right)\left[\frac{-gd}{2\omega\sqrt{Cg}\,ch q}\left(\alpha_1 q\, ch q + \right.\right.\right.$$

$$\left.\tilde{\alpha}_2 q\, sh q + \alpha_3 q^2 ch q\right)\Big] - \frac{\omega^2}{g}\frac{\partial \Phi_{00}}{\partial t_1}\left[\frac{-gdk}{2\omega\sqrt{Cg}\,ch q}\left(\alpha_1[ch q\right.\right.$$

$$\left.+ q\, sh q] + \tilde{\alpha}_2[sh q + q\, ch q] + \alpha_3[2q\, ch q\right.$$

$$\left.\left.\left.+ q^2 sh q]\right)\right] + i(\cdots\cdots)\Big\} e^{i\theta}$$

(iv) P''' as given by (III.7) has no contribution to G_1:

$$P''' = i\frac{g\omega d}{\sqrt{Cg}}\left[\frac{k^2 d^2}{16 Cg}\left(9\coth^4 q - 10\coth^2 q + 9\right)\right] e^{i\theta}$$

(v) P" is given by (II.9). Collecting contributions term by term we get:

$$P'' = \Big\{-\frac{\partial^2 \Phi_{00}}{\partial x_1 \partial t_1}\left(\frac{gkd}{2\omega\sqrt{Cg}}\right) + \frac{gd}{2}\left(\frac{1}{\sqrt{Cg}}\right)_{x_1}\frac{\partial \Phi_{00}}{\partial x_1} - \frac{\omega^2 d}{2g\sqrt{Cg}}\frac{\partial^2 \Phi_{00}}{\partial t_1^2}$$

$$- \frac{gkd}{2\omega}\left(\frac{1}{\sqrt{Cg}}\right)_{x_1}\frac{\partial \Phi_{00}}{\partial t_1} - \left[\frac{\partial \Phi_{00}}{\partial x_1}\left(\frac{-gd}{2\sqrt{Cg}}\right) + \frac{\partial \Phi_{00}}{\partial t_1}\left(\frac{gkd}{2\omega\sqrt{Cg}}\right)\right]_{x_1}$$

$$+ \frac{\partial^2 \Phi_{00}}{\partial y_1^2}\left(\frac{gd}{2\sqrt{Cg}}\right) + i(\cdots\cdots)\Big\} e^{i\theta}$$

Thus, collecting the contributions from (i) to (v) we get the total contribution from P_1:

$$I_3 = Re\left(-\frac{\sqrt{G}}{g} P_1 e^{-i\theta}\right) = -\frac{\sqrt{G}}{g}\left(\sqrt{G_\infty} A_{0\infty}\right)\left\{\frac{-g}{2\omega\sqrt{G}}\theta_{t_1 t_1}\right.$$

$$+ \theta_{t_1}\frac{g}{\sqrt{G}}\left[\alpha_1 q + \tilde{\alpha}_2 q\,th q + \alpha_3 q^2\right] + \theta_{x_1 t_1}\frac{g}{k\sqrt{G}} q\,th q$$

$$-\frac{g}{2\omega\sqrt{G}}\left(\alpha_1 q + \tilde{\alpha}_2 q\,th q + \alpha_3 q^2\right)\cdot\left(-2k\omega\frac{\partial\Phi_{00}}{\partial x_1} + k^2\frac{\partial\Phi_{00}}{\partial t_1}\right)$$

$$-\frac{gk}{2\omega\sqrt{G}}\left[\alpha_1(1+q\,th q) + \tilde{\alpha}_2(th q + q) + \alpha_3(2q + q^2 th q)\right]\cdot$$

$$\left(\frac{-\omega^2}{g}\frac{\partial\Phi_{00}}{\partial t_1}\right) - \frac{\partial^2\Phi_{00}}{\partial x_1 \partial t_1}\left(\frac{gk}{2\omega\sqrt{G}}\right) + \frac{g}{2}\left(\frac{1}{\sqrt{G}}\right)_{x_1}\frac{\partial\Phi_{00}}{\partial x_1}$$

$$-\frac{\omega^2}{2g\sqrt{G}}\frac{\partial^2\Phi_{00}}{\partial t_1^2} - \frac{gk}{2\omega}\left(\frac{1}{\sqrt{G}}\right)_{x_1}\frac{\partial\Phi_{00}}{\partial t_1}$$

$$-\left[\frac{\partial\Phi_{00}}{\partial x_1}\left(\frac{-g}{2\sqrt{G}}\right) + \frac{\partial\Phi_{00}}{\partial t_1}\left(\frac{gk}{2\omega\sqrt{G}}\right)\right]_{x_1}$$

$$\left. + \frac{\partial^2\Phi_{00}}{\partial y_1^2}\left(\frac{g}{2\sqrt{G}}\right)\right\}$$

(III.13)

It is indeed seen, from (3.2) and (3.24) that all the terms of I_2 (III.10), and I_3 (III.13) are of the form (III.1). Thus, the summation $I_2 + I_3$ will give the complete secular forcing for A_1, i.e.,

$$P(x)\ \cos Ky_1 e^{-i\Omega t_1} + * = I_2 + I_3 \qquad \text{(III.14)}$$

APPENDIX IV

Derivation of the Function S_1 for Equation (3.35)

For the inhomogeneous equation for ℓ_2 (3.35), the forcing at the right-hand side contains terms which can be written as,

$$S = S_1(x_1, D_0)\cos Ky_1\, e^{-i\Omega t_1} \tag{IV.1}$$

and it is required to find the function S_1.

(i) $g\nabla_1\cdot\left(\frac{h^3}{6}\nabla_1 F_{20} - \frac{h^2}{2}\nabla_1 \ell_1\right)$:

From (3.30a) and (3.32), we see that

$$S_1^{(1)} = \left(\frac{-igD_0}{2\Omega}\right)\left\{g\frac{\partial}{\partial x_1}\left[\frac{h^3}{6}\left(-L_n''' + K^2 L_n'\right) - \frac{h^2}{2}\frac{\Omega^2}{g}L_n'\right]\right.$$

$$\left. + g\frac{K^2h^3}{6}\left(L_n'' - K^2 L_n\right) + K^2\frac{h^2\Omega^2}{2}L_n\right\} \tag{IV.2}$$

(ii) G'_{40}:

$$G'_{40} = G_{40} + \frac{\partial^2 \Phi_{20}}{\partial t_1^2}\Big|_{z=0} \qquad \text{(IV.3)}$$

where G_{40} is given by (II.11). Thus, from (II.11), we will only collect terms of the form (IV.1):

$$\text{(i)} \; -2\frac{\partial^2 \Phi_{00}}{\partial t_1 \partial t_3} = g\frac{\partial D_0}{\partial t_3} L_n \cos Ky_1 \, e^{-i\Omega t_1} + \cdots$$

$$\text{(ii)} \; -2\frac{\partial^2 \Phi_{10}}{\partial t_1 \partial t_2} = g\frac{\partial D_1}{\partial t_2} L_n \cos Ky_1 \, e^{-i\Omega t_1} + \cdots$$

$$\text{(iii)} \; -\frac{\partial}{\partial t_1}\left[\left(k^2 \Phi_{21}\Phi_{11}^* + \Phi_{21_z}\Phi_{11_z}^*\right) + *\right] + \frac{1}{g}\frac{\partial}{\partial t_1}\left[\left(\omega^2 \Phi_{11}\Phi_{21_z}^* + \omega^2 \Phi_{21}\Phi_{11_z}^*\right) + *\right]$$

$$= \frac{\partial}{\partial t_1}\left\{2(A_0 A_1^* + A_0^* A_1)\left[\frac{-1}{2}\left[\left(\frac{gk}{2\omega}\right)^2 + \left(\frac{gk\,th q}{2\omega}\right)^2\right] + \frac{1}{g}\left[\frac{-g}{2}\cdot\frac{-gk\,th q}{2}\right]\right]\right\}$$

$$-\frac{\partial}{\partial t_1}\left[\left(k^2 \Phi_{21}^P \Phi_{11}^* + \Phi_{21_z}^P \Phi_{11_z}^*\right) + *\right] + \frac{1}{g}\frac{\partial}{\partial t_1}\left[\left(\omega^2 \Phi_{11}\Phi_{21_z}^{P*} + \omega^2 \Phi_{21}^P \Phi_{11_z}^*\right) + *\right]$$

$$= \frac{\partial}{\partial t_1}\left\{-2(A_0 A_1^* + A_0^* A_1)\left[\frac{\omega^2 ch^2 q}{8\, sh^2 q} + \frac{\omega^2}{8} - \frac{\omega^2}{4}\right]\right\}$$

$$+2\left\{\frac{ig^2 kq\, sh q}{8\omega^2 ch q} + \frac{ig}{8 ch q}(sh q + q\, ch q)\right\}\left(A_0^* \frac{\partial A_0}{\partial x_1} - *\right)_{t_1}$$

$$+\frac{\omega^2}{2g\, ch q}\left\{\frac{-igq\, sh q}{2k} - \frac{-ig^2}{2\omega^2}(sh q + q\, ch q)\right\}\left(A_0^* \frac{\partial A_0}{\partial x_1} - *\right)_{t_1}$$

(where we used the linear dispersion relation (3.9)),

$$= -\frac{\omega^2}{4\sinh^2 q}\frac{\partial}{\partial t_1}\left(A_0 A_1^* + *\right) - \frac{gd^2}{2C_g}\left(\tanh q + 2q\right)\Theta_{x_1 t_1}$$

$$+ \frac{\omega^2 d^2}{g C_g}\left(\frac{\omega^2 h}{2k} + \frac{g^2}{2\omega^2}\left(\tanh q + q\right)\right)\Theta_{x_1 t_1}$$

(where for brevity we write $d = \sqrt{C g_\infty}\ A_{0\infty}$). This is further simplified, using (3.24), (3.68), and (3.72), to give:

$$\frac{i\Omega\omega^2}{4\sinh^2 q} d^2\left[\left(\frac{A_{1\infty}}{A_{0\infty}}\right)\frac{e^{i\Omega\int^{x_1}\frac{ds}{C_g}}}{C_g} + \left(\frac{-igD_0}{2\Omega}\right)\frac{2q_1}{C_g}^{P}\right]$$

$$-\frac{i\Omega d^2}{C_g}\left\{\frac{-g}{2}\left(\tanh q + 2q\right) + \frac{\omega^2}{g}\left(\frac{\omega^2 h}{2k} + \frac{g^2}{2\omega^2}\left[\tanh q + q\right]\right)\right\}\left(\frac{-igD_0}{2\Omega}\right)\textcircled{H}\cos Ky_1 e^{-i\Omega t_1} + \cdots.$$

(iv) $$-\frac{\partial}{\partial t_1}\left[-ik\,\phi_{11}^*\,\phi_{11_{x_1}} + *\right] = \frac{ig^2 k}{4\omega^2}\left(A_0^*\frac{\partial A_0}{\partial x_1} - *\right)_{t_1} = \frac{-g^2 k d^2}{2\omega^2 C_g}\Theta_{x_1 t_1}$$

$$= \frac{i\Omega g^2 k d^2}{2\omega^2 C_g}\left(\frac{-igD_0}{2\Omega}\right)\textcircled{H}\cos Ky_1 e^{-i\Omega t_1} + \cdots$$

(v) $\frac{1}{g}\frac{\partial}{\partial t_2}\left[\omega^2\phi_{11}\phi_{11_2}^* + *\right]$ not proportional to $\cos Ky_1 e^{-i\Omega t_1}$

(vi) $$\frac{1}{g}\frac{\partial}{\partial t_1}\left[(i\omega\Phi_{11_{t_1}}\Phi_{11_z}^{*} + i\omega\Phi_{11}\Phi_{11_{zt_1}}^{*}) + *\right] = \frac{i\omega}{2}\left(A_0^{*}\frac{\partial A_0}{\partial t_1} - *\right)_{t_1}$$

$$= \frac{-\omega d^2}{C_g}\Theta_{t_1t_1} = \frac{\omega\Omega^2 d^2}{C_g}\left(\frac{-igD_0}{2\Omega}\right)\Theta\cos Ky_1 e^{-i\Omega t_1} + \cdots$$

(vii) $$\frac{\partial}{\partial x_2}\left(2\omega k|\Phi_{11}|^2\right)$$ not proportional to $\cos Ky_1 e^{-i\Omega t_1}$

(viii) $$-\left\{(i\omega\Phi_{11_{x_1}}\Phi_{11}^{*} - ik\Phi_{11_{t_1}}\Phi_{11}^{*}) + *\right\}_{x_1}$$

$$= -\left\{\frac{ig^2}{4\omega}\left(A_0^{*}\frac{\partial A_0}{\partial x_1} - *\right) - \frac{ig^2k}{4\omega^2}\left(A_0^{*}\frac{\partial A_0}{\partial t_1} - *\right)\right\}_{x_1}$$

$$= \left\{\frac{g^2d^2}{2\omega C_g}\Theta_{x_1} - \frac{g^2kd^2}{2\omega^2 C_g}\Theta_{t_1}\right\}_{x_1}$$

$$= \left(\frac{-igD_0}{2\Omega}\right)\left[\frac{g^2d^2}{2\omega C_g}\Theta' + \frac{ig^2\Omega kd^2}{2\omega^2 C_g}\Theta\right]' \cos Ky_1 e^{-i\Omega t_1} + \cdots$$

(ix)

$$-\left\{-2\omega k\Phi_{11}^{*}\Phi_{21} + *\right\}_{x_1}$$

$$= \frac{g^2}{2\omega}\frac{\partial}{\partial x_1}\left[k(A_0A_1^{*} + *)\right] + \left(gd^2\frac{\omega h}{C_g}\Theta_{x_1}\right)_{x_1}$$

$$= \frac{g^2d^2}{2\omega}\left[\frac{k}{C_g}\left(\frac{A_{1\infty}}{A_{0\infty}}\right)e^{i\Omega\int^{x_1}\frac{d\varrho}{C_g}} + \left(\frac{-igD_0}{2\Omega}\right)\frac{2k}{C_g}a_1^{P}\right]_{x_1}\cos Ky_1 e^{-i\Omega t_1}$$

$$+\left(d^2\frac{g\omega h}{C_g}\Theta_{x_1}\right)_{x_1}\cos Ky_1 e^{-i\Omega t_1} + \cdots\cdots$$

(x) $$-\left(i\omega\Phi_{11y_1}\Phi_{11}^{*}+*\right)_{y_1}=\frac{-ig^2}{4\omega}\left(A_0^{*}\frac{\partial A_0}{\partial y_1}-*\right)_{y_1}$$

$$=\frac{g^2d^2}{2\omega C_g}\,\Theta_{y_1y_1}$$

$$=\frac{-g^2d^2K^2}{2\omega C_g}\cdot\Theta\cdot\left(\frac{-igD_0}{2\Omega}\right)\cos Ky_1\,e^{-i\Omega t_1}+\cdots$$

(xi) $$-\left[\left(\frac{\partial\Phi_{00}}{\partial x_1}\right)\left(\frac{\partial\Phi_{10}}{\partial x_1}\right)-\left(\frac{\partial\Phi_{00}}{\partial y_1}\right)\left(\frac{\partial\Phi_{10}}{\partial y_1}\right)\right]_{t_1}-\left[\frac{\partial\Phi_{00}}{\partial x_1}\frac{\partial\Phi_{10}}{\partial t_1}\right.$$

$$\left.+\frac{\partial\Phi_{10}}{\partial x_1}\frac{\partial\Phi_{00}}{\partial t_1}\right]_{x_1}-\left[\frac{\partial\Phi_{00}}{\partial y_1}\frac{\partial\Phi_{10}}{\partial t_1}+\frac{\partial\Phi_{10}}{\partial y_1}\frac{\partial\Phi_{00}}{\partial t_1}\right]_{y_1}$$

$$=\left\{\left(\frac{-igD_0}{2\Omega}\right)\left[-i\Omega\frac{gkd^2L_n'}{2\omega hC_g}+\left(\frac{-i\Omega gkd^2L_n}{2\omega hC_g}\right)'\right]+i\Omega\left[K^2L_n(3\Psi_2-2\Psi_1)\right.\right.$$

$$\left.\left.+L_n'\Psi_1'+\tfrac{1}{2}L_n'\Psi_2'+\left[2L_n'(\Psi_1+\tfrac{1}{2}\Psi_2)-L_n'(\Psi_1'+\tfrac{1}{2}\Psi_1')\right]'\right]\left(\frac{-ig^3}{8\Omega^2}|D_0|^2D_0\right)\right\}\cdot$$

$$\cos Ky_1\,e^{-i\Omega t_1}+\cdots.$$

where use has been made of the trigonometric identieies:

$$\cos Ky_1\cos 2Ky_1=\tfrac{1}{2}\cos Ky_1+\tfrac{1}{2}\cos 3Ky_1$$

$$\sin Ky_1\sin 2Ky_1=\tfrac{1}{2}\cos Ky_1-\tfrac{1}{2}\cos 3Ky_1\quad\text{etc.}$$

(xii) $\frac{1}{2g}\left[\Phi_t(\nabla\Phi)^2\right]_z \rightarrow$

$$d^2\left(-\frac{\Omega^2 k^2}{C_g}L_n + \frac{i\Omega k}{C_g}\omega L_n'\right)\left(\frac{-igD_0}{2\Omega}\right)\cos Ky_1\, e^{-i\Omega t_1}$$

(xiii) $\frac{-1}{g^2}\left[\Phi_t \Phi_{zt}^2\right]_t \rightarrow$

$$\frac{-1}{g^2}\left[\frac{\partial\Phi_{00}}{\partial t_1}\left(\omega^2\Phi_{11z}\Phi_{11z}^* + *\right)\right]_{t_1}$$

$$= \frac{\omega^4\Omega^2 d^2}{2g^2 C_g}L_n\left(\frac{-igD_0}{2\Omega}\right)\cos Ky_1\, e^{-i\Omega t_1} + *$$

(xiv) $\frac{-1}{2g^2}\left[\Phi_{zzt}\Phi_t^2\right]_t \rightarrow \frac{-1}{g^2}\left[\frac{\partial\Phi_{00}}{\partial t_1}\left(\omega^2\Phi_{11zz}\Phi_{11}^* + *\right)\right]_{t_1}$

$$= \frac{\Omega^2 k^2 d^2}{2C_g}L_n\left(\frac{-igD_0}{2\Omega}\right)\cos Ky_1\, e^{-i\Omega t_1} + *$$

(xv) $\frac{-1}{2}\left[\Phi_x(\nabla\Phi)^2\right]_x \longrightarrow \frac{-1}{2}\left\{\frac{\partial\Phi_{00}}{\partial x_1}\left[\left(\frac{\partial\Phi_{00}}{\partial x_1}\right)^2 + \left(\frac{\partial\Phi_{00}}{\partial y_1}\right)^2\right]\right\}_{x_1}$

$$-\left[\frac{\partial\Phi_{00}}{\partial x_1}\frac{d^2}{C_g}\left(\frac{g^2k^2}{4\omega^2}+\frac{\omega^2}{4}\right)\right]_{x_1} - 2\left[\frac{\partial\Phi_{00}}{\partial x_1}\frac{d^2}{C_g}\frac{g^2k^2}{4\omega^2}\right]_{x_1}$$

$$= \frac{-1}{4}\left(3L_n'^3 + K^2L_n'L_n^2\right)\left(\frac{-ig^3}{8\Omega^3}|D_0|D_0\right)\cos Ky_1\, e^{-i\Omega t_1}$$

$$-\left\{L_n'\frac{d^2}{C_g}\left(\frac{g^2k^2}{4\omega^2}+\frac{\omega^2}{4}\right) + 2L_n\frac{d^2}{C_g}\frac{g^2k^2}{4\omega^2}\right\}'\left(\frac{-igD_0}{2\Omega}\right)\cos Ky_1\, e^{-i\Omega t_1}$$

(xvi) $$\frac{1}{g}\left[\Phi_x \Phi_t \Phi_{zt}\right]_x \longrightarrow \frac{1}{g}\left[\left(\omega^2 \Phi_{11}^* \Phi_{11z} \frac{\partial \Phi_{00}}{\partial x_1} - k\omega \Phi_{11z} \Phi_{11}^* \frac{\partial \Phi_{00}}{\partial t_1}\right) + *\right]_{x_1}$$

$$= \frac{2}{g}\left[\frac{g\omega^2 d^2}{4C_g} L_n' + \frac{igk\omega\Omega d^2}{4C_g} L_n\right]' \left(\frac{-igD_0}{2\Omega}\right) \cos Ky_1 \, e^{-i\Omega t_1} + *$$

(xvii) $$\frac{1}{2g}\left[\Phi_t^2 \Phi_{xz}\right]_x \longrightarrow \frac{1}{g}\left[\frac{\partial \Phi_{00}}{\partial t_1}\left(\omega k \Phi_{11z} \Phi_{11}^* + *\right)\right]_{x_1}$$

$$= \frac{2}{g}\left(\frac{-igk\omega\Omega d^2}{4g} L_n\right)' \left(\frac{-igD_0}{2\Omega}\right) \cos Ky_1 \, e^{-i\Omega t_1} + *$$

(xviii) $$\frac{-1}{2}\left[\Phi_y (\nabla\Phi)^2\right]_y \rightarrow \frac{-1}{2}\left\{\frac{\partial \Phi_{00}}{\partial y_1}\left[\left(\frac{\partial \Phi_{00}}{\partial x_1}\right)^2 + \left(\frac{\partial \Phi_{00}}{\partial y_1}\right)^2\right]\right\}_{y_1}$$

$$- \left[\frac{\partial \Phi_{00}}{\partial y_1}\left(k^2 \Phi_{11} \Phi_{11}^* + \Phi_{11z} \Phi_{11z}^*\right)\right]_{y_1}$$

$$= \frac{K^2}{4}\left(L_n L_n'^2 + 3K^2 L_n^3\right)\left(\frac{-ig^3}{8\Omega^3} |D_0|^2 D_0\right) \cos Ky_1 \, e^{-i\Omega t_1}$$

$$+ \left(\frac{g^2 k^2}{4\omega^2} + \frac{\omega^2}{4}\right) \frac{d^2}{C_g} K^2 L_n \left(\frac{-igD_0}{2\Omega}\right) \cos Ky_1 \, e^{-i\Omega t_1} + \cdots\cdots$$

(xix) $$\frac{1}{g}\left[\Phi_y \Phi_t \Phi_{zt}\right]_y \rightarrow \frac{1}{g}\left[\frac{\partial \Phi_{00}}{\partial y_1}\left(\omega^2 \Phi_{11z} \Phi_{11}^* + *\right)\right]_{y_1}$$

$$= \frac{-2}{g}\left(\frac{g\omega^2}{4} \frac{d^2}{C_g} K^2 L_n\right)\left(\frac{-igD_0}{2\Omega}\right) \cos Ky_1 \, e^{-i\Omega t_1} + *$$

The terms given in (i) to (xix), plus (IV.2), will give us S_1. Thus, summing these terms with little rearrangement, gives:

$$S_1 = gL_n\frac{\partial D_0}{\partial t_3} + gL_n\frac{\partial D_1}{\partial t_2} + \left(\frac{-igD_0}{2\Omega}\right)\left\{ g\frac{\partial}{\partial x_1}\left[\frac{h^3}{6}\left(-L_n''' + K^2L_n'\right)\right.\right.$$

$$\left. - \frac{h^2\Omega^2}{g}L_n'\right] + \frac{gK^2h^3}{6}\left(L_n'' - K^2L_n\right) + \frac{1}{2}K^2h^2\Omega^2L_n + A_{0\infty}^2\frac{C_{g\infty}}{C_g}\left[\frac{i\Omega g}{2}\cdot\right.$$

$$\left(\frac{q}{ch^2q} + \frac{1}{thq}\right)\textcircled{H}' + \left(2\omega^2\Omega^2 - g^2K^2\right)\frac{\textcircled{H}}{2\omega} + \frac{i\Omega\omega^2}{2sh^2q}a_1^P - \frac{i\Omega gkL_n}{2\omega h}$$

$$+ i\Omega\omega kL_n' + \frac{\omega^4\Omega^2L_n}{2g^2} - \frac{1}{2}k^2\Omega^2L_n + \left(\frac{g^2k^2}{4\omega^2} - \frac{\omega^2}{4}\right)K^2L_n\Big]$$

$$+ C_{g\infty}A_{0\infty}^2\left[\frac{1}{2C_g}\left(\frac{g}{\omega}\left(g + 2\omega^2h\right)\textcircled{H}' + \frac{i\Omega g^2k}{\omega^2}\textcircled{H} + \frac{2g^2k}{\omega}a_1^P\right.\right.$$

$$\left.\left. - \frac{i\Omega gkL_n}{\omega h} - \left(\frac{3g^2k^2}{2\omega^2} - \frac{\omega^2}{2}\right)L_n'\right)\right]'\Big\} + \left(\frac{-ig^3}{8\Omega^3}|D_0|^2D_0\right)\Big\{i\Omega\cdot$$

$$\left[K^2L_n\left(3\psi_2 - 2\psi_1\right) + L_n'\psi_1' + \frac{1}{2}L_n'\psi_2' + \left(2L_n'\left(\psi_1 + \frac{1}{2}\psi_2\right) - L_n\left(\psi_1' + \frac{1}{2}\psi_2'\right)\right)'\right]$$

$$+ \frac{K^2}{4}\left(L_nL_n'^2 + 3K^2L_n^2\right) - \frac{1}{4}\left(3L_n'^3 + K^2L_n'L_n^2\right)'\Big\} + A_{1\infty}A_{0\infty}\Big\{\frac{g^2C_{g\infty}}{2\omega}\cdot$$

$$\left[\frac{k}{C_g}e^{i\Omega\int^{x_1}\frac{d\varsigma}{C_g}}\right]' + \frac{i\Omega\omega^2C_{g\infty}}{4sh^2qC_g}e^{i\Omega\int^{x_1}\frac{d\varsigma}{C_g}}\Big\} \qquad \text{(IV.4)}$$

APPENDIX V

Numerical Scheme for the Determination of the Large Scale Motions ϕ_{oo} and ϕ_{10}

1) The Free Edge Wave ϕ_{oo}:

The first task is to determine the free edge wave modal shapes $L_n(x_1)$, and dispersion relation $\Omega(K)$ for arbitrary bottom shape. The edge wave homogeneous equation is (3.1):

$$\frac{\partial^2 \Phi_{oo}}{\partial t_1^2} - g\nabla_1 \cdot (h \nabla_1 \Phi_{oo}) = 0 \qquad (V.1)$$

For, $\phi_{oo} = (\frac{-gD_o}{2\Omega} L_n(x_1) \cos Ky_1 e^{-i\Omega t_1} + *$

L_n satisfies,

$$(hL_n')' + \frac{1}{g}(\Omega^2 - ghK^2) L_n = 0 \qquad (V.2)$$

We may non-dimensionalize (V.2) by using $1/k_o$ as a length scale and $1/\omega$ as a time scale, where k_o and ω are, respectively, the incident wave wavenumber and frequency at some reference depth h_o, so that from the dispersion relation (3.9), they are related by:

$$k_o = \frac{\omega^2}{gT} \quad ; \quad T = \text{th}\, k_o h_o \qquad (V.3)$$

Thus, we let

$$(x_1, h) = \frac{1}{k_o}(\bar{x}_1, \bar{h}), \; K = k_o \bar{K} \quad \text{and} \quad \Omega = \frac{1}{\omega}\bar{\Omega} \qquad (V.4)$$

where overbars denote nondimensional variables.

Hence, (V.2) becomes:

$$(\bar{h} L_n')' + \lambda L_n = 0 \tag{V.5}$$

where

$$\lambda = T \bar{\Omega}^2 - \bar{h} \bar{K}^2 \tag{V.6}$$

and primes now denote differentiation with respect to $\bar{x}_1$.

Equation (V.5) should be solved with the boundary conditions:

$$L_n \to 0 \qquad \text{as} \quad \bar{x}_1 \to \pm\infty \tag{V.7}$$

If the bottom is in the shape of a submerged ridge, symmetric about $\bar{x}_1 = 0$ (Figure 1,2), we have the following boundary conditions:

(a) for even modes

$L_n' = 0$ at $\bar{x}_1 = 0$, $L_n \to 0$ as $\bar{x}_1 \to \infty$

(b) for odd modes

$L_n = 0$ at $\bar{x}_1 = 0$, $L_n \to 0$ as $\bar{x}_1 \to \infty$

where now, Equation (V.5) is solved for $\bar{x}_1 \geq 0$.

This eigen-value problem can be solved numerically using the Hybrid Element Method, developed by Chen and Mei (1974) for water wave problems.

To illustrate the procedure, we discuss the solution for the even mode over symmetric ridge:

First, introduce the vertical line, $\bar{x}_1 = L$ which divides the domain into two regions, the first one ($0 \leq \bar{x}_1 \leq L$) containing the variable depth ($\bar{h}(\bar{x}_1)$) zone, while the second ($\bar{x}_1 \geq L$) being the constant depth ($\bar{h}=\bar{h}_o$) outer region.

In the outer region, the solution to (V.5) that satisfies the boundary condition at infinity is:

(V.9)

where $\alpha^2 = \bar{K}^2 - \frac{T}{\bar{h}_o}\bar{\Omega}^2 > 0$, a is a constant.

In the variable depth zone, a finite element 1-D discretization is constructed in order to satisfy (V.5) there. Furthermore, two matching conditions between the finite element solution and the analytical solution (V.9) are required. They are given by:

$$L_n^{(o)} = L_n^{(i)}$$

$$\bar{h}\frac{\partial}{\partial \bar{x}_1} L_n^{(o)} = \bar{h}\frac{\partial}{\partial \bar{x}_1} L_n^{(i)} \qquad \text{at } \bar{x}_1 = L \tag{V.10}$$

where $L_n^{(0)}$ = outer solution given by (V.9); $L_n^{(i)}$ = finite element solution.

The above problem can be shown to be equivalent to the stationarity of the functional:

$$J(L_n^{(o)}, L_n^{(i)}) = \int_o^L \left[\frac{\bar{h}}{2}\left(\frac{\partial L_n^{(i)}}{\partial \bar{x}_1}\right)^2 - \frac{\lambda}{2} L_n^{(i)2} \right] d\bar{x}_1 + \left[\bar{h}\left(\frac{L_n^{(o)}}{2} - L_n^{(i)}\right) \frac{\partial L_n^{(o)}}{\partial \bar{x}_1} \right]_{\bar{x}_1 = L} \tag{V.11}$$

Proof:

Taking the first variation of (V.11)

$$\delta J = \int_o^L \left[\bar{h} \frac{\partial L_n^{(i)}}{\partial \bar{x}_1} \cdot \frac{\partial \delta L_n^{(i)}}{\partial \bar{x}_1} - \lambda L_n^{(i)} \delta L_n^{(i)} \right] d\bar{x}_1 + \left[\bar{h}\left(\frac{\delta L_n^{(o)}}{2} - \delta L_n^{(i)}\right) \cdot \frac{\partial L_n^{(o)}}{\partial \bar{x}_1} + \bar{h}\left(\frac{L_n^{(o)}}{2} - L_n^{(i)}\right) \frac{\partial \delta L_n^{(o)}}{\partial \bar{x}_1} \right]_{\bar{x}_1 = L}$$

Integrating by parts:

$$\delta J = \left[\left(\bar{h} \frac{\partial L_n^{(i)}}{\partial \bar{x}_1}\right) \delta L_n^{(i)} \right]_o^L - \int_o^L \left[\left(\bar{h} L_n^{(i)\prime}\right)' + \lambda L_n^{(i)} \right] \delta L_n^{(i)} \, d\bar{x}_1 + \left[\bar{h}\left(\frac{\delta L_n^{(o)}}{2} - \delta L_n^{(i)}\right) \frac{\partial L_n^{(o)}}{\partial \bar{x}_1} + \bar{h}\left(\frac{L_n^{(o)}}{2} - L_n^{(i)}\right) \frac{\partial \delta L_n^{(o)}}{\partial \bar{x}_1} \right]_{\bar{x} = L} \tag{V.12}$$

$$I_1 = \int_0^L \frac{\bar{h}}{2}\left(\frac{\partial L_n^{(i)}}{\partial \bar{x}_1}\right)^2 d\bar{x}_1 = \sum_{m=1}^{M-1} \frac{1}{2}\bar{h}_m \left(\frac{\ell_{m+1} - \ell_m}{\delta}\right)^2 \cdot \delta$$

$$= \sum_{m=1}^{M-1} \frac{\bar{h}_m}{2\delta}\left(\ell_{m+1}^2 - 2\ell_m \ell_{m+1} + \ell_m^2\right)$$

(V.16)

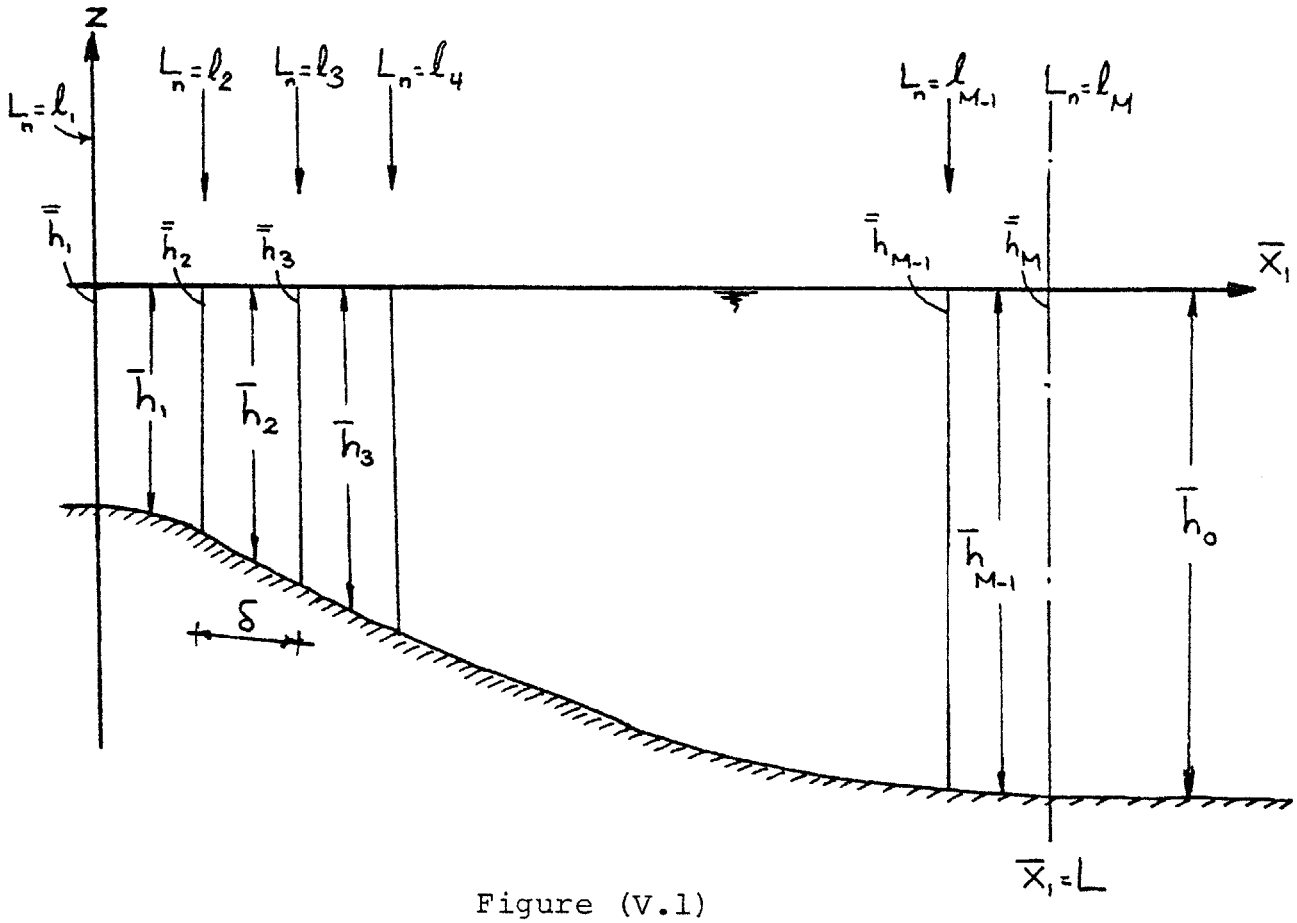

Figure (V.1)

But, applying Green's formula on L_n and δL_n we get:

$$\left[\bar{h} L_n' \delta L_n - \bar{h} \delta L_n' L_n \right]_0^L = 0$$

But at $\bar{x}_1 = 0$

$$L_n' = \delta L_n' = 0 \tag{V.13}$$

Hence,

$$\bar{h} L_n' \delta L_n = \bar{h} \delta L_n' L_n \qquad \text{at } \bar{x}_1 = L \tag{V.14}$$

Using (V.13) and (V.14) in (V.12) we get

$$\delta J = -\int_0^L \left\{ \left(\bar{h} L_n^{(i)\prime} \right)' + \lambda L_n^{(i)} \right\} \delta L_n^{(i)} \, d\bar{x}_1 + \left[\bar{h} \left(\frac{\partial L_n^{(i)}}{\partial \bar{x}_1} - \frac{\partial L_n^{(o)}}{\partial \bar{x}_1} \right) \delta L_n^{(i)} \right.$$

$$\left. + \bar{h} \left(L_n^{(o)} - L_n^{(i)} \right) \frac{\partial \delta L_n^{(o)}}{\partial \bar{x}_1} \right]_{\bar{x}_1 = L} \tag{V.15}$$

Hence, for J to be stationary, i.e., $\delta F = 0$ for arbitrary $\delta L_n^{(i)}$ and $\delta L_n^{(0)}$, Equations (V.5) and (V.10) are to be satisfied. This completes the proof.

Now, by discretizing the region ($0 \leq \bar{x}_1 \leq L$) as shown in Figure (V.1), we can approximate the expression (V.11) in terms of the nodal values ℓ_m (m=1,M) and a.

Thus, the integral:

where δ is the grid size, and where Taylor series expansion is used to approximate the first derivatives, with truncation error $\sim 0(\delta^2)$.

Similarly,

$$I_2 = \int_0^L -\frac{\lambda}{2} L_n^{(i)2} d\bar{x}_1 = \sum_{m=2}^{M-1} \frac{\delta}{2}\left(\bar{\bar{h}}_m \bar{K}^2 - T\bar{\Omega}^2\right) \ell_m^2$$

$$+ \frac{\delta}{4}\left(\bar{\bar{h}}_1 \bar{K}^2 - T\bar{\Omega}^2\right) \ell_1 + \frac{\delta}{4}\left(\bar{\bar{h}}_M \bar{K}^2 - T\bar{\Omega}^2\right) \ell_M^2 \qquad \text{(V.17)}$$

And,

$$I_3 = \left[\bar{h}\left(\frac{L_n^{(o)}}{2} - L_n^{(i)}\right)\frac{\partial L_n^{(o)}}{\partial \bar{x}_1}\right]_{\bar{x}_1 = L} = a^2\left(-\frac{\bar{h}_o}{2}\alpha e^{-2\alpha L}\right) + a\ell_M \bar{h}_o \alpha e^{-\alpha L} \qquad \text{(V.18)}$$

Thus, adding (V.16), (V.17) and (V.18), we get

$$J = I_1 + I_2 + I_3 = \vec{x}^T [A] \vec{x} \qquad \text{(V.19)}$$

where

$$\vec{x}^T = \{ \ell_1, \ell_2, \ell_3, \ldots, \ell_{M-1}, \ell_M, a \}$$

and [A] is the coefficients matrix, whose components a_{ij} are given by:

$$a_{11} = \frac{\bar{h}_1}{2\delta} + \frac{\delta}{4}\left[\bar{\bar{h}}_1 \bar{K}^2 - T\bar{\Omega}^2\right]$$

$$a_{MM} = \frac{\bar{h}_{M-1}}{2\delta} + \frac{\delta}{4}\left[\bar{\bar{h}}_M \bar{K}^2 - T\bar{\Omega}^2\right]$$

$$a_{mm} = \frac{\bar{h}_m + \bar{h}_{m-1}}{2\delta} + \frac{\delta}{2}\left[\bar{\bar{h}}_m \bar{K}^2 - T\bar{\Omega}^2\right] \qquad \text{for } m \neq 1 \text{ or } M$$

$$a_{m,m+1} = a_{m+1,m} = \frac{-\bar{h}_m}{2\delta} \qquad m = 1, 2, \ldots, M-1$$

$$a_{M+1,M+1} = \frac{-\alpha \bar{h}_0}{2} e^{-2\alpha L}$$

$$a_{M,M+1} = a_{M+1,M} = \frac{\alpha \bar{h}_0}{2} e^{-\alpha L}$$

while all the other a_{ij} are zeroes. Hence, A is a symmetric, tridiagonal matrix.

Thus, F=0 implies:

$$[A]\,\vec{x} = 0 \tag{V.20}$$

This is a homogeneous set of algebraic equations. For nontrivial solution for $\vec{x}$, [A] has to be singular, i.e.,

$$\det.|A| = 0 \tag{V.21}$$

Thus, for a given wave number $\bar{K}$, Equation (V.21) will determine the possible frequencies $\bar{\Omega}$, i.e., determine the dispersion relations of the edge wave. However, instead of

solving (V.21), which is an algebraic equation for M+1st order, one can use the following alternative:

By factoring out the term $-\frac{\delta}{2} T \bar{\Omega}^2$ off the diagonal terms of [A], (V.20) becomes

$$[A'] \vec{x} = \mu_e \vec{x} \qquad ; \mu_e = \frac{\delta}{2} T \bar{\Omega}^2 \tag{V.22}$$

where [A'] is still a symmetric, tridiagonal matrix. However, some [A'] elements depend on the value of μ_e (or $\bar{\Omega}^2$). Thus, we solve (V.22) by a trial-and-error procedure. First we can write $\bar{\Omega}^2$ as follows:

$$\bar{\Omega}^2 = (1-\beta^2) \frac{\bar{h}_o}{T} \bar{K}^2 \qquad ; \quad 0 < \beta < 1 \tag{V.23}$$

so that α in (V.9) is real.

Now, try a value of β, between zero and unity, into the elements of [A']. Then, solve the obtained eigenvalue problem (V.22). The simple method of Bisection (Wilkinson, p. 299) whichis most suitable for tridiagonal symmetric matrices can be used for the solution. Repeat by trying various values of $(0 < \beta < 1)$ until one eigenvalue coincides with that assumed in [A'] elements.

For the obtained pair $(\bar{\Omega}, \bar{K})$ the eigenvector x can be found, up to a constant, arbitrary multiplier, from (V.20). This arbitrary constant can be fixed by letting L_n at the

origin ($\bar{x}_1$=0) to be unity. The procedure can be repeated to get the dispersion relation $\bar{\Omega} = \bar{\Omega}(\bar{K})$ for the various modes.

2) Solutions for the induced motion ϕ_{10}:

The potential $_{10}$ is given by:

$$\Phi_{10} = \Phi_{10}^{(0)} + (\Phi_{10}^{(2)} + *) \qquad (V.24)$$

where $\phi_{10}^{(1)}$ is term representing the mass transport current solution, given by (3.42).

$\phi_{10}^{(2)}$ has the form:

$$\Phi_{10}^{(2)} = \left(\frac{-igD_0}{2\Omega}\right)^2 \left[\psi_1(x_1) e^{-2i\Omega t_1} + \psi_2(x_1) \cos 2Ky_1 \, e^{-2i\Omega t_1}\right] \qquad (V.25)$$

where, from (3.44) and (3.45), ψ_1 and ψ_2 satisfy:

$$-g(h\psi_1')' - 4\Omega^2\psi_1 = \frac{i\Omega}{2}\left[L_n'^2 + K^2L_n^2 + \frac{1}{2}(L_n^2)''\right] \qquad (V.26a)$$

$$-g(h\psi_2') + 4(ghK^2 - \Omega^2)\psi_2 = \frac{i\Omega}{2}\left[L_n'^2 - 3K^2L_n^2 + \frac{1}{2}(L_n^2)''\right] \qquad (V.26b)$$

The same numerical technique, Hybrid Element Method, which was used to solve for ϕ_{oo}, will be used also to solve

for ψ_1 and ψ_2. First, we non-dimensionalize the equations, using the same scalings and letting:

$$(\psi_1 , \psi_2) = \frac{\omega k_o}{g} (\bar{\psi}_1 , \bar{\psi}_2) \tag{V.27}$$

to get

$$(\bar{h}\bar{\psi}_1')' + 4T\bar{\Omega}^2\bar{\psi}_1 = \frac{-i\bar{\Omega}}{2}\left[L_n'^2 + \bar{K}^2 L_n^2 + \frac{1}{2}(L_n^2)'' \right] \tag{V.28a}$$

$$(\bar{h}\bar{\psi}_2')' - 4(\bar{h}\bar{K}^2 - T\bar{\Omega}^2)\bar{\psi}_2 = \frac{-i\bar{\Omega}}{2}\left[L_n'^2 - 3\bar{K}^2 L_n^2 + \frac{1}{2}(L_n^2)'' \right] \tag{V.28b}$$

with the boundary conditions

$$\bar{\psi}_1 \sim e^{\pm i\hat{\lambda}\bar{x}_1} \qquad \text{as } \bar{x}_1 \longrightarrow \pm\infty \tag{V.29a}$$

$$\bar{\psi}_2 \longrightarrow 0 \qquad \text{as } \bar{x}_1 \longrightarrow \pm\infty \tag{V.29b}$$

where, $\hat{\lambda} = 2\bar{\Omega}\sqrt{T/\bar{h}_o}$. (V.30a) is the radiation condition of Sommerfeld, that is $\bar{\psi}_1$ behaves as an outgoing wave at infinity.

For symmetric ridge, and for even or odd mode L_n, it is seen from (V.28) and (V.29) that $\bar{\psi}_1$ and $\bar{\psi}_2$ should

be even functions of $\bar{x}_1$. Thus, the boundary conditions are,

$$\bar{\psi}_1' = 0 \quad ; \bar{x}_1 = 0 \qquad \text{and} \qquad \bar{\psi}_1 \sim e^{i\hat{\lambda}\bar{x}_1} \qquad \text{as } \bar{x}_1 \to \infty \tag{V.30a}$$

$$\bar{\psi}_2' = 0 \quad ; \bar{x}_1 = 0 \qquad \text{and} \qquad \bar{\psi}_2 \to 0 \qquad \text{as } \bar{x}_1 \to \infty \tag{V.30b}$$

and (V.28) are solved for $\bar{x}_1 \geq 0$.

We start the solution, as before, by introducing the vertical line $\bar{x}_1$=L, such that in the region $\bar{x}_1 > L$, the R.H.S. of (V.28aorb) is negligible. In the outer region, we have the solutions:

$$\bar{\psi}_1 = \sigma_1 = a_1 e^{i\hat{\lambda}\bar{x}_1}$$

$$\bar{\psi}_2 = \sigma_2 = a_2 e^{-\alpha_2\bar{x}_1} \tag{V.31}$$

where $\alpha_2^2 = 4(\bar{K}^2 - \frac{T}{\bar{h}}\bar{\Omega}^2)$, a_1 and a_2 are constants.

In the region ($0 \leq \bar{x}_1 \leq L$), the finite element discretization is made as when solving for ϕ_{oo} (Figure V.1). Matching conditions at $\bar{x}_1$=L are similar to (V.10):

$$\psi_j^i = \sigma_j$$

$$\bar{h}\,\psi_j^{i\,\prime} = \bar{h}\,\sigma_j' \qquad \text{at } \bar{x}_1 = L \;;\; j = 1,2 \tag{V.32}$$

where ψ_1^i, ψ_2^i are the finite element solution to $\bar{\psi}_1$ and $\bar{\psi}_2$.

The above two problems can be shown to be equivalent to the stationarity of the functionals:

$$J_j(\sigma_j, \psi_j^i) = \int_0^L \left[\frac{\bar{h}}{2}(\psi_j^{i\prime})^2 - \frac{\lambda_j}{2}\psi_j^{i\,2} + f_j\,\psi_j^i \right] d\bar{x}_1$$

$$+ \left[\bar{h}\left(\frac{\sigma_j}{2} - \psi_j^i\right)\sigma_j' \right]_{\bar{x}_1 = L} \;;\; \text{for } j = 1,2 \tag{V.33}$$

where

$$\lambda_1 = 4T\bar{\Omega}^2 \tag{V.34a}$$

$$\lambda_2 = -4(\bar{h}\bar{K}^2 - T\bar{\Omega}^2) \tag{V.34b}$$

and, f_1 and f_2 are the right hand sides of (V.28a and b) respectively.

This is very similar to (V.11), and it is straightforward to follow the same approximation procedure to express (V.33) in terms of the nodal values $\ell_m^{(j)}$

(j=1,2 and m=1,M) and a_j. Hence, we have

$$J_j = \frac{1}{2} \vec{x}_j^T [A_j] \vec{x}_j + \vec{x}_j^T \cdot \vec{F}_j \qquad ; j=1,2 \qquad \text{(V.35)}$$

where $[A_j]$ is a symmetric, tridiagonal matrix, similar to [A] in (V.19) and the extra term $\vec{x}_j^T \vec{F}_j$ comes from the extra contribution to the integrand $f_j \psi_j^i$.

Thus, the stationarity of J_j implies

$$[A_j] \vec{x}_j + \vec{F}_j = 0 \qquad ; j=1,2 \qquad \text{(V.36)}$$

These sets of algebraic equations can easily be solved, using Gaussian Elimination Technique, for example, to get the unknown vector

$$x_j = (\ell_1^j, \ell_2^j, \ldots \ell_M^j, a_j).$$

where, ℓ_m^j is the value of ψ_j^i at the mth node.